Identification of Small RNAs as potential biomarkers and regulators of chemoradiotherapy response in Oesophageal Adenocarcinoma (EAC)

by

Guoqian Ding

Thesis

Submitted to Flinders University

for the degree of

Master of Science

College of Medicine and Public Health

May 2023

Declaration

I certify that this thesis does not incorporate, without acknowledgment, any material previously submitted for a degree or diploma in any university; and that the research within will not be submitted for any other future degree or diploma without the permission of Flinders University; and that to the best of my knowledge and belief it does not contain any material previously published or written by another person except where due reference is made in the text.

Guoqian Ding May 1st, 2023

TABLE OF CONTENTS

Identification of potential small RNA biomarkers of response to chemoradiotherapy in pre-treatment blood from patients with locally advanced EAC

Acknowledgements

This thesis would not have been possible without the financial support --- Flinders International Postgraduate Research Scholarship (FIPRS) from Flinders University and the Australian Government. Research is a team sport and this thesis would not have been possible without the continued support of my supervisors, laboratory and Department colleagues, friends and my family.

First and foremost, I wish to acknowledge my primary supervisor Damian Hussey for the opportunity to learn from him and study within his laboratory for the past four years. His continued guidance, encouragement, expertise and friendship have been invaluable throughout my study. He has nurtured my love of research and knowledge and I am very appreciative of the training and experience I acquired throughout my candidature.

I extend my gratitude to my associate supervisor, Professor David Watson. His clinical and experimental knowledge was very valuable and I thank him for his continued support throughout my project. I also would like to thank Karen Chiam and Steve Due. Your friendship, mentorship and the time you spent helping me with experiments throughout my research training was very much appreciated.

I wish to thank the members of the Upper Gastrointestinal Research Laboratory (especially Isabell Bastian and George Mayne, and others including Tingting Wang, Benjamin Eyck, Frederike Butz, Ann-Kathrin Eichelmann and Tanya Irvine) headed by Dr Damian Hussey with whom our laboratory is strongly affiliated.

I would also like to thank the ACRF CGF, Michael Michael and FCIC and Flinders Genomics Facility staff, Flow cytometry staff. Both of you help me a lot during my study.

Thanks Editage company for the English language and grammatical editing.

Finally, I would like to thank my family for their support and patience over the last four years.

The paper is too short to describe my feelings. My gratitude to you all will always remain in my heart and illuminate my future path.

Abbreviations

Oesophageal adenocarcinoma	EAC
Oesophageal carcinoma	EC
Oesophageal squamous cell cancer	ESCC
Epidermal growth factor receptor	EGFR
Estrogen receptor	ER
Vascular endothelial growth factor	VEGF
Human epidermal growth factor receptor 2	HER2
PIWI-interacting RNAs	piRNAs
Small nucleolar RNAs	snoRNAs
Small nuclear RNA	snRNAs

AMP-activated protein kinase	AMPK
American Joint Cancer Committee	AJCC
False discovery rates	FDR
Formalin-fixed paraffin-embedded	FFPE
Area under the ROC Curve	AUC
3-(4,5-dimethylthiazol-2-yl)-5-(3-carboxymethoxyphenyl)-2-(4-sulfophenyl)-2H-tetrazolium	MTS
Vehicle control	VC
Plating efficiency	PE
Survival fraction	SF
Tumor regression grade	TRG
Crystal violet	CV

Abstract

It is reported that neoadjuvant chemoradiotherapy for esophageal cancer can significantly improve overall survival. However, not all patients have a good response to chemoradiotherapy and achieve significant survival improvement. Therefore, it is important to find biomarkers that are associated with chemoradiotherapy response to treat patients individually and adjust the treatment approach in a response-guided manner in neoadjuvant settings. It would be ideal if these biomarkers enabled prediction of response prior to administering of therapy.

Emerging evidence demonstrates that small RNAs, such as miRNAs, piRNAs, snRNAs, and snoRNAs play a pivotal role in the development and progression of numerous cancers. However, there are few studies on the roles of small RNAs in

tissue or in blood as biomarkers and regulator of treatment response in oesophageal adenocarcinoma (EAC).

In this thesis, the top differentially expressed tissue small RNAs between EAC neoadjuvant chemoradiotherapy responders and non-responders were identified as potential biomarkers. The potential functions and mechanisms underlying their actions were studied using EAC cell lines. miR-451a was the top biomarker for prediction of responders. The functional study showed that miR-451a enhanced EAC cell proliferation and decreased apoptosis in these cells. miR-451a rendered the EAC cells more resistant to drug treatment. Protein analysis indicated that miR-451a might regulate the treatment response by affecting pAMPK, Thr172/AMPK, 14-3-3 zeta phos Ser58/14-3-3 zeta/delta and pEGFR/EGFR.

Exosomes circulating in peripheral blood contain numerous small RNAs, some of which come from tumor tissues and might be useful biomarkers. Therefore, in this study response based differentially expressed small RNAs were identified using serum exosomes from patients with EAC. Some reports have suggested that circulating exosomes can modulate the local tumor environment to influence tumor response to chemoradiotherapy. Therefore, this study tested the ability of serum exosomes from patients with EAC to modulate the proliferation and/or drug or radiation response behavior of EAC cells. The results showed that the exosomes from non-responders made the cells less resistant to cisplatin while the exosomes from non-responders made the cells more resistant to 5-FU in most experiments.

Collectively, this study identified specific small RNAs as potentially useful biomarkers of response to chemoradiotherapy in EAC and provided information on the potential roles of these small RNAs in regulating the response to chemoradiotherapy.

CHAPTER 1
INTRODUCTION

The aim of this thesis was to identify small RNAs as biomarkers of response to chemoradiotherapy in esophageal adenocarcinoma (EAC) and study the roles of significant microRNAs (miRNAs) in regulating chemoradiotherapy responses and the mechanisms underlying these roles.

Ongoing research to identify differentially expressed small RNAs between responders and non-responders to chemoradiotherapy in cancer would help to discover specific small RNAs that could be used as biomarkers for chemoradiotherapy response and could also be therapeutic targets for patients showing chemoradioresistance.

This chapter introduces esophageal carcinoma (EC), the origin and function of circulating small RNAs, current biomarkers in esophageal carcinoma for diagnosis, prognosis, and chemoradiotherapy response, and the mechanisms underlying the roles of small RNAs in regulating chemoradiotherapy response.

1.1 A brief overview of EC

1.1.1 Epidemiology

EC is an esophageal malignancy and is the sixth highest cause of mortality in cancer patients and the eighth most common carcinoma in the world[1, 2], with an estimated 45,000 new global patients every year. The number of new EC patients per year is rapidly increasing, with approximately 80% occurring in developing countries[3], and men in Eastern Asia with the highest incidence rate of EC globally[2].

There are two main EC subtypes, with the primary being esophageal squamous cell cancer (ESCC), accounting for approximately 90–95% of global cases, and the other being EAC which constitutes approximately 50–80% of cases in western countries, including the USA[4]. ESCC and EAC have different risk factors, with environment, nutrition, low socioeconomic status, tobacco, alcohol, lack of whole-grain consumption, and genetic influences playing a pivotal role in ESCC patients[5-7], while Caucasian ethnicity, male sex, obesity, postmenopausal status[8], the length of

Barrett's esophagus[9], and a chronic history of reflux disease[10] being the main risk factors for EAC patients.

1.1.2 Clinical features and diagnosis

Dysphagia, which refers to difficulty in swallowing is a common clinical symptom of EC, with the other symptoms being chest pain, weight loss, chronic cough, and vomiting. Patients show different symptoms depending on individual differences[11].

EC is typically diagnosed using X-ray barium radiography, computed tomography (CT), endoscopic ultrasonography, and Positron Emission Tomography (PET)[12]. Endoscopy is used for diagnosis and CT scan for staging. Barium X-ray is rare for diagnosis today but as a basic tool it still can find EC occasionally. However, these methods of detection are limited in scope, and more than half of patients already have metastasis at the time of diagnosis[13]. Therefore, effective biomarkers for earlier clinical diagnosis of EC need to be urgently investigated.

1.1.3 Treatment

The primary therapeutic approach for the treatment of EC involves surgical resection, when possible. Complete surgical excision is associated with lower recurrence rates and a longer survival time[14]. Unfortunately, only 30–40% of patients diagnosed with EC are potential candidates for surgical resection[15]. Therefore, early diagnosis is critical [16]. In some countries, the government recommends that all patients with dysphagia undergo endoscopy for the screening of EC [17]. Moreover, endoscopy not only enables the screening and diagnosis of EC but is also a tool for treatment during the early stage of EC, such as for T1a lesions[18, 19].

Chemotherapy and radiotherapy are the main therapeutic approaches for patients who cannot undergo surgical resection. Both chemotherapy and radiotherapy are also used in neoadjuvant therapy. However, the benefits of neoadjuvant therapy in prolonging patient survival time remains debatable [20-22]. Clinically, chemoradiotherapy shows polarized effects in patients, with some patients being responders with increased survival time, while others are non-responders with

decreased survival time. Therefore, it is important for physicians to determine the patients who could benefit from chemoradiotherapy.

In short, biomarkers for early diagnosis and the prediction of prognosis and chemo-radiotherapy response are necessary to guide the treatment of patients with EC.

1.2 Current biomarkers for EC

Several types of biomarkers are currently available for EC, including immunohistochemical (IHC) biomarkers, antibodies, genes, and small RNA biomarkers[10].

IHC biomarkers are popular for the detection of associated protein expression to predict the diagnosis and outcome for several cancers. A number of EC biomarkers have been detected using IHC including epidermal growth factor receptor (EGFR)[23], estrogen receptor (ER)[24], vascular endothelial growth factor (VEGF)[25, 26], P53[27], and epidermal growth factor receptor 2(HER2)[28]. Researchers have also identified the biomarker SLC39A6 via large-scale genome-wide association studies, and used IHC to demonstrate that this gene could be used for the early detection and as a prognostic biomarker for EC[29]. However, several potential problems affect the final IHC staining results including strong background staining, weak target antigen staining, and autofluorescence.

The antibody against tumor-associated antigen (TAA) can also be used as a biomarker for the diagnosis of EC. Some researchers[30] reported that TAAs are detectable much earlier in the circulation of patients with EC and can be used as potential biomarkers for the early diagnosis of EC[31]. Antibodies against p53 have been identified as a biomarker for the diagnosis of ESCC[32]. Several publications have reported that other antibodies such as SURF1, HOOK2, LOC146223, CEA, SCC-Ag, and CYFRA211 could also be used as potential biomarkers[33, 34]. Unfortunately, the sensitivity of these antibodies is only about 26.7% even though their specificity is reported to be above 90%[35].

The advent of microarray-based analysis has made tremendous clinical impact by identifying differential gene expression as biomarkers for EC[36, 37]. Matthias et

al.[38] used microarray-based analysis to demonstrate differential gene expression of Ephrin B3 receptor between EAC responders and non-responders, which can serve as a biomarker for patient treatment response. Xie et al.[39] reported that integrin **α** 5 plays an important role in ESCC progression and can be used as a new biomarker for ESCC prognosis. De Bruijn K et al.[40] observed that decreased expression of IGF-1R is related to EAC invasiveness and aggressiveness and thus, it could serve as a biomarker for the screening of EAC from Barrett's esophagus (BE). However, using these genes as potential biomarkers has some limitations[41]. For example, age-associated alterations in gene expression patterns would hinder their long-term use as a biomarker. These drawbacks underscore the importance of finding new kinds of biomarkers in circulation, such as RNAs, for the clinical diagnosis and prognosis of cancer.

The first described circulating RNA species was that of messenger RNAs (mRNAs) in the 1990s from several kinds of carcinomas[42-44]. The circulating mRNAs reflect the status of the intracellular process of protein translation; therefore, they could be used as potential biomarkers for the diagnosis and prognosis of carcinoma. However, mRNAs are easily degraded and unabundant in circulation, furthermore, they are prone to contamination during sample handling[45, 46]. Therefore, the application of mRNAs as biomarkers is very limited.

Circulating small RNAs are more stable and conserved across species[47]. Small RNAs including miRNAs, PIWI-interacting RNAs (piRNAs), small nucleolar RNAs (snoRNAs), and small nuclear RNA (snRNAs) have become the focus of current biomarker research. miRNAs were first identified in circulation in 2008 by Chim et al.[48], and several circulating miRNAs have since been reported. However, little is known about the other small RNA species including piRNAs, snRNA and snoRNAs. piRNAs are 26–31 nt in length and are derived from a Dicer-independent mechanism. They have been reported in circulation, with functions extending beyond transposon silencing[49, 50]. snoRNAs have also been identified in circulation[51] and are thought to regulate chemical modifications for other RNAs. Blood is one of the most accessible biological fluids as it contacts all bodily tissues

and carries disease-specific biomarkers. Therefore, identifying small RNAs as biomarkers in circulating blood is practical and promising[52].

1.3 Circulating small RNAs

1.3.1 Potential source of circulating small RNAs

Small RNAs have been reported to be stable in biological fluids enabling their use as potential biomarkers[53]. Small RNAs can be detected in several bodily fluids, such as breast milk, blood, urine, vaginal secretion, saliva, tears, and semen[54-56]. The expression of small RNAs in bodily fluids can change according to the development of diseases, indicating that these small RNAs can be used as biomarkers to assess and screen the pathological status of the body. For example, miRNAs in saliva have been identified as potential biomarkers for the diagnosis of EC[57]. However, the ideal biomarker should be minimally invasive, accessible, reliable, and specific to the disease being investigated[47, 58]. Compared to other bodily fluids, blood is the most accessible biological fluid and carries unique biomarkers for several diseases[59] especially cancer, because it makes close contact with almost all body tissues. Furthermore, repeated follow-up and monitoring of treatment efficacy can be conveniently performed using blood.

Biomarkers for analysis can be derived from whole blood, serum, or plasma [60]. Previous research has indicated that using whole blood is inefficient for small RNA detection due to the detrimental effect of red blood cells on the expression of small RNAs. There is no general consensus about the use of circulating serum or plasma for biomarker detection, but most researchers believe that serum might work better for small RNA detection as plasma contains cellular debris which might cause contamination by small RNAs from apoptotic and lysed cells[61].

1.3.2 The origin of small RNAs in circulation

Small RNAs can be detected in blood samples of patients with several diseases, especially in patients with cancer, including pleural mesothelioma[53], cholangiocarcinoma[58], lymphoma[62], thyroid carcinoma[63], pancreatic cancer[64], nasopharyngeal carcinoma[65], and gastric cancer[66-68]. Moreover, circulating small RNAs can also be detected in some benign diseases, such as

polycystic ovary syndrome[69]. Other small RNAs such as piRNAs and snoRNAs have also been detected in circulation[50, 70, 71], such as in bladder cancer[72], hepatocellular carcinoma[73], and renal carcinoma[74]. Small RNAs in circulation are abundant, but the source of these small RNAs remains unclear as they could be derived from the cell death and lysis of cancer cells or from direct secretion from cancer cells.

The subcellular origin of small RNAs is known, for example, miRNA originate from the cell nucleus, where they are transcribed and cleaved by Drosha, forming pre-miRNA, which are translocated to the cytoplasm by exportin-5, where the mature miRNAs are formed by further trimming by dicer[75]. Cellular piRNAs are derived from transposons, mRNAs, and lncRNAs[76], and are processed to mature piRNAs by either a primary synthesis mechanism or by 'ping-pong' amplification[77]. Cellular snoRNAs mainly originate from RNApol-II activity, with the majority being processed from the introns of certain protein-coding and noncoding transcripts[70]. However, how these small RNAs enter into the circulation and whether they are derived from circulation alone, especially for piRNAs and snoRNAs, remains unknown.

Several studies indicate that the level of small RNAs in tissue is consistent with their levels in circulation. For example, Brase et al.[78] reported elevated levels of miR-375 and miR-141 in both tissue samples and the serum of patients with prostate cancer. Moreover, Ng et al.[79] reported five miRNAs with elevated levels in both the blood and tissue of patients with colorectal cancer. However, another study[80] showed that only a small number of small RNAs in circulation reflect the status of small RNAs in cells or cancer tissue, indicating that cells have specific mechanisms whereby they choose the small RNAs that should be released in circulation; this makes the origin of circulating small RNAs a complicated research subject.

Currently, several probable approaches have been reported to investigate the origin of circulating small RNAs, such as from cancer cells, active secretion by extracellular vesicles, active secretion in protein complexes, and foreign organisms and viruses.

1.3.2.1 Cellular Origin

Most of the circulating small RNAs are derived from human cells, but it is not clear which specific cells contribute to these small RNAs[81]. Cancer cells could release miRNAs into the bloodstream and could also secrete miRNA-containing extracellular vesicles[82]. Circulating small RNAs from cancer cells would depend on the size of cancer and accessibility of the blood supply. Pigati et al.[83]indicated that circulating small RNAs, such as miR-451 and miR-1246, can be derived from malignant mammary epithelial cells, indicating that cells are an important source of the circulating small RNAs. However, the contribution of cancer cells to the entire pool of circulating small RNAs is little, making it hard to detect cancer-associated small RNAs, especially in the early stages of cancer[84]. Moreover, the small RNAs produced by cancer cells have little effect on immunocytes to create an immune response. Therefore, immunocytes may produce miRNAs as the process or result of their activity against cancer.

Numerous studies have attempted to demonstrate that the circulating small RNAs are derived from blood cells. Radha et al.[85] reported that blood cells could play a pivotal role in the origin of circulating miRNAs, indicating that the circulating miRNAs might be derived from blood cells. Pritchard et al.[86] showed that circulating miRNAs are mainly derived from blood cells and alterations in blood cell counts or hemolysis changed the levels of plasma miRNA biomarkers by up to 50-fold, indicating that the circulating miRNAs have a close relationship with blood cells.

1.3.2.2 Extracellular vesicles

Research has shown that the circulating small RNAs can be actively secreted from extracellular vesicles (EV). Extracellular vesicles include exosomes, microvesicles, apoptotic bodies, exosome-like vesicles, and membrane particles[87]. The exact mechanisms underlying the release of EVs and the kinds of cells that release them remain unclear. Several mechanisms have been proposed for EV release., including[88]: 1) exosome production via the exocytic fusion of multivesicular bodies; 2) direct microvesicle release by the budding of vesicles derived from the plasma membranes; and 3) apoptotic bodies resulting from cell death (Figure 1-1).

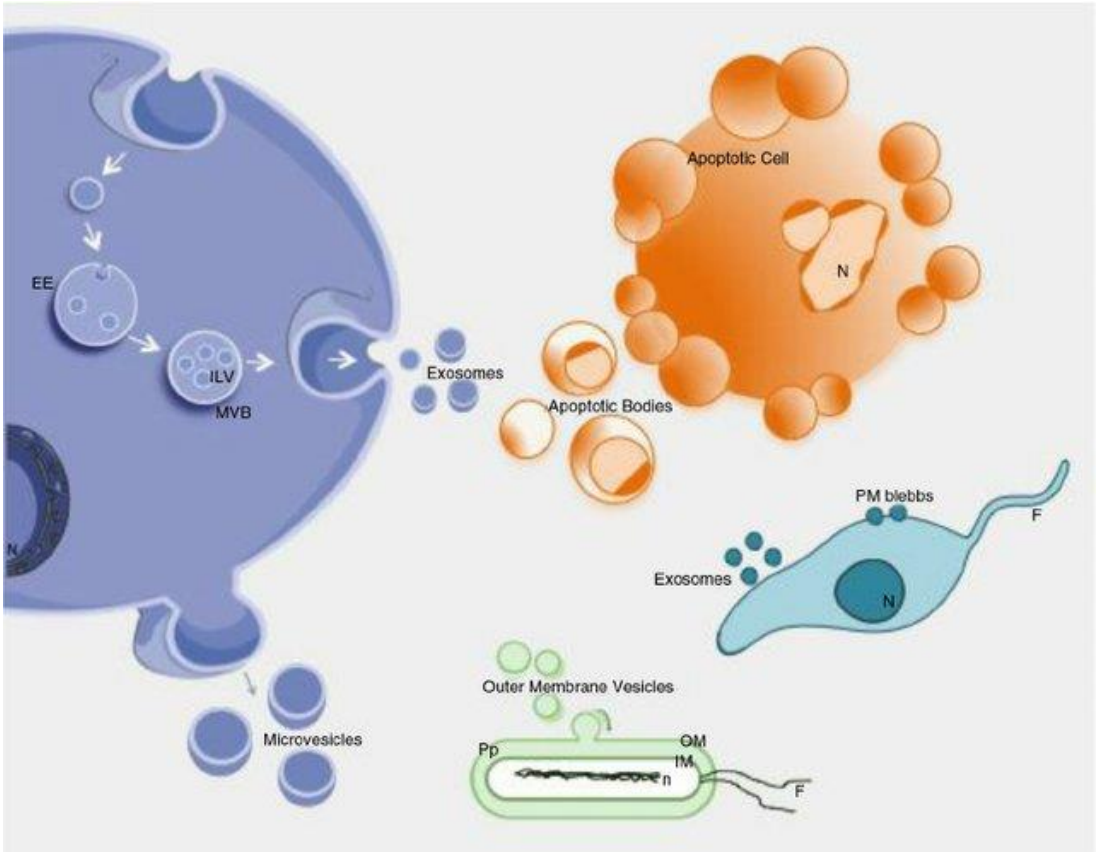

Figure 1-1: Biogenesis, and release of extracellular vesicles. Reproduced from Yanez et al.[89] with permission from the corresponding author (María Yáñez-Mó) and the publisher (Wiley).

Current research is predominantly focused on two major types of EVs: exosomes, and microvesicles and apoptotic bodies. Exosomes are smaller, ranging in size from 30–200 nm and form by the fusion of multiple microvesicles with the plasma membrane as discussed above. Microvesicles are 0.1–1 um in size and form by cellular blebbing. Apoptotic bodies are released through blebbing from cells undergoing apoptosis, and are more than 1000 nm in size[90, 91] (Figure 1-2).

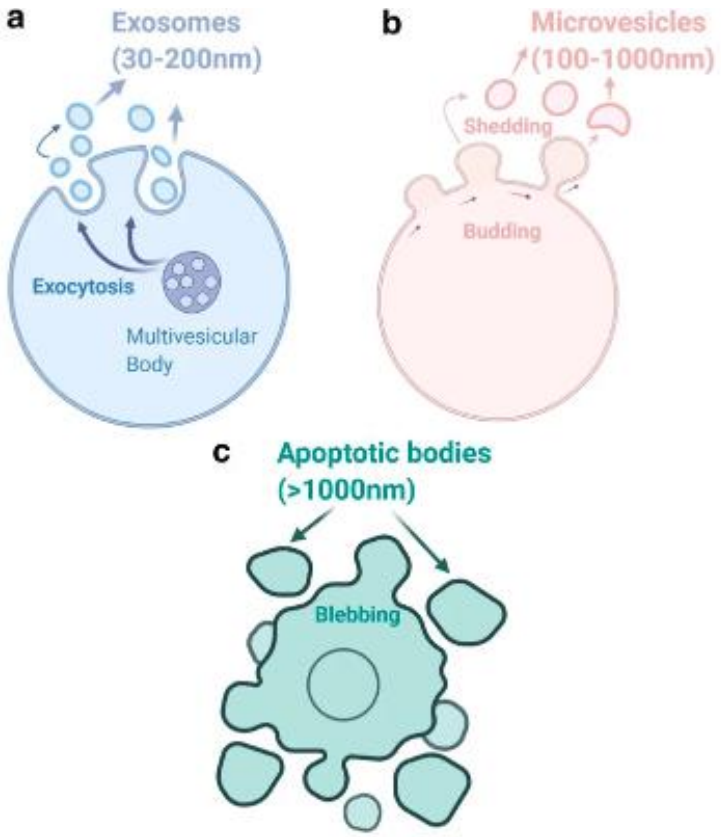

Figure 1-2: Characteristics of different subtypes of extracellular vesicles, a: exosomes, b: microvesicles, c: apoptotic bodies. Reproduced from Gurung et al.[92] with permission from the corresponding author (ulien Baruteau) and the publisher (BMC).

These vesicles protect the small RNAs against external factors, such as enzymatic degradation and pH conditions, making the small RNAs contained in exosomes and microvesicles as potential biomarkers of cancer[93]. Small RNA packaging into EVs enables the small RNAs to circulate throughout the body in circulating blood. The EVs communicate with other cells for proper cargo delivery to the target cells. The EVs deliver the small RNAs by fusing directly with the plasma membrane of recipient cells, or via endocytotic pathways[94], or by protein-protein interactions such as Toll-like receptors[95] (Figure 1-3).

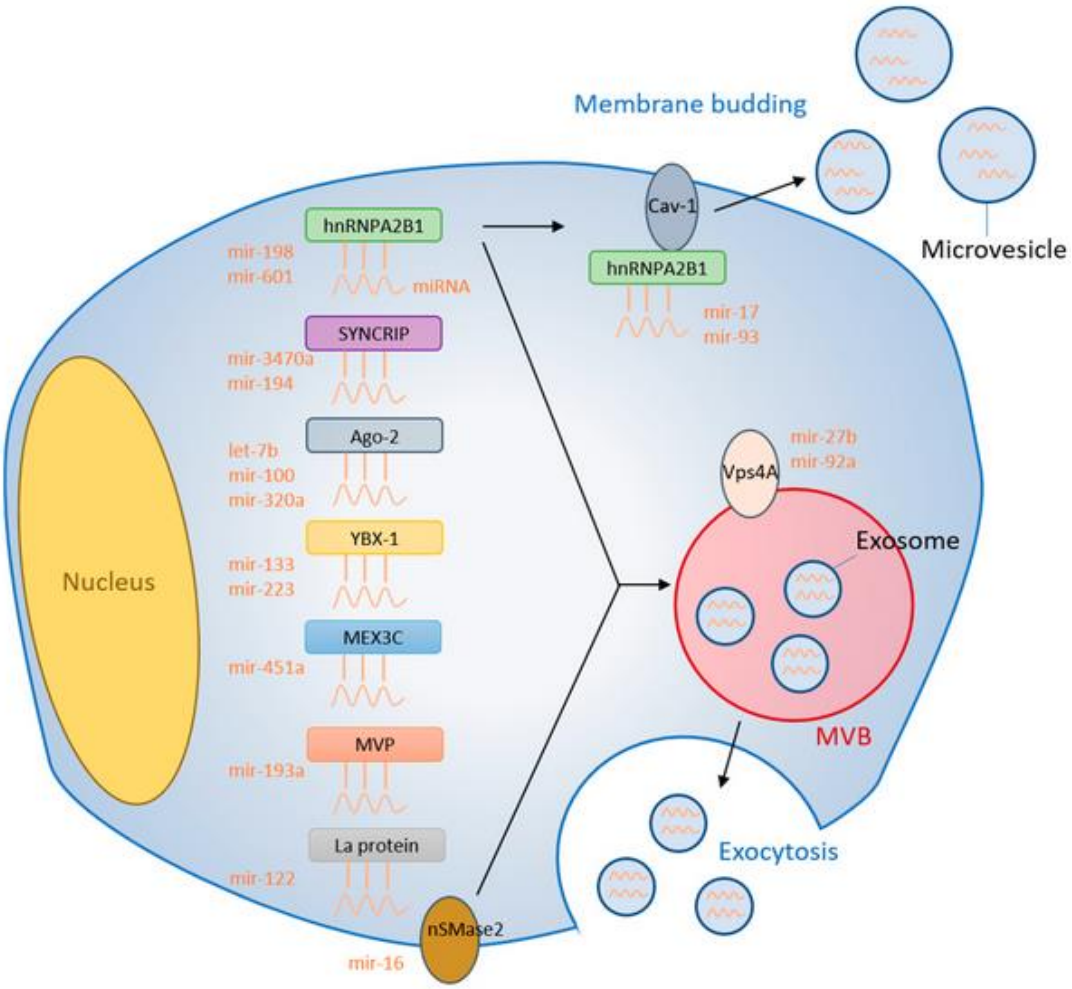

Figure 1-3: Packaging of miRNA into EVs. RNA binding proteins and membranous proteins are involved in binding specific miRNAs and selectively sorting them into EVs. Reproduced from Groot and Lee.[96] with permission under the Creative Commons Attribution License.

Small RNAs in exosomes or vesicles can be detected in several kinds of cancer, such as prostate carcinoma[97], breast carcinoma [98], non-small-cell lung carcinoma [99], and even in some other diseases such as sickle cell anemia[100], and Alzheimer's disease[101]. The EVs contain a variety of small RNAs. Ben-Dov et al.[46] demonstrated the presence of both miRNAs and piRNAs in circulating exosomes in healthy and cancer patients, and showed that these small RNAs are associated with age, sex, and cancer type.

1.3.2.3 Protein complex

Several studies have reported that the circulating small RNAs are not always derived from active secretion by EVs. Turchinovich et al.[102] reported that most circulating miRNAs could pass through 0.22 μm filters, indicating that these miRNAs are free of EVs and further described a close relationship between miRNAs and Ago2, an RNA-induced silencing complex-related protein. This kind of protein-miRNA complex could be the secondary product of dead cells. These Ago2-miRNA complexes protect the circulating miRNAs against degradation by plasma RNases [103].

Apart from Ago2, researchers[104] have demonstrated that nucleophosmin 1 (NPM1) can also secure miRNAs from degradation, and that NPM1 might be an important player in the exportation and packaging of circulating miRNAs. Other studies have claimed that some lipoproteins such as high-density lipoproteins and low-density lipoproteins have the ability to transfer miRNAs[105, 106], and this ability could enable their response to fatty acids intake[107].

It is not clear whether piRNAs, snRNAs, and snoRNAs are also actively secreted with protein complexes. However, piRNAs play a critical role by interacting with PIWI proteins and they work together to regulate transposable elements at the transcriptional level, and piRNAs also interact with other proteins such as argonaut proteins and regulate cytoplasmic mRNAs in the cytoplasm[108]. Whether this kind of phenomenon happens in circulation is still not clear.

1.3.2.4 Foreign factors

Some studies[109, 110] have indicated that the circulating small RNAs could originate from exogenous organisms, such as the microbiome, fungi, bacteria, and diet-derived organisms. Zhang et al.[111] reported that exogenous miR-168a, which is abundant in rice, could enter the circulation after digestion and can be detected in the human plasma. These miRNAs can also be detected in the plasma of animals after consuming plant materials containing miRNAs. Similarly, Pastrello et al.[112] found that the level of circulating Brassica miRNA is consistent with Brassica plant intake.

However, several questions remain about RNA survival during the process of cooking and passing through the digestive tract. Furthermore, how these miRNAs are released from the gut epithelium to circulation also remains unclear. Since miRNAs can be derived from the diet, small RNAs from the foreign environment could alter gene expression in the human body and affect the development of diseases. Zhang et al.[113] observed that the ingestion of plant miRNAs might play a pivotal role in humans in a cross-kingdom way at the genetic level. Similarly, Pirro et al.[114] found that the miRNAs in Moringa have a potential ability to regulate gene expression in humans in a cross-species manner. Furthermore, Chin et al.[115] reported that oral intake of plant miR-159 from dietary consumption could suppress the development of breast cancer in mice.

Conversely, some researchers argue against the origin of the circulating small RNAs from foreign intake. Mico et al.[116] argued that plant miRNAs could not be detected in circulating plasma after the ingestion of beer and extra virgin olive oil. Similarly, Bagci et al.[117] pointed out that many food-born miRNAs are not from actual food sources, and doubt that plant miRNAs could regulate human gene expression.

1.4 The potential roles of small RNAs in cancer

1.4.1 Tumorigenesis

miRNA expression has been related to tumorigenesis in several types of carcinoma. Fu et al.[118] found that miR-592 plays an oncogenic role in colorectal cancer by targeting forkhead Box O3A. Furthermore, other studies indicated that miR-199b[119], miR-544a[120], and miR-103 are correlated with invasion and migration in colorectal cancer. Wu et al.[121] observed that miR-4835p promotes the growth of gastric cancer, and miR-19[122], miR-135a[68], miR-1, miR-133, miR-206[123], miR-558a[124], and miR-181b[125] were all associated with the development and metastasis of gastric cancer. miR-155-3p[126] and miR-548a-5p[127] are related to hepatic cancer while miR-183, miR-33a[128], miR-454[129], miR-182[130], and miR-429[131] promote the growth of lung cancer. Among other cancers, miR-211 is related with oral cancer[132], miR-200c promotes the migration and invasion of

bladder cancer[133], miR-663 expression is correlated with poor prognosis in patients with nasopharyngeal cancer, miR-194[134] and miR-203[135] promote ovarian cancer cell growth and metastasis by targeting protein tyrosine phosphatases, and miR-20b[136] promotes the growth invasion of esophageal cancer. Moreover, miRNAs can affect tumorigenesis according to their differential expression: miRNAs with increased expression in tumor cells are referred to as oncogenes, while those whose expression levels are decreased can be considered tumor suppressors.

Apart from miRNAs, piRNAs also play pivotal roles in the regulation of tumorigenesis. Cheng et al.[137] demonstrated increased piR-651 expression in colon, gastric, lung, and breast cancers, compared to that in the normal adjacent tissues, indicating that piRNAs are associated with tumorigenesis. Moreover, Yan et al.[138] showed that piRNA-823 contributes to tumorigenesis in multiple myeloma by regulating DNA methylation, providing an ideal candidate for piRNA-targeted therapies for multiple myeloma treatment. Cui et al.[49] showed that piR-615 and piR-823 levels are reduced in the circulation of patients with gastric cancer and that piR-823 levels are related with lymphatic and distant metastasis.

snoRNAs can also regulate tumorigenesis, and some snoRNAs are called oncogenic snoRNAs[139]. The snoRNAs, SNORD50A and SNORD50B, regulate K-Ras by GTPase-binding, which induces tumorigenesis[140]. Liao et al.[141] reported that the expression of SNORD33, SNORD66, and SNORD76 are elevated in the plasma of patients with non-small-cell lung cancer (NSCLC). Similarly, Mei et al.[142] indicated that snoRNA 42 acts as an oncogene in NSCLC, and this snoRNA was also identified as a new oncogene and prognostic biomarker in colorectal cancer[143]. Ma et al.[144] indicated that SNORD78 is related to the survival of hepatocellular carcinoma, and knocking down SNORD78 inhibits the growth, migration, and metastasis of SK-Hep-1 cells by causing cell cycle arrest and apoptosis. Another study showed that snoRNA U50 plays an important role in the evolution of breast cancer[145]. snRNAs have also been identified to modulate cancer gene expression, such as U1 snRNA[146]. Circulating snRNA U2 has been identified as a biomarker for diagnosis and prognosis in lung cancer[147]. These findings indicate that

snRNAs and snoRNAs are important players in cancer biology and their activation could play pivotal roles in tumorigenesis and could be potential biomarkers in cancer.

1.4.2 Tumor Suppressors

Recent research has focused on the tumor suppressor role of miRNAs. Kano et al.[148] observed that miR-145, miR-133a, and miR-133b could be tumor-suppressive in ESCC. miRNAs may play the role of suppressors in several ways. miR-133[149] can impede lung cancer cells by directly targeting FOXQ1; miR-503[150] restrains prostate cancer by inhibiting ZNF217 expression; miR-7 inhibits the growth and infiltration of thyroid carcinoma cells by targeting CKS2[151]; miR-98 plays the role of suppressor in hepatic cancer by targeting SALL4[152]; miR-143 inhibits breast cancer by targeting CD44[153]; miR-377 suppresses pancreatic cancer by targeting Pim-3[154]. Other mechanisms are also involved in the role of miRNAs as cancer suppressor, such as miR-106a inhibits bladder cancer cells by MAPK signaling[155]; miR-561 suppresses gastric cancer cell growth and invasion by regulating c-Myc[156]. Moreover, miRNAs can inhibit cancer growth by promoting apoptosis, such as miR-155 suppresses ovarian cancer cells by promoting their apoptosis[157]; miR-9501 inhibits lung cancer by activating apoptosis[158]; and miR-5582-5p can suppress cancer cells by inducing apoptosis[159].

Moreover, studies have reported that reduced piR-823 expression suppresses gastric cancer [137, 160]. Hashim et al.[161] found an active piRNA pathway in breast cancer. Peng et al.[162] showed that piR-55490 is a suppressor in the development of lung cancer, and that piR-55490 could induce mTOR mRNA degradation similar to miRNAs. Another study[137] showed that piR-615 can inhibit the development of gastric cancer cells and induce apoptosis in these cells at the G2/M phase.

Previous research has established that some snoRNAs can inhibit cancer cell growth. Dong et al.[163] found that snoRNA U50 is a candidate as a cancer-suppressor gene in patients with prostate carcinoma. Chen et al.[164] reported that SNORD76 is a cancer suppressor in glioblastoma by leading to cell cycle arrest at the S phase and stirring the Rb-associated cell cycle regulation. Su et al.[165] observed a key role of fibrillarin in Myc-induced elevated snoRNA biogenesis in cancer, and that inhibiting

snoRNA biogenesis in cancer cells activated p53 and inhibited tumorigenicity. Langhendries et al.[166] showed that the depletion of snoRNA (U3 and U8) induces p53 stabilization and expression. p53 is a tumor suppression gene and this finding might provide a way to control cancers by silencing a single snoRNA. snRNAs have also been identified as a suppressor in cancer, such as the U1 snRNA inhibits polyadenylation affording a new opportunity for cancer therapy[167].

1.4.3 Regulating chemoradiotherapy response

The exact mechanisms underlying chemoradiotherapy resistance are unclear, but it is believed that miRNAs play pivotal roles in regulating such resistance. Several miRNAs are altered after chemoradiotherapy in patients and in cells, indicating a close relationship between chemoradiotherapy resistance and miRNAs.

In general, there are two types of miRNAs according to their role in treatment response. The first are desensitizer miRNAs, for example, miR-221-3p increases the chemoresistance to 5-FU by targeting RB1 in pancreatic cancer [168]; miR-20a increases cisplatin resistance in gastric cancer by targeting cylindromatosis (CYLD)[169]; and miR-96 increases cisplatin resistance in non-small cell lung cancer cells by targeting gene of sterile α motif domain-containing (SAMD9) [170]. The second type represents miRNAs that enhance sensitivity, for example, Zhou et al.[171] reported that the upregulation of miR-375 could increase the sensitivity of gastric cancer cells to cisplatin by targeting gene erb-b2 receptor tyrosine kinase 2(ERBB2), and miR-30a[172] plays a similar role by suppressing the EMT (epithelia-to-mesenchymal transition); miR-770-5p[173] could suppress cisplatin resistance by targeting excision repair cross-complementation group 2 (ERCC2) in ovarian cancer; and miR-621 could increase the sensitivity to chemotherapy in breast cancer by promoting p53 activity[174].

miRNAs could also affect radiotherapy resistance, for example, miR-208a[175] expression is increased after radiation in human lung cancer cells, inducing radio-resistance. While increased miR-328-3p[176] and miR-95[177] expression sensitize non-small cell lung cancer cells to radiotherapy, miR-216b[178] increases the sensitivity to radiotherapy in pancreatic cancer.

Only a few studies have reported the roles of piRNA, snoRNAs, and snRNA in modulating chemoradiotherapy response. Chu et al.[179] indicated that ACA11, an snoRNA, could inhibit oxidative stress, thus conferring resistance to chemotherapy and promoted the growth of multiple myeloma cells. A piRNA-like small RNA, piR-L-138 was observed to induce cisplatin resistance by inhibiting apoptosis in lung squamous cell cancer[180]. The snRNA-U2-1f is abundant in circulation and persists positively after chemotherapy, indicating that it might play an important role in chemotherapy response[181].

1.5 Small RNAs in EC

1.5.1 The diagnostic value of circulating small RNAs in EC

EC incidence has increased markedly worldwide in recent decades, especially the incidence of EAC in western countries. Even with significant clinical advancements, the prognosis for EC has not improved much. The primary reason is the unavailability of useful and specific markers for the early diagnosis of EC in patients who have no symptoms. Moreover, there are no high-quality biomarkers for screening EAC from Barrett's esophagus (BE). Most of the patients with EC are diagnosed late. BE is an established precursor lesion for EAC, and the incidence of EAC in patients with BE is ~30-fold higher than patients without BE[182]. Moreover, BE is not diagnosed in more than 90% of new EAC patients, therefore, it is especially important to monitor patients with BE because the early diagnosis of EAC from BE changes the survival time significantly. Our clinical experience reveals that the resection of early EC (T1–2) contributes to an increased survival time, while the prognosis is very poor for advanced stages (T3–4) even after surgical intervention.

Small RNAs are 21–25 bp in size, and are specific and important in circulation to detect early-stage cancers and can serve as biomarkers for the diagnosis of EC. Zhang et al.[183] reported on the use of circulating small RNAs as biomarkers for the first time in 2010, and observed that miR-10a, miR-22, miR-100, miR-148b, miR-223, miR-133a, and miR-127-3p have diagnostic value for ESCC by analyzing

290 ESCC patients and 140 controls. Since then, an increasing number of miRNAs have been identified as biomarkers in EC (Table 1-1).

There are some inconsistent reports concerning the use of small RNAs as biomarkers for diagnosis in patients with EC. For example, Kang et al.[184] and Chen et al.[185] indicated that decreased miR-129 expression could be found in cancer tissues, while others[186] argued that its levels increased, rather than decreased. The reasons for this could be due to other factors in the body, which could affect the expression of the small RNAs in circulating blood. Another reason could be data analysis, which would result in the different observations, such as the housekeeping gene chosen for data normalizing[187].

Table 1-1. The diagnostic value of circulating small RNAs in EC *(PubMed, search terms: small RNAs/miRNA/piRNA/piRNA/snoRNA/snRNA and diagnosis /diagnostic and esophageal cancer, 2000–2021, Up means increased expression while Down means decreased expression compared to non-cancer tissue)*

Tumor	*Samples*	*Small RNAs*	*Methods*	*Up/down*	*Association*	*Ref*
EAC	*Serum*	*miR-25-3p, miR-151a-3p, miR-375, miR-100-5p*	*Sequencing +qRT-PCR*	*Up, up, down, down*	*Early diagnosis*	*[188]*
EAC	*Plasma*	*miR-382-5p, miR-133a-3p*	*qRT-PCR*	*Up, down*	*Screening of BE and EAC*	*[189]*
EAC	*Exosome from serum*	*RNU6-1/miR-16-5p, miR-25-3p/miR-320a, let-7e-5p/miR-15b-5p, miR-30a-5p/miR-324-5p, miR-17-5p/miR-194-5p*	*qRT-PCR*	*Up, up, up, down, down*	*Screening of BE and EAC*	*[190]*
ESCC	*Serum*	*miR-10a, miR-22, miR-100, miR-148b, miR-223, miR-133a, miR-127-3p*	*Solexa sequencing +qRT-PCR*	*Up (all)*	*The early diagnosis of ESCC*	*[183]*
ESCC	*Serum*	*miR-31*	*qRT-PCR*	*Up*	*Diagnostic biomarker for ESCC*	*[191]*
ESCC	*Plasma/seru*	*miR-18a*	*qRT-PCR*	*Up*	*Biomarker for detection and*	*[192]*

	m				*monitoring of tumor dynamics*	
ESCC	*Serum*	*miR-25, miR-100, miR-193-3p, miR-194, miR-223, miR-337-5p and miR-483-5p*	*TaqMan Low Density Array+qRT-PCR*	*Up*	*Diagnostic biomarker for ESCC*	*[193]*
ESCC	*Plasma*	*miR-25*	*Microarray +qRT-PCR*	*Up*	*Biomarker for detection and monitoring of tumor dynamics*	*[194]*
ESCC	*Serum*	*miR-146a*	*qRT-PCR*	*Down*	*Diagnostic biomarker for ESCC*	*[195]*
ESCC	*Plasma*	*miRNA-718*	*qRT-PCR*	*Down*	*Diagnostic biomarker for ESCC*	*[196]*
ESCC	*Serum*	*miR-10b, miR-29c, miR-205*	*qRT-PCR*	*Up, down, down*	*Diagnostic biomarker for ESCC*	*[197]*
ESCC	*Serum*	*miR-375*	*qRT-PCR*	*Down*	*Diagnostic biomarker for ESCC*	*[198, 199]*
ESCC	*Plasma*	*miR-16, miR-185, miR-375*	*qRT-PCR*	*All up*	*Diagnostic biomarker for ESCC*	*[200]*
EC (No type indicated)	*Serum*	*miR-218*	*qRT-PCR*	*Down*	*Early detection and clinical evaluation*	*[201]*
ESCC	*Serum*	*miR-129, miR-365*	*microarray +qRT-PCR*	*All up*	*miRNA-365 for the early prediction of miR-129 for prediction of clinical stage*	*[202]*

ESCC	*Serum*	*miR-1322*	*qRT-PCR*	*Up*	*Diagnostic biomarker for ESCC*	*[203]*
ESCC	*Serum*	*miR-107*	*qRT-PCR*	*Down*	*Diagnostic biomarker for ESCC*	*[204]*
ESCC	*Plasma*	*miR-506*	*qRT-PCR*	*Up*	*Diagnostic biomarker for ESCC*	*[205]*
ESCC	*Serum*	*miR-1246*	*Microarray +qRT-PCR*	*Up*	*Diagnostic biomarker for ESCC*	*[206]*
ESCC	*Serum*	*miR-7*	*qRT-PCR*	*Down*	*Diagnostic biomarker for ESCC*	*[207]*
EAC	*Plasma*	*miR-155*	*qRT-PCR*	*Up*	*Diagnostic biomarker for ESCC*	*[208]*
ESCC/EC	*Serum*	*miR-21*	*qRT-PCR*	*Up*	*Diagnostic biomarker for EC*	*[198, 199] [200, 209-211]*
EAC	*Exosome from serum*	*miR-223-5p*	*qRT-PCR*	*Up*	*Diagnostic biomarker for T2 and T3 category*	*[212]*
ESCC	*Plasma*	*miR-216a/b*	*qRT-PCR*	*Down*	*Diagnostic biomarker for ESCC*	*[213]*
ESCC	*Serum*	*miR-613*	*qRT-PCR*	*Down*	*Diagnostic biomarker for ESCC*	*[214]*
ESCC	*Plasma*	*miR-373*	*qRT-PCR*	*Up*	*Diagnostic biomarker for ESCC*	*[215]*
EC	*Serum*	*miR-144*	*qRT-PCR*	*Up*	*Diagnostic biomarker*	*[216]*

ESCC	*Serum*	*miR-1297*	*qRT-PCR*	*Down*	*Diagnostic biomarker for ESCC*	*[217]*
ESCC	*plasma*	*miR-9*	*qRT-PCR*	*Up*	*Diagnostic biomarker for ESCC*	*[218]*
Gastroesophageal adenocarcinoma	*Plasma*	*miR-223*	*qRT-PCR*	*Up*	*Diagnostic biomarker for gastroesophageal adenocarcinoma*	*[219]*
ESCC	*Exosome from serum*	*miR-296-5p*	*qRT-PCR*	*Up*	*Diagnostic biomarker for ESCC*	*[220]*
ESCC	*Serum*	*miR-296-5p, miR-20b-5p, miR-28-3p, miR-192-5p, miR-223-3p*	*qRT-PCR*	*Up*	*Diagnostic biomarker for ESCC*	*[220]*
ESCC	*Serum*	*miR-377*	*qRT-PCR*	*Down*	*Diagnostic biomarker for ESCC*	*[221]*
ESCC	*Serum*	*miR-15a*	*qRT-PCR*	*Down*	*Biomarker for ESCC*	*[222]*
ESCC	*Plasma*	*miR-106a, miR-18a, miR-20b, miR-486-5p, miR-584, miR-223-3p*	*qRT-PCR*	*Up, up, up, up, up, down*	*Biomarker for ESCC*	*[223]*
ESCC	*Exosome from Plasma*	*miR-584, miR-223-3p*	*qRT-PCR*	*Up, down*	*Biomarker for ESCC*	*[223]*

1.5.2 The prognostic value of circulating small RNAs in EC

Apart from their use as biomarkers in diagnosis, circulating small RNAs may also play pivotal roles in predicting the prognosis of patients with EC, for example, miR-31, miR-25, and miR-100, as shown in Table 1-2. Several miRNAs are related to the clinical stage and metastasis, consequently affecting the survival time. For instance,

Sun et al.[224] indicated that miR-367 is associated with the clinical stage and tumor metastasis, which is a prognostic factor and is associated with the overall survival of ESCC patients.

Multiple potential mechanisms could explain the association between small RNAs and their prognostic value. Liu et al.[225] indicated that decreased miR-1294 expression is associated with poor prognosis of ESCC because of the downregulation of c-Myc. Song et al.[226] indicated that miR-9 is related with clinical progression, lymph node metastasis, and the survival time in patients with ESCC by inducing the EMT. Moreover, Li et al.[227] reported that decreased miR-140 expression contributes to the suppression of EMT and promotes the invasion ability by targeting slug in patients with EC. Some miRNAs can predict prognosis in combination with mRNA, for example Sun et al.[228] found that combined miR-195 and Cdc42 mRNA expression can act as biomarkers for prognosis in patients with ESCC.

Apart from the EAC and ESCC, there is another kind of EC, called small cell carcinoma of esophagus (SCCE). This type of EC is not common but is very aggressive with poor prognosis. A study reported that some miRNAs could predict the outcomes for SCCE; for e.g., decreased miR-625 expression[229] is significantly associated with survival time and may thus, represent a new biomarker of prognosis in patients with SCCE.

Table 1-2. The prognostic value of circulating small RNAs in EC (PubMed, search terms: small RNAs/miRNA/piRNA/piRNA/snoRNA/snRNA and prognosis /prognostic and esophageal cancer, 2000–2021, Up means increased expression while Down means decreased expression compared to non-cancer tissue)

Tumor	*Samples*	*Small RNAs*	*Methods*	*Up/down*	*Association*	*Ref*
ESCC	*Serum*	*miR-31*	*qRT-PCR*	*Up*	*Poor prognosis in survival*	*[191]*
ESCC	*Serum*	*miR-25, miR-100*	*qRT-PCR*	*Up*	*Predict poor survival in ESCC*	*[193]*
ESCC	*Serum*	*miR-146a*	*qRT-PCR*	*Down*	*Predict worse overall survival and progression-free*	*[195]*

					survival	
ESCC	*Serum*	*miR-21, miR-375*	*qRT-PCR*	*Up, down*	*Independent factors affecting prognosis*	*[198, 199, 230]*
ESCC	*Plasma*	*miR-16, miR-21*	*qRT-PCR*	*Up, up*	*Shortened progression-free survival and overall survival*	*[200, 231]*
ESCC	*Plasma*	*miR-506*	*qRT-PCR*	*Up*	*High expression had shorter survival time*	*[205]*
ESCC	*Serum*	*miR-367*	*qRT-PCR*	*Up*	*Associated with overall survival and independent prognostic factor*	*[224]*
Advanced adenocarcinomas of the gastroesophageal junction	*Serum*	*miR-302c, miR-222*	*Microarray +qRT-PCR*	*Up, down*	*Associated with better overall survival*	*[232]*
ESCC	*Serum*	*miR-1246*	*Microarray +qRT-PCR*	*Up*	*Independent risk factor for poor survival*	*[206]*
ESCC	*Serum*	*miR-613*	*qRT-PCR*	*Down*	*Worse overall survival and progression-free survival*	*[214]*
ESCC	*plasma*	*miR-9*	*qRT-PCR*	*Up*	*Poor survival and independent prognostic factor for ESCC*	*[218]*
ESCC	*Serum*	*miR-377*	*qRT-PCR*	*Down*	*Poor survival*	*[221]*
ESCC	*Serum*	*miR-15a*	*qRT-PCR*	*Down*	*Advanced tumor-node-metastasis and stages, short overall survival*	*[222]*
ESCC	*Serum*	*miR-200c*	*qRT-PCR*	*Up*	*Shortened progression-free survival*	*[233, 234]*

1.5.3 The predictive values of circulating small RNAs for chemoradiotherapy in EC

It is reported that neoadjuvant radiochemotherapy or chemotherapy could improve the overall survival of patients with EC by about 10% in five-year survival rate[235, 236]. However, a number of researchers pointed out that the patients with increased survival also show a good histopathological response[237, 238]. Therefore, it is important to assess chemoradiation response in order to treat patients individually and adjust the treatment approach guided by their response.

Several studies have reported on miRNAs as biomarkers for chemotherapy, as shown in Table 1-3. For example, Tanake et al.[239]found that miR-27 is related to chemoresistance in EC. These small RNAs can also predict the treatment response to neoadjuvant chemotherapy in EC. For instance, circulating miR-21 can act as a biomarker for chemoresistance to cisplatin plus 5-FU in ESCC[240]. Small RNAs can also predict treatment response to radiotherapy. Such as Lv et al.[198] indicated that increased miR-21 expression could indicate increased resistance to radiotherapy (Table 1-3).

Table 1-3. The predictive values of circulating small RNAs for chemoradiotherapy in EC *(PubMed, search terms: small RNAs/miRNA/piRNA/piRNA/snoRNA/snRNA and chemotherapy/radiotherapy/chemoradiotherapy and esophageal cancer, 2000–2021)*

Tumor	*Samples*	*Small RNAs*	*Methods*	*Up/down*	*Association*	*Ref*
ESCC	*Serum*	*miR-21*	*qRT-PCR*	*Up*	*Reduced the sensitivity of radiotherapy*	*[198]*
ESCC	*Serum*	*miR-27a/b*	*miRNA array+qRT-PCR*	*Up*	*Poor response to chemotherapy (cisplatin+5-fluorouracil+docetaxel , cisplatin+5-fluorouracil+adriamycin)*	*[239]*

ESCC	*Serum*	*miR-7*	*qRT-PCR*	*Down*	*Poor chemoradiotherapy response (no regimen details)*	*[207]*
ESCC	*Serum*	*miR-200c*	*qRT-PCR*	*Up*	*Poor response to chemotherapy (cisplatin+5-fluorouracil +Adriamycin, cisplatin+5-fluorouracil+docetaxel)*	*[233]*
ESCC	*Serum*	*miR-377*	*qRT-PCR*	*Down*	*Predict the poor response to chemoradiation with 5-fluorouracil and cisplatin*	*[221]*
ESCC	*Serum*	*miR-21*	*qRT-PCR*	*Up*	*Poor response to docetaxel/cisplatin/5-fluorouracil*	*[211]*
ESCC	*Serum*	*miR-200c*	*qRT-PCR*	*Up*	*Higher response to platinum-containing chemotherapy was associated with low miR-200c expression*	*[234]*
ESCC	*Plasma*	*miR-16*	*qRT-PCR*	*Up*	*More sensitive to radiotherapy*	*[231]*
ESCC	*Serum*	*miR-21*	*qRT-PCR*	*Up*	*Biomarker for chemoresistance(cisplatin/5-fluorouracil)*	*[240]*

1.6 The mechanisms whereby small RNAs regulate the responses to chemoradiotherapy

There are several mechanisms underlying the regulation of chemoradiotherapy response by miRNAs, such as multidrug resistance (MDR) transporters, cell cycle, autophagy, drug targets, DNA repair, EMT, and cancer stem cells. piRNAs are

involved in cancer regulation by affecting gene expression patterns via a mechanism similar to that for miRNAs[241] or by regulating chemoradiotherapy response with the assistance of PIWI proteins. For example, piRNA-54265 binds to the PIWIL2 protein and activates the STAT3 signaling pathway, making the colorectal cancer cells more resistant to Oxaliplatin or 5-FU[242]. However, no study has reported on the mechanisms whereby piRNAs, snoRNAs, and snRNAs regulate chemoradiotherapy response in EC. Here, we only discuss the mechanisms related to this study and miRNAs.

1.6.1 Hypoxia

Hypoxia refers to a low level of oxygen. Tumor hypoxia happens due to uncontrolled cell proliferation, altered metabolism, and abnormal tumor blood vessels, which reduce the transport of oxygen and nutrients[243]. Hypoxia is a common characteristic of the cancer microenvironment. Hypoxia affects the chemoradiotherapy response in several ways, such as the delivery of drugs and their cellular uptake are affected by hypoxia because of the acidity. Besides, some chemotherapeutic drugs require oxygen to generate free radicals and induce cytotoxicity. Hypoxia also affects adaptation by post-translational or transcriptional modifications that facilitate cell proliferation and chemoresistance[244]. The hypoxia-inducible factor-1 (HIF-1) is an established contributor to the development of drug resistance in several cancers. HIF-1 is induced by hypoxia and binds to various target genes and regulates their response to hypoxia. Recent findings show that the mechanisms underlying hypoxia-induced chemoresistance are not only dependent on HIF-1, but also involve a number of genetic and biochemical responses that modulate one another[245].

miRNAs have been identified to be involved in hypoxia, thus affecting chemoradiotherapy response. For example, miR-21 was identified by Jiang et al.[246] to regulate radiation response by modulating HIF-1α in non-small cell lung cancer cells. Moreover, miR-24 induces chemo-resistance and hypoxic advantage in breast cancer[247].

1.6.2 AMP-activated protein kinase (AMPK) signaling pathway

Several signaling pathways are involved in chemoradiotherapy response. For example, the AMP-activated protein kinase (AMPK) signaling pathway, which is an energy sensor that modulates cell metabolism. The AMPK pathway is activated upon sensing a lack of energy in the body, resulting in the uptake of glucose and lipid oxidation to generate more energy. Thus, AMPK plays an important role in whole-body energy balance[248].

Several miRNAs regulate the chemoradiotherapy response by targeting the AMPK signaling pathway. For instance, miR-301a regulates the chemoresistance of doxorubicin in osteosarcoma cells by targeting AMPK[249]. LKB1 promotes radioresistance in EC cells by targeting the AMPK signaling pathway[250], while miR-451a could regulate the LKB1/AMPK signaling by targeting CAB39[251, 252]. Therefore, miR-451a might regulate the chemoradiotherapy response via AMPK. miR-25-5p was also reported to activate the AMPK signaling pathway and suppress the proliferation of colorectal cancer cells[253].

1.6.3 Hippo signaling pathway

The Hippo pathway plays important roles in the physiology and pathology of mammals, such as control of organ size, renewal of stem cells, and regulation of cancer[254-256]. There are four main components in the mammalian Hippo pathway: MST1/2, LATS1/2, YAP, and its paralog TAZ. Currently, the core components of the Hippo pathway have been found to regulate chemotherapy response in several types of cancer cells[257]. For example, decreased MST levels causes the resistance of prostate cancer cells to cisplatin, while increasing the level of MST sensitizes these cells to cisplatin[258]. Decreased LATS2 levels can upregulate the transcription of estrogen receptor alpha (ERα), which contributes to tamoxifen resistance[259]. Increased YAP and Taxol induce cisplatin resistance in ovarian cancer cells[260], and 5-FU resistance in colon cancer cells[261, 262]. TAZ increases the level of the multi-drug resistance protein (MRP) and results in resistance to paclitaxel and doxorubicin[263]. The core components of the Hippo pathway are also involved in the regulation of radiotherapy. For instance, the

sensitivity to radiation is increased upon YAP knockdown by siRNA in endometrial cancer[264].

Many miRNAs regulate the chemoradiotherapy response by targeting the Hippo pathway components. For instance, miR-455-3p increases the resistance to gemcitabine by targeting TAZ in pancreatic cancer[265]. miR-874-3p regulates the chemotherapy response to 5-FU in colorectal cancer by targeting YAP and TAZ, inducing the inactivation of the Hippo signaling pathway[266]. Some other miRNAs, such as miR-135b target tumor suppressor kinase 2 (LATS2) directly to regulate the chemotherapy response in colorectal cancer via the Hippo signaling pathway[267].

1.6.4 PI3K/Akt/mTOR signaling pathway

The PI3K/Akt/mTOR signaling pathway is an important pathway in regulating the cell cycle. Several small RNAs are involved in this pathway by targeting PTEN, which inhibits the PI3K/Akt/mTOR signaling pathway through its lipid phosphatase activity. miR-130b targets PTEN to modulate multidrug resistance by the PI3K/Akt signaling pathway in breast cancer[268]. miR-497 regulates the cisplatin sensitivity in osteosarcoma cell lines via PI3K/Akt. miR-21 is unregulated in cisplatin-resistant gastric cancer cell lines, and increases cisplatin resistance by downregulating PTEN and activating PIA3K/Akt[269]. Besides, the exosomal transfer of tumor-associated macrophage-derived miR-21 also induces drug resistance to cisplatin by this mechanism[270].

1.6.5 Epidermal growth factor receptor (EGFR)

The epidermal growth factor receptor (EGFR) family contains four members, EGFR/ErbB1, ErbB2, ErbB3, and ErbB4. EGFR is a cell surface receptor and plays a pivotal role in cell proliferation, survival, and invasion. Therefore, it is one of the most important mechanisms for the miRNA-mediated regulation of chemoradiotherapy response.

The EGFR pathways are involved in crosstalk with miRNAs during chemoradiotherapy, thus affecting each other. For example, inhibition of miR-21 decreases EGFR expression in glioblastoma, while EGFR positively regulates the expression of miR-21[271]. Some miRNAs have been identified to regulate

chemoresistance via EGFR related signaling pathway, such as miR-34c-5p targets amphiregulin (AREG) directly, while AREG induces stemness and chemoresistance via the EGFR signaling pathway in ovarian cancer[272]. Besides, a few miRNAs have been identified to target EGFR directly, such as miR-27a[273], miR-200a[274], miR-133a[275], and miR-27b[276]. These studies indicate that miRNAs might regulate the chemoradiotherapy response via EGFR.

1.6.6 Estrogen Receptor (ER)

ER is one of the oldest molecules of targeted therapy, and there is a close relationship between ER and chemoradiotherapy response. Studies have found that ER could influence the chemotherapy response of cancer cells to many chemotherapeutic agents, such as cisplatin. Matsumura et al.[277] found that estrogen (E2) and cisplatin could trigger the activation of Erα, which could induce cisplatin resistance in ovarian cancer cells by promoting the activation of apoptosis. Besides, miR-873 was reported to modulate the chemotherapy response to tamoxifen via ERα [278].

Similarly, ERβ could also influence the chemotherapy response. For example, Luo et al.[279] reported that an ERβ agonist increases the cytotoxic effect of cisplatin and results in the resistance of the upper urinary tract urothelial carcinoma cells to cisplatin. In malignant mesotheliomas cell, ERβ agonist further sensitizes the cisplatin cytotoxicity[280]. Furthermore, Wilk et al. found that inhibition of ERβ regulates cisplatin cytotoxicity in medulloblastoma cell lines by promoting Rad51-mediated DNA repair[281].

Several miRNAs have been found to regulate ERα, ERβ, and ER coregulators, including miR-18a, miR-193b, miR-302c, miR-22[282], miR-206[283], miR-222-3p[284], miR-373[285], miR-4728-3p[286], miR-615-3p[287], and miR-92a-3p[288]. These miRNAs were also found to regulate the drug or radiation response. For example, miR-4728-3p has a crucial effect in the regulation of breast cancer by modulating estrogen receptor 1 (ESR1) by a non-canonical internal seed interaction[289]. Furthermore, Wang et al.[290] used microarray profiling and reported that miR-4728-3p was downregulated in the 5-FU-resistant gastric cancer

cell line and might serve as a biomarker for multidrug resistance. miR-615-3p has also been pointed out as a potential biomarker in chemotherapy response. For examples, miR-615-3p was reported to regulate Bortezomib resistance in patients with multiple myeloma[291]. In lung cancer, exosomal H19 facilitated Erlotinib resistance by the miR-615-3p/ATG7 axis, and this might be a potential target for the diagnosis and treatment of lung cancer[292]. Mukai et al.[293] used miRNA microarray analysis to indicate that miR-615-3p was related to the malignant proliferation of hepatocellular carcinoma cells, and induced chemoresistance, indicating that miR-615-3p could be a potential biomarker of chemotherapy response. miR-92a-3p was also a popular miRNA as a biomarker in chemoradiotherapy response, and was identified in several cancers. For example, miR-92a-3p was regarded as a biomarker of treatment response in hepatocellular carcinoma by targeting Smad7[294]. Besides, serum miR-92a-3p was identified as a biomarker of chemotherapy response in metastatic colorectal cancer[295]. Furthermore, miR-92a-3p was shown to regulate the cellular growth, development, and chemotherapy response to cisplatin in an NSCC cell line by targeting PTEN [296].

Thus, several small RNAs have been found to regulate Erα, Erβ, and ER coregulators, taking part in the regulation of drug treatment. Therefore, small RNAs could regulate chemoradiotherapy response via ER.

1.6.7 p53

p53 plays an important role in tumor repression through the transcriptional regulation of many genes. P53 responds to various stress signals including DNA damage and hypoxia. Most drugs and radiation act as anti-cancer agents through DNA damage, thus p53 can be easily activated during chemoradiotherapy.

Several miRNAs have been identified to modulate p53 directly, such as miR-125b and miR-504[297]. These miRNAs bind to the 3'-UTR of the p53 mRNA, thus decreasing the levels and function of p53. Some miRNAs work together with p53 and other genes as the signaling axis to regulate chemoradiotherapy response, for example, the p53-miR520-p21 signaling axis plays an important role in regulating chemotherapy response in colorectal cancer[298]. Moreover, the p53-miR200-

moesin axis modulates metastasis and drug resistance in breast cancer[299]. A recent study provided evidence that mutant p53 regulates chemoradiotherapy sensitivity in EAC cells by working together with miRNAs and the cystine/glutamate antiporter SLC7A11[300].

1.6.8 Warburg effect

Warburg effect is a feature of cancer in which aerobic glycolysis is enhanced in many types of cancers. The differential metabolism of cancer cells creates an environment that makes them more drug-resistant. The mechanisms involved in this process are complicated, including glucose transport, glycolytic enzymes, glycolysis and hypoglycemia, stress response elements, and energy sensors[301].

Many signaling pathways contribute to the Warburg Effect. For example, growth factor stimulation triggers signaling through RTKs to activate PI3K/Akt and Ras. Akt increases glucose transporter activity and promotes glycolysis. The p53 oncogene facilitates TP-53-induced glycolysis and apoptosis. AMPK is a central energy sensor that modulates cell metabolism and play a pivotal role in the Warburg effect. The Hippo signaling pathway regulates metabolism adaptation in cancer development[302]. These signaling pathways might work together and regulate mechanisms of chemoradiotherapy.

1.7 Aims:

The above literature review provides an overview of EC, and shows that identifying biomarkers for the early diagnosis, prognosis, and chemoradiotherapy response is necessary and valuable to guide the treatment of patients with EC. The review described the current biomarkers for EC and illustrated that identifying small RNAs as biomarkers in circulating blood is practical and promising. Moreover, the review illustrated the origin and potential roles of circulating small RNAs in cancers. However, currently there are no small RNAs that could be used as biomarkers of response to chemotherapy reported in patients with EAC, especially piRNA, snoRNA, and snRNAs. Therefore, the first aim of this study is **to investigate the expression of small RNAs in pre-treatment tumor tissues of locally advanced**

patients with EAC (Chapter 3). The top small RNAs in the pre-treatment tumor tissues of locally advanced patients with EAC were identified.

Several mechanisms could underlie small RNA-mediated regulation of chemoradiotherapy response. However, the mechanism underlying the regulation of chemoradiotherapy responses by small RNAs in EAC is not known. Therefore, Chapter 4 describes the **investigation of the function of miR-451a (biomarker selected from chapter 3) in regulating chemoradiotherapy response in EAC**.

The circulating small RNAs in exosomes could also be potential biomarkers of response to chemotherapy. Chapter 5 **identifies potential small RNA biomarkers of response to chemoradiotherapy treatment in pre-treatment blood from locally advanced patients with EAC.** The circulating small RNAs in exosomes as biomarkers of response to chemoradiotherapy were further explored using RNA sequencing analysis. The exosomal small RNAs selected as candidate biomarkers of response to chemoradiotherapy were tested in the cohort of EAC patients.

The small RNAs from serum exosomes might play an important role in regulating chemoradiotherapy response. Blood exosomes include several small RNAs, and these exosomes could modulate the local tumor environment so as to influence tumor response to chemoradiotherapy. Therefore, the aim of Chapter 6 was **to investigate the role of blood small RNAs in regulating chemoradiotherapy response in EAC cells.**

Thus, the aim of this study was to investigate whether the small RNAs in tissue and blood could be suitable biomarkers for chemoradiotherapy response and whether they could regulate chemoradiotherapy response.

CHAPTER 2
MATERIALS AND METHODS

2.1. Materials

General reagents: All chemicals, cell culture media, and supplements were of analytical grade and were used without further purification and were purchased from several companies.

The esophageal adenocarcinoma cell lines OE19, OE33, JHEsoAD1, ESO51, ESO26, SKGT4, OACP4C (gastro-esophageal junction), and FLO1 were purchased from Sigma (Castle Hill NSW 1765) and cultured in RPMI +10% FBS medium.

2.1.1. Buffers and solutions

Drugs: 5-Fluorouracil (5-FU): Sigma-Aldrich, United States (containing 1.05 mM Sodium Hydroxide).

Cisplatin: Sigma-Aldrich, United States (containing 4.62 mM Sodium Chloride and 0.16 mM Mannitol).

Carboplatin: DBL Carboplatin Injection (Hospira Australia Pty Ltd.), 100 mL, 0.1 g in stock (containing Sodium Chloride 900 mg, Mannitol 100 mg, water for injection to 100 mL).

Paclitaxel: ANZATAX injection concentrate (Hospira Australia Pty Ltd.), 50 mL, 0.3 g in stock (containing PEG 35 Castor Oil NF: 26.35 g. Citric Acid (anhydrous): 100 mg, Ethanol to 50 mL).

The vehicles for the drugs: 5-FU vehicle: Sodium Hydroxide (Lot# RNBC4129) at 1.05 mM (Sigma-Aldrich, United States).

Cisplatin vehicle: Sodium chloride (Lot# SLBD3098V) at 4.62 mM and D-Mannitol (Lot# SLBG6345V) at 0.16 mM (Sigma-Aldrich, United States).

Carboplatin vehicle: ultra-pure water from our lab by filtering through a 0.22-µm membrane.

Paclitaxel Vehicle: Citric acid (Lot# SLBP9972V) (Sigma-Aldrich, Item number: C2404). Kolliphor EL (PEG 35 castor oil NF, Lot# BCBS4515V) (Sigma-Aldrich, Item number: C5135, United States).

The 10X Annexin V binding buffer: 100 mL (ab14084, Lot#: GR214723-1, abcam, Australia; 1:10 dilution with sterile H2O).

Annexin V-FITC: ab14082, Lot# GR270442-9, abcam, Australia; diluted to 0.3 µg/mL with PBS for flow cytometry.

Propidium Iodide: ab14083, Lot# GR266276-25, abcam, Australia; diluted to 0.5 µg/mL with PBS for flow cytometry.

Transfection reagents: miRCURY LNA™ Mimic hsa-miR-451a (Cat# 471387-001, Lot# 190371, at a concentration of 66.667 µM). miRCURY LNA™ Negative (Cat# 479903-001, Lot# 190372, at a concentration of 66.667 µM). Vehicle: 30 mM HEPES and 100 mM Potassium Acetate. Lipofectamine™ 2000 (Cat# 11668019 Invitrogen).

Trypan blue solution: Cat# 15250-061, Invitrogen

RNA extraction: QIAzol (miRNeasy Kit), Qiagen

Protein lysis buffer:

5 mL of 1 M Tris/HCl pH 7.5

3 mL of 5 M NaCl

0.5 mL of 200 mM EGTA

20 mL of 500 mM Sodium fluoride (NaF)

10 mL of 100 mM Tetrasodiumpyrophosphate decahydrate

1 mL of 100 mM Sodium vanadate ($NaVO_4$)

0.2 mL of 2 mM Sodium azide

1 mL 1% NP40

Exosome extraction: Exoquick, System Biosciences (Cat No.: EXOQ5A-1, 5 mL).

MTS/PMS solution: Dissolved MTS G1111 from Promega at 2 mg/mL in PBS (1x) and PMS P9625 from Sigma at 184 mg/mL in PBS (200x), and then prepared MTS/PMS aliquots: 500 mL MTS at 2 mg/mL (1x), 125 μL PMS at 184 mg/mL (200x), 25 mL PBS.

PCR reagents: miScript II RT kit, Qiagen. miScript Single Cell qPCR Kit, Qiagen. , United States

Apoptosis Assay Reagent: IncuCyte® Caspase-3/7 Green (Cat#: 4440, Lot: 14N0308-103711), Essen BioScience, Ltd. , United States

Western blotting reagents:

10X PBS

NaCl: 80 g

KCl: 2 g

$Na_2HPO_4.2H_2O$: 18.05 g

KH_2PO_4: 2.4 g

MQ: 1 L

Lysis buffer 50 mL

Tris/+HCl (pH 7.4): 6.05 g TRIS base

Sodium Chloride (NaCl) :14.61 g

Ethyleneglycol tetraacetic acid (EGTA): 3.8 g

Sodium fluoride (NaF): 1.05 g

Tetrasodiumpyrophosphate decahydrate: 2.23 g

Sodium vanadate (Na_3VO_4): 0.92 g

Sodium azide (NaN_3): 65 mg

10X Running Buffer for Gel electrophoresis:

Tris Base: 30.3 g

Glycine: 144 g

SDS: 10 g

MQ: 800 mL

Adjust the pH to 8.3

MQ to 1 L

1X Transfer Buffer for protein transfer from gel to PVDF membrane

Tris base: 12.12 g

Glycine: 57.6 g

MQ: 3 L

Methanol: 800 mL

Add MQ to 4 L

PBS-T

PBS

1% Tween-20

Blocking Buffer

5% Non-fat dried milk in PBS-T

2.1.2. Media

RPMI+10% FBS medium: 500 mL RPMI (Life Technologies, Carlsbad, CA) supplemented with 50 mL fetal bovine serum (FBS, 10%, Fisher scientific, USA), 5 mL penicillin & streptomycin (Life Technologies, Carlsbad, CA), 1 mL Normocin (Invivogen, San Diego, CA).

RPMI+10% CSS medium: 500 mL RPMI (Life Technologies, USA) supplemented with 50 mL charcoal stripped serum (CSS, made of 10% FBS, from our lab), 5 mL penicillin & streptomycin (Life Technologies, Carlsbad, CA), 1 mL Normocin (Invivogen, USA).

RPMI+10% CSS medium without antibiotics: 500 mL RPMI (Life Technologies, USA) supplemented with 50 mL charcoal stripped serum (CSS, 10%).

RPMI+10% exosome-depleted FBS: 500 mL RPMI (Life Technologies, Cat# A2720803) supplemented with 50 mL exosome-depleted FBS (exosome-depleted FBS, 10%), 5 mL penicillin & streptomycin (Life Technologies), 1 mL Normocin (Invivogen, USA).

Exosome Depletion CSS: (Product# 61200, Norgen): Media (5 mL) was added to 20 mL CSS, followed by the addition of 400 µL of ExoC Buffer. The solution was mixed well by vortexing for 10 seconds and incubated at room temperature for 10 minutes. The mixture (15 mL) was transferred into a Maxi Spin column assembled with one of the provided collection tubes and centrifuged for 15 minutes at 500 *g* (~1,000 RPM). The flowthrough was transferred (containing the Exosome-depleted CSS) into a fresh 50 cc tube and the spin column was reassembled with its collection tube. The above steps were repeated once more. The Exosome-depleted CSS was aliquoted and stored at -20°C for future use. For experimental usage, the Exosome-Depleted CSS was thawed overnight at 4°C. Exosome-depleted CSS (62.5 mL) was combined with 5 mL of antibiotics (Antimycotic stock of interest in 500 mL media of interest).

Charcoal stripped exosome-depleted FBS: Added 20 g of charcoal (C6241, Sigma-Aldrich) to 1 L Exosome-depleted FBS and mixed gently overnight on a

shaker table at 0–5°C. The charcoal was removed from the suspension by centrifugation at about 2000 *g* for 15 minutes. The top layer was carefully removed by aspiration. We filtrated the medium after centrifugation to ensure purity.

2.2. Methods

2.2.1. The cohort of patients

For chapter 3, we identified patients with pre-treatment archival tumor tissues of locally advanced EAC in Adelaide from 2002–2012 and selected those with comprehensive clinical records on treatment response and long-term follow-up. A total of 31 patients were recruited in our cohort. The 31 patients underwent endoscopy before being treated by neoadjuvant chemoradiotherapy (5-FU, cisplatin, and radiotherapy). We received samples from the biopsy. The patients underwent the surgery and we assessed the chemoradiotherapy response based on the American Joint Committee Cancer (AJCC) tumor regression grading system on the resected specimens.

For chapter 5, patients from South Australia (SA) and Netherlands were recruited for the exosomes serum studies. The SA cohort included 11 patients, RSAB01031 (AJCC0), RSAB01055(AJCC0), RSAB 01074(AJCC0), RSAB 01084(AJCC0), RSAB01029(AJCC3), RSAB 01082(AJCC3), and RSAB01015(AJCC3). However, only four of them passed the PCR quality control. The Netherlands cohort samples were kindly provided by Bas Wijnhoven and Eelke Toxopeus from Erasmus University medical centre and included 10 patients (five responders and five non-responders). The patients were divided into responders and non-responders and the small RNAs were compared between the two groups.

Ethics approval for the study was obtained from the Southern Adelaide Clinical Human Research Ethics Committee (Projects 197.08 and 145.11), the Royal Adelaide Hospital Human Research Ethics Committee (Project 070910) and the Medical Ethics Committee Erasmus MC (Project MEC-2012-191).

2.2.2. The assessment of chemoradiotherapy response

For the neoadjuvant patients, the response to chemoradiotherapy was assessed based on histological tumor regression assessment with the AJCC (American Joint Cancer Committee) staging manual (7th edition) system[303]. AJCC grade 0 represents complete histological tumor regression (no residual cancer cells), while AJCC 1 (few cancer cells) and AJCC 2 (residual cancer outgrowing fibrosis) represent intermediate tumor regression, and AJCC 3 (No regressive change) represents no tumor regression[304]. Collectively the AJCC 1, 2, and 3 are considered as partial and non-responders to neoadjuvant chemoradiotherapy, while AJCC0 are regarded as complete responders. The Netherlands cohort used the Mandard TRG system, which is different from the AJCC system. The Mandard TRG system is[304]: TRG1: No viable cancer cells; TRG2: few cancer cells; TRG3: Predominant fibrosis with increased number of residual cancer cells; TRG4: Residual cancer outgrown by fibrosis; TRG5: no cancer cells killed. TRG1 represents responders to neoadjuvant chemoradiotherapy, while TRG5 represents non-responders.

Another method for assessment is five-tier classification for the definitive chemoradiotherapy patients (patients who had chemoradiotherapy **without** surgery):

1) Complete response

complete disappearance of tumor at endoscopy and CT, and no local recurrence within two years

2) Near complete response

complete disappearance of tumor at endoscopy and CT, but local recurrence within two years.

3) Good partial response

persistent tumor at endoscopy or on macroscopic inspection of resection specimen but reduced in size by at least 50% compared to pre-chemo assessment.

4) Poor partial response

persistent tumor at endoscopy or on macroscopic inspection of resection specimen but reduced in size by less than 50% compared to pre-chemo assessment.

5) No response

persistent tumor at endoscopy or on macroscopic inspection of resection specimen, and no reduction in size compared to pre-chemo assessment.

2.2.3. Tissue sample preparation

The patients underwent endoscopy before being treated by neoadjuvant chemoradiotherapy (5-FU, cisplatin, and radiotherapy). We received the samples from the biopsy. The pre-treatment biopsy tissue blocks were sectioned at a thickness of 4 μm for hematoxylin and eosin staining. Consecutive tissue sections were then cut at 10 μM for RNA extraction with RecoverAll™ Total Nucleic Acid Isolation kit (Ambion) as per the manufacturer's protocol. Then the RNA purity and concentration was performed by Nanodrop. The purified RNAs were used for the sequencing study.

2.2.4. Blood sample preparation

Written consents were received from the patients before the blood collection. The blood was collected in a serum clot activator tube. The preparation of blood was different between different hospitals (chapter 5, table 5-1). After centrifugation, the serum was divided into 1-mL aliquots respectively. The aliquots were stored in Eppendorf tubes at −80 °C for future use. The serum aliquots used in this study were recovered from storage by quick thawing. Before use, the samples were centrifuged at 16000 *g* at 4 °C for about 30 minutes to eliminate particles.

2.2.5. Exosome extraction from serum

The exosome isolation from serum samples was performed by Exoquick assay (Cat No.: EXOQ5A-1, 5 mL), because ExoQuick is considered better for specific exosomal miRNAs recovery from cryopreserved serum[305]. The processes were followed strictly according to the manual from the company.

The serum was thawed quickly, and then centrifuged using a bench-top centrifuge at 16000 *g* at 4°C for 30 minutes. The supernatant was collected very carefully to avoid the pellet, and 250 μL of the supernatant was taken out into 1.5 mL tubes and 63 μL of Exoquick was added into the tubes and kept at 4°C overnight. We centrifuged the sample using a bench top centrifuge at 1500 *g* at 4°C for 30 minutes the following day and aspirated out the supernatant. The centrifugation and aspiration was repeated once more. Next, DPBS (50 μL) was added to the pellet for resuspension and the exosomal solution was stored at -80°C.

2.2.6. Counting the exosomes

The exosomes were counted by Nanosight (NTA version: NTA3.0 0060). To begin with, the exosomes were diluted in PBS to a final dilution of 1:3200 . This was done in two steps : 1:400 dilution=1 ul exosomes solution + 399 ul PBS. Then1:8 dilution= 100 ul exosomes solution (from the first dilution) + 700 ul DPBS.

Second, 400 μL of the solution was withdrawn with a 1 mL syringe and pushed into the chamber. After fitting the block, we turned on the thermometer to record the temperature and turned on the laser switch. Third, we captured the computer screen and finally analyzed the video.

Capture settings:

Camera type: SCMOS

Camera level: 13

Slider shutter: 800

Slider gain: 350

FPS: 28.1

Number of frames: 1687

Temperature: 22.1–22.2

Viscosity: (water) 0.948–0.951cP

Analysis settings:

Detect threshold: 10

Blur size: auto

Max jump distance: auto; 7.8–8.1 pix

2.2.7. RNA extraction from the Cell/Tissue/Exosome

RNA extraction from the Tissue/Exosomes was conducted by QIAzol lysis. The QIAzol lysis reagent (700 μL) was added to the sample and incubated at room temperature (15–25°C) for 5 minutes. Then, 140 μL chloroform was added and shaken vigorously for about 15 seconds, followed by incubation at room temperature for two–three minutes and centrifugation for 15 minutes at 12000 *g* at 4°C. We transferred the upper aqueous phase (approximately 350 μL), containing the RNA, to a new 2 mL collection tube by carefully avoiding transferring any interphase. We then added 1.5 volumes (usually 525 μL) of 100% ethanol and mixed thoroughly by pipetting. We pipetted up to 700 μL sample, including any precipitate, into an RNeasy® Mini column in a 2 mL collection tube and centrifuged at 8000 g for 15 seconds at room temperature and then discarded the flow-through. Buffer RWT (700 μL) was added to the RNeasy Mini column and centrifuged for 15 seconds at ≥8000 *g*. The flow-through was discarded and we pipetted 500 μL buffer RPE into the RNeasy Mini column, and centrifuged for 15 seconds at ≥8000 *g* and discarded the flow-through. Buffer RPE (500 μL) was added to the RNeasy Mini column and centrifuged for two minutes at ≥8000 *g*, and then transferred the RNeasy Mini column to a new 1.5-mL collection tube. We pipetted 30–50 μL RNase-free water directly onto the RNeasy Mini column membrane and centrifuged for one min at ≥8000 *g* for elution.

2.2.8. RNA sequencing

Samples were sequenced on the Illumina HiSeq 2500 Platform using the single-end protocol with a read length of 52. Raw reads were trimmed and filtered for short sequences using cutadapt v.1.3[306] setting minimum-length option to 18, error-rate 0.2 and overlap 5. The trimmed FASTQ files averaging 22 million reads per sample were analyzed, and quality checked using FastQC program (v.0.10.1)[307]. Reads were mapped against the human reference genome (Ensembl GRCh38) using BWA (Burrows-Wheeler Aligner) (version 0.7.9a-r786)[308] with default parameters returning an average of unique alignment rate of 83%. HTSeq-count (v.0.61p1)[309] was used to extract the counts for the mature miRNAs, snoRNA and snRNAs, and piRNAs, based on the hg19 annotations provided by miRbase (release 21)[310], Ensembl/Gencode (release 21) and piRbase (version 1.0)[311], respectively.

The miRNA, snRNA, snoRNA, and piRNA counts were normalized based on GC content using EDASeq (v.2.4.1) [312], and differential expression analysis was evaluated from GC normalized counts using DESeq2 statistical tool (v.1.10.1)[313] and edgeR (v.3.12.0)[314]. The normalization and differential expression analysis was carried out in the R environment (v.3.2.1; https://cran.r-project.org/).

GC and length normalization was performed using a Full-Quantile method in R using the EDASeq package[312] (https://bioconductor.org/packages/release/bioc/html/EDASeq.html), with the number of bins optimized separately for CG-content, and then for length of the RNA, by using bias plots (for details of the optimization process see https://bioconductor.org/packages/release/bioc/vignettes/EDASeq/inst/doc/EDASeq.html#normalization).

2.2.9. Cell culture

2.2.9.1. Thawing the cells

Cells were thawed quickly from liquid nitrogen by transferring quickly to a water bath at 37°C. We immediately transferred the thawed cells into a centrifuge tube containing the culture medium, and inverted to mix and centrifuged at 1500 rcf for 5

minutes. The supernatant was removed using an aspirator and the cell pellet was resuspended in 1 mL of culture medium with gentle pipetting, and then transferred the cells to a new flask with the appropriate quantity of media and resuspended cells. The cells were cultured in a 5% CO_2 incubator at 37°C and the media was changed every 2–3 days.

2.2.9.2. Subculture

The cells were split when the confluence reached around 70~80%. The spent medium was removed using the aspirator and cells were washed with 2–5 mL PBS. Then, 1–2 mL of Trypsin-EDTA was added to the cells and placed in the incubator for about 1~5 minutes. The cells were checked under the microscope to confirm that all the cells had detached. The reaction was stopped by adding complete media at least twice the volume of Trypsin-EDTA. The cell suspension was transferred to a 10-mL centrifuge tube using a disposable transfer pipette and centrifuged at 1500 rcf for 5 minutes. The supernatant was aspirated, and the cells were resuspended in fresh media (1 mL) by repeated pipetting; then, the cells were transferred to a new flask with the appropriate quantity of media and resuspended cells. The cells were cultured in a 5% CO_2 incubator at 37°C and media was changed every 2–3 days.

2.2.9.3. Trypan blue cell count

The Trypan blue (solution from Invitrogen cat# 15250-061) was diluted 1:10 in a 1.5 mL tube with the cell suspension and mixed well. After breathing to generate condensation, the cover slip was quickly placed onto the hemocytometer with gentle pressure. The solution (20 µL) was then loaded onto the hemocytometer by pipetting the aliquot to the edge of the cover slip. The cell numbers were counted in the four outer squares (the 4 x 4 squares in each corner) and then the total number of cells in the 1-mL sample were counted by using the following formula: Total cell number = average cell no. ×10000 × dilution factor.

2.2.9.4. Harvesting of cells for RNA extraction

The Trizol Kit was used according to the manufacturer's instructions. The cells were scraped off and transferred into a 10-mL tube. The wells were washed with 1 mL

PBS and the solution was transferred into the same 10-mL tube and centrifuged at 1500 rcf for 5 minutes. The supernatant was removed and 500 μL of Trizol was added, resuspended and transferred into 2-mL Eppendorf tube. The samples were centrifuged to ensure that the samples were at the bottom of tube; then, the tube was placed into a heating block for 5 minutes at 37°C. The samples were frozen at -80°C.

2.2.9.5. Harvesting of cells for protein extraction

When the confluence was about 60–80%, the cells were harvested for protein extraction. We scraped the cells off from the plate by wiping several times, and then transferred the cells to a centrifuge tube and centrifuged at 1500 rcf for 5 minutes at room temperature. Lysis buffer (1 mL) was added after removing the supernatant. The centrifuge tube was placed vertically with the probe in the middle of the tube, and then the lysate was sonicated with probe sonicator for 10–20 seconds till the solution was clear. The samples were frozen at -80°C.

2.2.10. Transfection of miRNA mimics

2.2.10.1. miRNA mimics

The optimization of transfection concentration and cell density was conducted before transfection. Several concentrations of mimics with a number of cell densities were set for the studies. The transfection efficiency was assessed by qRT-PCR. The final concentration of mimics and cell density were used for the transfection.

The OE33 cell line was picked for transfection. The transfection was conducted by miRCURY LNA™ Mimic of hsa-miR-451a at the optimized concentration, with the appropriate concentration of Lipofectamine 2000 (Invitrogen, Life technologies). The transfection was performed when the cell confluence was around 70%. The medium was changed after 6 hours of transfection and the cells were re-plated after 24 hours of transfection. The transfected cells underwent the drug treatment and radiation after 48 hours of transfection. The treatment response was assessed using flow cytometry and Incucyte analyses.

2.2.11. Drug treatment on cells

The drug treatment on cells was performed after 24 hours of seeding in the plate. The drugs and the vehicle controls of the drugs were prepared on the day of treatment. The spent media was replaced with fresh media containing the drugs or vehicle controls and then the plates were put back into the incubator at 5% CO2 and 37°C. The drug treatment response was assessed by flow cytometry or Incucyte after treatment for 72 or 96 hours.

2.2.12. Radiation on cells

The cells were subjected to irradiation by Xrad320 (Precision X-Ray) at 2 Gy. The clonogenic assay was used for the assessment of the radiotherapy response in cell lines.

2.2.13. Measuring the cell growth/viability /proliferation/apoptosis

2.2.13.1. MTS(3-(4,5-dimethylthiazol-2-yl)-5-(3-carboxymethoxyphenyl)-2-(4-sulfophenyl)-2H-tetrazolium) assay

The MTS assay was used for measuring the cell viability by assessing cell metabolic activity. MTS reagent (20 μL) was added directly to each well of a 96-well plate. After incubating for two hours under standard conditions, the absorbance of each well was read using a BioRad Plate reader at 490 nm. The data was corrected by subtracting the mean absorbance of the background wells. The survival fraction was calculated by dividing the corrected absorbance of a treated sample by the mean of the corrected absorbance of the respective vehicle controls.

2.2.13.2. Flow cytometry

The cells were harvested as described above and resuspended in 250 μL binding buffer. Annexin V-FITC (0.3 μg/mL) was added to the samples and incubated in the dark for five minutes. Propidium Iodide (0.5 μg/mL) was added to each sample just before performing the flow cytometry. The unstained, PI only, and FITC only

samples were read first, followed by the other samples using the Flow Cytometer. The setup for Flow Cytometry was as follows:

Events: 10000

Fluidics: fast

Threshold: 1.5 million

Gating: P6 in P5

Compensation: 3.5%

2.2.13.3. Incucyte

The Incucyte assay served as the live-cell monitor; it analyzed the cell confluence from the captured images. The cells were incubated in the Incucyte system; the cell viability and proliferation were assessed on the basis of the confluence. The data in the treatment group were normalized with the data of vehicle control.

2.2.13.4. Caspase-3/7 Apoptosis Assay

This assay was used together with the Incucyte test, and the Caspase-3/7 was added directly to cell culture wells to get live cell images of cells undergoing apoptosis. The assay reagent did not disturb the cell proliferation and morphology. Upon addition to cell culture medium, the inert non-fluorescent substrate went through the cell membrane where it was cleaved by activated Caspase-3/7, resulting in the release of the DNA-binding dye and fluorescent staining of the nuclear DNA. With the IncuCyte® integrated analysis software, fluorescent objects can be quantified and the background fluorescence can be minimized.

The full strength for Caspase 3/7 reagent was 5 μM per well in 100 μl solution per well. Our preliminary experiment revealed that 2.5 μM was the optimized dose for most experiments, therefore we used a final concentration of 2.5 μM for all experiments in this study.

2.2.13.5. Clonogenic assay

The appropriate cells were seeded into the plates, then incubated for the respective incubation times in a 5% CO2 incubator at 37°C and with media change every 2–3 days. When a sufficient number of colonies were formed, the fixing and staining were performed. The media was aspirated, and the cells were washed with 1 mL PBS, followed by the addition of 1 mL of 10% neutral buffered formalin for 20 minutes. After aspirating the formalin, the colonies were stained with 1 mL 0.01% crystal violet solution in deionized water for 1 hour. The staining solution was removed and the plates were allowed to dry, and the colonies were counted by the software Image J. Every colony that consisted of more than 50 cells was identified and counted as one.

2.2.13.6. Crystal violet Assay

The media was gently removed from each well of the plates, and then each well was washed with 1 mL of PBS and the plates were transferred to the fume hood. In the fume hood, the PBS was removed and the colonies were fixed with 1 mL 10% neutral buffered formalin solution for 20 minutes. The formalin was removed and then plates were stained with 1 mL 0.01% crystal violet in dH_2O for 60 minutes. Excess crystal violet was washed with dH_2O and dishes were allowed to dry, and quantified by solubilizing dye in 1 mL of 1% SDS in H_2O. The solubilization took up to 1 hour with occasionally shaking of the plate. The absorbance of the samples was read at 595 nm using a BioRad Microplate reader. The area coverage analysis was performed using the ImageJ software.

2.2.13.7. xCelligence

The xCelligence provides dynamic, real-time cellular analysis. It uses electrical impedance as the readout to monitor the cell proliferation. The cells were subcultured until they reached 70% confluency on the day of exosome transfection. The cell suspension was prepared at 4.72E+05 cells/mL, different types of exosomes were added at a concentration of 1.57E+09/μL separately to the cells. After 24 hours, the cells were replated at a density of 60k (60000 cells/mL) and subjected to

xCelligence analysis. The cells were treated with drugs/vehicle for 72 hours and the data were analyzed by the xCelligence software.

2.2.14. qRT-PCR

2.2.14.1. RNA extraction

QIAzol lysis reagent (700 μL) was added to the samples and homogenized using the appropriate methods. The homogenate was incubated at room temperature (15–25°C) for 5 minutes and 140 μL chloroform was loaded into the homogenate and shaken vigorously for 15 seconds. Samples were incubated at room temperature (15–25°C) for 2~3 minutes and then centrifuged for 15 minutes at 12,000 *g* at 4°C. The upper aqueous phase containing the RNA was transferred to a new 2-mL collection tube and then 1.5 volumes of 100% ethanol was added and mixed thoroughly by pipetting. We then pipetted 700 μL sample into an RNeasy® Mini column in a 2-mL collection tube and then centrifuged at ≥8000 *g* for 15 seconds at room temperature and discarded the flow-through and repeated the above steps using the remainder of the sample. The RNeasy Mini column was transferred to a new 1.5 mL collection tube and 30‑50 μL RNase-free water was pipetted directly onto the RNeasy Mini column membrane, and then centrifuged for 1 min at ≥8000 *g* to elute.

2.2.14.2. miScript Single Cell qPCR Kit

The 3’ ligation was first performed using 5 μL purified RNA (1 ng for cell lysate; 1 μL for serum sample diluted by UPW(ultra pure water) to 5 μL). The 3’ ligation master mix (miScript SC 3’ ligation buffer, nuclease-free water, miScript SC 3’ RNA ligase) was made and 2 μL was added into the tube containing 5 μL cell lysate/RNA. The miScript SC ligation activator was added to each well and mixed by pipetting briefly, and then incubated for 1 hour at 16ºC in the thermal cycler.

Immediately prior to setting up the 5’ ligation reactions, we allowed the completed 3’ ligation reactions to equilibrate to room temperature for about 2 minutes. At room temperature, 5 μL of 5’ ligation master mix (miScript SC 5’ ligation buffer, miScript SC 5’ RNA ligase) was added into the tube containing the completed 3’ ligation

reaction and then incubated for 5 minutes at 37ºC and 15 minutes at 65ºC to inactivate the miScript SC 5' RNA ligase.

The reverse-transcription reaction was started from the completed 20 μL 5' ligation reactions. The reverse-transcription master mix (miScript SC 5X RT buffer, miScript SC 10X RT nucleics, nuclease-free water and miScript SC reverse-transcriptase) was prepared on ice and 20 μL of the reverse-transcription master mix was loaded into the tubes containing the completed 5' ligation reaction and mix well. The reactions were incubated at 37ºC for 2 hours and another 5 minutes at 95ºC to inactivate the miScript SC reverse transcriptase.

The cDNA needed to be cleaned up before performing the PCR. The beads and bind mixture (miScript SC cleanup beads, miScript SC cleanup bind) were prepared for the clean-up of cDNA and 40 μL solution of beads and bind mixture was added to the cDNA and shaken at 1100 rpm using the Eppendorf MixMate for 10 minutes. The supernatant was discarded and 150 μL of freshly prepared 80% ethanol was added to the beads twice. We allowed the beads to air dry for 10 minutes and then added 20 μL buffer EB to the beads and mixed using Eppendorf MixMate at 1110 rpm for 5 minutes. The beads were separated from the suspension using a magnet stand, and the cleaned up products were used for the next step.

This unbiased amplification was performed to make sure that sufficient target was present for quantification in subsequent real-time PCR. The 9 μL preamplification components (miScript SC preAMP buffer, miScript SC preamp universal primer, Hotstar Taq DNA polymerase) were added directly to the wells containing the cleaned up products. The preamplification reaction was placed in the thermal cycler and started to run (the set-up is shown below, Table 2-1).

Table 2-1: The thermal cycler program for the amplification (reproduced from handbook of miScript single cell kit)

Step	Time	Temperature
PCR initial activation step	15 min	95°C
3-step cycling (2 cycles)		
Denaturation	30s	94°C
Annealing	60s	55°C
Extension	60s	70°C
2-step cycling (11 cycles)		
Denaturation	30s	94°C
Annealing/extension	3 min	60°C
Hold at 4°C for at least 5 min		

The PCR quality control test for a small number of representative samples was recommended by the company manual; thus, we tested the quality control for all the samples for the sake of preciseness. The PCR quality control master mix ((2x QuantiTect SYBR Green PCR Master Mix, 10x miScript Universal Primer, and nuclease-free water) was prepared at room temperature and 18 μL of the master mix was added into five individual tubes, and the five tubes contained five kinds of primers, which were, miSC3 (Assessment of 3' ligation performance), miSC5 (Assessment of 5' ligation performance), miSCRT (Assessment of reverse-transcription performance), miSCPA (Assessment of preamplification performance) and PPC (Assessment of real-time PCR performance). The cycling conditions were as shown below. If the samples passed the quality control, the preamplification products were diluted 1:3 with nuclease-free water and used for the real-time PCR with 17 μL master mix (2× QuantiTect SYBR, 10× miScript Universal primer, 10× miScript primer assay, UPW) and 3 μL cDNA loaded into the corresponding tubes and run immediately on the Rotorgene (the set-up is shown below, Table 2-2).

Table 2-2: The thermal cycler program for the quality control (reproduced from handbook of miScript single cell kit)

Step	Time	Temperature
PCR initial activation step	15 min	95°C
3-step cycling (35 cycles)		
Denaturation	15s	94°C
Annealing	30s	55°C
Extension	30s	70°C

2.2.14.3. miScript II RT Kit

The template was 1 μg of RNA in 8 μL volume with UPW and we added 2 μL Master Mix (miScript 5× Hispec/Hiflex buffer, 10× nucleics mix, reverse transcriptase, UPW), and then loaded onto thermocycler at 37ºC for 60 minutes and 95ºC for 5 minutes. The cDNA was diluted by adding 180 μL UPW and prepared for the PCR. The Master Mix (2× QuantiTect SYBR, 10× miScript universal Primer, 10× miScript primer assay, UPW) was prepared and 17 μL was added into the tube, and 3 μL of each cDNA sample was added into the corresponding tubes, and then loaded on the RotorGene for the PCR reaction.

2.2.15. Obtaining custom made primers of piRNA and snoRNA

We selected the piRNA candidates and looked up their sequence from the piRNA database (http://www.regulatoryrna.org/database/piRNA/browse.php). The sequence of snoRNA was obtained from PubMed. We used the online primer design tool on the company's website (https://www.qiagen.com/au/shop/genes-and-pathways/custom-products/custom-assay-products/custom-mirna-products/) and enter the information required on the website, submitted the order to the company, and the company prepared and tested the primers.

2.2.16. Western blotting

2.2.16.1. EZQ protein quantification

The EZQ™ Protein Quantitation Kit (R33200, Invitrogen) was used for testing the protein concentration. The handbook of the kit was strictly followed. First, the protein standards (Ovalbumin from chicken egg, Invitrogen R33200), assay paper,

and the samples were prepared and 1 μL of each standard and sample were loaded onto the assay paper in triplicate, allowing the samples to dry. The assay paper was carefully removed from the microplate with clean tweezers and then we placed the trimmed assay paper in a clean large weighing tray and added 40 mL of methanol, and then poured off the methanol. The paper was dried on low heat using Easy Breeze Gel Dryer for 3 minutes or until completely dry. We added 35 mL of EZQ Protein Quantification Reagent and then placed on the shaker for 30 minutes and poured off the reagent and added 40 mL of EZQ stain and placed on the shaker for 2 minutes, and then scanned the assay paper.

The results were analyzed by calculating the fluorescence values of the experimental samples and normalized by subtracting the fluorescence value of the no-protein control. We created a standard curve by plotting the corrected fluorescence values of the standards and the protein concentration respectively and determined the concentration of the experimental samples from the standard curve.

2.2.16.2. Bio-rad Precast Gel Set Up

The sodium dodecyl sulfate polyacrylamide gel electrophoresis was bought from Epitomics (Epitomics Inc., CA, USA). The comb was gently removed and the wrap and solution were discarded. The wells were rinsed with 1× Running Buffer and then the gel was placed in the Bio-Rad gel holder. We filled up the top tank (holder) with 1× Top Tank Running Buffer and filled up the bottom tank with 1× Bottom Tank Running Buffer.

2.2.16.3. Running the gel/ Sample preparation

We mixed the desired amount/concentration of sample with 4× Loading/sample buffer. For reducing conditions, DTT was added to loading/sample buffer (4 mg DTT to 100 ml 4× loading/sample buffer). The samples were placed in a 95°C heating block for 2 minutes, and then quick spined. The samples were evenly loaded into each well along with the dual color protein standard. The tank lid was placed on and attached to a power pack, and then run at 200 volts for 30 minutes.

2.2.16.4. Transfer

We cut 2 pieces of Bio-Rad extra thick blotting paper and 1 piece of PVDF membrane (8.5 cm × 7 cm), and then soaked the blotting papers in 1× Transfer buffer for about 30 minutes. We took the gel out of the electrophoresis tank and placed in a tray containing 1× Transfer buffer and allowed for equilibration to occur for 10 minutes. At the same time, we soaked the PVDF membrane briefly in methanol and then in 1× Transfer buffer for 10 minutes. We measured the dimensions of the gel/blotting pads and cut out the same sizes from the middle of a transparency sheet. We poured some water in the semi-dry transfer unit to keep the base moist and placed the remainder of the transparency in the unit. We placed one soaked blotting pad in the middle of the transparency sheet where the square piece was cut out and then slid the soaked membrane underneath the gel (in the tray containing 1x Transfer buffer) and gently lifted the gel and placed both the membrane and gel (as it was lifted) on top of the blotting pad in the transfer unit. We cut one corner of the membrane to mark the lane orientations and placed the other blotting pad on top of the gel. After ensuring that there were no air bubbles, we placed the lid over the transfer unit and placed a heavy object on top of the unit and allowed the transfer to occur for approximately 2 hours at 65 mA (per membrane).

2.2.16.5. Blocking

After the transfer was completed, we removed the blotting pads and the gel from the unit and then removed the membrane from the unit and placed in a tray containing 5% skim milk powder solution in 1× TBS-T (0.1% Tween 20) and allowed blocking to occur for 1 hour while shaking.

2.2.16.6. Primary antibody

The primary antibody was diluted in 0.1% skim milk powder solution (in 1 × TBS-T). The blocking solution was discarded and the membrane was washed briefly with wash buffer (1× TBS-T (0.1% Tween 20) + 0.1% Skim Milk) for 5 minutes at room temperature while shaking. We applied the diluted primary antibody to the membrane in the tray after discarding the wash buffer. We covered the tray (glass

plate) to avoid drying of the membrane and incubated at room temperature for 1–2 hours while shaking.

2.2.16.7. Secondary antibody

The membrane was washed twice with the wash buffer for 5 minutes and 15 minutes. We diluted the appropriate secondary antibody at 1:5000 in 0.1% skim milk powder solution in 1× TBS-T (prepare 10 mL if the tray is being used); then, we treated the membranes with the diluted secondary antibody and covered the tray with a glass plate, followed by incubation at room temperature for 1 hour while shaking.

2.2.16.8. Development (using ECL)

The membranes were washed several times as follows: 2 × 5 minutes (wash buffer), 2 × 15 minutes (wash buffer), 1 × 5 min (TBS). We placed a piece of Glad plastic wrap on the bench and then applied at least 1 mL of each ECL Substrate (2 mL Final Volume, GE health care, Buckinghamshire, England) to the middle of the wrap (less can be used but can give uneven background). We took the membrane out of TBS and placed on top of the 2 mL ECL substrate and incubated for five minutes and then imaged the membrane using the Fuji ChemiDoc™ MP Imaging System (Bio-Rad, California, USA).

2.2.16.9. Image processing

Bands were visualized using the ChemiDoc™ MP Imaging System (Bio-Rad, California, USA) and photographed using MultiGauge version 3.0 image capture software (Fujifilm Life Science). Band intensity for the protein of interest and the loading control protein was quantified using Carstream Image Analysis software (Carestream, Rochester, NY). After western blotting, the total protein load control method was used to normalize protein of interest band intensities [300]. Differences in the experimental group and control band intensities were assessed for statistical significance using the Mann-Whitney test.

2.2.16.10. Instructions for background subtraction

We quantified the band intensities by drawing a rectangle around the bands of interest and quantified the intensity of pixels of the band of interest as well as pixels surrounding the band of interest (non-data pixels), if they are within the rectangle. Background subtraction was performed to subtract non-data pixels from the entire pixels in the rectangle so that only data-pixels remained. We used two methods to do this, which are local and global background subtraction. Either of the two methods can be used if the blot is very clear, if there is hardly any background, or if the background looks the same over the entire membrane. In these cases, both methods will give very similar values. But there are occasions where one of the two methods is more appropriate than the other method.

2.2.16.10.1. Local background subtraction

For local background subtraction, it is important to identify whether the background is due to non-specific binding of the antibody or due to artefacts of the detection reagent. If the background is due to non-specific binding, then local background should NOT be used.

Local background subtraction calculates separate background intensities for each unknown and standard volume you create. For each volume, the intensities of the pixels in a 1-pixel border around the volume are added together and divided by the total number of border pixels. This gives an average intensity for the background around each band, which is then subtracted from the intensity of each pixel inside the volume.

2.2.16.10.2. Global background subtraction

Global background subtraction should be used if the signal around the rectangle containing the band of interest is due to specific binding of the antibody (for example if the antibody binds to two isoforms with a very small difference in MW (a few kDa), the two bands can run very close to each other and the signal of one isoform may contribute to the pixels surrounding the band of the other isoform.

Global background subtraction calculates only one single background intensity for the entire gel. This average background intensity is then subtracted from all the volumes in the gel. The average intensity of the pixels in the background volume is calculated and subtracted from each pixel in all standard and unknown volumes. Therefore, it is not necessary for the background volume area to be the same size as your unknown.

2.2.17. Bioinformatics analysis for identifying potential small RNA-associated signaling pathways

We used the miRWalk2.0 (http://zmf.umm.uni-heidelberg.de/apps/zmf/mirwalk2/) to predict the potential target genes for the miRNAs. The high score target genes were picked according to the results and then put into the Innate DB website for the pathway analysis (http://www.innatedb.com/redirect.do?go=batchPw).

The detailed steps were as follows:

The target gene prediction: miRWalk2.0, Predicted target module, miRNA-gen targets, microRNA information retrieval system: select human, miRBase, miRNA, past has-miR-xx; step2: default; step 3: tick all the database; step 4: default, search, putative target genes table, pick the target gene data, copy to the InnateDB data analysis.

Signaling pathway analysis: Data analysis, pathway analysis, web form, upload, column, choose cross-reference ID, Refseq, Ok, next, pathway ORA, Analysis algorithm: hypergeometric, p-value correction method: Benjamini–Hochberg, Do analysis, pathway over-representation analysis results, all, download.

Another method is to use the DIANA mirPath v.3 to conduct the KEGG analysis: add miRNA, choose data base (Tarbase, microT-CDS, or TargetScan), set the p-value threshold 0.05, MicroT threshold 0.8, if we use the TargetScan, the p-value threshold 0.05, TargetScan Score Type: context+, TargetScan context score-0.4, TargetScan conservation score 0.1, apply.

CHAPTER 3
IDENTIFICATION OF POTENTIAL SMALL RNAS AS BIOMARKERS OF RESPONSE TO CHEMORADIOTHERAPY IN PRE-TREATMENT TUMOR TISSUES FROM PATIENTS WITH LOCALLY ADVANCED EAC

3.1 Introduction

It is reported that neoadjuvant chemoradiotherapy for esophageal cancer could improve the overall survival of esophageal cancer patients by about 10% in a five-year survival rate[235, 236]. However, not all patients have a good response to chemoradiotherapy and achieve significant survival improvement. About 25–30% of patients with locally advanced esophageal carcinoma fail to respond to chemoradiotherapy and 40–43% suffer from the therapy-related toxicities more than grade 3[315]. Unsuccessful chemoradiotherapy makes the patient unfit or delays the surgery, giving rise to increased morbidity and mortality. Therefore, it is important to assess chemoradiotherapy response, preferably prior to therapy, in order to treat patients individually and adjust the treatment approach in a response-guided manner in neoadjuvant settings.

Small RNAs, such as miRNAs, piRNAs, snRNAs, and snoRNAs have been reported to play a pivotal role in the development and progression of numerous cancers. Recent progress in next generation sequencing technology has enabled researchers to investigate the roles of small RNAs in cancer progression. Several miRNAs have been identified as biomarkers for predicting the neoadjuvant chemoradiotherapy response in ESCC, such as miR-200c[233], miR-145-5p, miR-152, miR-193b-3p, and miR-376a-3p[316]. miR-21[198] and miR-98[317] were also identified to predict the radiotherapy response for EC. RNA-seq technology promoted the study of the other small non-coding RNAs. For example, Koduru et al.[318][319] identified several snoRNAs and piRNAs differentially expressed in colorectal cancer

and breast cancer by RNA-seq. However, very few studies have mentioned the relationship between small non-coding RNAs and chemoradiotherapy response. Chu et al.[179] indicated that ACA11, an snoRNA, inhibited oxidative stress, which promoted resistance to chemotherapy and the growth of multiple myeloma cells. Wang et al.[320] found that piR-L-138 increased resistance to cisplatin in lung squamous cell carcinoma. However, the roles of piRNAs, snRNAs, and snoRNAs as biomarkers for chemoradiotherapy response in EAC have not been reported.

This chapter describes the identification of the top differentially expressed small RNAs between esophageal adenocarcinoma neoadjuvant chemoradiotherapy responders and non-responders, and the analysis of these small RNAs as biomarkers for chemoradiotherapy response in locally advanced patients with EAC.

3.2 Methods

This study was a retrospective study and the archival formalin fixed pre-treatment endoscopy biopsies between 2002–2012 were used for the lab analysis. The sample cohort was described in a previous publication from our laboratory[1] [321]. A total of 31 patients were selected with comprehensive clinical records on treatment response and long-term follow-up (Chapter 2: 2.2.1).

The treatment response of specimens was assessed by American Joint Cancer Committee (AJCC) staging manual (7th edition) system (Chapter 2: 2.2.2). The cohort consisted of nine complete responders (AJCC-0) and 22 partial (11 AJCC-1, five AJCC-2) or non-responders (six AJCC-3). To determine potential small RNA biomarkers for responders, the complete responders were compared to the combined partial and non-responders (AJCC-0 vs. AJCC-1.2.3). To determine potential small

[1] This publication described the use of the miRNA sequencing data to derive a miRNA ratio-based biomarker model. The approach utilized cross validation to derive the least complex multi-biomarker prediction model so that it was not overfitted. This differs from the approach taken in this thesis, which was to discover as many response associated miRNAs (and other small RNAs) as possible, and use FDR estimation to determine that the false positive rate was acceptable. This thesis focused on discovering individual miRNAs (and other small RNAs), rather than miRNA ratios, to explore the biology underpinning these individual candidate small RNA biomarkers [Chapter 4].

RNA biomarkers for non-responders, the combined complete and partial responders were compared to the non-responders (AJCC-0.1.2 vs. AJCC-3). To ensure that any potential biomarkers identified were also evident in a comparison of extreme response phenotypes the complete responders were compared to the non-responders (AJCC-0 vs. AJCC-3). In our previous paper[321] there were no differences in relapse free survival between partial and non-responders (AJCC-1 vs. -2, AJCC-1 vs. -3, & AJCC-2 vs. -3). For our analyses the patients were therefore grouped together in order to get sufficient sample size and power. The AJCC-0 and AJCC-3 was checked as well to ensure that the biomarkers selected from the above analysis were supported in an analysis of extreme response phenotypes.

The presence of cancer in a 4 micron tissue section was confirmed by a histopathologist then RNA extraction was conducted as described in Chapter 2 : 2.2.3 and the small RNAs were profiled by RNA sequencing (Chapter 2:2.2.8). Mann-Whitney U tests (non-parametric; $p < 0.05$) were utilized to select small RNAs with potentially diagnostic utility. False discovery rates (FDR) were estimated to ensure that the majority of differentially expressed small RNAs were not selected due to chance alone. ROC curves were then used to estimate diagnostic accuracy, which was utilized for final biomarker selection. ROC curve analysis was performed in R by building a logistic regression model, and then using the predictions from the model to build a ROC curve using the pROC package (https://cran.r-project.org/web/packages/pROC/index.html) The area under the ROC curve is considered: excellent for AUC values between 0.9–1; good for AUC values between 0.8–0.9; fair for AUC values between 0.7–0.8; poor for AUC values between 0.6–0.7; failed for AUC values between 0.5–0.6 [322-324]. Candidate biomarkers were selected when the value of their AUC was above 0.8. The biomarkers were selected further based on their ROC curve derived specificity and sensitivity and 95% confidence intervals for the specificity and sensitivity estimates were determined via bootstrap resampling using the ci.se and ci.sp functions in the pROC package in R (for details see: https://cran.r-project.org/web/packages/pROC/pROC.pdf). Specificity estimates the true negative rate, and therefore the chance of making a false positive prediction. The lower bound of the 95% confidence interval of the false positive rate is the worst-case estimate of making a false positive prediction.

Sensitivity estimates the proportion of actual positives that could potentially be correctly identified. A perfect biomarker would achieve 100% sensitivity and 0% false positives. In practice, there is a trade-off between sensitivity and specificity, and in the clinical context of this study, we focused on maximizing the ability of small RNA biomarkers to detect good responders, which entails maximizing sensitivity. Therefore, in our study, biomarkers were selected that had greater than 85% sensitivity and less than a 65% false positive rate at the confidence interval lower bounds.

The selected small RNAs that were differently expressed between responders and non-responders were subsequently assessed by qRT-PCR (Chapter 2: 2.2.14). The qRT-PCR results were normalized using let-7g-5p. The data were analyzed by Mann Whitney test, and $p<0.05$ was regarded as significant. Correlations between the PCR data, the NGS data, and the age of the formalin-fixed paraffin-embedded (FFPE) blocks were also analyzed by Linear Regression.

3.3 Results

3.3.1 Small RNAs as biomarkers for the prediction of responders

3.3.1.1 miRNAs

The results showed that miR-451a, miR-340-5p, and miR-576-5p might be potential biomarkers for the prediction of responders by analysis of AJCC-0 vs. AJCC-1.2.3 (Table 3.1, Figure 3.1), However, the lower bound of the false positive rate was 90% at a lower bound on the sensitivity of 85% for miR-576-5p (Figure 3.2). Therefore, this miRNA was unacceptable as a biomarker. As for the other two miRNAs, the lower bound of the false positive rate of miR-340-5p was 55% when the lower bound of the sensitivity was 85% and the lower bound of the false positive rate of miR-451a was 65% when the lower bound of the sensitivity was 85%. Therefore, miR-451a and miR-340-5p were considered as potential biomarkers compared to the other miRNAs. The extreme situation was checked as well, that is AJCC-0 vs. AJCC-3 (Table 3.2), and miR-451a was further supported as a potential biomarker in this analysis of extreme response phenotypes. Therefore, miR-451a was selected as a biomarker for the prediction of responders. Although miR-340-5p was not

significant in AJCC-0 vs. AJCC-3 (P=0.088), it was selected because the lower bound of the false positive rate estimate for AJCC-0 vs. AJCC-1.2.3 (55%) was lower than that of miR-451a (65%) at a lower bound sensitivity of 85%.

Table 3.1: *miRNAs as biomarkers for the prediction of responders (AJCC0 vs. AJCC123). A thick black line borders the miRNAs with AUC>0.8. The pink colour represents p value<0.05, the orange colour represents AUC>0.8.*

miRNA	**AJCC 0** vs. **1.2.3 MWU p value**	**AUC**
hsa.-miR-451a	0.000	0.924
hsa-miR-340-5p	0.000	0.909
hsa-miR-576-5p	0.004	0.828
hsa-miR-17-3p	0.014	0.788
hsa-miR-103a-3p	0.014	0.783
hsa-miR-10a-5p	0.020	0.768
hsa-miR-27b-3p	0.020	0.768
hsa-miR-147b	0.020	0.768
hsa-miR-361-3p	0.023	0.763
hsa-miR-3613-5p	0.023	0.763
hsa-miR-449c-5p	0.026	0.760
hsa-miR-365a-5p	0.026	0.760
hsa-miR-769-5p	0.033	0.747

hsa-miR-4521	0.033	0.747
hsa-miR-26a-2-3p	0.036	0.745
hsa-miR-141-3p	0.041	0.737
hsa-miR-10b-5p	0.046	0.732
hsa-miR-424-3p	0.046	0.732

Table 3.2: *miRNAs as biomarkers for the prediction of responders (AJCC-0 vs. AJCC-3). A thick black line borders the miRNAs that were significant in the analysis of AJCC-0 vs. AJCC-1.2.3. The pink colour represents p value<0.05, the orange colour represents AUC>0.8.*

miRNA	**AJCC 0** vs. **3** **MWU p value**	**AUC**
hsa-miR-451a	0.003	0.944
hsa-miR-1301-3p	0.003	0.944
hsa-miR-361-3p	0.008	0.907
hsa-miR-552-3p	0.008	0.907
hsa-miR-503-5p	0.008	0.907
hsa-miR-15b-3p	0.012	0.889
hsa-miR-767-5p	0.014	0.889
hsa-miR-10a-5p	0.026	0.852

hsa-miR-127-5p	0.032	0.843
hsa-miR-26b-3p	0.034	0.843
hsa-miR-31-5p	0.036	0.833
hsa-miR-130a-3p	0.036	0.833
hsa-miR-552-5p	0.042	0.778
hsa-miR-1269a	0.048	0.815
hsa-miR-99a-5p	0.050	0.815
hsa-miR-93-3p	0.050	0.815
hsa-miR-664a-5p	0.050	0.815
hsa-miR-139-3p	0.050	0.815
hsa-miR-3609	0.050	0.815
hsa-miR-32-5p	0.050	0.815

Figure 3.1: *miRNAs as biomarkers for the prediction of responders.*

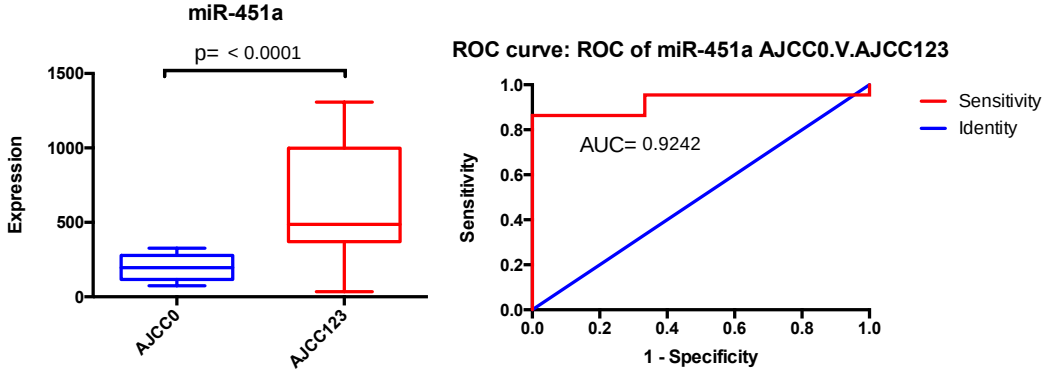

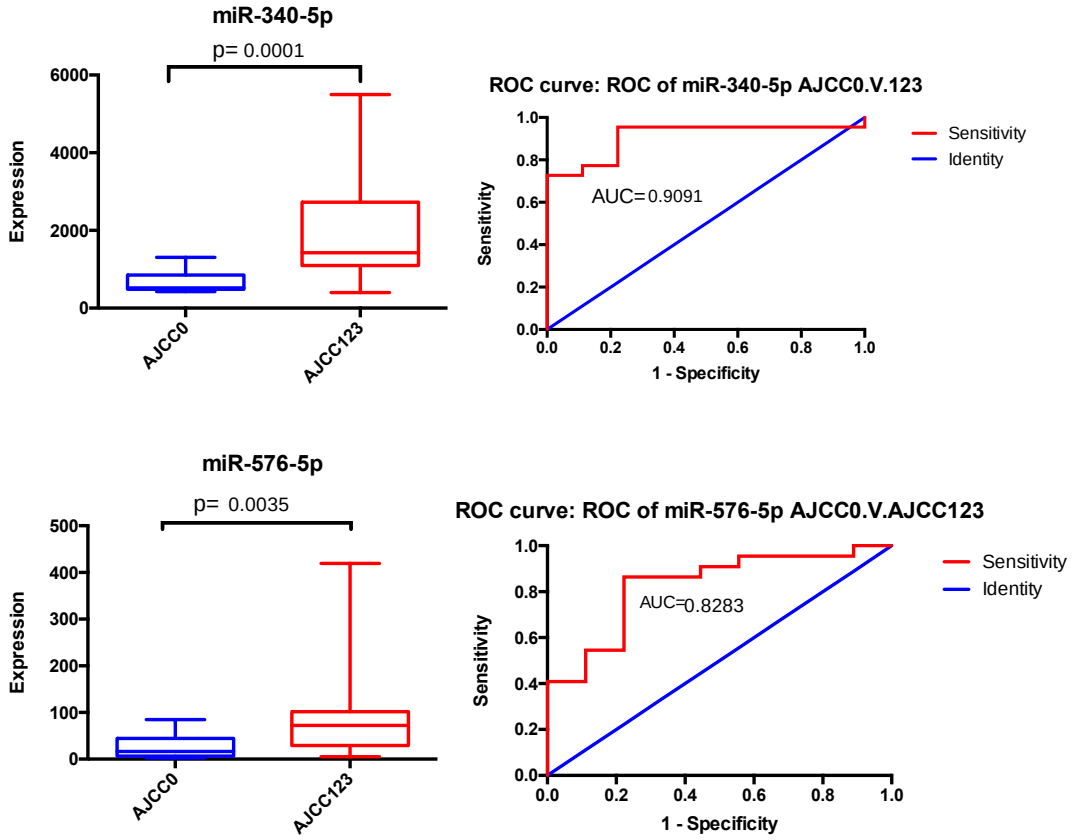

Figure 3.2: *The lower bound of the false positive rate and the sensitivity of the miRNAs.*

A: miR-340-5p: The lower bound of the false positive rate is 55% (green arrow), when the lower bound of the sensitivity is 85% (blue arrow).

B: miR-451a: The lower bound of the false positive rate is 65% (green arrow), when the lower bound of the sensitivity is 85% (blue arrow).

C: miR-576-5p: The lower bound of the false positive rate is 90% (green arrow), when the lower bound of the sensitivity is 85% (blue arrow).

A B

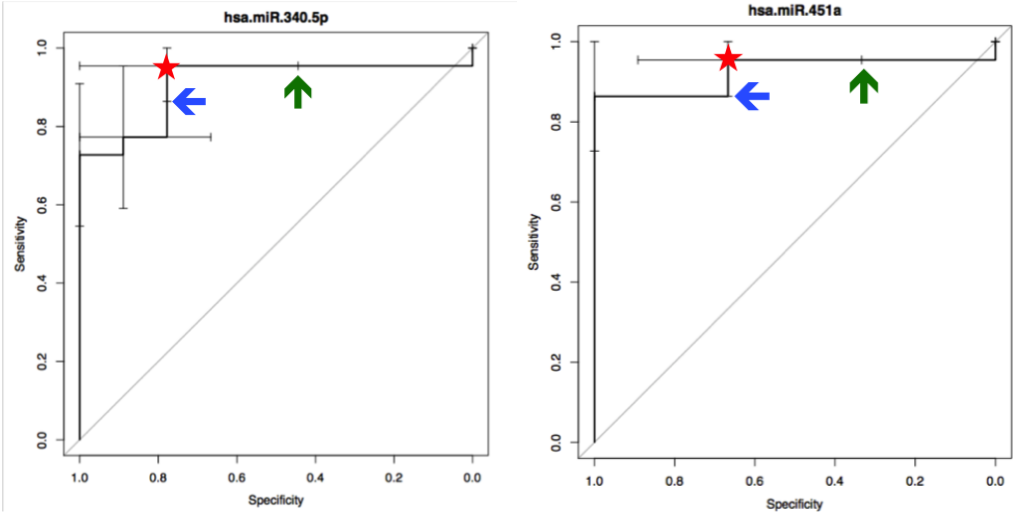

C

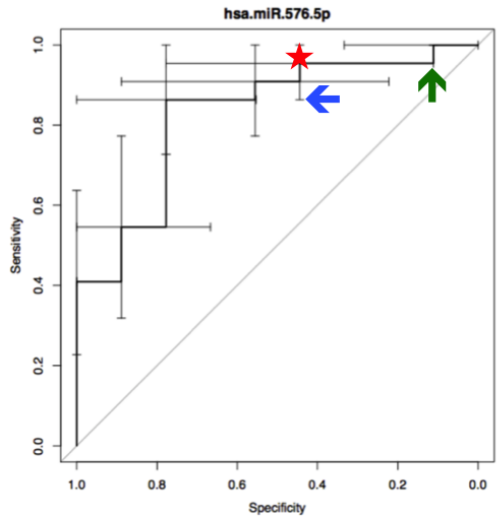

3.3.1.2 piRNAs

We identified three piRNAs as potential biomarkers for the prediction of responders, DQ576665, DQ598428, and DQ590407, and they were supported in an analysis of extreme response phenotypes as well, that was AJCC-0 vs. AJCC-3(p=0.026, p=0.018 and p=0.036, respectively; Table 3.3 and Table 3.4). The ROC curve showed that all of them were excellent biomarkers (Figure 3.3). However, only DQ576665 and DQ598428 were adequate for the biomarkers of responders according to the lower bound of the false positive rate (Figure 3.4).

Table 3.3: *piRNAs as biomarkers for the prediction of responders (AJCC-0 vs. AJCC-1.2.3). A thick black line borders the piRNAs with AUC>0.8. The pink colour represents p value<0.05, the orange colour represents AUC>0.8.*

piRNA	AJCC 0 vs. 1.2.3 MWU p value	AUC
DQ576665	0.002	0.869
DQ598428	0.003	0.843
DQ590407	0.005	0.818
DQ596723	0.009	0.798
DQ591185	0.010	0.793
DQ588486	0.016	0.780
DQ570117	0.018	0.773
DQ570640	0.023	0.763
DQ596993	0.023	0.763
DQ580344	0.023	0.763
DQ588165	0.023	0.765
DQ573947	0.028	0.758
DQ595103	0.033	0.747
DQ576917	0.033	0.747
DQ592780	0.034	0.747
DQ581701	0.039	0.742
DQ575658	0.039	0.742
DQ576780	0.046	0.732
DQ598130	0.046	0.732

Table 3.4: *piRNAs as biomarkers for the prediction of responders (AJCC-0 vs. AJCC-3). A thick black line borders the piRNAs that were significant in the analysis of AJCC-0 vs. AJCC-1.2.3. The pink colour represents p value<0.05, the orange colour represents AUC>0.8.*

piRNA	AJCC 0 vs. 3 MWU p value	AUC

DQ570640	0.008	0.907
DQ599822	0.008	0.907
DQ598428	0.018	0.870
DQ571591	0.018	0.870
DQ580344	0.021	0.870
DQ588165	0.021	0.870
DQ576665	0.026	0.852
DQ571335	0.026	0.852
DQ590407	0.036	0.833
DQ598130	0.036	0.833
DQ593767	0.036	0.833
DQ598263	0.050	0.815
DQ596932	0.050	0.815
DQ593671	0.050	0.815
piR-hsa-32187	0.050	0.815
DQ580946	0.051	0.815
DQ588486	0.057	0.806
DQ586779	0.059	0.806
DQ596993	0.066	0.796

Figure 3.3: *piRNAs as biomarkers for the prediction of responders.*

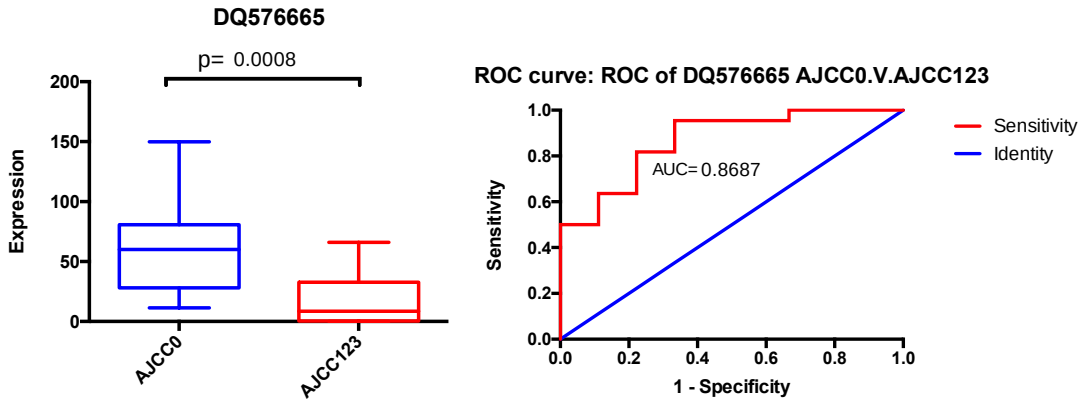

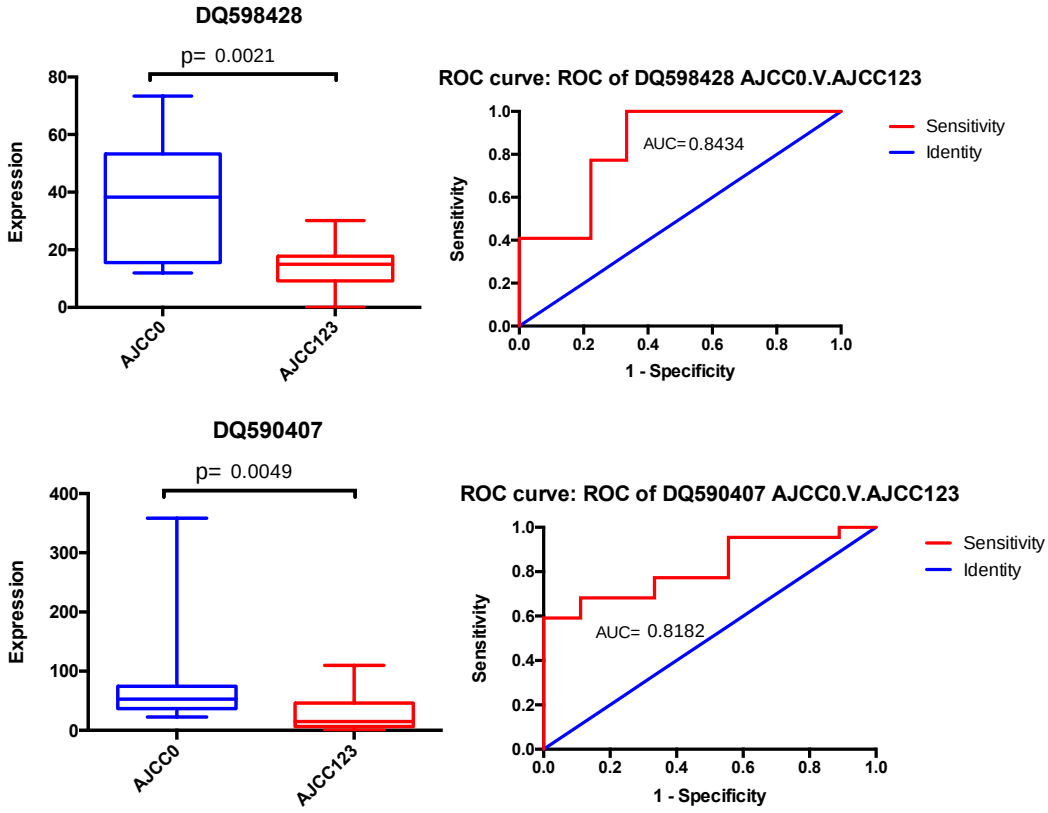

Figure 3.4: *The lower bound of the false positive rate and sensitivity of the piRNAs.*

A: DQ576665: The lower bound of the false positive rate is 65% (green arrow) when the lower bound of the sensitivity is 83% (blue arrow).

B: DQ598428: The lower bound of the false positive rate is 65% (green arrow) when the lower bound of the sensitivity is 100%.

C: DQ590407: The lower bound of the false positive rate is 90% (green arrow) when the lower bound of the sensitivity is 85%(blue arrow).

A B

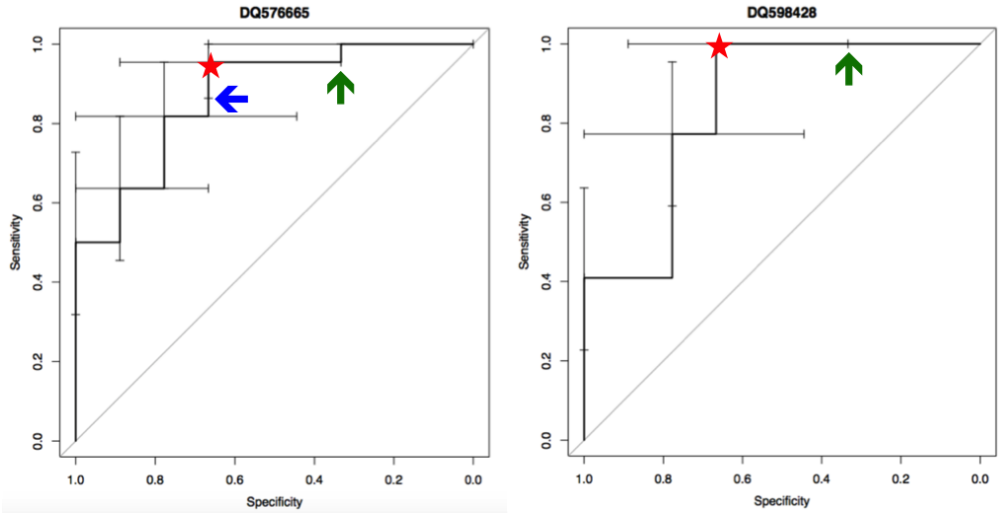

C

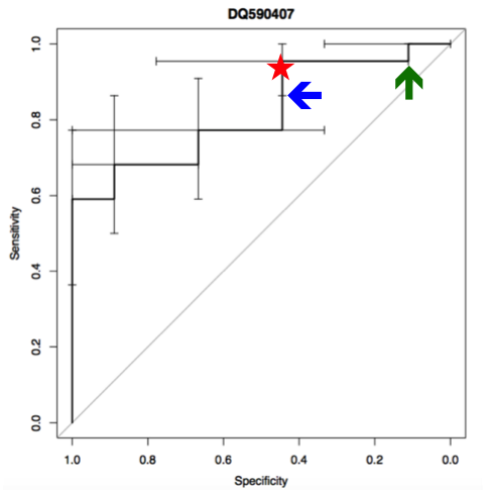

3.3.1.3 snoRNAs

There were 4 snoRNAs selected as biomarkers for the prediction of responders, which were SNORD58B.201, SNORD123.201, SNORA2B.201, and SNORD18A.201 (Table 3.5, Figure 3.5). SNORD58B.201, SNORD123.201, and SNORD18A.201 were significant in AJCC-0 vs. AJCC-3 (Table 3.6). However, all of them were unacceptable according to the lower bound of the false positive rate and the lower bound of the sensitivity (Figure 3.6).

Table 3.5: *snoRNAs as biomarkers for the prediction of responders (AJCC-0 vs. AJCC-1.2.3). A thick black line borders the snoRNAs with AUC>0.8. The pink colour represents p value<0.05, the orange colour represents AUC>0.8.*

snoRNA	**AJCC 0** vs. **1.2.3** **MWUp value**	**AUC**
SNORD58B-201	0.006	0.813
SNORD123-201	0.006	0.813
SNORA2B-201	0.006	0.813
SNORD18A-201	0.008	0.803
SNORD42B-201	0.009	0.798
SNORD54-201	0.016	0.778
U8-4-201	0.016	0.778
SNORD6-201	0.039	0.742
SNORD52-201	0.039	0.742
SNORD5-201	0.046	0.732
SNORA31-201	0.053	0.727
SNORD117-201	0.057	0.722
SNORA38-201	0.057	0.722
SNORD37-201	0.064	0.717

Table 3.6: *snoRNAs as biomarkers for the prediction of responders (AJCC-0 vs. AJCC-3). A thick black line borders the snoRNAs that were significant in the analysis of AJCC-0 vs. AJCC-1.2.3. The pink colour represents p value<0.05, the orange colour represents AUC>0.8.*

snoRNA	**AJCC 0** vs. **3** **MWU p value**	**AUC**
SNORD58B-201	0.003	0.944
SNORD54-201	0.003	0.944
SNORA8-201	0.005	0.926
SNORD42B-201	0.008	0.907
SNORD114-17-201	0.008	0.907
SNORD18A-201	0.018	0.870
SNORD37-201	0.018	0.870
SNORD14A-201	0.018	0.870
SNORA38-201	0.026	0.852
SNORD92-201	0.026	0.852
SNORA77-201	0.026	0.852
SNORD123-201	0.036	0.833
SNORA27-201	0.050	0.815
SNORD113-8-201	0.050	0.815

Figure 3.5: *snoRNAs as biomarkers for the prediction of responders.*

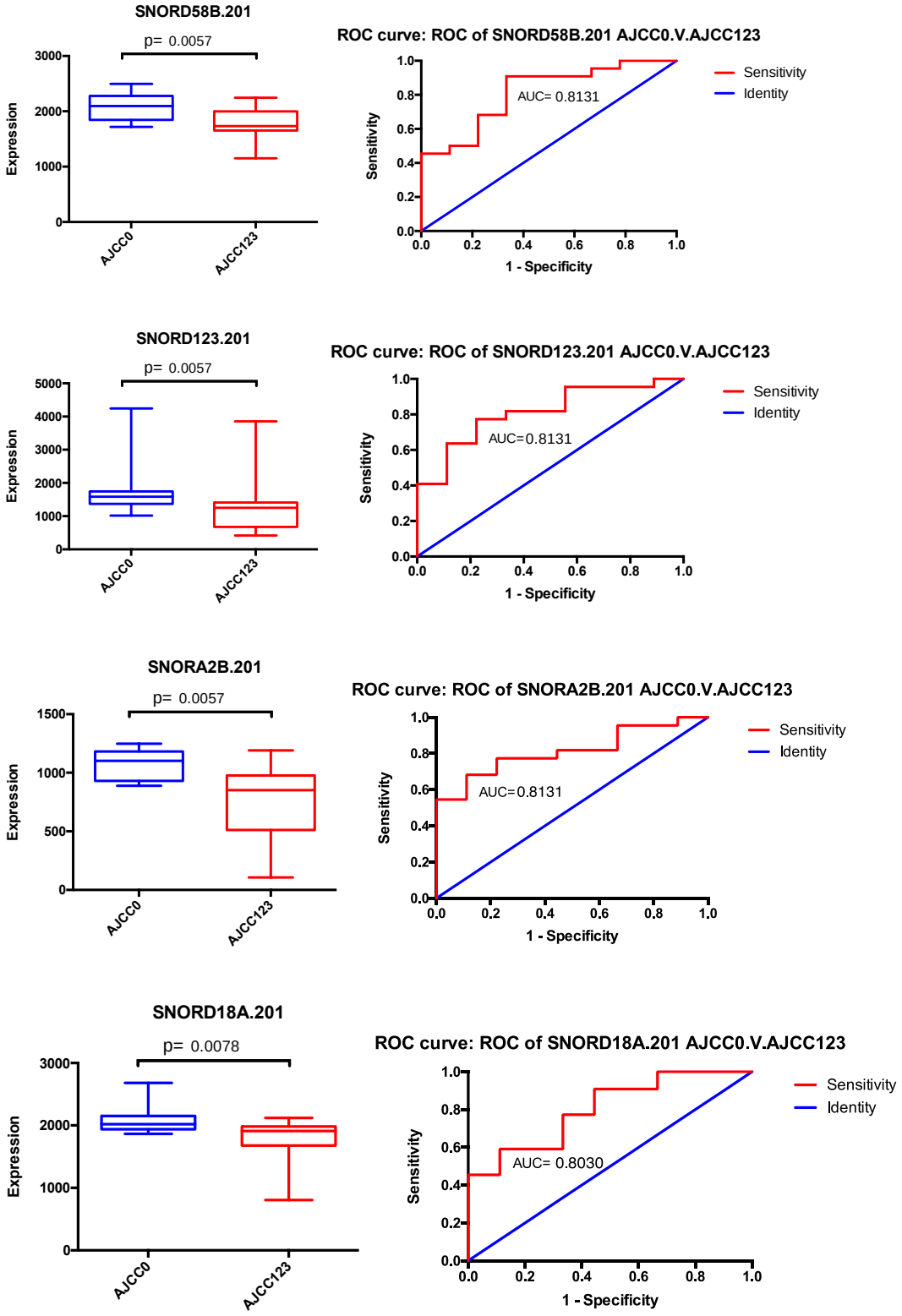

Figure 3.6: *The lower bound of the false positive rate and sensitivity of the snoRNAs.*

A: SNORD58B.201: The lower bound of the false positive rate is 65% (green arrow) when the lower bound of the sensitivity is 75% (blue arrow).

B: SNORD123.201: The lower bound of the false positive rate is 90% (green arrow) when the lower bound of the sensitivity is 85% (blue arrow).

C: SNORA2B.201: The lower bound of the false positive rate is 100% (green arrow), when the lower bound of the sensitivity is 85% (blue arrow).

D: SNORD18A.201: The lower bound of the false positive rate is 80% (green arrow), when the lower bound of the sensitivity is 92% (blue arrow).

A

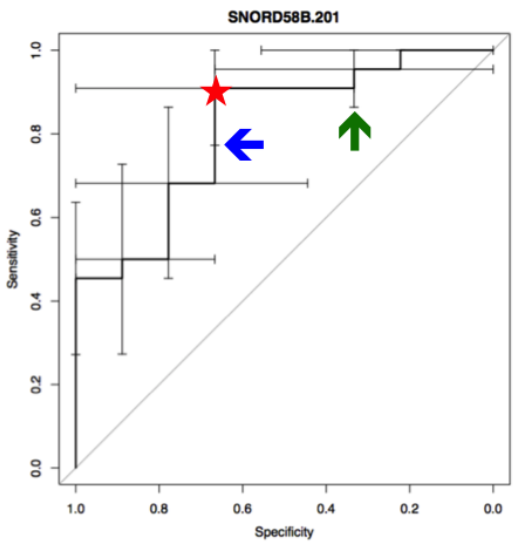

B

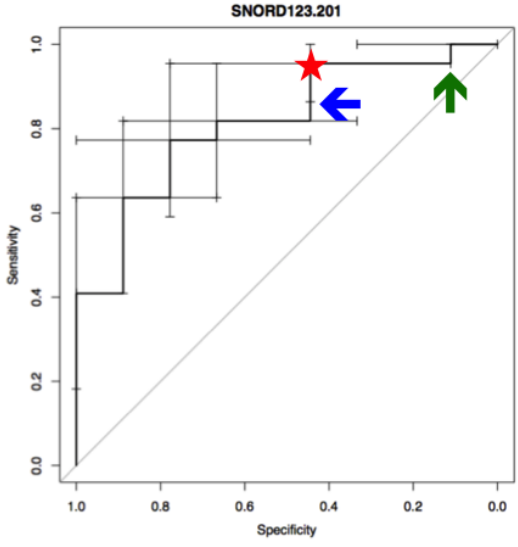

C

D

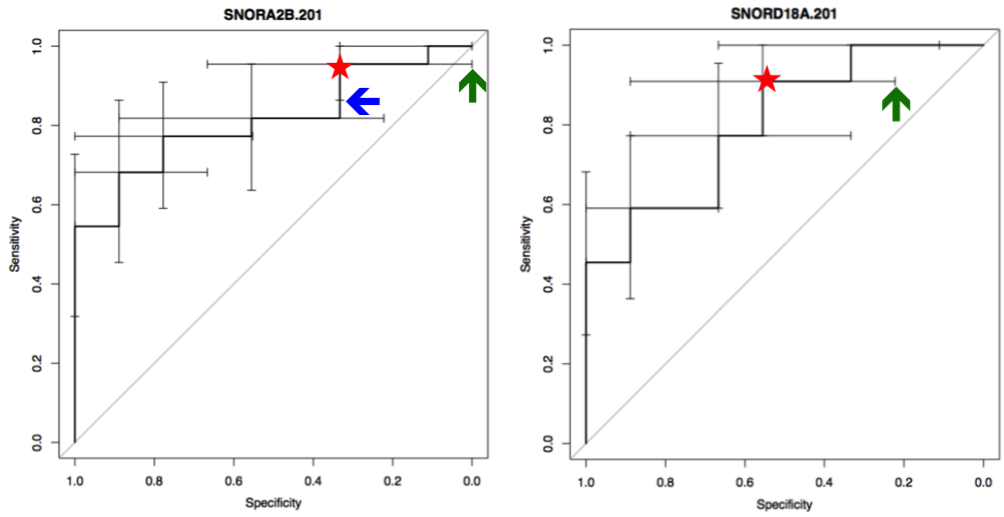

3.3.1.4 snRNAs

As for the snRNAs, RNU1.148P.201 was identified as a potential biomarker for the prediction of responders (Table 3.7, Figure 3.7), but this snRNA was not significant in the extreme situation that was AJCC-0 vs. AJCC-3 (Table 3.8). Furthermore, the lower bound of the false positive rate was as high as 90% when the lower bound of the sensitivity was 75%. Therefore, there were no suitable snRNAs as biomarkers of treatment response (Figure 3.8).

Table 3.7: *snRNAs as biomarkers for the prediction of responders (AJCC-0 vs. AJCC-1.2.3). A thick black line borders the snRNAs with AUC>0.8. The pink colour represents p value<0.05, the orange colour represents AUC>0.8.*

snRNA	**AJCC 0 vs. 1.2.3 MWU p value**	**AUC**
RNU1-148P-201	0.008	0.803
RNU6-1016P-201	0.064	0.717
U2-6-201	0.086	0.702

RNU4ATAC-201	0.086	0.702

Table 3.8: *snRNAs as biomarkers for the prediction of responders (AJCC-0 vs. AJCC-3). . The pink colour represents p value<0.05, the orange colour represents AUC>0.8.*

snRNA	**AJCC 0** vs. **3** **MWU p value**	**AUC**
RNU5E-4P-201	0.005	0.926
RNU5E-6P-201	0.018	0.870
RNU5F-1-201	0.036	0.833
RNU6ATAC25P-201	0.050	0.815

Figure 3.7: *snRNAs as biomarkers for the prediction of responders.*

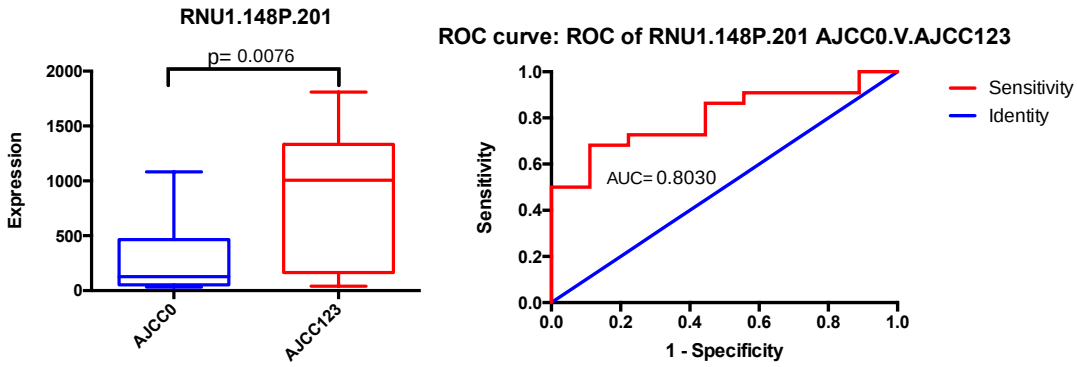

Figure 3.8: *The lower bound of the false positive rate and sensitivity of the snoRNAs.*

RNU1.148P.201: The lower bound of the false positive rate is 90% (green arrow) when the lower bound of the sensitivity is 74% (blue arrow).

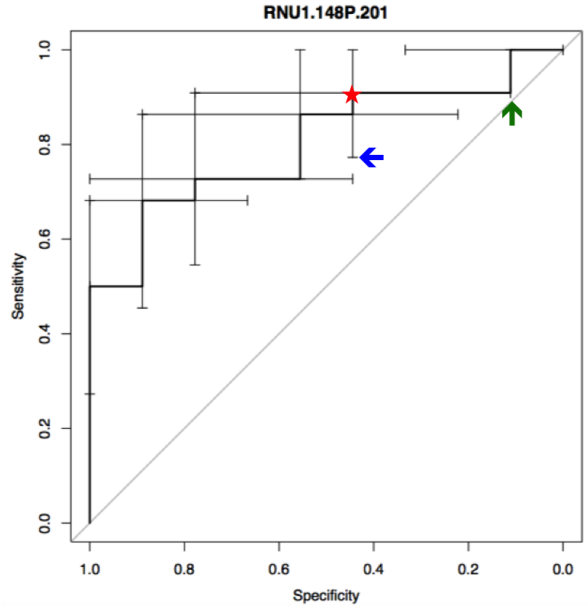

3.3.2 Small RNAs as biomarkers for the prediction of non-responders

3.3.2.1 miRNAs

The results revealed that 12 miRNAs might be potential biomarkers for the prediction of non-responders (Table 3.9, Figure 3.9), and nine of them were supported in the extreme situation of AJCC-0 vs. AJCC-3 (the 12 miRNAs all had $p<0.05$). However, only five of them were selected according to the lower bound of the false positive rate and the lower bound of the sensitivity, that were miR-767-5p, miR-1301-3p, miR-552-3p, miR-99a-5p, and miR-206 (Figure 3.10).

Table 3.9: *miRNAs as biomarkers for the prediction of non-responders (AJCC-0.1.2 vs. AJCC-3). A thick black line borders the miRNAs with AUC>0.8. The pink colour represents p value<0.05, the orange colour represents AUC>0.8.*

3.3.2.1.1.1 miRNA	**AJCC 0.1.2** vs. **3 MWU p value**	AUC
hsa-miR-503-5p	0.003	0.873

hsa-miR-767-5p	0.006	0.867
hsa-miR-1301-3p	0.007	0.847
hsa-miR-130a-3p	0.009	0.840
hsa-miR-15b-3p	0.010	0.833
hsa-miR-552-3p	0.015	0.820
hsa-miR-26b-3p	0.018	0.820
hsa-miR-99a-5p	0.017	0.813
hsa-miR-32-5p	0.017	0.813
hsa-miR-31-3p	0.020	0.813
hsa-miR-24-1-5p	0.023	0.807
hsa-miR-206	0.026	0.800
hsa-miR-197-3p	0.031	0.787
hsa-miR-455-5p	0.031	0.787
hsa-miR-628-3p	0.033	0.787
hsa-miR-125b-1-3p	0.035	0.780
hsa-miR-7706	0.035	0.780
hsa-miR-146a-3p	0.040	0.777
hsa-miR-139-3p	0.048	0.767
hsa-miR-154-5p	0.043	0.767

hsa-miR-425-5p	0.046	0.767
hsa-miR-370-3p	0.046	0.767

Table 3.10: *miRNAs as biomarkers for the prediction of non-responders (AJCC-0 vs. AJCC-3). A thick black line borders the miRNAs that were significant in the analysis of AJCC-0.1.2 VS AJCC-3. The pink colour represents p value<0.05, the orange colour represents AUC>0.8.*

miRNA	**AJCC 0** vs. **3** **MWU p value**	**AUC**
hsa-miR-451a	0.003	0.944
hsa-miR-1301-3p	0.003	0.944
hsa-miR-361-3p	0.008	0.907
hsa-miR-552-3p	0.008	0.907
hsa-miR-503-5p	0.008	0.907
hsa-miR-15b-3p	0.012	0.889
hsa-miR-767-5p	0.014	0.889
hsa-miR-10a-5p	0.026	0.852
hsa-miR-127-5p	0.032	0.843
hsa-miR-26b-3p	0.034	0.843

hsa-miR-31-5p	0.036	0.833
hsa-miR-130a-3p	0.036	0.833
hsa-miR-552-5p	0.042	0.778
hsa-miR-1269a	0.048	0.815
hsa-miR-99a-5p	0.050	0.815
hsa-miR-93-3p	0.050	0.815
hsa-miR-664a-5p	0.050	0.815
hsa-miR-139-3p	0.050	0.815
hsa-miR-3609	0.050	0.815
hsa-miR-32-5p	0.050	0.815

Figure 3.9: *miRNAs as biomarkers for the prediction of non-responders.*

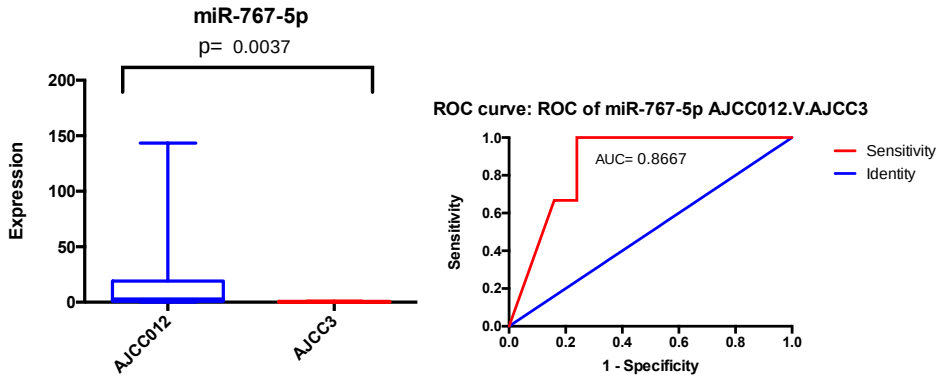

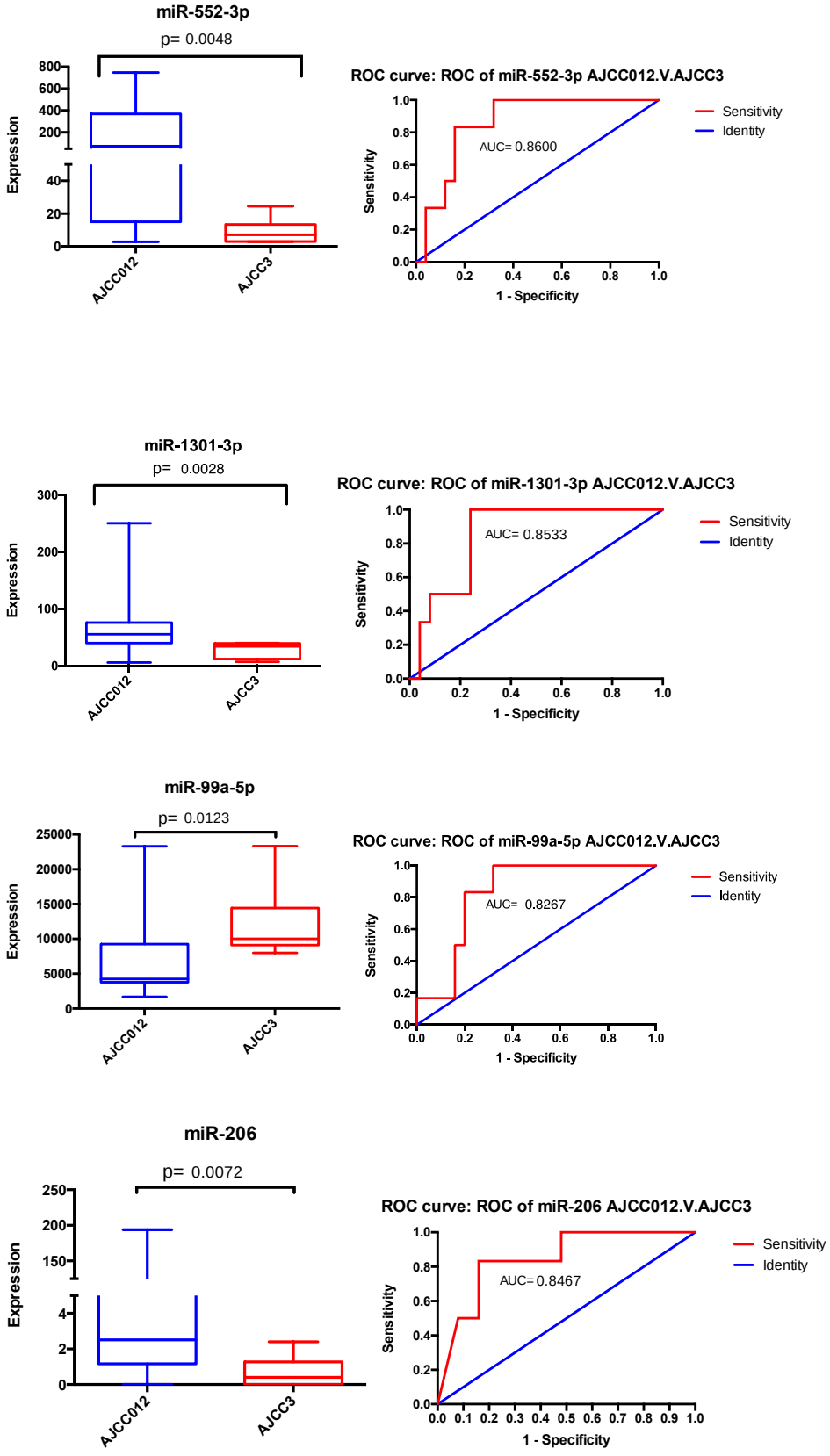

Figure 3.10: *The lower bound of the false positive rate and sensitivity of the miRNAs.*

A: miR-767-5P: The lower bound of the false positive rate is 45% (green arrow) when the sensitivity is 100%.
B: miR-1301-3p: The lower bound of the false positive rate is 47% (green arrow) when the sensitivity is 100%.
C: miR-552-3p: The lower bound of the false positive rate is 48% (green arrow) when the sensitivity is 100%.
D: miR-99a-5p: The lower bound of the false positive rate is 55% (green arrow) when the sensitivity is 100%.
E: miR-206: The lower bound of the false positive rate is 60% (green arrow) when the sensitivity is 100%.

A

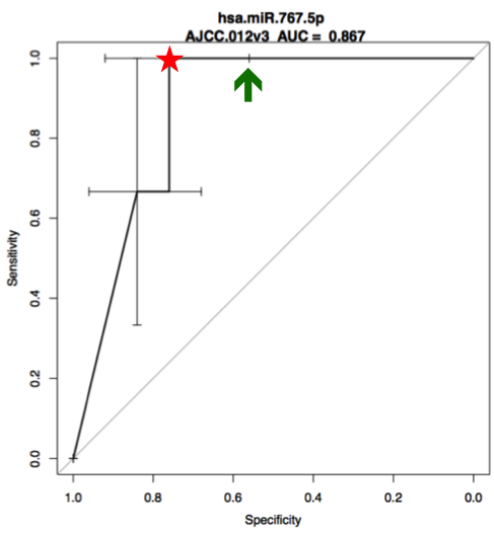

B

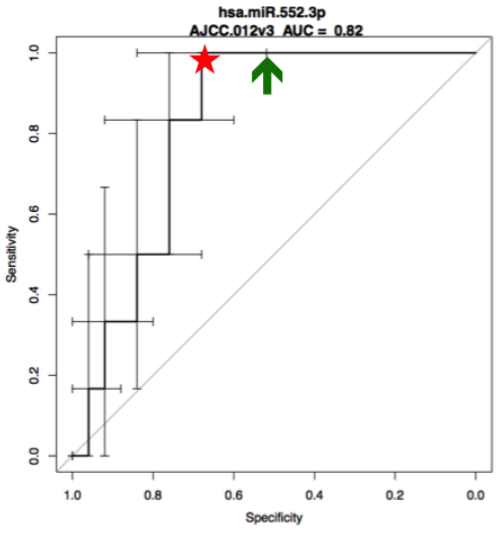

C

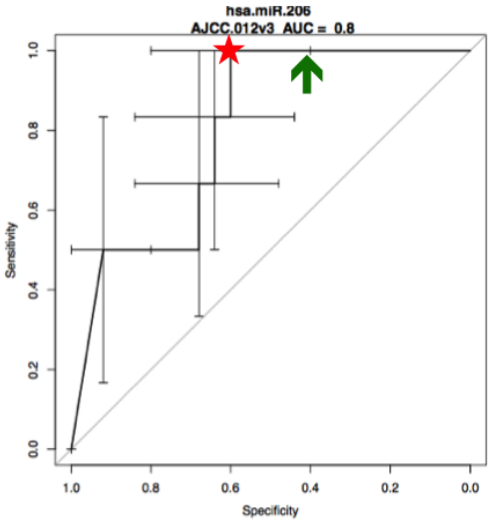

D

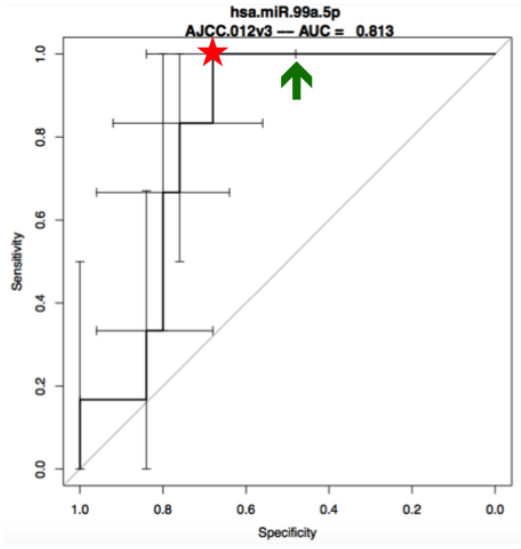

E

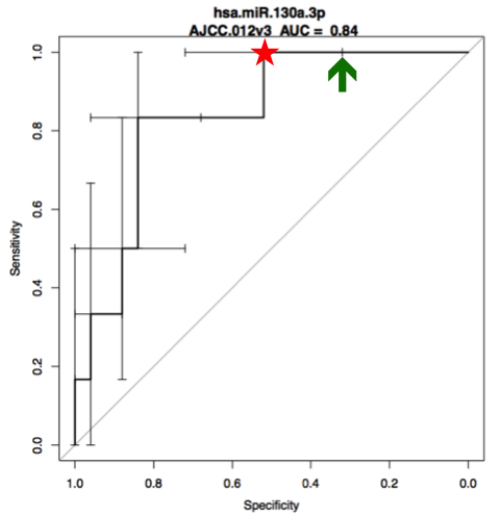

3.3.2.2 piRNAs

We identified five piRNAs as potential biomarkers for the prediction of non-responders that were piR-hsa-32187, DQ598641, DQ599147, DQ582265, and DQ599822 (Table 3.11 and Figure 3.11) and two of them were significant in AJCC-0 vs. AJCC-3 (Table 3.12, DQ599822 p=0.008, piR-hsa-32187 p=0.050). However, only piR-has-32187, DQ598641, DQ599147 were picked for the biomarkers of responders according to the lower bound of the false positive rate (Figure 3.12).

Table 3.11: *piRNAs as biomarkers for the prediction of non-responders (AJCC-0.1.2 vs. AJCC-3). A thick black line borders the piRNAs with AUC>0.8. The pink colour represents p value<0.05, the orange colour represents AUC>0.8.*

piRNA	**AJCC 0.1.2** vs. **3 MWU p value**	AUC
piR-hsa-32187	0.003	0.880
DQ598641	0.006	0.853
DQ599147	0.011	0.840
DQ582265	0.012	0.837
DQ599822	0.015	0.820
DQ580256	0.031	0.787
DQ593767	0.031	0.787
DQ580084	0.033	0.787

DQ597990	0.041	0.773
DQ573323	0.043	0.740

Table 3.12: *piRNAs as biomarkers for the prediction of non-responders (AJCC-0 vs. AJCC-3). A thick black line borders the piRNAs that were significant in the analysis of AJCC-0.1.2 vs. AJCC-3. The pink colour represents p value<0.05, the orange colour represents AUC>0.8.*

piRNA	**AJCC 0** vs. **3** **MWU p value**	**AUC**
DQ570640	0.008	0.907
DQ599822	0.008	0.907
DQ598428	0.018	0.870
DQ571591	0.018	0.870
DQ580344	0.021	0.870
DQ588165	0.021	0.870
DQ576665	0.026	0.852
DQ571335	0.026	0.852
DQ590407	0.036	0.833
DQ598130	0.036	0.833
DQ593767	0.036	0.833
DQ598263	0.050	0.815
DQ596932	0.050	0.815
DQ593671	0.050	0.815
piR-hsa-32187	0.050	0.815
DQ580946	0.051	0.815
DQ588486	0.057	0.806
DQ586779	0.059	0.806
DQ596993	0.066	0.796

Figure 3.11: *piRNAs as biomarkers for the prediction of non-responders.*

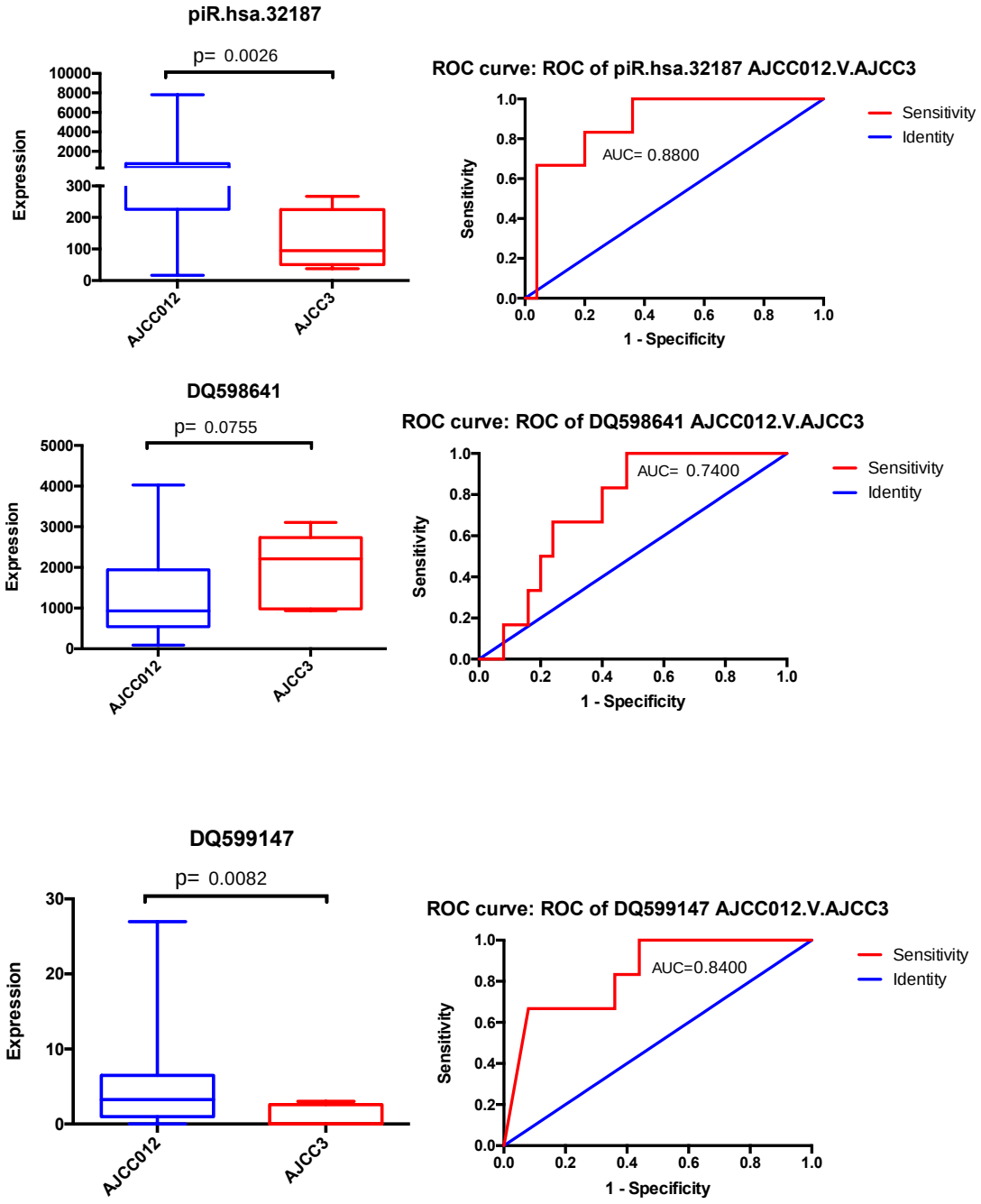

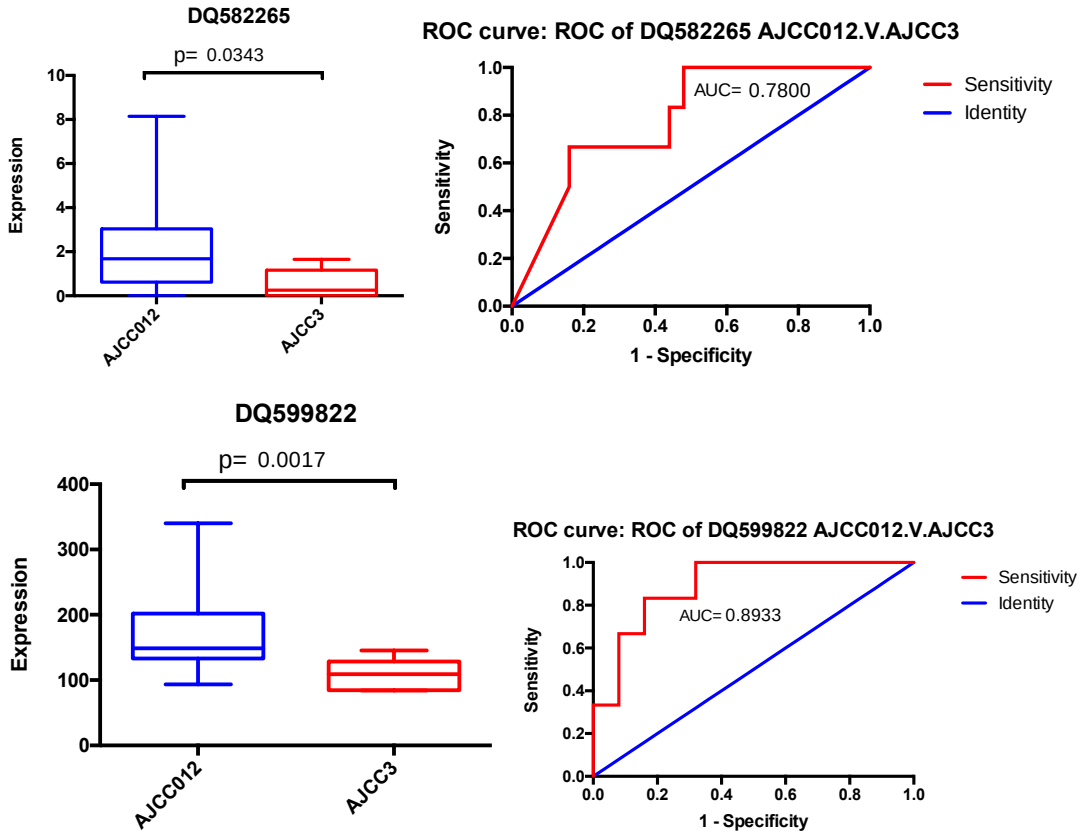

Figure 3.12: *The lower bound of the false positive rate and sensitivity of the piRNAs.*

A: piR-has-32187: The lower bound of the false positive rate is 50% (green arrow) when the lower bound of the sensitivity is 100%.

B: DQ598641: The lower bound of the false positive rate is 48% (green arrow) when the lower bound of the sensitivity is 100%.

C: DQ599147: The lower bound of the false positive rate is 65% (green arrow) when the lower bound of the sensitivity is 100%.

D: DQ582265: The lower bound of the false positive rate is 68% (green arrow) when the lower bound of the sensitivity is 100%.

E: DQ599822: The lower bound of the false positive rate was 70% (green arrow) when the lower bound of the sensitivity is 100%.

A

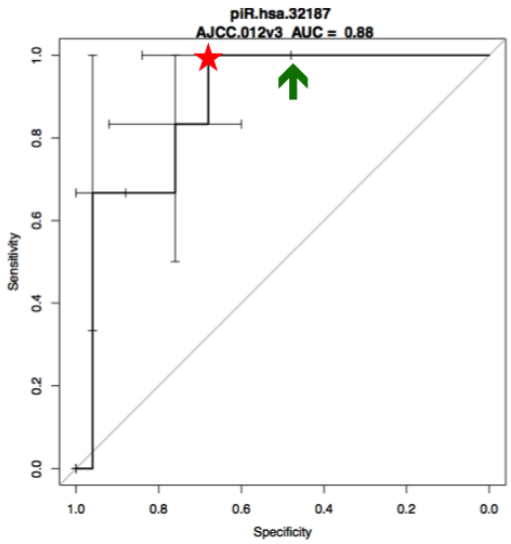
piR.hsa.32187
AJCC.012v3 AUC = 0.88
Sensitivity
Specificity
1.0
0.8
0.6
0.4
0.2
0.0

B

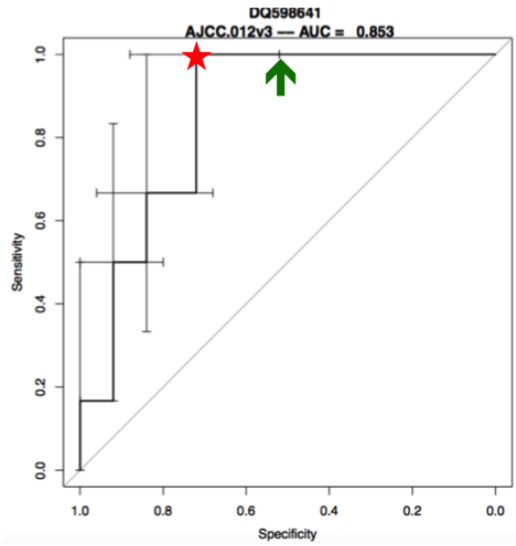
DQ598641
AJCC.012v3 — AUC = 0.853
Sensitivity
Specificity
1.0
0.8
0.6
0.4
0.2
0.0

C

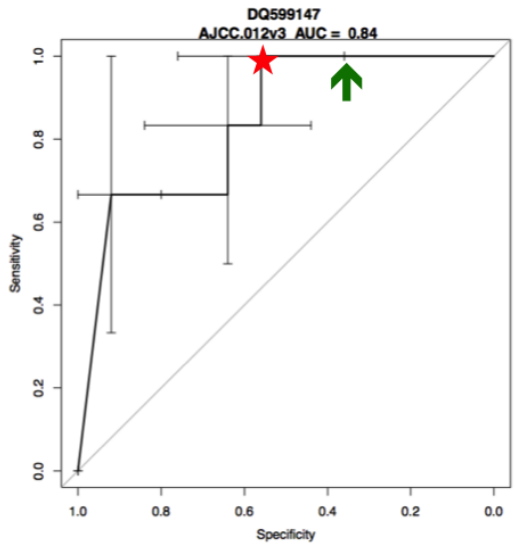
DQ599147
AJCC.012v3 AUC = 0.84
Sensitivity
Specificity
1.0
0.8
0.6
0.4
0.2
0.0

D

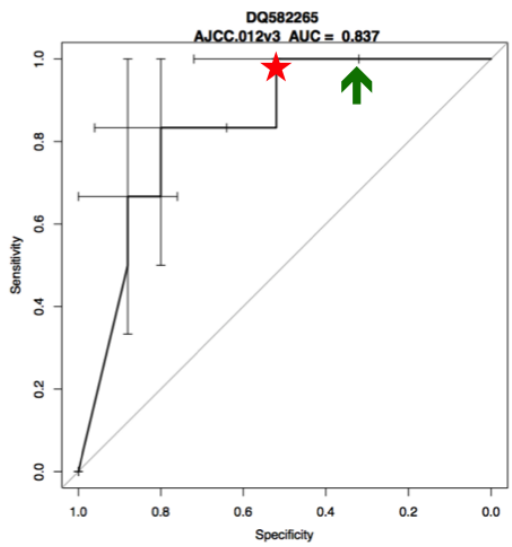
DQ582265
AJCC.012v3 AUC = 0.837
Sensitivity
Specificity
1.0
0.8
0.6
0.4
0.2
0.0

E

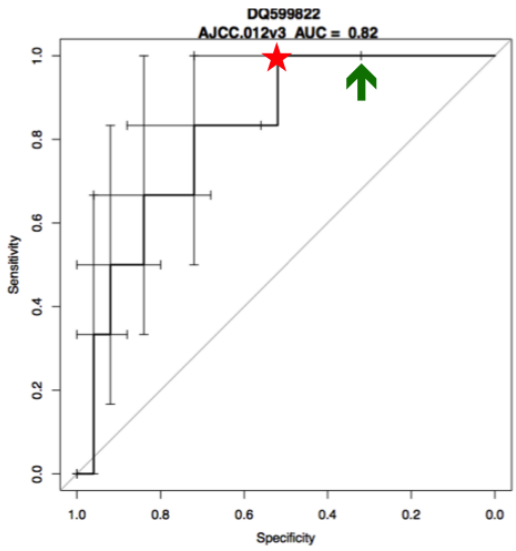

Table 3.13: *snoRNAs as biomarkers for the prediction of non-responders (AJCC-0.1.2 vs. AJCC-3). A thick black line borders the snoRNAs with AUC>0.8. The pink colour represents p value<0.05, the orange colour represents AUC>0.8.*

snoRNA	**AJCC 012** vs. **3** **MWU p value**	**AUC**
SNORD114-17-201	0.003	0.873
SNORD14A-201	0.007	0.847
SNORD92-201	0.007	0.847
SNORD58B-201	0.012	0.827
SNORD15A-201	0.015	0.820
SNORD46-201	0.017	0.813
SNORD113-8-201	0.027	0.793
SNORA42-1-201	0.027	0.793
SNORA77-201	0.031	0.787

SNORA8-201	0.035	0.780
SNORD113-6-201	0.035	0.780
SNORD116-24-201	0.035	0.780
SNORA21-1-201	0.035	0.780
SNORD15B-201	0.041	0.773
SNORD36-1-201	0.041	0.773
SNORD54-201	0.041	0.773

3.3.2.3 snoRNAs

We identified six snoRNAs as biomarkers for the prediction of non-responders, which were SNORD114.17.201, SNORD14A.201, SNORD92.201, SNORD58B.201, SNORD15A.201, and SNORD46.201 (Table 3.13 and Figure 3.13) and four of them were significant between AJCC-0 and AJCC-3 (Table 3.14). However, only SNORD58B.201, SNORD46.201, and SNORD114.17.201 were chosen as potential biomarkers for the prediction of non-responders according to the lower bound of the false positive rate and the lower bound of the sensitivity (Figure 3.14).

Table 3.14: *snoRNAs as biomarkers for the prediction of non-responders (AJCC-0 vs. AJCC-3). A thick black line borders the snoRNAs that were significant in the analysis of AJCC-0.1.2 vs. AJCC-3. The pink colour represents p value<0.05, the orange colour represents AUC>0.8.*

snoRNA	**AJCC 0** vs. **3** **MWU p value**	**AUC**
SNORD58B-201	0.003	0.944

SNORD54-201	0.003	0.944
SNORA8-201	0.005	0.926
SNORD42B-201	0.008	0.907
SNORD114-17-201	0.008	0.907
SNORD18A-201	0.018	0.870
SNORD37-201	0.018	0.870
SNORD14A-201	0.018	0.870
SNORA38-201	0.026	0.852
SNORD92-201	0.026	0.852
SNORA77-201	0.026	0.852
SNORD123-201	0.036	0.833
SNORA27-201	0.050	0.815
SNORD113-8-201	0.050	0.815

Figure 3.13: *snoRNAs as biomarkers for the prediction of non-responders.*

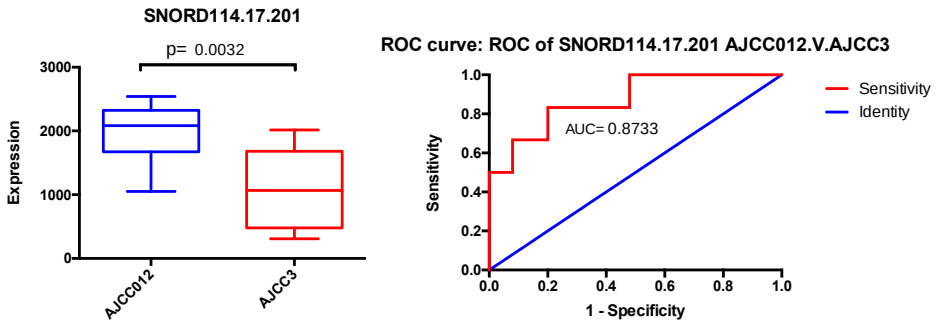

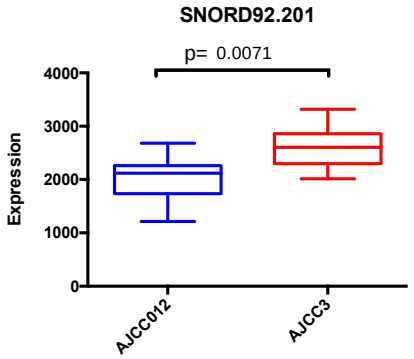
SNORD92.201
p= 0.0071
Expression
4000
3000
2000
1000
0
AJCC012
AJCC3

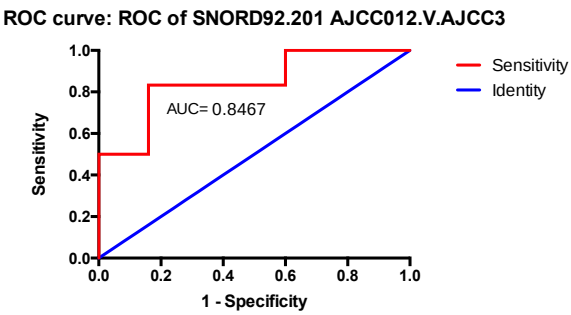
ROC curve: ROC of SNORD92.201 AJCC012.V.AJCC3
Sensitivity
1 - Specificity
AUC= 0.8467
Sensitivity
Identity

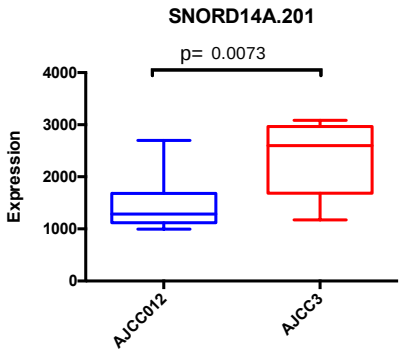
SNORD14A.201
p= 0.0073
Expression
4000
3000
2000
1000
0
AJCC012
AJCC3

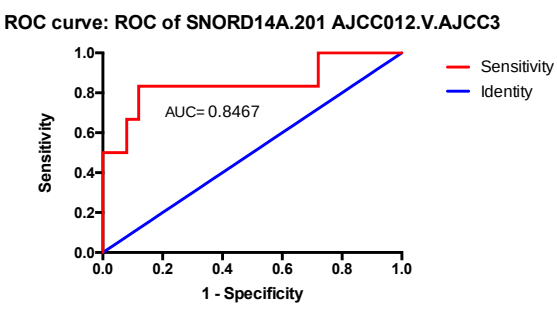
ROC curve: ROC of SNORD14A.201 AJCC012.V.AJCC3
Sensitivity
1 - Specificity
AUC= 0.8467
Sensitivity
Identity

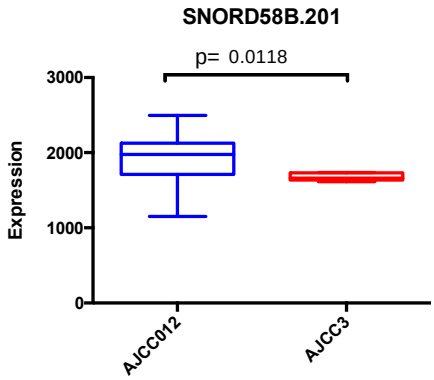
SNORD58B.201
p= 0.0118
Expression
3000
2000
1000
0
AJCC012
AJCC3

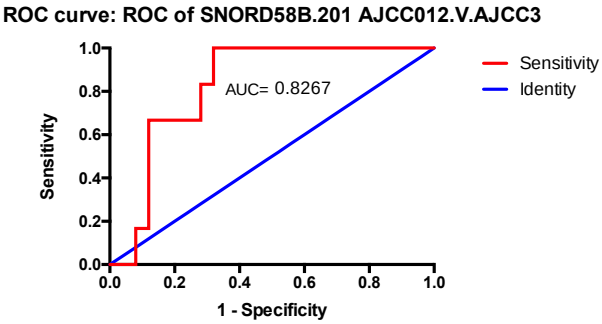
ROC curve: ROC of SNORD58B.201 AJCC012.V.AJCC3
Sensitivity
1 - Specificity
AUC= 0.8267
Sensitivity
Identity

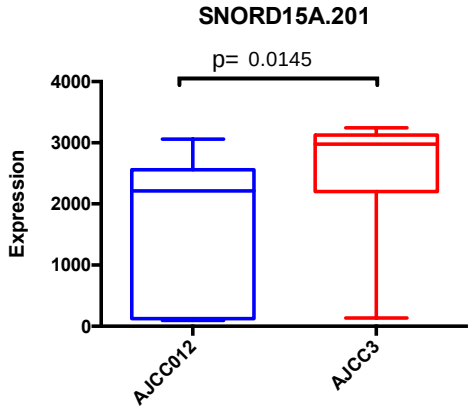
SNORD15A.201
p= 0.0145
Expression
4000
3000
2000
1000
0
AJCC012
AJCC3

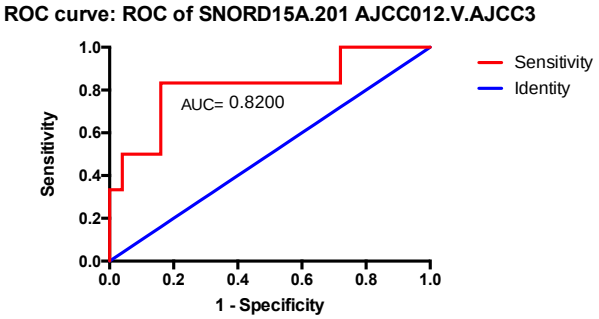
ROC curve: ROC of SNORD15A.201 AJCC012.V.AJCC3
Sensitivity
1 - Specificity
AUC= 0.8200
Sensitivity
Identity

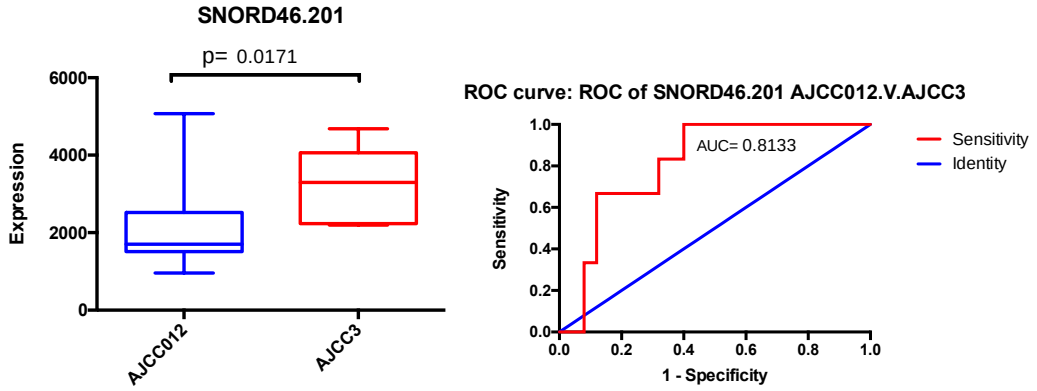

Figure 3.14: *The lower bound of the false positive rate and sensitivity of the snoRNAs.*

A: SNORD114.17.201: The lower bound of the false positive rate is 65% (green arrow) when the lower bound of the sensitivity is 100%.
B: SNORD14A.201: The lower bound of the false positive rate is 85% (green arrow) when the lower bound of the sensitivity is 100%.
C: SNORD92.201: The lower bound of the false positive rate is 80% (green arrow) when the lower bound of the sensitivity is 100%.
D: SNORD58B.201: The lower bound of the false positive rate is 55% (green arrow) when the lower bound of the sensitivity is 100%.
E: SNORD15A.201: The lower bound of the false positive rate is 90% (green arrow), when the lower bound of the sensitivity is 100%.
F: SNORD46.201: The lower bound of the false positive rate is 60% (green arrow) when the lower bound of the sensitivity is 100%.

A B

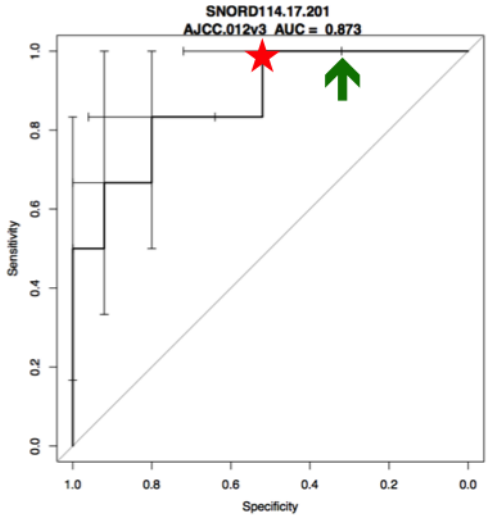
SNORD114.17.201
AJCC.012v3 AUC = 0.873
Sensitivity
Specificity
1.0
0.8
0.6
0.4
0.2
0.0

C

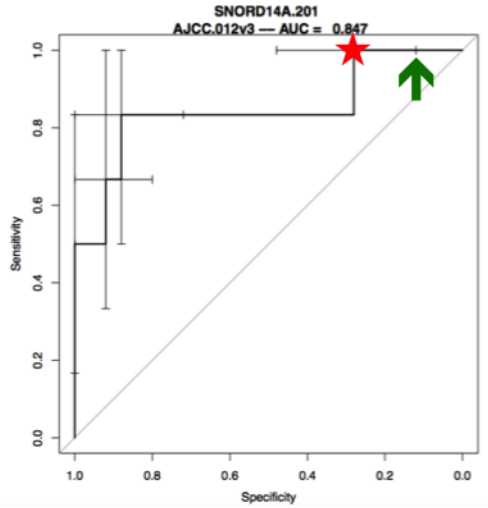
SNORD14A.201
AJCC.012v3 — AUC = 0.847
Sensitivity
Specificity
1.0
0.8
0.6
0.4
0.2
0.0

D

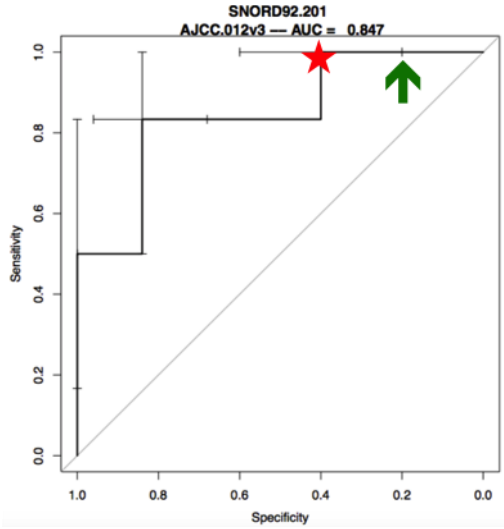
SNORD92.201
AJCC.012v3 — AUC = 0.847
Sensitivity
Specificity
1.0
0.8
0.6
0.4
0.2
0.0

E

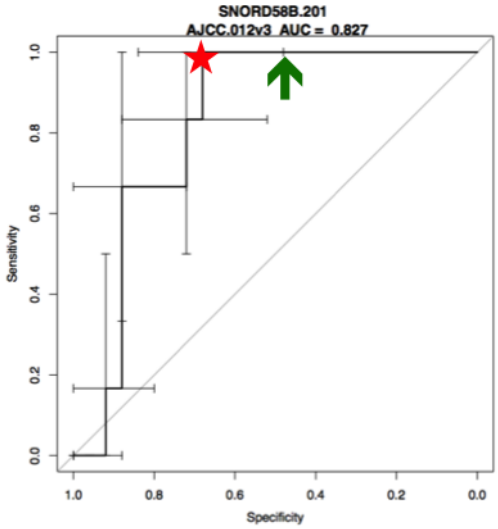
SNORD58B.201
AJCC.012v3 AUC = 0.827
Sensitivity
Specificity
1.0
0.8
0.6
0.4
0.2
0.0

F

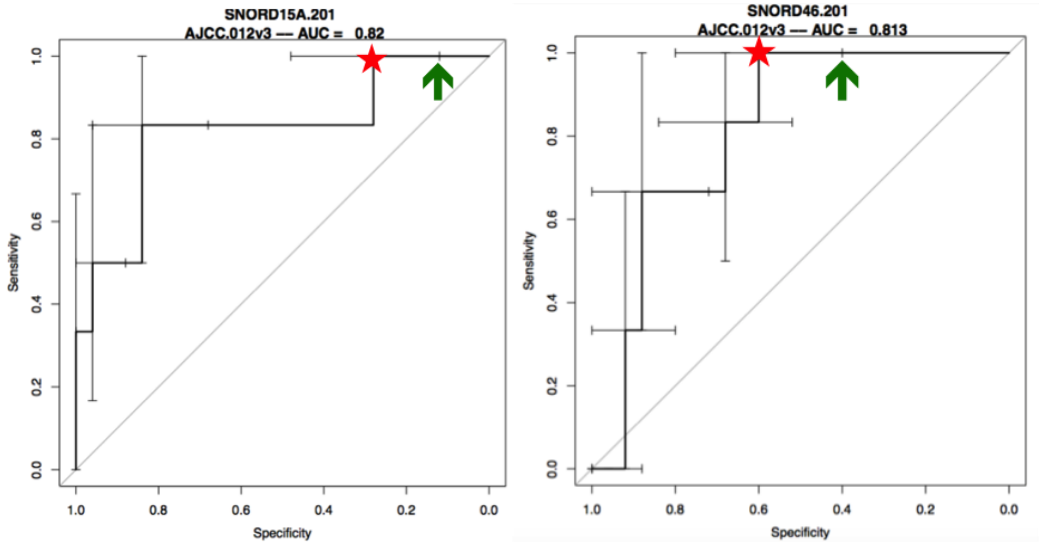

3.3.2.4 snRNAs

As for the snRNAs, RNU5E-4P-201, RNU5E-6P-201, and RNU6ATAC25P-201 were identified as potential biomarkers for the prediction of non-responders (Table 3.15, Figure 3.15), and all of them were significant in the extreme situation AJCC-0 vs. AJCC-3 ($p<0.05$, Table 3.16). However, the lower bound of the false positive rate was too high when the lower bound of the sensitivity was over 80%, therefore, they were not valid biomarkers (Figure 3.16).

Table 3.15: *snRNAs as biomarkers for the prediction of non-responders (AJCC-0.1.2 vs. AJCC-3). A thick black line borders the snRNAs with AUC>0.8. The pink colour represents p value<0.05, the orange colour represents AUC>0.8.*

snRNA	**AJCC 012 vs. 3** **MWU p value**	**AUC**
RNU5E-4P-201	0.015	0.820
RNU5E-6P-201	0.020	0.807
RNU6ATAC25P-201	0.020	0.807

Table 3.16: *snRNAs as biomarkers for the prediction of non-responders (AJCC-0 VS AJCC-3). The thick black line borders the snRNAs that were significant in the analysis of AJCC-0.1.2 VS AJCC-3. The pink colour represents p value<0.05, the orange colour represents AUC>0.8.*

snRNA	AJCC 0 vs. 3 MWU p value	AUC
RNU5E.4P.201	0.005	0.926
RNU5E.6P.201	0.018	0.870
RNU5F.1.201	0.036	0.833
RNU6ATAC25P.201	0.050	0.815

Figure 3.15: *snRNAs as biomarkers for the prediction of non-responders.*

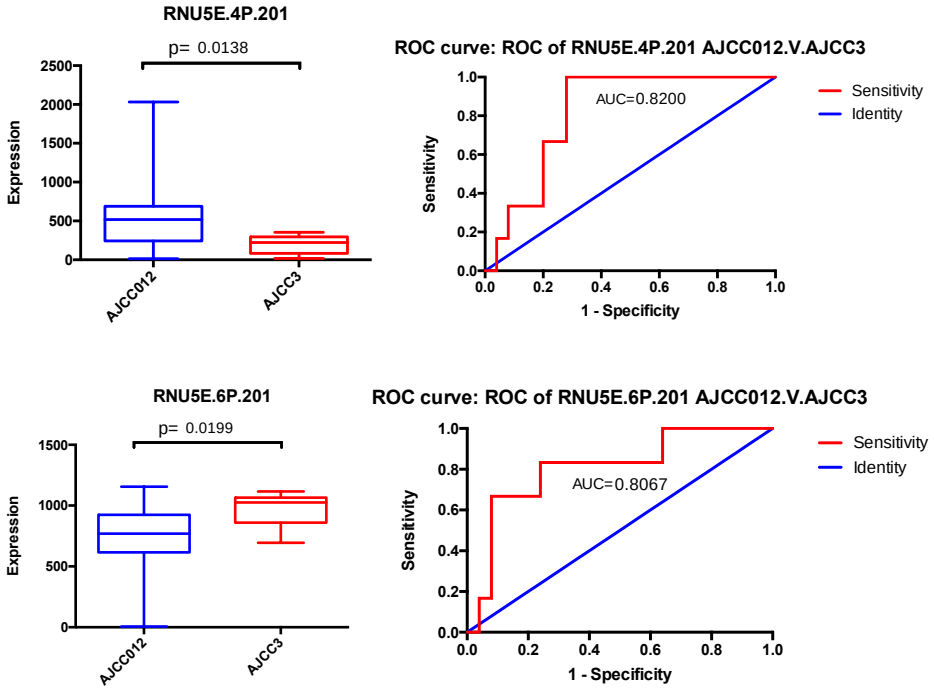

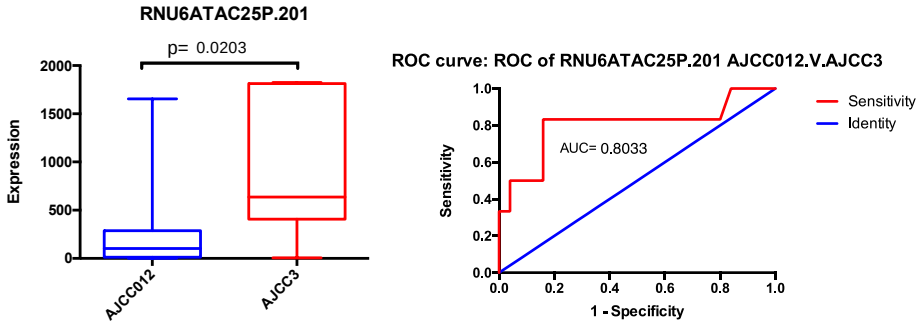

Figure 3.16: *The lower bound of the false positive rate and sensitivity of the snoRNAs.*

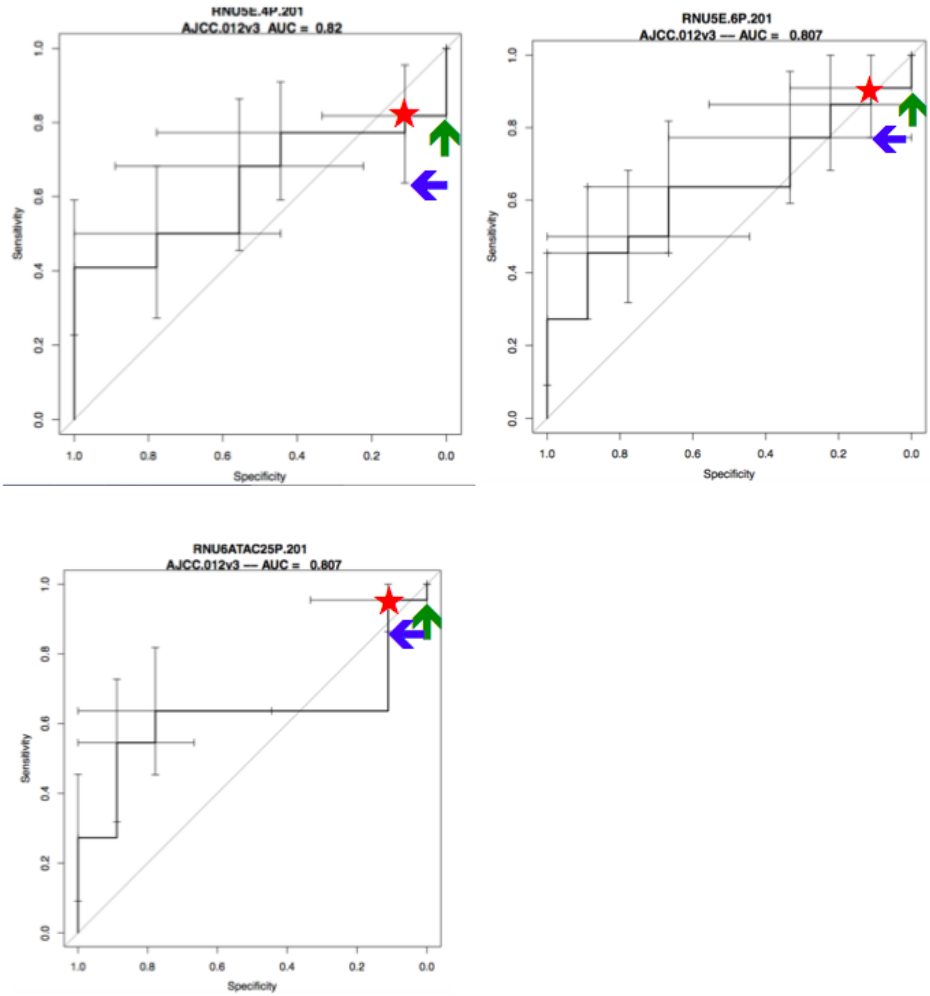

3.3.3 The summary of candidate biomarkers selected from tissue

The biomarkers with potential for predicting chemoradiotherapy response prior to commencing therapy are as follows (Figure 3.17):

Prediction of responders: miR-451a, miR-340-5p, DQ598428, and DQ576665.

Prediction of non-responders: miR-767-5p, miR-1301-3p, miR-552-3p, miR-99a-5p, miR-206, DQ598641, piR-has-32187, SNORD58B-201, SNORD46-2-201, and SNORD114-17-201.

The rank of the table was determined by following factors:

a) The lower bound of the sensitivity and the lower bound of the false positive rate
b) AUC
c) p value between AJCC 0 vs. AJCC 1.2.3.
d) p value between AJCC 0 vs. AJCC 3.

Figure 3.17: *The summary of biomarkers with potential for predicting chemoradiotherapy response prior to commencing therapy.*

Rank	miRNA		piRNA		snoRNA		snRNA	
	Prediction of responders	Prediction of non-responders	Prediction of responders	Prediction of non-responders	Prediction of responders	Prediction of non-responders	Prediction of responders	Prediction of non-responders
1	miR-340-5p	miR-767-5p	DQ598428	DQ598641	None	SNORD58B-201	None	None
2	miR-451a	miR-1301-3p	DQ576665	piR-hsa-32187		SNORD46-201		
3		miR-552-3p				SNORD114-17-201		
4		miR-99a-5p						
5		miR-206						

3.3.4 The detection of the top differentially expressed small RNAs in pretreatment tumor tissues of EAC patients by qRT-PCR

3.3.4.1 The miR-451a and miR-340-5p expression by qRT-PCR

The top miRNA biomarkers were detected by qRT-PCR. The results showed that the expression of miR-451a was significant between responders and non-responders (p=0.0018), which was consistent with our sequencing data (Figure 3.18 A). However, the qRT-PCR data of miR-340-5p produced a less significant difference in miRNA expression between responders and non-responders (p=0.35) than that observed in the sequencing counts (Figure 3.18 B). According to the literature, the miRNA levels (measured by qRT-PCR) gradually decrease with the increase in the age of the FFPE tissue blocks[325]. Therefore, it was hypothesized that the age of the FFPE tissue block might significantly impact the performance of the qRT-PCR assay more so than performance of the sequencing assay. This hypothesis was explored by examining various associations as described below.

Figure 3.18: *The miR-451a (A) and miR-340-5p (B) expression in pretreatment tumor tissues of EAC patients, as assessed by qRT-PCR; the data were normalized with let-7g-5p.*

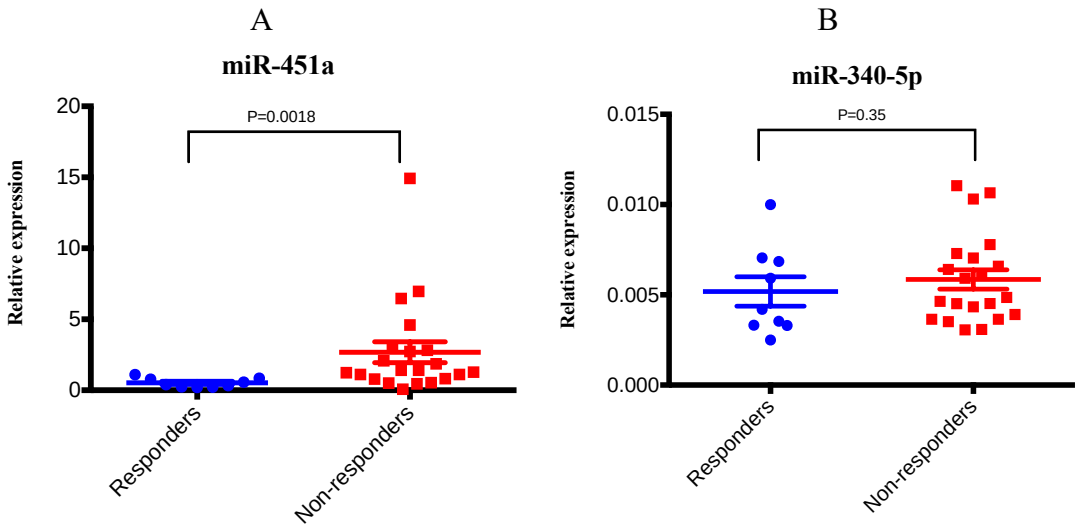

3.3.4.2 The associations between the PCR and NGS data

The association between the two data was performed by the accepted guidelines for interpreting the correlation coefficient by Linear Regression: Values between 0 and 0.3 (0 and -0.3) indicate a weak positive (negative) linear relationship, values

between 0.3 and 0.7 (-0.3 and -0.7) indicate a moderate positive (negative) linear relationship, while values between 0.7 and 1.0 (-0.7 and -1.0) indicate a strong positive (negative) linear relationship (DM STAT-1 articles, http://www.dmstat1.com/res/TheCorrelationCoefficientDefined.html).

The results showed that PCR data of miR-451a has a positive correlation with the NGS data (R=0.74, Figure 3.19 A). There was a weak relationship between PCR and NGS data for miR-340-5p expression (R=0.16, Figure 3.19 B), which could mean that the age of the FFPE block might strongly affect miR-340-5p expression. This could be the reason why the PCR data of miR-451a is significant between responders and non-responders but not miR-340-5p.

Figure 3.19: *The associations between the PCR data and NGS data (A: miR-451a, B: miR-340-5p), the x-axes show the PCR data or ranked PCR data while the y-axes show the NGS data or ranked NGS data.*

A: miR-451a

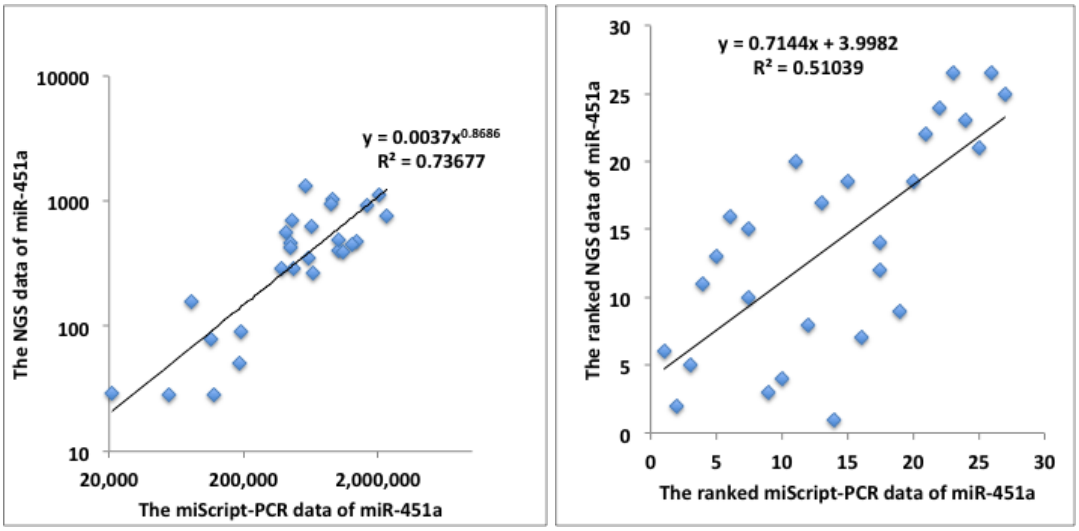

B: miR-340-5p

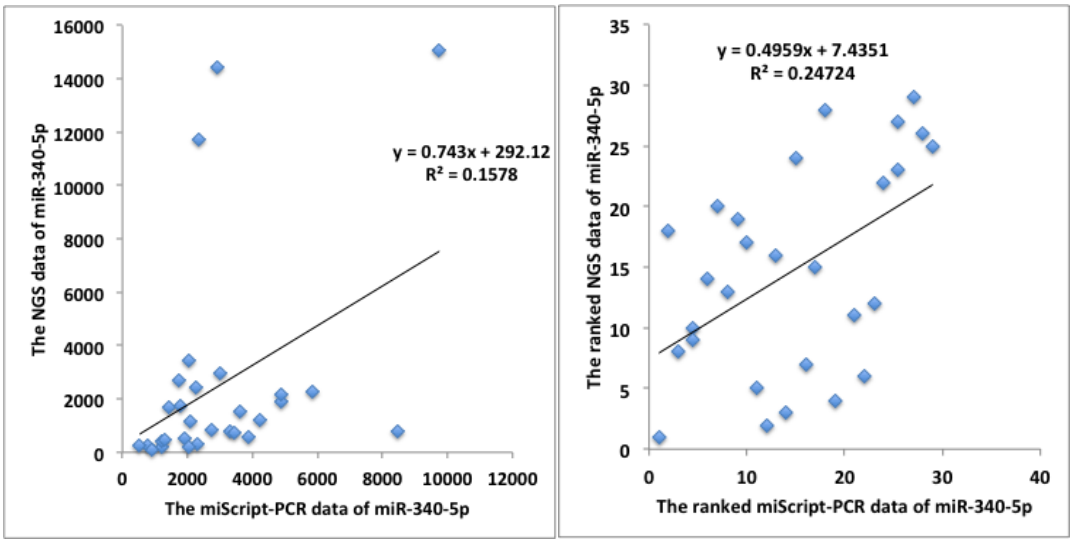

3.3.4.3 *The associations between the age of the FFPE block and the NGS results*

The results showed that there were no correlations between the age of the FFPE block and the NGS data for miR-451a (R=0.077), with similar results in the ranked data (Figure 3.20 A). As for miR-340-5p, the expression level was slightly decreased with age, but there was no correlation between the FFPE block and the NGS results (R=0.104), and the ranked data showed similar results (Figure 3.20 B), suggesting that the NGS data is not impacted by the age of the FFPE blocks.

Figure 3.20: *The association between the age of the FFPE block and the NGS results (A: miR-451a, B: miR-340-5p).*

A: miR-451a

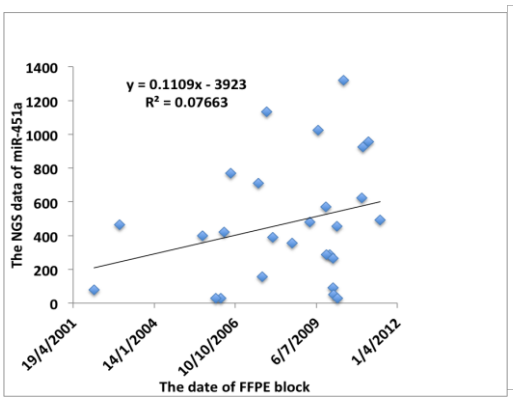

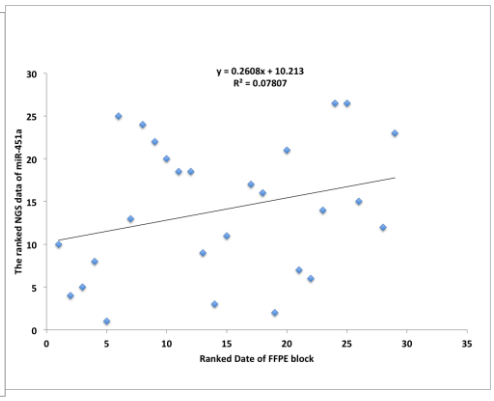

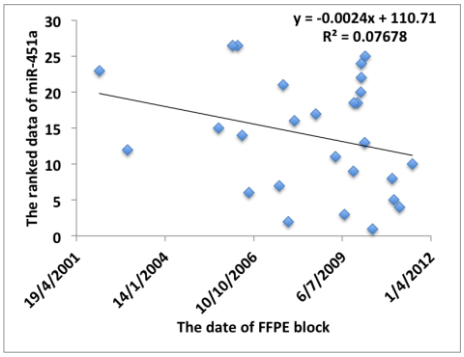

B: miR-340-5p

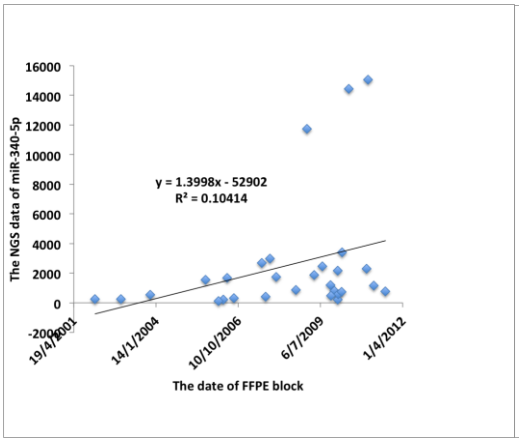

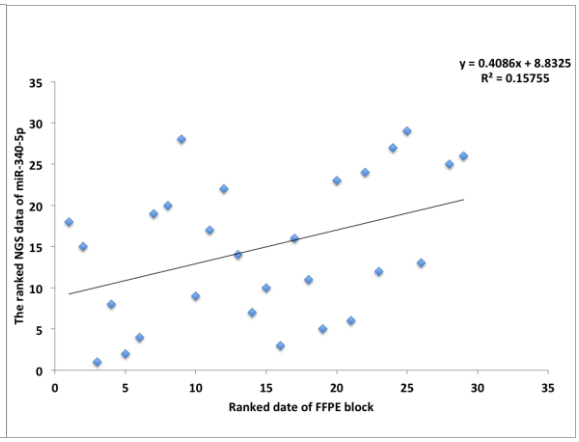

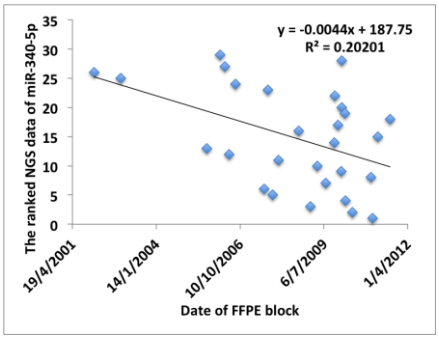

3.3.4.4 *The associations between the age of the FFPE block and the qRT-PCR results*

The results showed that there are very weak correlations between the age of the FFPE block and the PCR data of miR-451a (R=0.021), with similar results in the ranked data (Figure 3.21 A). However, for miR-340-5p, the expression level decreased over time more than that of miR-451a (R=0.35), and the ranked data showed similar results (Figure 3.21 B), indicating that the age of the FFPE block affected the PCR results. Therefore, the remaining small RNAs were not tested by qRT-PCR.

Figure 3.21: *The association between the age of the FFPE block and the PCR data (A: miR-451a, B: miR-340-5p).*

A: miR-451a

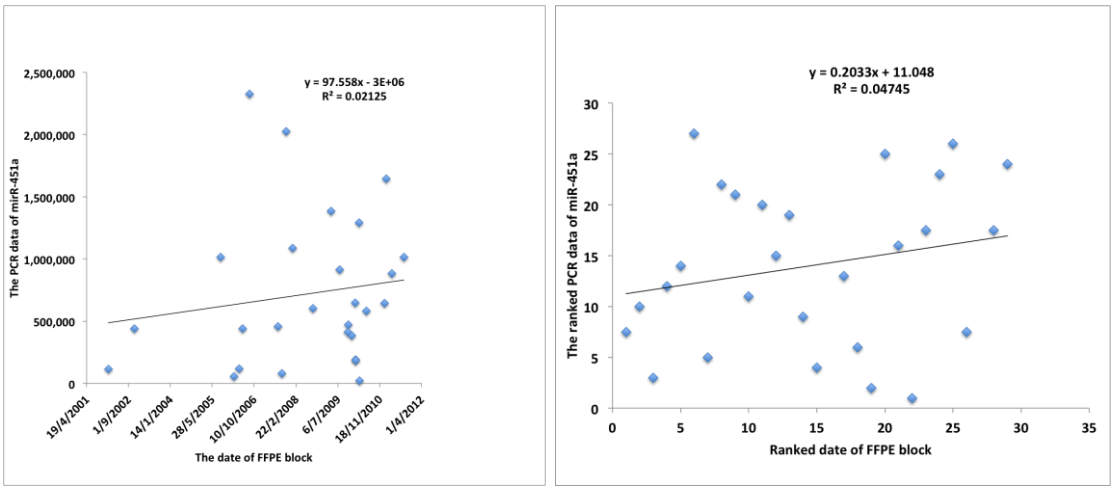

B: miR-340-5p

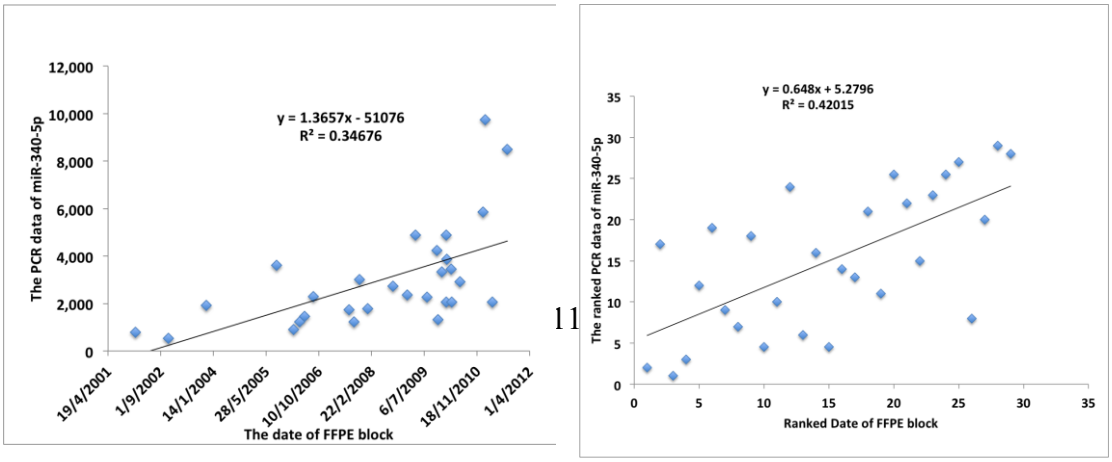

3.4 Discussion

It was reported that neoadjuvant chemoradiotherapy increases the survival rate of patients with EAC[326]. However, a number of researchers pointed out that the patients with significantly improved survival time also have a good histopathologic response[237, 238]. Therefore, it is important to identify biomarkers for chemoradiotherapy response prior to treatment so as to maximize the benefits for patients who underwent the neoadjuvant chemoradiotherapy.

3.4.1 miRNAs as potential biomarkers for chemoradiotherapy response

miRNAs are good candidates as biomarkers of treatment response and previous research has identified some miRNAs as biomarkers for neoadjuvant chemoradiotherapy response in EC. Wen et al.[316] showed that miR-145-5p, miR-152, miR-193b-3p, and miR-376a-3p predict the neoadjuvant chemoradiotherapy response in ESCC. Serum levels of miR-200c[233] can serve as potential biomarkers in predicting chemotherapy response in ESCC patients who received neoadjuvant chemotherapy.

small RNAs are also the biomarkers of treatment response for the EC patients who received chemoradiotherapy after surgery or palliative treatment. For example, a study reported that there is a relationship between low let-7c expression and poor response to chemotherapy in patients with ESCC[327]. Sugimura et al.[327] reported that both let-7c and let-7b are associated with poor response to chemotherapy. Tanake et al.[239] found that miR-27 is related to chemoresistance in EC. Chen et al.[328] indicated that decreased miR-133a and miR-133b expression could be biomarkers of response to chemotherapy in ESCC patients who underwent

paclitaxel-based treatment. Wang et al.[329] found that miR-221 regulates 5-FU resistance in EC patients by the Wnt/beta-catenin-EMT pathways, suggesting that miR-221 could serve as a therapeutic biomarker. Dong et al.[207] reported that miR-7 is a biomarker for predicting the chemoradiation response. While there are several studies about miRNAs as biomarkers of treatment response in ESCC, there are few reports on miRNAs as biomarkers for EAC.

The results of our study showed that miR-340-5p, miR-451a, and miR-576-5p might be biomarkers of responders in EAC. However, only miR-451a and miR-340-5p were acceptable as the biomarker of responders according to the analysis of lower bound of the false positive rate. The lower bound of the false positive rate is 90%, when the lower bound of the sensitivity is 85% for miR-576-5p, which indicates a high error probability. Therefore, miR-451a and miR-340-5p were selected for further study. These two miRNAs had a greater than 85% sensitivity and less than a 65% false positive rate. According to this cut-off, a small number of small RNAs were selected as biomarkers of response to chemoradiotherapy. Therefore, this cut-off was used in this study to ensure the quality of biomarkers. miR-340-5p and miR-451a have been reported as biomarkers of response to chemoradiotherapy in other cancers. For example, Song L et al.[330]showed that miR-340-5p modulates cisplatin resistance in osteosarcoma. Michal Wozniak et al.[331] identified miR-340-5p to be involved in drug resistance in melanoma by influencing the expression of ABCB5. miR-451a is widely dysregulated in cancers, and plays an important role in cancer diagnosis, prognosis, and chemoradiotherapy response[332]. The studies by Wang et al.[333] and Guet al.[334] reported that miR-451a has a relationship with paclitaxel resistance in breast cancer. Other researchers found that miR-451a promotes the sensitivity of lung cancer cells to cisplatin[335], and sensitizes breast cancer cells to tamoxifen[336]. Our study showed increased miR-340-5p and miR-451a expression in non-responders. The AUC of these miRNAs were above 0.9, indicating that they are very good biomarkers for prediction of responders in patients with EAC.

As for the biomarkers of non-responders, we identified 12 miRNAs in our study, however, only five of them are good enough as biomarkers of non-responders

according to the analysis of lower bound of the false positive rate: miR-767-5p, miR-1301-3p, miR-552-3p, miR-99a-5p, and miR-206. These miRNAs have a close relationship with chemoradiotherapy response in other cancers. For example, miR-99a regulates cisplatin resistance in gastric cancer[337], miR-206 plays important role in cisplatin resistance of ovarian serous carcinoma[338] and lung adenocarcinoma cells[339]. Besides, it also regulates 5-FU resistance in colon cancer cells[340], indicating that these miRNAs might play an important role in regulation of chemoradiotherapy response.

3.4.2 piRNAs/snoRNAs/snRNAs as potential biomarkers of response to chemoradiotherapy

Very few studies have mentioned the relationship between piRNA/snoRNAs/snRNAs and chemoradiotherapy response. For examples, Chu et al.[179] indicated that ACA11, an snoRNA, inhibits oxidative stress, which provides resistance to chemotherapy and promotes the growth of multiple myeloma cells. Wang et al.[320] found that piR-L-138 increases chemotherapy resistance to cisplatin in lung squamous cell carcinoma. However, no study has reported these small RNAs as biomarkers of response to chemoradiotherapy in EAC.

Our study showed that these small RNAs could be potential biomarkers of response to chemoradiotherapy in EAC. piRNAs, such as DQ598428 and DQ576665, snoRNAs, such as SNORD58B.201, SNORD46.201, and SNORD114.17.201, were potential biomarkers of response to chemoradiotherapy by seq2 and AUC analysis. It would be worthwhile to validate them in independent cohorts in future studies. We believe these small RNAs have an important role in regulation of chemoradiotherapy response and they might be new treatment targets for improving the efficiency of chemoradiotherapy.

3.4.3 The detection of top differentially expressed small RNAs by qRT-PCR

We only tested miR-451a and miR-340-5P by qRT-PCR and found that miR-340-5p was not significant between responders and non-responders. According to the literature, miRNA levels gradually decrease over time in FFPE tissue blocks[325].

Therefore, we suspected that the age of FFPE tissue block might significantly impact the qRT-PCR results.

The results suggested that the age of FFPE tissue block did not significantly affect miR-451a levels because there was a positive correlation between the PCR and NGS data. The NGS data was not affected by the age of the FFPE block as well. However, the age of FFPE tissue seemed to impact on miR-340-5p more than miR-451a, which could explain why miR-340-5p was not significant in our PCR data. Small RNAs can be affected by the age of the FFPE tissue block, such as miRNAs and snRNAs[325]. Therefore, the remaining small RNAs were not tested by qRT-PCR. miRNA sequencing analysis showed that the preparation of small RNA cDNA libraries can be conducted on up to 35-year FFPE specimens[341]. Besides, our data showed that there is no correlation between the age of FFPE and NGS data. Therefore, the data from the sequencing analysis in this study could be reliable even without PCR further detection.

3.4.4 Clinical relevance

Our current hypothesis is that small RNAs might be useful biomarkers of response to chemoradiotherapy in EAC patients. In clinical work, these small RNAs could be tested to guide the treatment measures and decide which patients could benefit from chemoradiotherapy. Thus, predicting chemoradiotherapy response prior to treatment will greatly impact the clinical decision-making and improve both the quality of life and treatment outcomes. Moreover, uncovering the mechanisms underlying the role of small RNAs in chemoradiotherapy response will promote research to identify the target gene or signaling pathway to improve the chemoradiotherapy response and survival time.

3.4.5 Limitations

This study has some limitations. First, the sample size should be expanded further to make stronger conclusions. Besides, qPCR detection should be performed in the same samples and the results should be validated in independent cohorts. Second, the potential mechanisms for the role of small RNAs in regulating chemoradiotherapy response should be studied using cell lines; we will do this in chapter 4. Third, we

only detected some top small RNAs by qRT-PCR because of the possible problems associated with the age of FFPE tissues. More small RNAs should be validated in the future if newer samples are available. Finally, we did not micro-dissect the tumour tissue from the paraffin sections, so potential variability in inflammatory cell infiltrate and contribution of stroma may have impacted on the results.

3.4.6 Summary

In summary, this study showed the small RNA expression profile in EAC, and identified small RNAs as potential biomarkers of response to neoadjuvant chemoradiotherapy for EAC. Clinically, these small RNAs could be tested to guide the treatment measures and decide which patients could benefit from chemoradiotherapy. Thus, predicting chemoradiotherapy response prior to treatment will greatly impact the clinical decision-making and improve both quality of life and treatment outcomes. Further investigation is warranted to evaluate the functions of these small RNAs and finally to translate the results from the bench to the bedside.

CHAPTER 4
INVESTIGATING THE ROLE OF CELLULAR SMALL RNAS IN REGULATING CHEMORADIOTHERAPY RESPONSE IN EAC CELLS

4.1 Introduction

As described in chapter 3, the biomarkers with the potential for predicting chemoradiotherapy response prior to commencing therapy by sequencing the pre-treatment archival tumor tissues of patients with EAC were as follows: miR-451a, miR-340-5p, DQ598428, DQ576665, miR-767-5p, miR-1301-3p, miR-552-3p, miR-99a-5p, miR-206, DQ598641, piR-hsa-32187, SNORD58B-201, SNORD46-2-201, and SNORD114-17-201. These small RNAs might play a pivotal role in regulating chemoradiotherapy response in EAC.

miR-451a was the top biomarker for prediction of responders and was validated by qRT-PCR (Chapter 3, 3.3.1 and 3.3.4). Several studies have assessed the role and mechanisms of miR-451a in regulating chemotherapy and radiotherapy response in other kinds of cancer. For example, Tian et al.[342] reported that miR-451a sensitized lung cancer cells to radiotherapy by promoting apoptosis, and Cheng et al.[335] observed that increased miR-451a expression could promote the sensitivity to cisplatin in lung cancer cells by targeting Mcl-1. In renal cell cancer, Sun et al.[343] found that miR-451a regulated chemotherapy resistance by targeting ATF-2(activating transcription factor 2). miR-451a was also identified to have a relationship with Imatinib resistance in chronic myeloid leukemia[344]. Overexpression of miR-451a was also found to regulate autophagy and sensitization of breast cancer cells to tamoxifen [336]. Liu et al.[345] reported the opposite results that decreased miR-451a expression increased the tamoxifen sensitivity by targeting the macrophage migration inhibitory factor in breast cancer. The inconsistency between these studies indicate that the function of miR-451a is complicated in regulating chemoradiotherapy response. In our lab, the expression of miR-451a was positively correlated with resistance to radiation treatment in EAC cell lines (OE19), and with the response to neoadjuvant chemoradiotherapy in patient serum[346].

Another identified biomarker, miR-340-5p has been reported to regulate chemoradiotherapy response as well. For example, miR-340-5p was reported as a promising biomarker of chemoradiotherapy response in gastric cancer[347]. Overexpression of miR-340-5p decreased cell proliferation and induced cellular drug resistance in breast cancer by targeting the Wnt/β-catenin pathway[348]. miR-340-5p was also reported to modulate cisplatin resistance in osteosarcoma[330]. Besides, this miRNA was tumor-suppressive and could be a biomarker of prognosis and treatment response in colorectal cancer[349]. In hepatocellular cancer, miR-340-5p interacted with long non-coding RNAs to regulate cisplatin resistance[350].

The other miRNAs identified as biomarkers of response to chemoradiotherapy have been mentioned in the literature as well. For instance, miR-99a regulated cisplatin resistance in gastric cancer[337]. miR-206 played an important role in cisplatin resistance of ovarian serous carcinoma[338] and lung adenocarcinoma cells[339], and also regulated 5-FU resistance in colon cancer cells[340].

Studies have mentioned the relationship between piRNA/snoRNAs/snRNAs and chemoradiotherapy response as well. For example, Chu et al.[179] showed that ACA11, an snoRNA, inhibited oxidative stress, which provided resistance to chemotherapy and promoted the growth of multiple myeloma cells. Wang et al.[320] found that piR-L-138 increased chemotherapy resistance to cisplatin in lung squamous cell carcinoma. However, no previous study has identified that these piRNA/snoRNAs/snRNAs, selected as biomarkers in Chapter 3, are related with chemoradiotherapy response.

Some studies have shown the role of small RNAs in regulating other cancers, however, there are few studies on the roles of small RNAs in regulating treatment response in EAC cell lines. Therefore, in this chapter, we explored the function of small RNAs and the potential mechanisms underlying their action in EAC cell lines.

4.2 Methods

We used eight cell lines in this study: six adherent cell lines (OE19, OE33, JHEsoAd1, SKGT4, FLO1, and OACP4C), one suspension cell line (ESO51), and

one semi-adherent cell line (ESO26). All cell lines were cultured at 37°C under 5% CO_2 conditions.

The first experiment was to investigate the relationship between the biomarkers selected from tissue in chapter 3 and the response to drug treatment or radiation treatment in eight EAC cell lines. We utilized drug and radiation response data as well as qRT-PCR data generated by other laboratory members for their own research that was provided to me for my own analysis. The cells for drug treatment were seeded in 12-well plates with RPMI or CSS medium (medium was changed 24 hours before seeding from complete medium to CSS, because the CSS was charcoal stripped serum which removed the hormones that might affect the mechanistic studies) at a density of 45,000 cells per mL, and then the cells were treated with 20 μM cisplatin or 50 μM 5-FU after seeding for 24 hours. The drug treatment response to cisplatin or 5-FU was assessed in the eight EAC cell lines using flow cytometry (Annexin V-FITC/PI assay) and MTS assay after 72 hours of treatment. The MTS Assay was used because it was a colorimetric assay that determined metabolic activity in cells and indicated mitochondrial activity. The survival Fraction (SF) was used for assessment of the treatment response, obtained by dividing the number of viable cells of a treated sample by the mean of the number of viable cells of the respective untreated vehicle controls in flow cytometry. In MTS data, SF was calculated by dividing the corrected absorbance of a treated sample by the mean of the corrected absorbance of the respective vehicle controls. For radiation response analysis, the cells were seeded in 6-well plates in complete medium at a density that allowed them to reach about 80% confluence 24 hours after seeding (SK-GT-4: 300000 cells/well, OE-19: 450,000 cells/well, and the other cell lines: 400,000 cells/well). These cells received irradiation with 2 Gy after seeding for 24 hours. The radiotherapy response was assessed by clonogenic assay (Chapter2: 2.2.13.5). In Clonogenic data, the SF was obtained by dividing the plating efficiency (PE) of each irradiated well by the mean of the PEs of non-irradiated controls .All the pre-treated cells were harvested in QIAzol for RNA extraction and in RIPA buffer for western blotting. The qRT-PCR was performed using miScript II kit (Chapter 2, 2.2.14.3) on the RNA extracted from the above cells. The expression of all small RNAs was

tested by qRT-PCR. let-7g-5p was chosen as the housekeeping gene and all miRNAs were normalized with let-7g-5p. The use of Let-7g-5p as a housekeeper gene has been previously reported[351] and has been confirmed by other members of my lab. The relationship between treatment response and small RNAs was analyzed by Spearman rank correlation.

miR-451a was the strongest biomarker and its expression was associated with drug and radiation response in EAC cell lines. Therefore, for the second experiment, this miRNA was selected for further investigation into its possible role in regulating drug and radiation response in EAC cells. The EAC cell line OE33 was used for transfection because OE33 cells have a lower baseline level of miR-451a and was one of the most sensitive cell lines to cisplatin, 5-FU, and radiation. Several drug concentrations were tried first in OE33 to find the appropriate concentration for transfection. The miRNA mimics were performed to upregulate miR-451a expression. The transfected cells were treated with cisplatin, 5-FU, carboplatin, paclitaxel, or irradiation. Carboplatin and paclitaxel were included as they are the chemotherapy agents currently used for the treatment of EAC in neoadjuvant settings[352]. Incucyte, Caspase assay, and Clonogenic assay were used to assess the treatment response, respectively. The data from the miR-451a mimics in OE-33 experiments assessed by Incucyte consistently indicated that miR-451a promotes cellular proliferation, which might make it difficult to assess the effect of miR-451a mimic on drug treatment response. Therefore, the clonogenic assay was performed for further analysis.

The third experiment investigated the miR-451a signaling pathways and networks by using a combination of bioinformatics tools and literature searching. miRWalk2 was used for predicting target genes[353, 354]. The InnateDB was used for the pathway analysis[355]. The most highly predicted target genes and the top 30 signaling pathways were used for the literature search. We validated the bioinformatics prediction by studying the expression of miR-451a and targeted proteins in EAC cell lines. miR451a expression was measured by qRT-PCR (Chapter 2, 2.2.14.3) while the proteins were detected by western blotting (Chapter 2, 2.2.16). The Spearman rank correlation was used to test the correlation between miR-451a expression and

targeted protein expression. Based on the importance of proteins in regulating treatment response, and their close relationship with miR451a, the protein expression might change by altering the expression of miR-451a. To explore this, we measured the expression of these proteins in OE-33 cells after transfection with miR-451a mimics. The miR-451a targeted proteins were analyzed between miR451a mimics and controls. The background subtraction was used for the control in the western blots. Such as local background subtraction, global background subtraction(Chapter2:2.2.16.10).

4.3 Results

4.3.1 The relationship between small RNAs expression and drug/radiation treatment response in EAC cell lines

The small RNAs that were selected as candidate biomarkers from tissue were tested in eight EAC cell lines by treatment with drugs (5-FU or cisplatin) or radiation. Flow Cytometry and MTS assay were used for testing treatment response in the drug experiments, while Clonogenic assay was used for testing treatment response in the radiation experiments. The treatment response was tested in three independent experiments.

The flow cytometry results are presented in Table 4-1 (column header “Flow cytometry”) and Figure 4-1 (graph title “Flow data”). There were associations between miR-451a expression and cisplatin treatment response (rho=0.667, p=0.083), and between miR-1301-3p and cisplatin treatment response (rho=0.667, p=0.083). However, these did not reach statistical significance. In the 5-FU treatment experiment, there was an association between miR-767-5p expression and 5-FU treatment response by flow cytometry (rho=0.714, p=0.058). However, it did not reach statistical significance.

The MTS assay was also used for investigating the relationship between treatment response and the expression of small RNAs. These results are presented in Table 4-1 (column header “MTS”) and Figure 4-1 (graph title “MTS data”). There was a positive correlation between miR-767-5p expression and cisplatin treatment response (rho=0.738, p=0.046). There was also a positive correlation between miR-1301-3p

expression and cisplatin treatment response (rho=0.810, p=0.022). However, in the 5-FU treatment experiment, there was no correlation between any small RNA expression and 5-FU treatment response by MTS.

As for the radiation experiment, the results showed a positive correlation between miR-451a expression and radiation treatment response (p=0.024; Table 4-1 (column header "Clonogenic assay"), Figure 4-1 (graph title "Clonogenic data")).

See the complete Figures in appendix 4.3.

Although only eight of 14 selected biomarkers from chapter 3 were tested in cell lines because the Qiagen company could not design a functional qRT-PCR assay for some piRNAs and snoRNAs (the process for obtaining custom made primers in Chapter 2, 2.2.17), the results supported the hypothesis that some of the selected tissue biomarkers of response to chemoradiotherapy might exert a direct biological role in controlling drug and or radiation response in EAC cells, especially for miR-451a, that gave significant effect in irradiation treatment response and $p<0.1$ in drug treatment response. Besides, our lab previously reported that miR-451a regulated treatment response in OE19 cells[346]. Therefore, miR-451a was selected for the functional study.

***Table 4-1**. The relationship between the candidate small RNA tissue biomarkers and drug and radiation treatment response in eight EAC cell lines (The rho value is in bold when rho is greater than or equal to 0.5. p-value is in red when the p value is less than 0.1.).*

Small RNAs	Cisplatin				5-FU				Radiation	
	Flow Cytometry		MTS		Flow Cytometry		MTS		Clonogenic assay	
	spearman		spearman		spearman		spearman		spearman	
	rho	*p value*	*rho*	*p value*	*rho*	*p value*	*rho*	*p value*	*rho*	*p value*
miR-340-5p	0.119	0.793	-0.286	0.501	-0.452	0.268	0.429	0.299	0.179	0.713
miR-451a	**0.667**	0.083	0.333	0.428	-0.405	0.327	0.262	0.536	**0.0857**	0.024
miR-767-5p	0.357	0.389	**0.738**	0.046	**0.714**	0.058	0.238	0.582	0.000	>0.999
miR-1301-3p	**0.667**	0.083	**0.810**	0.022	0.095	0.840	0.214	0.619	0.393	0.396
miR-206	-0.119	0.793	0.452	0.268	-0.191	0.665	0.476	0.243	**0.500**	0.267
DQ598428	0.000	>0.999	-0.476	0.243	0.071	0.882	0.119	0.793	-0.464	0.302
piR-32187	-0.214	0.619	-0.119	0.793	0.286	0.501	0.476	0.243	0.143	0.783
SNORD114	0.048	0.935	-0.214	0.619	**-0.524**	0.197	-0.214	0.619	-0.464	0.302

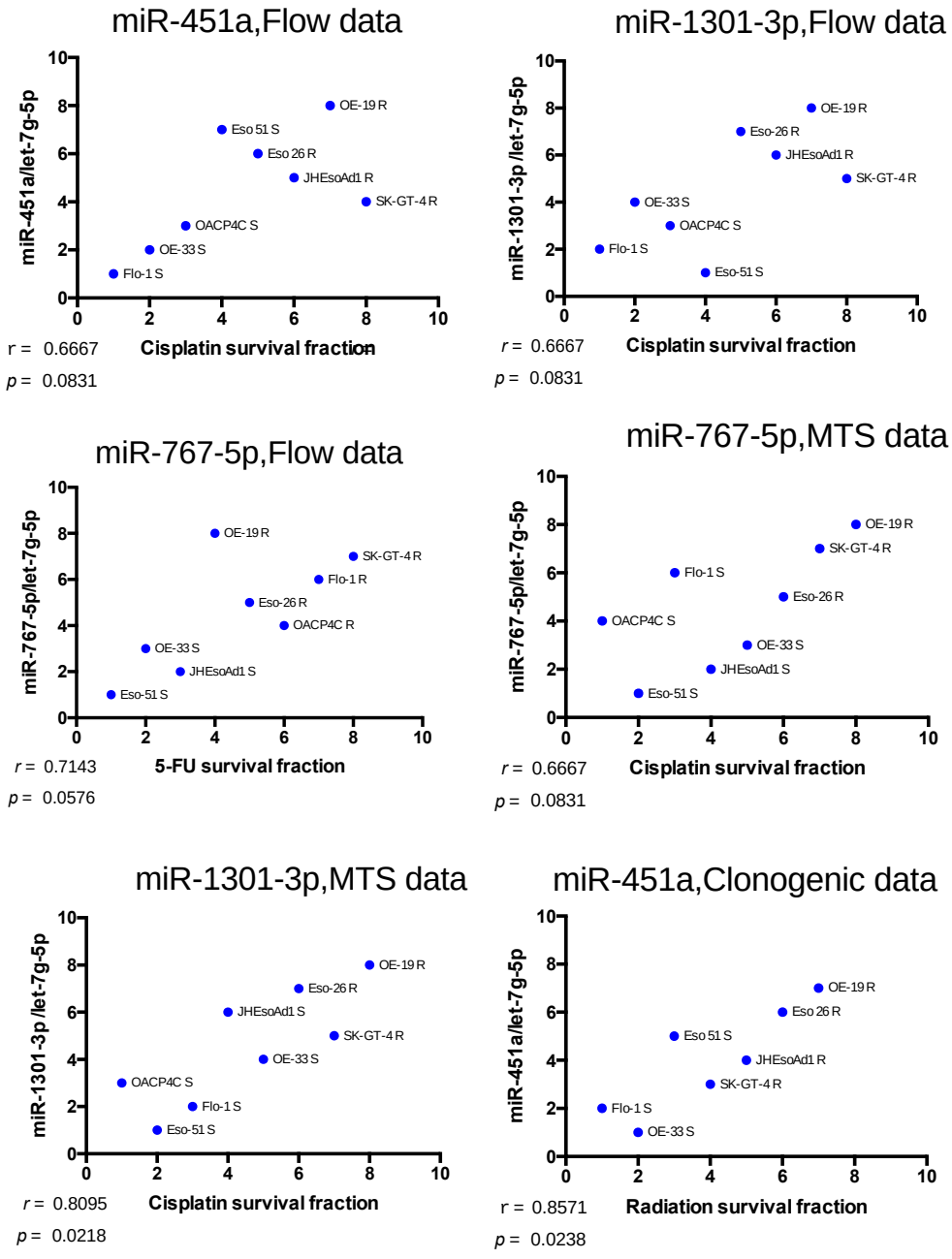

Figure 4-1. *The relationship between treatment response and the expression of small RNAs by flow cytometry, MTS, or Clonogenic Assay (Y-axis shows the expression of small RNAs normalized by let-7g-5p. The X-axis shows the SF). The experiment was performed in triplicate.*

4.3.2 The impact of miR-451a mimic molecule on proliferation of OE33 cells – Incucyte assay

OE33 cells were transfected with miR-451a mimics and corresponding non-targeting mimic controls. Three independent experiments were performed using 60,000 cells (written as 60k in graph titles) in 96-well plates and 0.05 nM mimic concentration was used for transfection. Fig 4.2 shows a diagram with details on the experimental

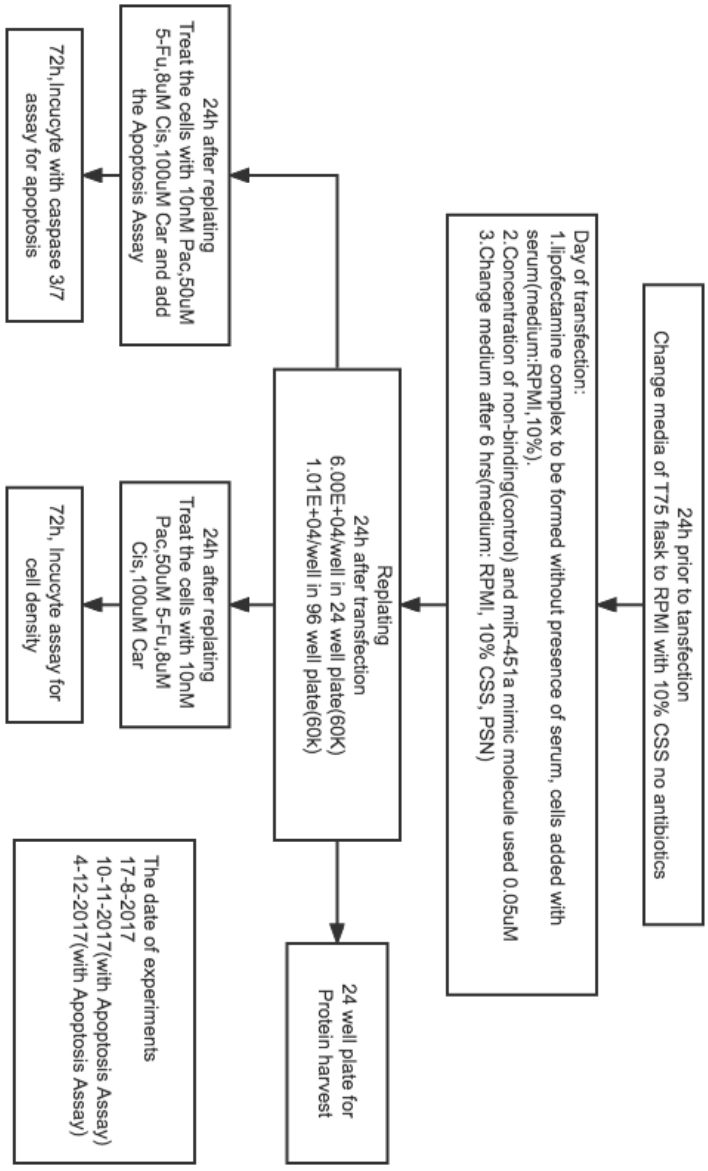

Figure 4-2*. The diagram of the experiments performed using Incucyte (drug treatment).*

design. Cells were cultured in the presence of the vehicles that were used for subsequent drug treatment (described in sections 4.3.3 onwards).

The results showed that the miR-451a mimic molecule increased the cell proliferation in three independent experiments (the dates of experiment were 17-8-2017, 10-11-2017, and 4-12-2017). This effect was observed in all three independent experiments. The results from one representative experiment are shown here, Figure 4-3 (see Appendix 4.4 for data from the other 2 experiments).

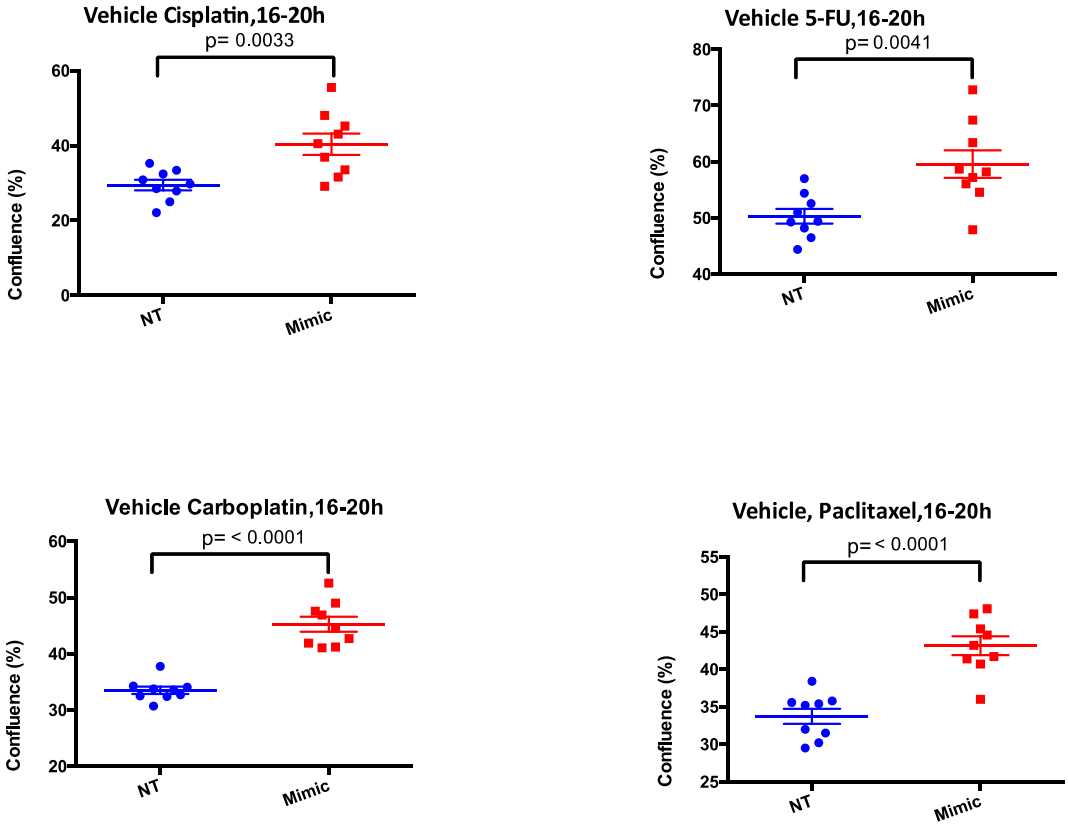

***Figure 4-3**. The miR-451a mimic molecule enhanced the proliferation of OE33 cells at 0.05 nM at the 60k cell density after 16–20 hours (combined data from timepoints 16, 18, and 20 hours after replating into 96-well plates, corresponding to 40–44 hours after transfection with miR-451a mimic or negative control mimic) treated with the vehicle of cisplatin, 5-FU, carboplatin, and paclitaxel. NT: non-targeting molecule. The date of the experiment was 10-11-2017.*

4.3.3 The impact of miR-451a mimic on the response of OE-33 cells to drug treatment - Incucyte assay for cell density

The effects of the miR-451a mimic on response to cisplatin, 5-FU, carboplatin, and paclitaxel were tested in the same three independent experiments described in section 4.3.2. The concentration of each drug was optimized prior to the experiments (see the Appendix 4.1, 4.2). The experimental design is shown in Figure 4-2. The results from the experiments conducted on 10-11-2017 and 4-12-2017, taken at 72 hours after drug treatment, are shown in Figures 4-4 and 4-5. This timepoint corresponds to 96 hours after transfection with miR-451a mimic or negative control mimic. In the experiment conducted on 10-11-2017, the mean confluence values indicated that there were more cells in the miR-451a mimic-transfected and drug-treated cultures than there were in the matched negative control mimic-transfected and drug-treated cultures. This difference was statistically significant for cisplatin ($p = 0.0004$), 5-FU ($p = 0.0273$), and carboplatin ($p = 0.0081$), suggesting that the miR-451 mimic resulted in increased drug resistance. The results of the experiment conducted on 4-12-2017 showed this same general trend, however the differences in mean confluence values between the miR-451a mimic-transfected and drug-treated cultures *vs* the matched negative control mimic-transfected and drug-treated cultures were lower than in the 10-11-2017 experiment. Further, the only statistically significant difference was found in case of the paclitaxel-treated cultures ($p=0.0.0021$) (See Appendix 4.5:Figure 4-15) for data from the 17-8-2017 experiment). This experiment did not include enough technical replicates to allow any conclusions to be drawn.

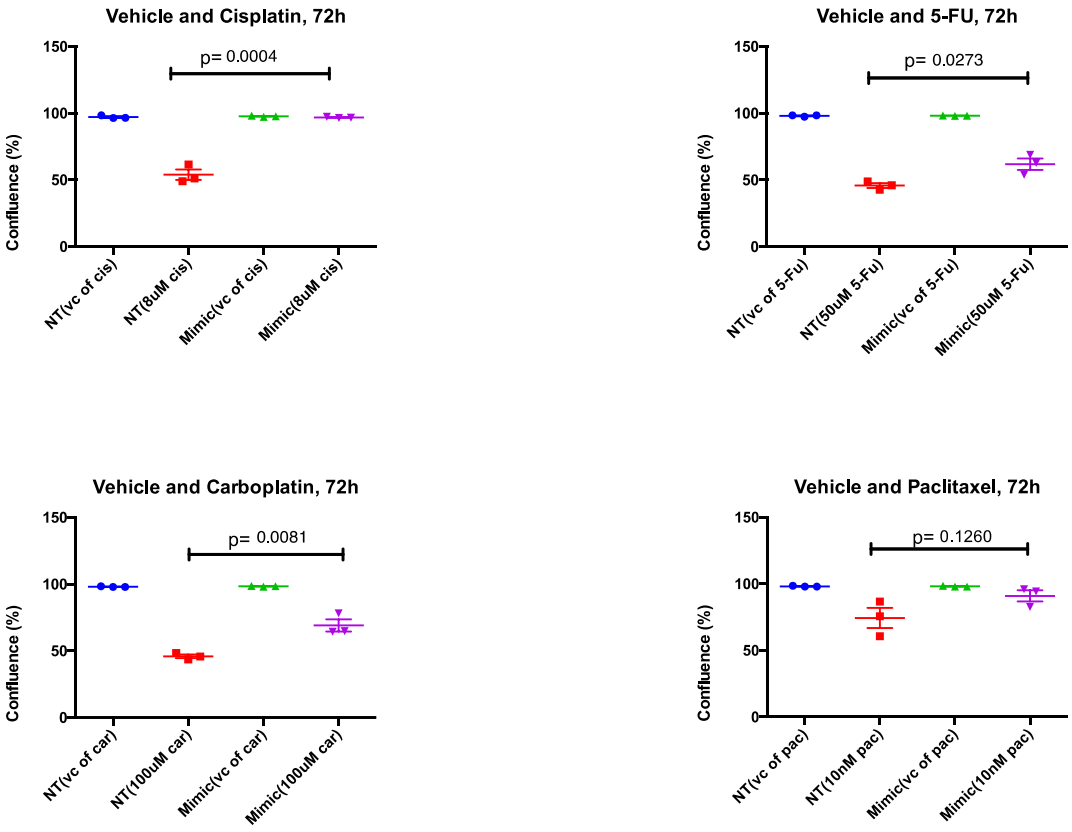

Figure 4-4. *The impact of miR-451a on drug response of OE33, as assessed by the Incucyte assay for cell density (Cisplatin, 5-FU, Carboplatin, and Paclitaxel, 10-11-2017, 60k cell density, 0.05 nM miR-451a mimic transfection, 72-hour treatment, single timepoint).*

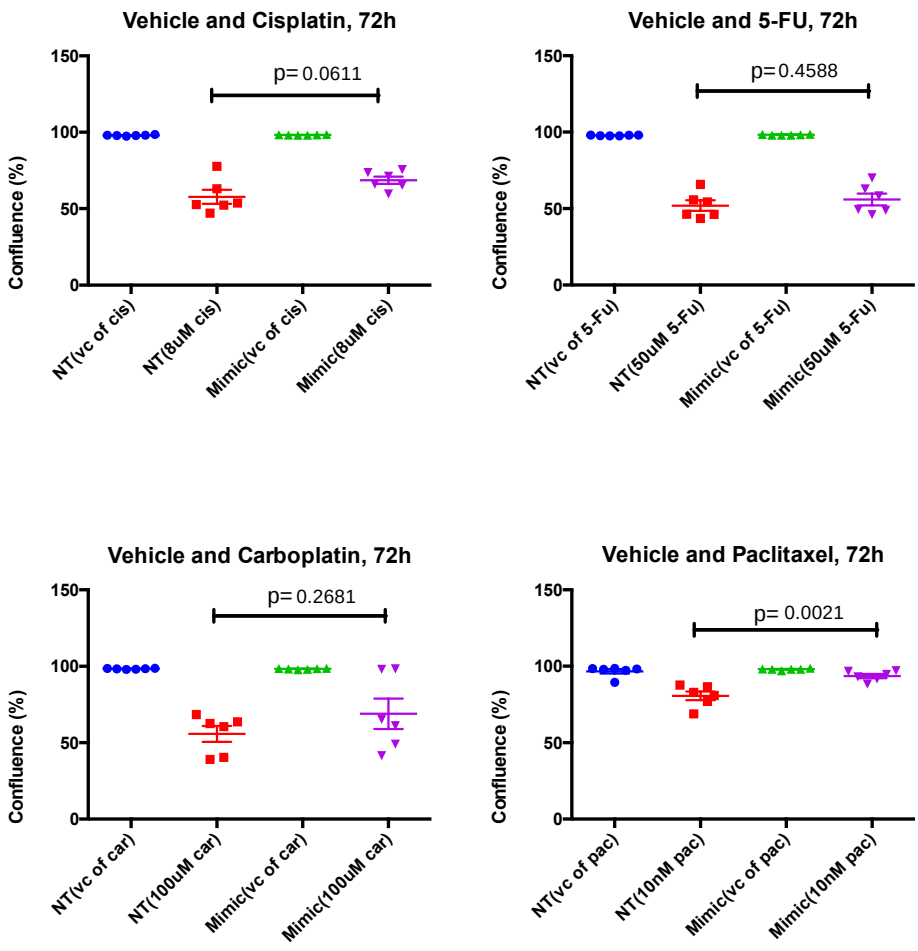

Figure 4-5. *The impact of miR-451a on drug response of OE33, as assessed by the Incucyte assay for cell density (Cisplatin, 5-FU, Carboplatin, and Paclitaxel, 4-12-2017, 60k cell density, 0.05 nM miR-451a mimic transfection, 72-hour treatment, single timepoint).*

4.3.4 The impact of miR-451a mimic on the response of OE-33 to drug treatment – Incucyte with caspase 3/7 assay for analysis of apoptosis

For two of the three experiments performed using the Incucyte live cell imager (10-11-2017 and 4-12-2017), the caspase 3/7 assay was used as an indicator of apoptosis in the miR-451a mimic and negative mimic control groups. The experimental design is shown in Figure 4-2. The data were normalized with confluence in order to take into account the impact of miR-451a transfection on cell number.

The results of the 10-11-2017 experiment are shown in Figure 4-6. Mean caspase 3/7 levels in miR-451a mimic-transfected cisplatin / 5-FU / carboplatin-treated cultures were lower than in matched negative control mimic-transfected drug-treated cultures. This difference was statistically significant for the cisplatin-treated (p=0.0465) and 5-FU-treated (p=0.0484) cultures and indicated that the miR-451a mimic inhibited drug induced apoptosis. There was no significant difference in mean caspase 3/7 levels between the miR-451a-transfected and paclitaxel-treated cultures and the negative control mimic-transfected and paclitaxel-treated cultures.

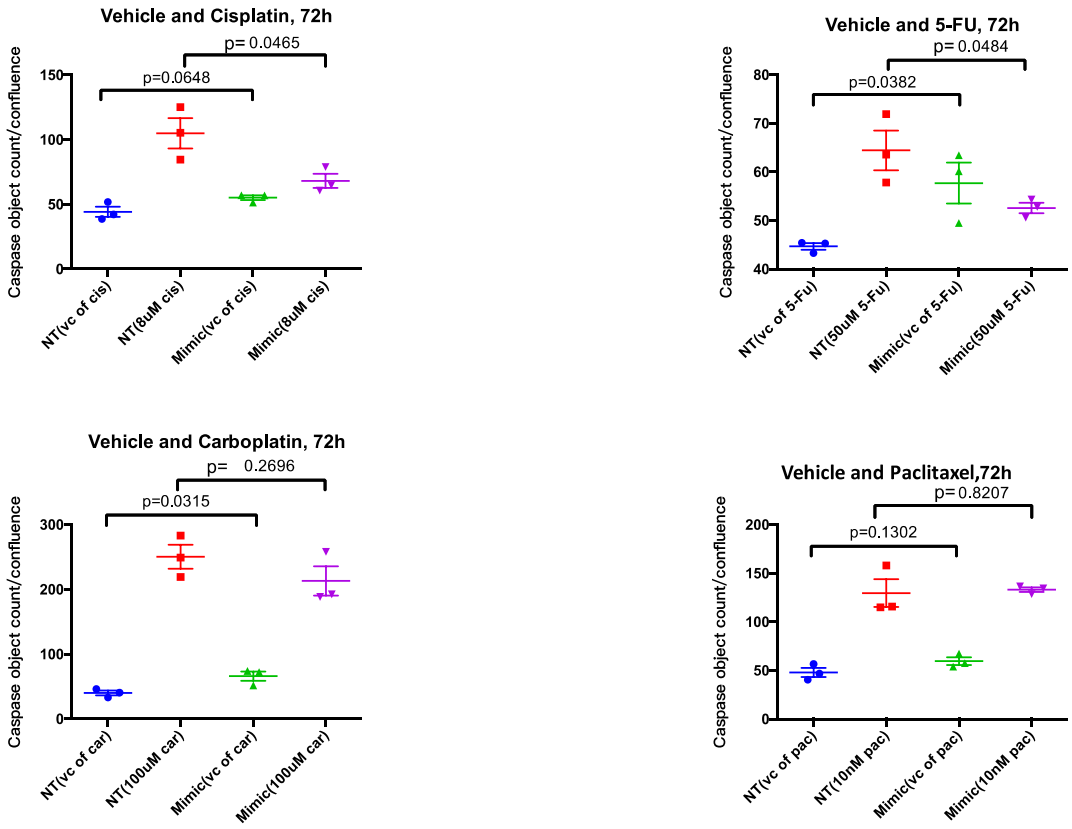

Figure 4-6*. The impact of miR-451a on drug response of OE33, as assessed by the Incucyte test, along with the caspase 3/7 assay for examining apoptosis (10-11-2017, 60k cell density, 0.05 nM miR-451a mimic transfection, 72-hour treatment, single timepoint).*

The results of the 4-12-2017 experiment are shown in Fig 4-7. Unlike the 10-11-2017 experiment, there was no clear impact of miR-451a on cisplatin / 5-FU / carboplatin induced apoptosis. Mean caspase 3/7 levels in the miR-451a-transfected

paclitaxel-treated culture were higher than those in the matched negative control mimic-transfected culture (p=0.0309), indicating that miR-451a promoted paclitaxel-induced apoptosis.

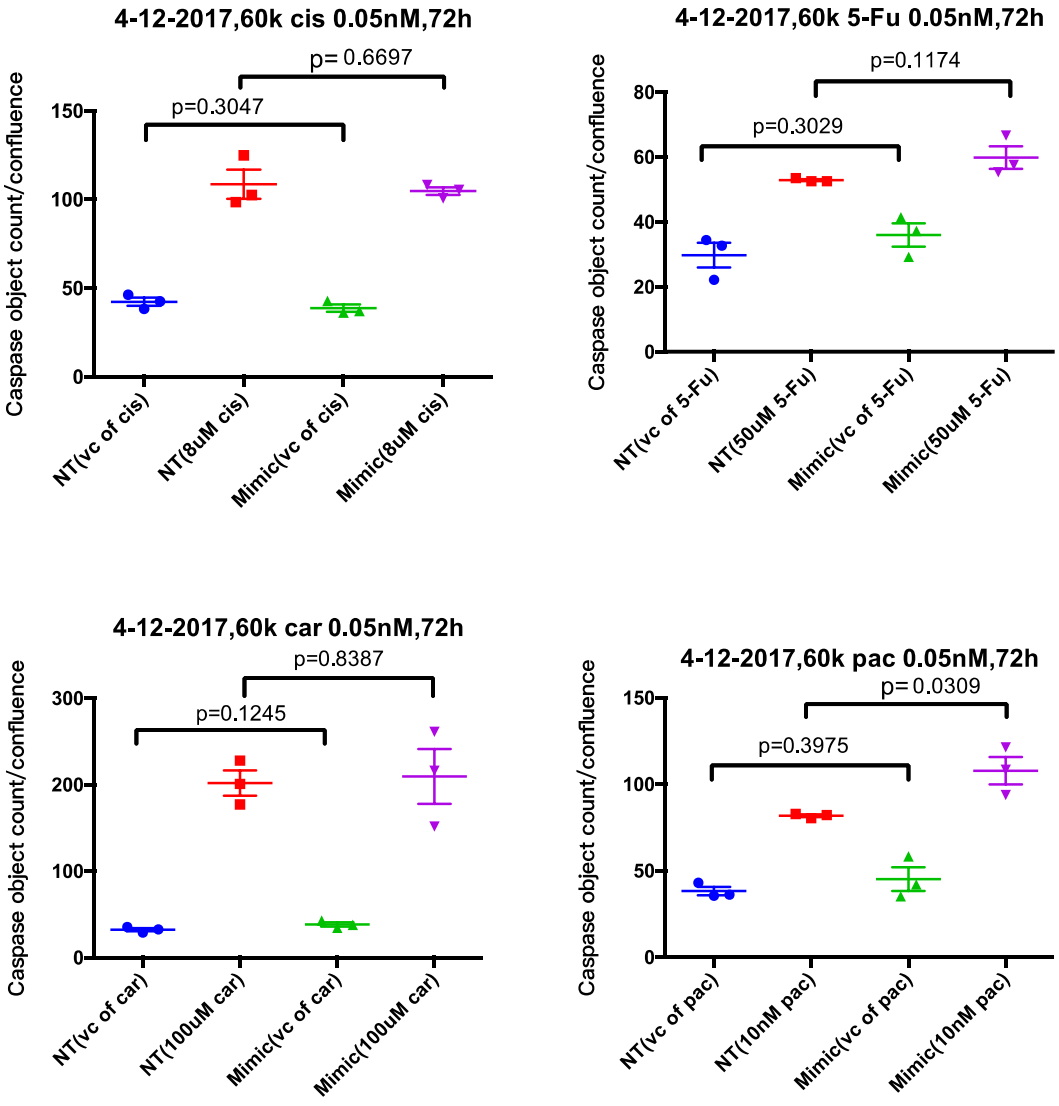

Figure 4-7*. The impact of miR-451a on drug response of OE33, as assessed by the Incucyte test, along with the caspase 3/7 assay for apoptosis (4-12-2017, 60k cell density, 0.05 nM miR-451a mimic transfection, 72-hour treatment, single timepoint).*

Closer inspection of the 10-11-2017 and 4-12-2017 results indicated that these two experiments also differed in the apoptosis behavior of the vehicle-treated cultures at the 72 hour timepoint.

In the 10-11-2017 experiment (Figure 4-6), mean caspase 3/7 levels were higher in miR-451a mimic-transfected vehicle control-treated cultures than in matched negative control mimic-transfected vehicle control-treated cultures. The difference in mean caspase levels was statistically significant for the vehicle controls of the 5-FU-treated ($p = 0.0382$) and carboplatin-treated cultures ($p= 0.0315$).

In contrast, the 4-12-2017 experiment (Fig 4-7) showed no statistically significant differences in mean caspase 3/7 levels between miR-451a mimic-transfected vehicle control-treated cultures and matched negative control mimic-transfected vehicle control-treated cultures.

This difference between the two experiments' apoptosis behavior in the vehicle-treated cultures at the 72-hour timepoint may be due to the more pronounced impact of miR-451a on cell proliferation in the 10-11-2017 experiment (see Fig 4-3 above, at 16–20 hours) *vs* the 4-12-2017 experiment (see Appendix 4.4, Figures 4.12 and 4.13, at 16–20 hours). Higher cell density in the 10-11-2017 experiment would result in greater competition for available nutrients at the 72-hour timepoint when the cells have grown beyond confluence, and this would reasonably be expected to result in higher levels of apoptosis.

4.3.5 miR-451a affected the clonogenic potential of OE33 cells

The data from the miR-451a mimics in OE-33 experiments assessed by Incucyte consistently indicated that miR-451a promoted cellular proliferation. This effect might make it difficult to isolate the assessment of the impact of miR-451a mimic on drug treatment response. Therefore, the clonogenic assay was performed for further analysis. This assay, also called the clonogenic survival assay or colony formation assay, tests the ability of a single cell to survive and reproduce to form colonies[356].

Three independent experiments were performed. The experimental design is shown in Figure 4-8. The optimal dose of each drug required to allow a sufficient number of colonies to form as well as observe a sufficient killing effect of the drugs was not known prior to conducting these experiments. Hence, a range of different concentrations were tried, with some guidance from available literature [357-362], and not all concentrations were included in each experiment. The clonogenic potential was assessed by calculating the plating efficiency (PE), which was the number of colonies formed divided by the number of seeded cells.

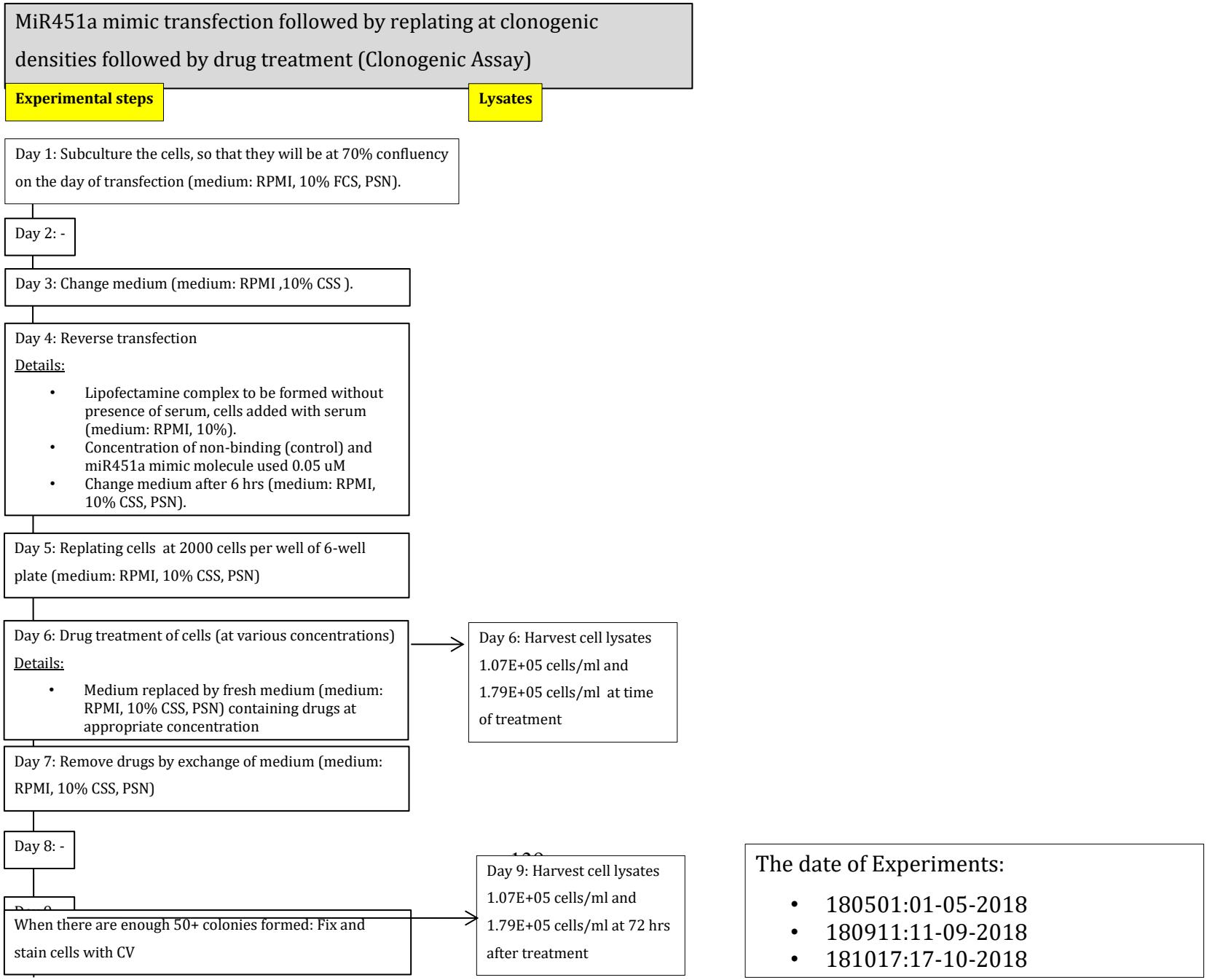
MiR451a mimic transfection followed by replating at clonogenic densities followed by drug treatment (Clonogenic Assay)
Experimental steps
Lysates
Day 1: Subculture the cells, so that they will be at 70% confluency on the day of transfection (medium: RPMI, 10% FCS, PSN).
Day 2: -
Day 3: Change medium (medium: RPMI ,10% CSS).
Day 4: Reverse transfection
Details:
Lipofectamine complex to be formed without presence of serum, cells added with serum (medium: RPMI, 10%).
Concentration of non-binding (control) and miR451a mimic molecule used 0.05 uM
Change medium after 6 hrs (medium: RPMI, 10% CSS, PSN).
Day 5: Replating cells at 2000 cells per well of 6-well plate (medium: RPMI, 10% CSS, PSN)
Day 6: Drug treatment of cells (at various concentrations)
Details:
Medium replaced by fresh medium (medium: RPMI, 10% CSS, PSN) containing drugs at appropriate concentration
Day 6: Harvest cell lysates 1.07E+05 cells/ml and 1.79E+05 cells/ml at time of treatment
Day 7: Remove drugs by exchange of medium (medium: RPMI, 10% CSS, PSN)
Day 8: -
When there are enough 50+ colonies formed: Fix and stain cells with CV
Day 9: Harvest cell lysates 1.07E+05 cells/ml and 1.79E+05 cells/ml at 72 hrs after treatment
The date of Experiments:
180501:01-05-2018
180911:11-09-2018
181017:17-10-2018

***Figure 4-8**. The diagram of the experiments performed using the Clonogenic Assay (drug treatment).*

Results from the first two experiments (180501 and 180911) indicated that the mean plating efficiencies were higher in the miR-451a-transfected and vehicle control (VC)-treated cells than in the negative control mimic transfected and vehicle control-treated cells (Figure 4-9, 4-10, 4-11, 4-12, top and middle graphs "VC" labels). In case of the cells treated with the vehicle controls of cisplatin-, 5-FU-, and carboplatin, these differences were statistically significant, indicating that miR-451a enhanced the clonogenic potential (i.e., survival potential) of the cells. Similarly, in the cisplatin-, 5-FU-, carboplatin-, and paclitaxel-treated cultures, the mean plating efficiencies were generally higher in the miR-451a-transfected cells than in the negative control mimic transfected cells.

In contrast to the first two experiments, the results from the third and final independent experiment on 181017 suggested that the miR-451a mimic decreased the clonogenic potential of OE33 cells (Figure 4-9, 4-10, 4-12, bottom graphs "VC" labels).

The discrepancy of PE could be due to the activation of potential signaling pathways, affecting PE. The potential mechanisms underlying this discrepancy will be investigated (see 4.3.10).

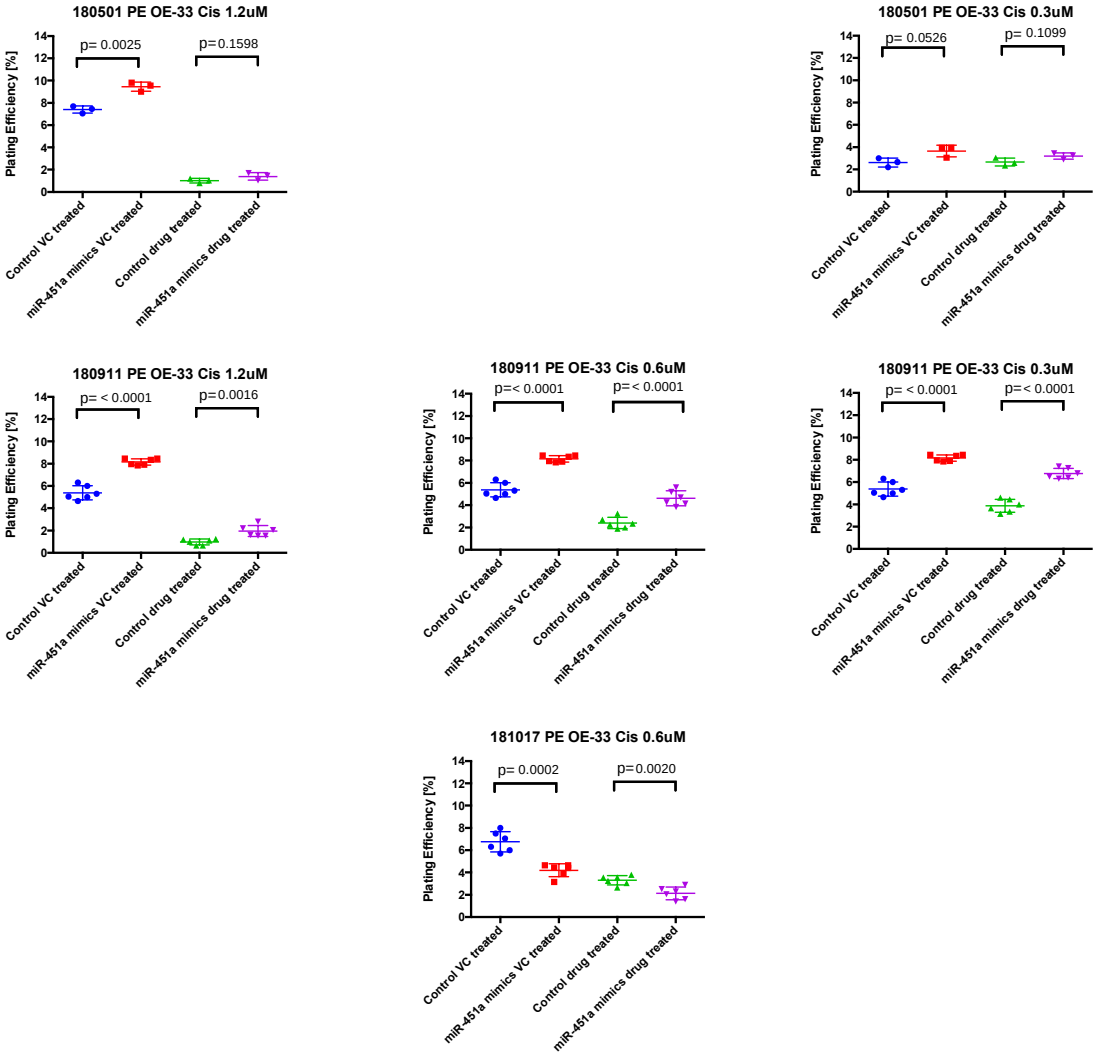

Figure 4-9*. The miR-451a mimics affected the PE in OE33 cells treated with VC of cisplatin and cisplatin. The title of the graph includes the date of the experiment and the drug concentration used in the experiment (there are two non-targeting mimic control (NT) groups: one is for the cells treated with the vehicle control (VC) and the other is for the cells treated with the drug).*

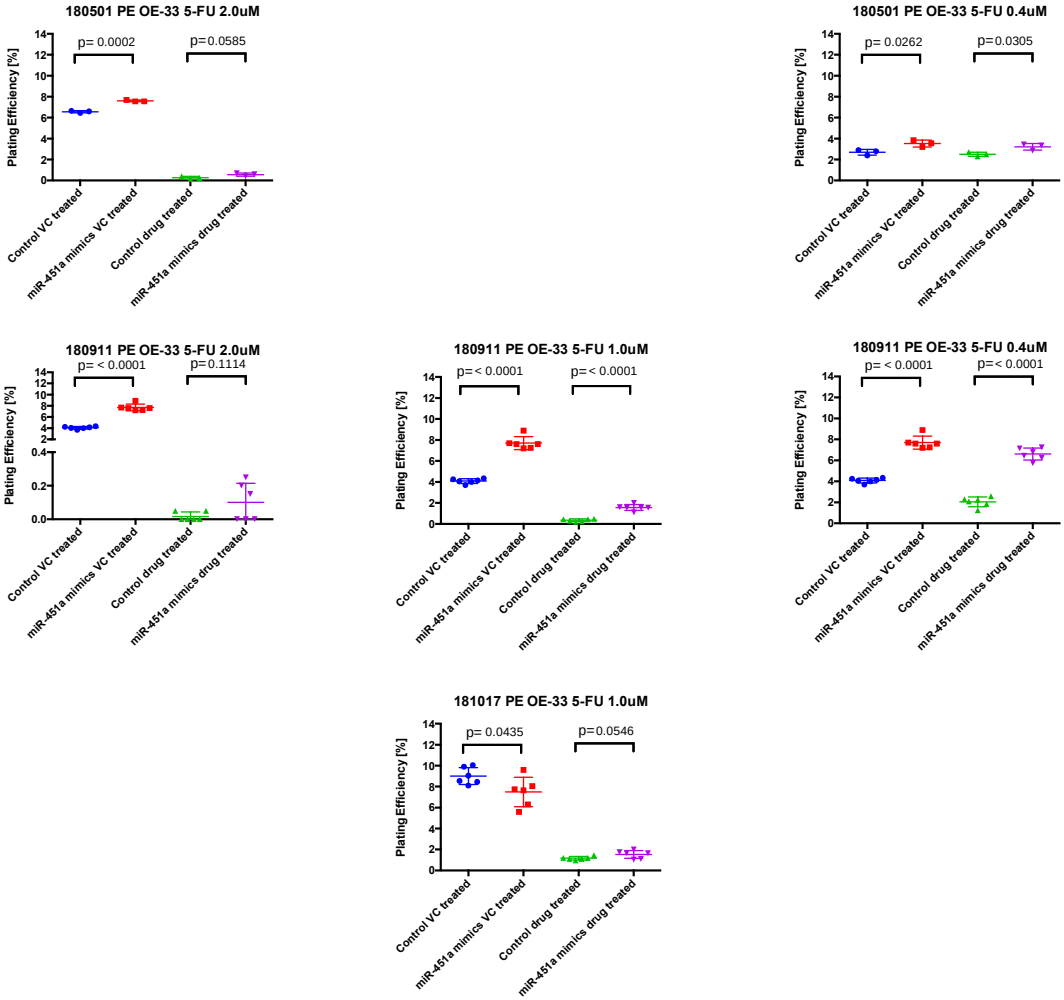

Figure 4-10. *The miR-451a mimics affected the PE in OE33 cells treated with the VC of 5-FU and 5-FU. The title of the graph includes the date of the experiment and the drug concentration used in the experiment (there are two non-targeting mimic control (NT) groups: one is for cells treated with the vehicle control (VC) and the other is for cells treated with the drug).*

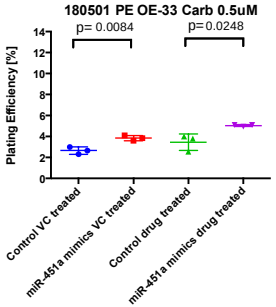
180501 PE OE-33 Carb 0.5uM
p= 0.0084
p=0.0248
Plating Efficiency [%]
Control VC treated
miR-451a mimics VC treated
Control drug treated
miR-451a mimics drug treated

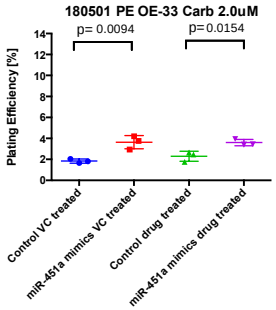
180501 PE OE-33 Carb 2.0uM
p= 0.0094
p=0.0154
Plating Efficiency [%]
Control VC treated
miR-451a mimics VC treated
Control drug treated
miR-451a mimics drug treated

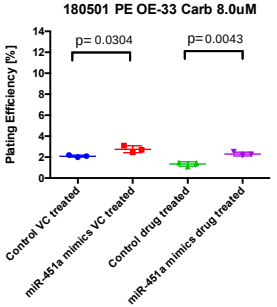
180501 PE OE-33 Carb 8.0uM
p= 0.0304
p=0.0043
Plating Efficiency [%]
Control VC treated
miR-451a mimics VC treated
Control drug treated
miR-451a mimics drug treated

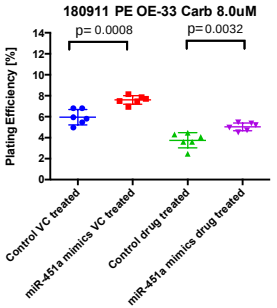
180911 PE OE-33 Carb 8.0uM
p= 0.0008
p=0.0032
Plating Efficiency [%]
Control VC treated
miR-451a mimics VC treated
Control drug treated
miR-451a mimics drug treated

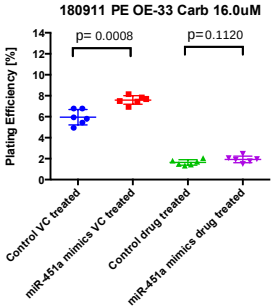
180911 PE OE-33 Carb 16.0uM
p= 0.0008
p=0.1120
Plating Efficiency [%]
Control VC treated
miR-451a mimics VC treated
Control drug treated
miR-451a mimics drug treated

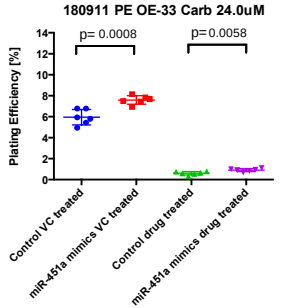
180911 PE OE-33 Carb 24.0uM
p= 0.0008
p=0.0058
Plating Efficiency [%]
Control VC treated
miR-451a mimics VC treated
Control drug treated
miR-451a mimics drug treated

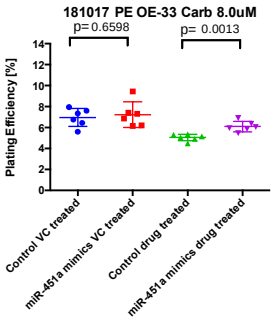
181017 PE OE-33 Carb 8.0uM
p=0.6598
p= 0.0013
Plating Efficiency [%]
Control VC treated
miR-451a mimics VC treated
Control drug treated
miR-451a mimics drug treated

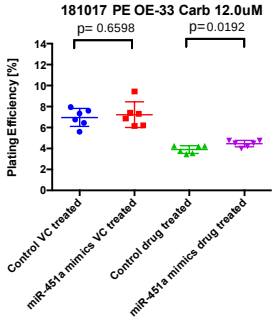
181017 PE OE-33 Carb 12.0uM
p= 0.6598
p=0.0192
Plating Efficiency [%]
Control VC treated
miR-451a mimics VC treated
Control drug treated
miR-451a mimics drug treated

Figure 4-11. *The miR-451a mimics affected the PE in OE33 cells treated with the VC of Carboplatin and Carboplatin. The title of the graph includes the date of the experiment and the drug concentration used in the experiment (there are two non-targeting mimic control (NT) groups: one is for cells treated with the vehicle control (VC) and the other is for cells treated with the drug.*

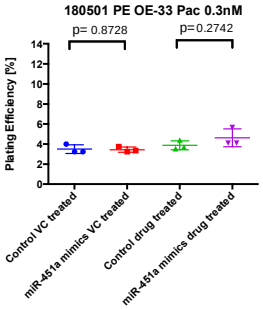
180501 PE OE-33 Pac 0.3nM
p= 0.8728
p=0.2742
Plating Efficiency [%]
Control VC treated
miR-451a mimics VC treated
Control drug treated
miR-451a mimics drug treated

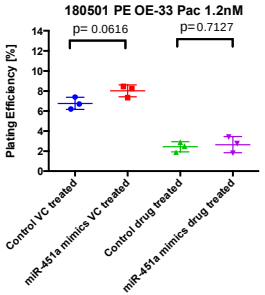
180501 PE OE-33 Pac 1.2nM
p= 0.0616
p=0.7127
Plating Efficiency [%]
Control VC treated
miR-451a mimics VC treated
Control drug treated
miR-451a mimics drug treated

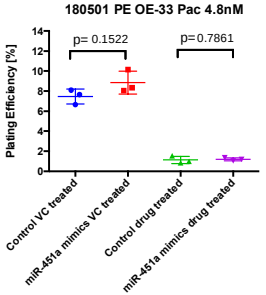
180501 PE OE-33 Pac 4.8nM
p= 0.1522
p=0.7861
Plating Efficiency [%]
Control VC treated
miR-451a mimics VC treated
Control drug treated
miR-451a mimics drug treated

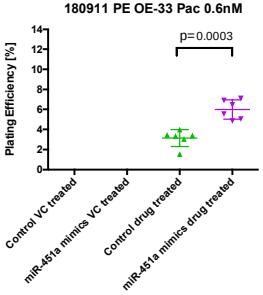
180911 PE OE-33 Pac 0.6nM
p=0.0003
Plating Efficiency [%]
Control VC treated
miR-451a mimics VC treated
Control drug treated
miR-451a mimics drug treated

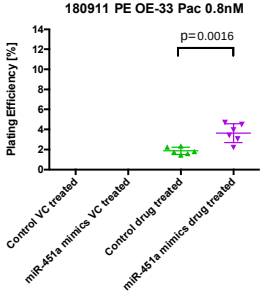
180911 PE OE-33 Pac 0.8nM
p=0.0016
Plating Efficiency [%]
Control VC treated
miR-451a mimics VC treated
Control drug treated
miR-451a mimics drug treated

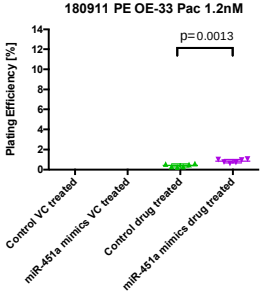
180911 PE OE-33 Pac 1.2nM
p=0.0013
Plating Efficiency [%]
Control VC treated
miR-451a mimics VC treated
Control drug treated
miR-451a mimics drug treated

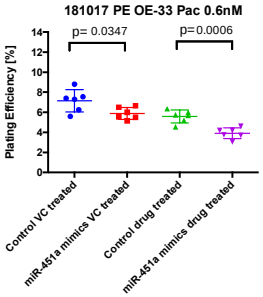
181017 PE OE-33 Pac 0.6nM
p= 0.0347
p=0.0006
Plating Efficiency [%]
Control VC treated
miR-451a mimics VC treated
Control drug treated
miR-451a mimics drug treated

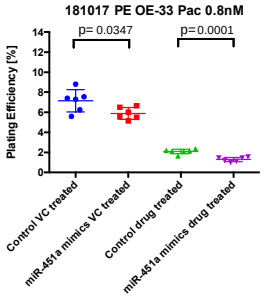
181017 PE OE-33 Pac 0.8nM
p= 0.0347
p=0.0001
Plating Efficiency [%]
Control VC treated
miR-451a mimics VC treated
Control drug treated
miR-451a mimics drug treated

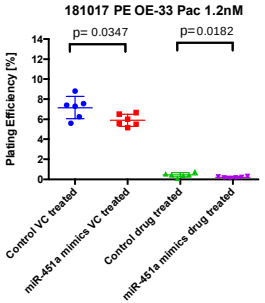
181017 PE OE-33 Pac 1.2nM
p= 0.0347
p=0.0182
Plating Efficiency [%]
Control VC treated
miR-451a mimics VC treated
Control drug treated
miR-451a mimics drug treated

Figure 4-12. *The miR-451a mimics affected the PE in OE33 cells treated with the VC of paclitaxel and paclitaxel. In the 180911 experiment, the wrong vial of working concentration was used to prepare the vehicle control and therefore the treatment was not included. The title of the graph includes the date of the experiment and the drug concentration used in the experiment (there are two non-targeting mimic control (NT) groups: one is for cells treated with the vehicle control (VC) and the other is for cells treated with the drug).*

4.3.6 The miR-451a mimics affected the drug treatment response in OE33 cells as measured by the clonogenic assay

The treatment response was assessed by calculating the survival fraction (SF), which was calculated by dividing the PE in the treated group with the PE in the control group.

In the cisplatin treatment, the results showed that the miR-451a mimics made the OE33 cells more resistant to cisplatin in the experiment conducted on 180911 (Figure 4-13, middle graphs labelled 180911). In the experiments conducted on 181017 and 180501, there were no significant differences between the miR-451a mimic group and the negative control group (Figure 4-13, top and bottom graphs).

In the 5-FU treatment, the miR-451a mimics made the OE33 cells more resistant to the 1 μM and 0.4 μM 5-FU doses in the 180911 experiment (Figure 4-13, middle graphs labelled 180911), and another experiment from 181017 confirmed this effect (Figure 4-14, bottom graphs labelled 181017). There were no significant differences observed in the 180501 experiment (Figure 4-14, top graphs label 180501).

In the Carboplatin treatment, the miR-451a mimics made the OE33 cells more resistant to 8 μM Carboplatin in the 181017 experiment (Figure 4-15, bottom graphs labelled 181017). There were no significant differences observed in the experiments conducted on 180501 and 180911 (Figure 4-15, top and middle graphs).

As for the paclitaxel treatment, the miR-451a mimics made the OE33 cells less resistant to paclitaxel in the 181017 experiment (Figure 4-16, bottom graphs labelled 181017). There was no significant difference in the 180501 experiment. (Figure 4-16, top graphs labelled 180501). The survival fraction in the 180911 experiment could not be calculated because the wrong working vial of Paclitaxel vehicle was used for

preparing the vehicle control treatments and therefore these treatments were not performed.

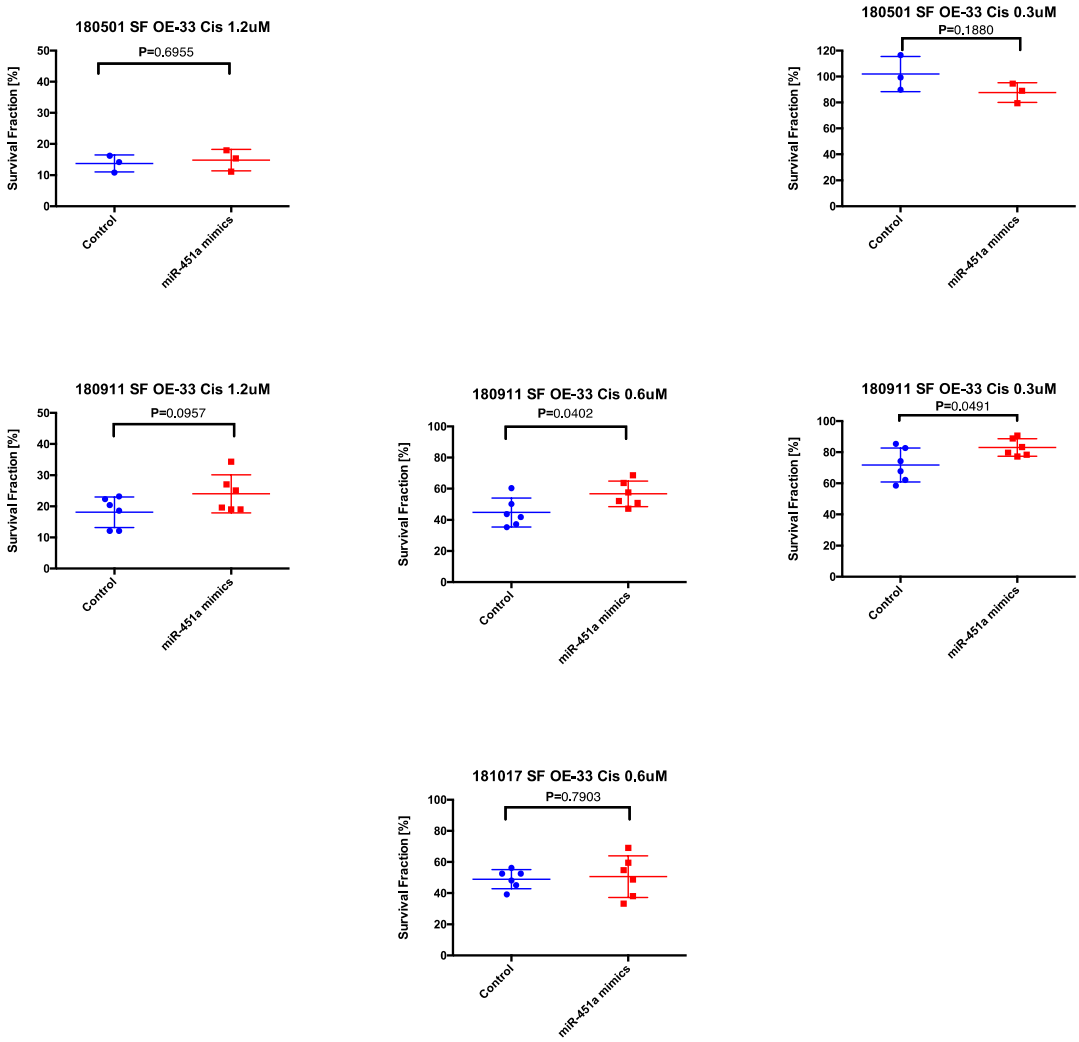

Figure 4-13. *The miR-451a mimics affected the SF in OE33 cells treated with cisplatin. The Y-axis is the SF, while the X-axis represents the different transfection groups; control refers to the cells that were transfected with the negative control, while miR-451a mimics refer to the cells that were transfected with the miR-451a mimics. The title of the graph includes the date of the experiment and the drug concentration used in the experiment.*

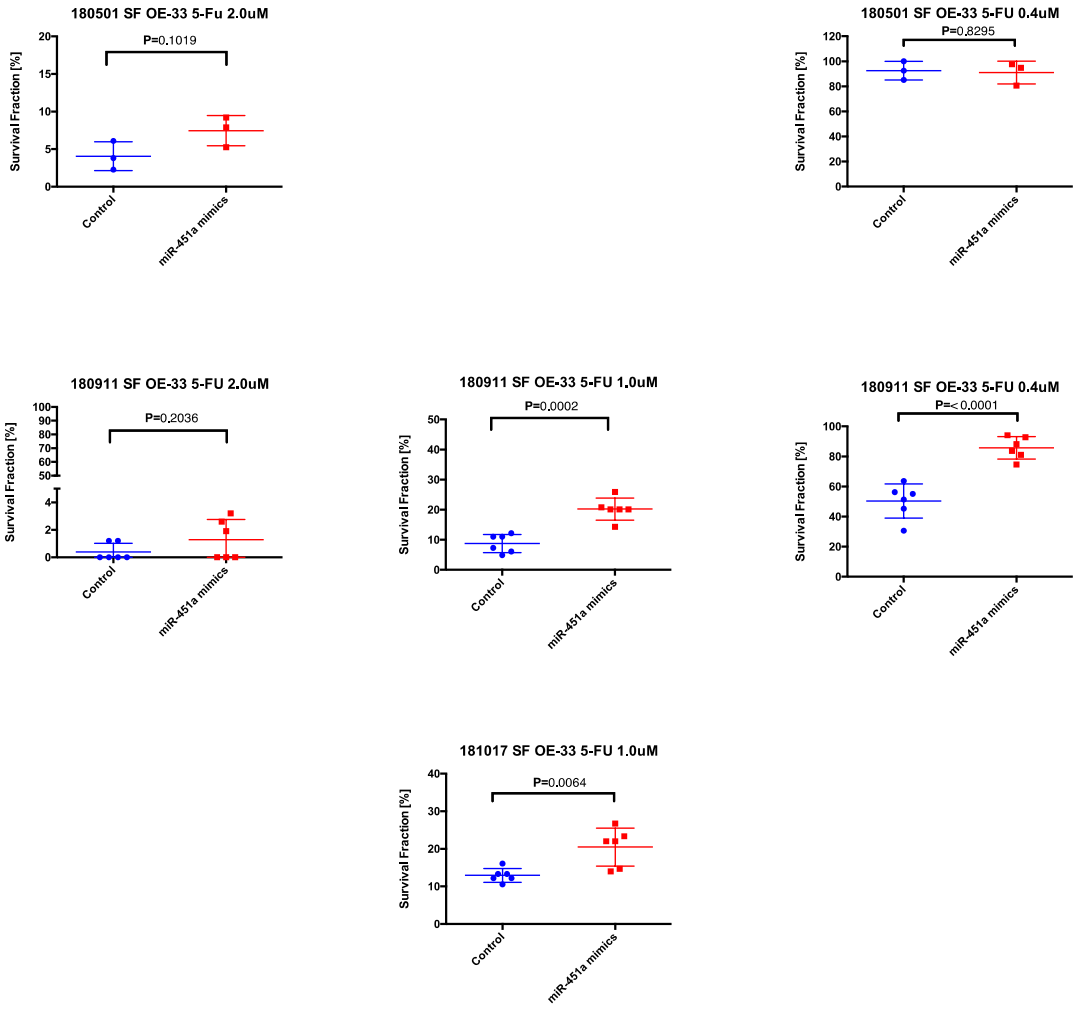

***Figure 4-14**. The miR-451a mimics affected the SF in OE33 cells treated with the VC of 5-FU and 5-FU. The title of the graph includes the date of the experiment and the drug concentration used in the experiment.*

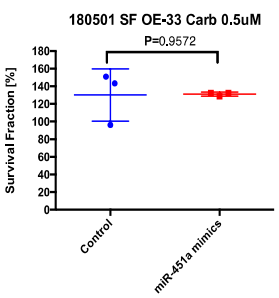
180501 SF OE-33 Carb 0.5uM
P=0.9572
Survival Fraction [%]
Control
miR-451a mimics

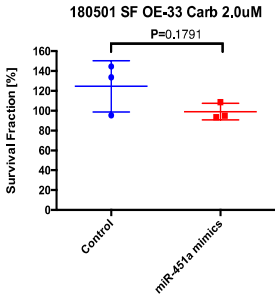
180501 SF OE-33 Carb 2.0uM
P=0.1791
Survival Fraction [%]
Control
miR-451a mimics

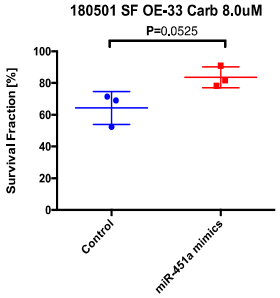
180501 SF OE-33 Carb 8.0uM
P=0.0525
Survival Fraction [%]
Control
miR-451a mimics

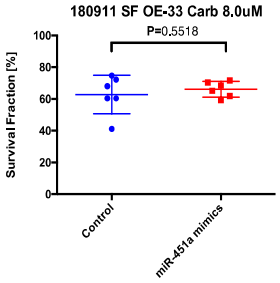
180911 SF OE-33 Carb 8.0uM
P=0.5518
Survival Fraction [%]
Control
miR-451a mimics

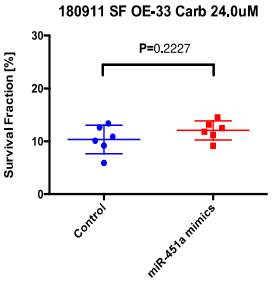
180911 SF OE-33 Carb 24.0uM
P=0.2227
Survival Fraction [%]
Control
miR-451a mimics

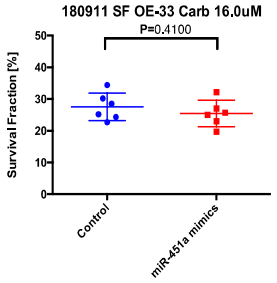
180911 SF OE-33 Carb 16.0uM
P=0.4100
Survival Fraction [%]
Control
miR-451a mimics

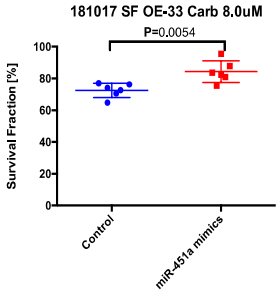
181017 SF OE-33 Carb 8.0uM
P=0.0054
Survival Fraction [%]
Control
miR-451a mimics

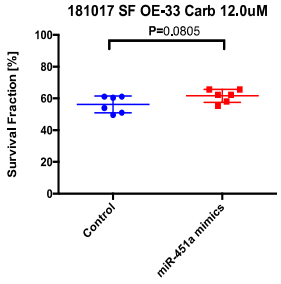
181017 SF OE-33 Carb 12.0uM
P=0.0805
Survival Fraction [%]
Control
miR-451a mimics

***Figure 4-15**. The miR-451a mimics affected the SF in OE33 cells treated with the VC of Carboplatin and Carboplatin. The title of the graph includes the date of the experiment and the drug concentration used in the experiment.*

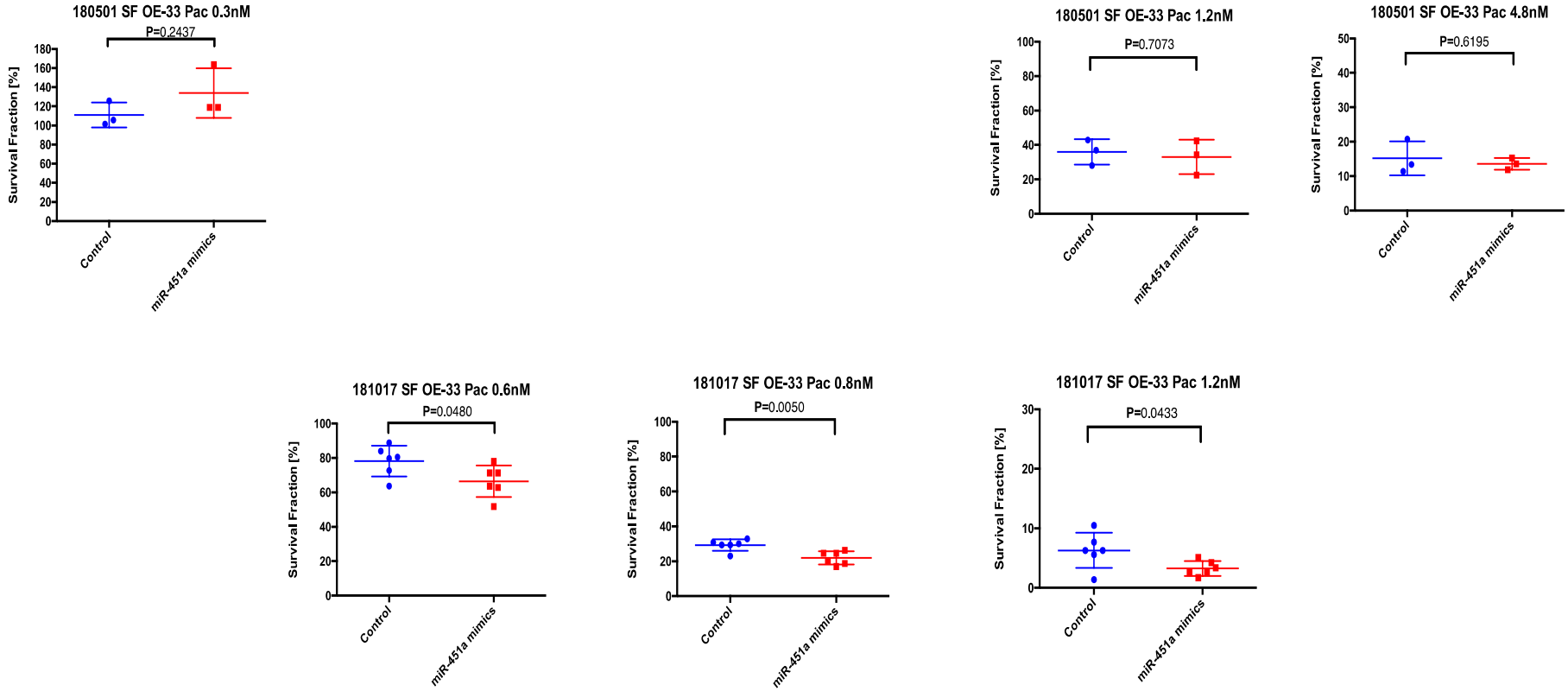

Figure 4-16. *The miR-451a mimics affected the SF in OE33 cells treated with the VC of paclitaxel and paclitaxel. The title of the graph includes the date of the experiment and the drug concentration used in the experiment.*

Table 4-2 presents a summary of the drug treatment response in OE33 cells using the SF of miR-451a mimic divided by the SF of negative control. Results are arranged from lowest to highest drug concentration tested. Overall, when a significant difference in drug response was observed, the results indicated that miR-451a mimics might make the cells more resistant to cisplatin, 5-FU, and carboplatin, but less resistant to paclitaxel (Table 4-2). This effect persisted even in the 181017 experiment, in which the direction of the effects of the miR-451a mimic on the clonogenic potential of the vehicle-treated cells was the opposite of that observed in case of the first two experiments. This suggests that miR-451a regulates cell survival and drug response via different mechanisms.

Table 4-2*, The summary of the drug treatment response in OE33 cells by the clonogenic assay (NT: negative control, the p-value is labeled in red when below 0.1. The arrow is up when SF miR-451a mimic/NT ratio is above 1, otherwise it is down. p<0.1 is labeled in red).*

Drug name	Drug conc.	Date	SF miR-451a mimic/SF NT	p-value
Cisplatin	0.6 μM	180911	1.267 ↑	0.04
	0.6 μM	181017	1.034	0.79
	1.2 μM	180501	1.078	0.69
	1.2 μM	180911	1.325 ↑	0.09
5-FU	1.0 μM	180911	2.303 ↑	0.0002
	1.0 μM	181017	1.582 ↑	0.006
	2.0 μM	180501	1.837	0.1

	2.0 μM	180911	3.171	0.2
Carboplatin	8.0 μM	180501	1.301 ↑	0.05
	8.0 μM	180911	1.053	0.55
	8.0 μM	181017	1.162 ↑	0.005
	12.0 μM	181017	1.095 ↑	0.08
	16.0 μM	180911	0.923	0.41
	24.0 μM	180911	1.165	0.22
Paclitaxel	0.6 nM	181017	0.850 ↓	0.05
	0.8 nM	181017	0.749 ↓	0.005
	1.2 nM	181017	0.517↓	0.04
	1.2 nM	180501	0.919	0.71
	4.8 nM	180501	0.893	0.62

4.3.7 The miR-451a mimics affect the response of OE-33 cells to irradiation – clonogenic assay.

Two independent clonogenic assay experiments were performed to study whether the miR-451a mimic affected the response of OE33 cells to irradiation. The experimental design is shown in Figure 4-17.

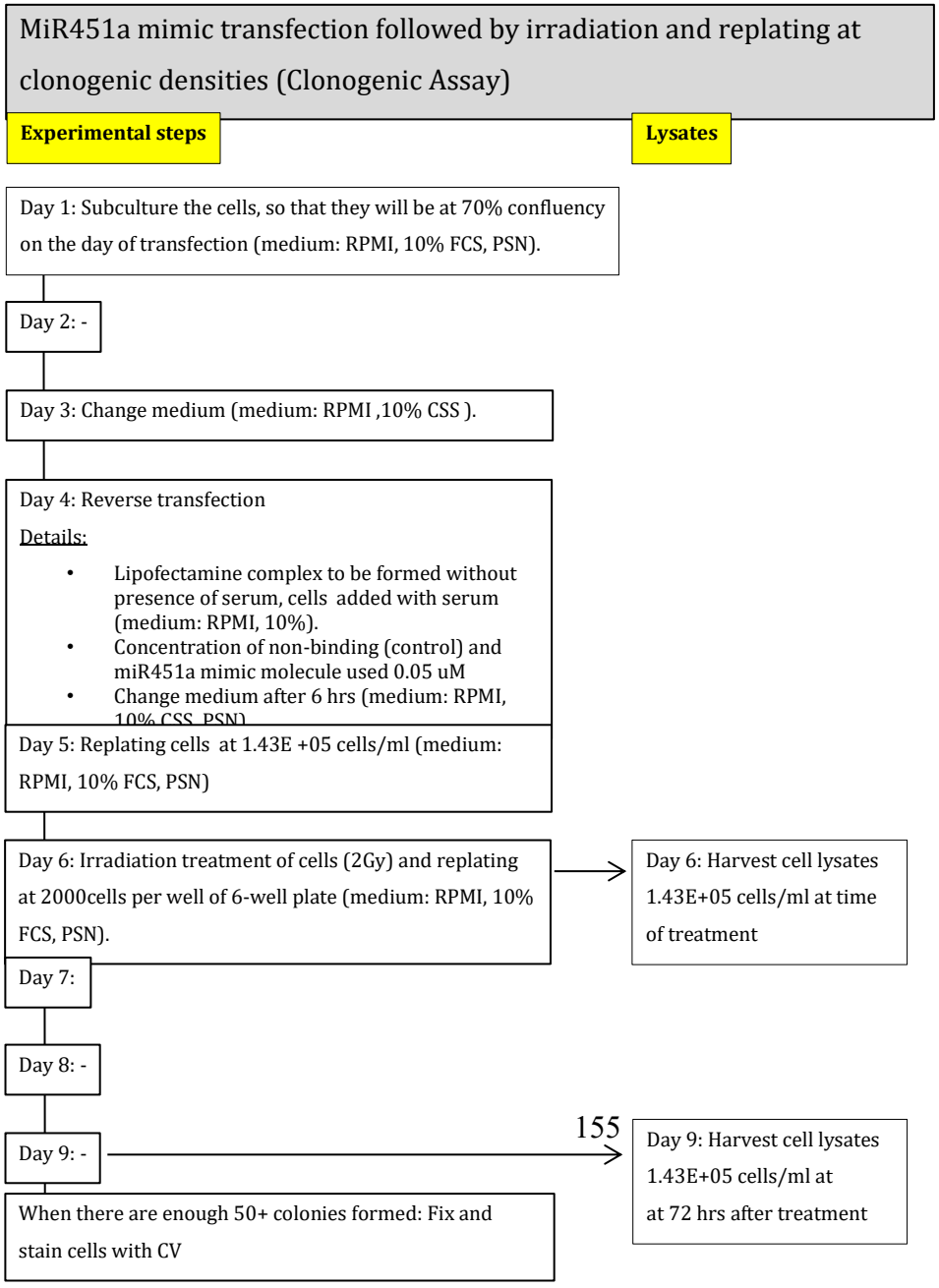

The date of Experiments:

- 180926:26-09-2018
- 181002:02-10-2018

***Figure 4-17**. The diagram of the experiments by Clonogenic Assay (irradiation treatment).*

In both experiments, the mean plating efficiency in the non-irradiated miR-451a mimic transfected cells was significantly lower than in the non-irradiated negative control mimic transfected cells (Figure 4-18). These results indicated that the miR-451a mimic decreased the clonogenic potential of OE33 cells in two independent experiments. The same result was observed in the irradiated cells.

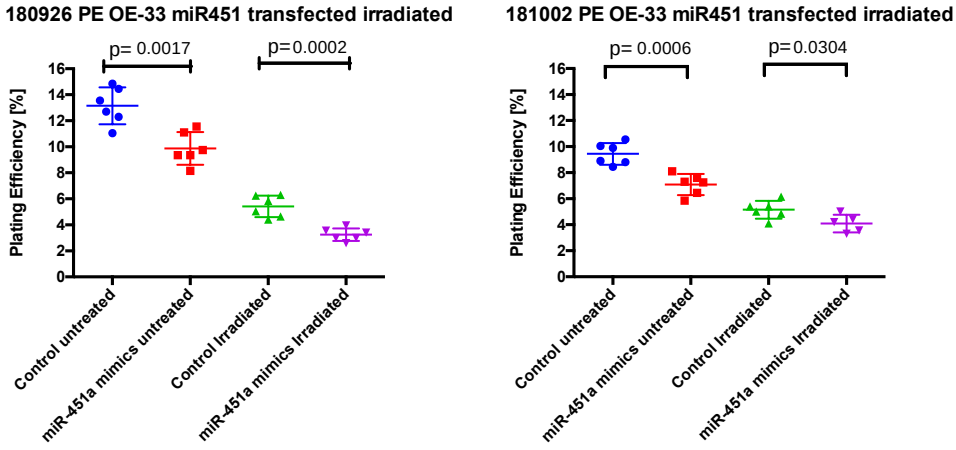

***Figure 4-18**. The miR-451a mimics affected the PE in OE33 cells treated with control and irradiation (control untreated group: the cells were transfected by non-targeting mimic control without undergoing radiation, miR-451a mimics untreated: the cells were transfected by miR-451a mimics without undergoing radiation. control irradiated group: the cells were transfected by non-targeting mimic control undergoing radiation, miR-451a irradiated: the cells were transfected by miR-451a mimics undergoing radiation).*

Calculation of survival fraction indicated that miR-451a mimic resulted in a small statistically significant decrease in the SF in the experiment conducted on 180926, suggesting that miR-451a mimic had a small sensitizing effect. There was no significant difference in the experiment conducted on 181002 (Figure 4-19).

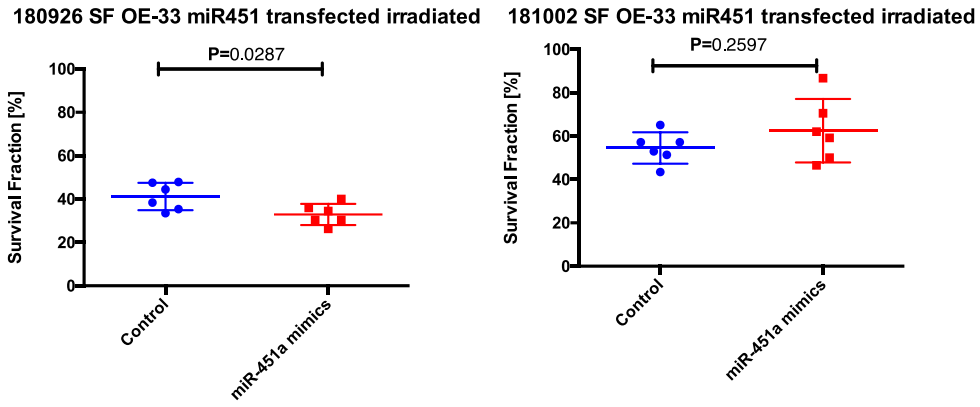

***Figure 4-19**. The miR-451a mimics affected the response of OE-33 cells to irradiation (control group: the cells were transfected by non-targeting mimic control undergoing radiation, miR-451a mimics: the cells were transfected by miR-451a mimics undergoing radiation).*

4.3.8 The potential mechanisms underlying the involvement of miR-451a in regulating the chemoradiotherapy response

4.3.8.1Investigation of Key Candidate Genes and Pathways for miR-451a using Integrated Bioinformatical Analysis

The potential functions of miR-451a were investigated by integrated bioinformatical analysis. The predicted target genes of miR-451a were obtained using miRWalk2.0 (http://zmf.umm.uni-heidelberg.de/apps/zmf/mirwalk2/) and 75 genes that were predicted by seven databases or more were chosen for further analysis by InnateDB (https://www.innatedb.com/). The InnateDB analysis included REACTOME, PID NCI, PID BIOCARTA, INOH, KEGG, and NETPATH. The results showed that there were 180 signaling pathways identified ($p<0.05$) by InnateDB (Table 4-2 shows $p<0.01$ only), on the top of the list were Mitotic G1-G1/S phases, energy dependent regulation of mTOR by LKB1-AMPK, and ErbB1 downstream signaling (Table 4-3).

***Table 4-3**: The predicted pathways of miR-451a by Innate DB ($p<0.01$)*

Pathway Name	Pathway p-value
Mitotic G1-G1/S phases	0.001
Energy dependent regulation of mTOR by LKB1-AMPK	0.001
ErbB1 downstream signaling	0.002
Regulation of mRNA stability by proteins that bind AU-rich elements	0.002
Cyclins and cell cycle regulation	0.002
RNF mutants show enhanced WNT signaling and proliferation	0.003
TCF dependent signaling in response to WNT	0.003
XAV939 inhibits tankyrase, stabilizing AXIN	0.003
Misspliced LRP5 mutants have enhanced beta-catenin-dependent signaling	0.003
mTOR signaling	0.003
PKB-mediated events	0.003
P38 MAPK signaling pathway	0.003
Oncogene Induced Senescence	0.004
Hedgehog signaling pathway	0.004
Signaling by WNT in cancer	0.004
Ceramide signaling pathway	0.004
deactivation of the beta-catenin transactivating complex	0.004

Angiotensin ii mediated activation of JNK pathway via Pyk2-dependent signaling	0.005
LKB1 signaling events	0.005
TNF receptor signaling pathway	0.005
TGF-beta signaling	0.005
Cyclin D associated events in G1	0.006
G1 Phase	0.006
Cell cycle	0.006
Toll-like receptor signaling pathway	0.007
TCR	0.007
Wnt signaling pathway	0.008
Proteasome	0.009
Cross-presentation of soluble exogenous antigens (endosomes)	0.009
Regulation of activated PAK-2p34 by proteasome mediated degradation	0.009

As we can see from the bioinformatical analysis, the AMPK signaling pathway might play a pivotal role in miR-451a regulation of the chemoradiotherapy response. AMPK is involved in the chemoresistance in several kinds of cancers[363-365]. Besides, elevated miR-451a suppressed its target, CAB39, in malignant glioma cells, leading to repression of LKB1 activity and its downstream substrate AMP-activated protein kinase (AMPK)[366]. In esophageal cancer cells, LKB1 promoted radioresistance by the AMPK pathway[367]. These studies support an important role of AMPK in regulating chemoradiotherapy response in EAC cells.

The AMPK signaling pathway plays an important role in regulating chemoradiotherapy response as discussed above. AMPK is a central regulator of metabolism. Therefore, we performed a literature research based around the regulators of metabolism. AMPK results in a rearrangement of the 14-3-3 interactome[368], and phosphorylates several 14-3-3 targets[369]. Besides, from the literature survey [370-373], YWHAZ (encoding the 14-3-3 zeta and delta protein) and AKT were validated targets of miR-451a, and the calcium-binding protein39 (CAB39) was a validated target of miR-451a in pancreatic cancer[251]. OXCT1 and SLC7A11 were also important in regulating metabolism and they were predicted targets of miR-451a and both are key molecules in several aspects of metabolism [374, 375]. MST1 was also a predicted target of miR-451a and was a key enzyme in the Hippo signaling pathway, while Hippo signaling regulated chemotherapy response and metabolism[257, 376]. p53 is a master regulator of cell growth and suppresses SLC7A11[377, 378]. These related proteins regulate energy metabolism, indicating that these miR-451a related proteins might work together to regulate the chemoradiotherapy response by affecting the Warburg effect (Chapter 1: 1.6.8). The network of miR-451a and related proteins could regulate chemoradiotherapy response, as showed in Figure 4-20. Therefore, these miR-451a related proteins would be further studied as part of this thesis.

It is worth mentioning that the gene-miRNA interactions of miR-451a showed that YWHAZ was the hub gene of miR-451a from the Innate-DB analysis. In gene expression networks, hub genes are genes with a high number of interactions with other genes in the network[379] (Figure 4-21). From the literature study, YWHAZ and miR-451a are known to play an important role in cancer and regulation of drug treatment response[333, 380, 381].

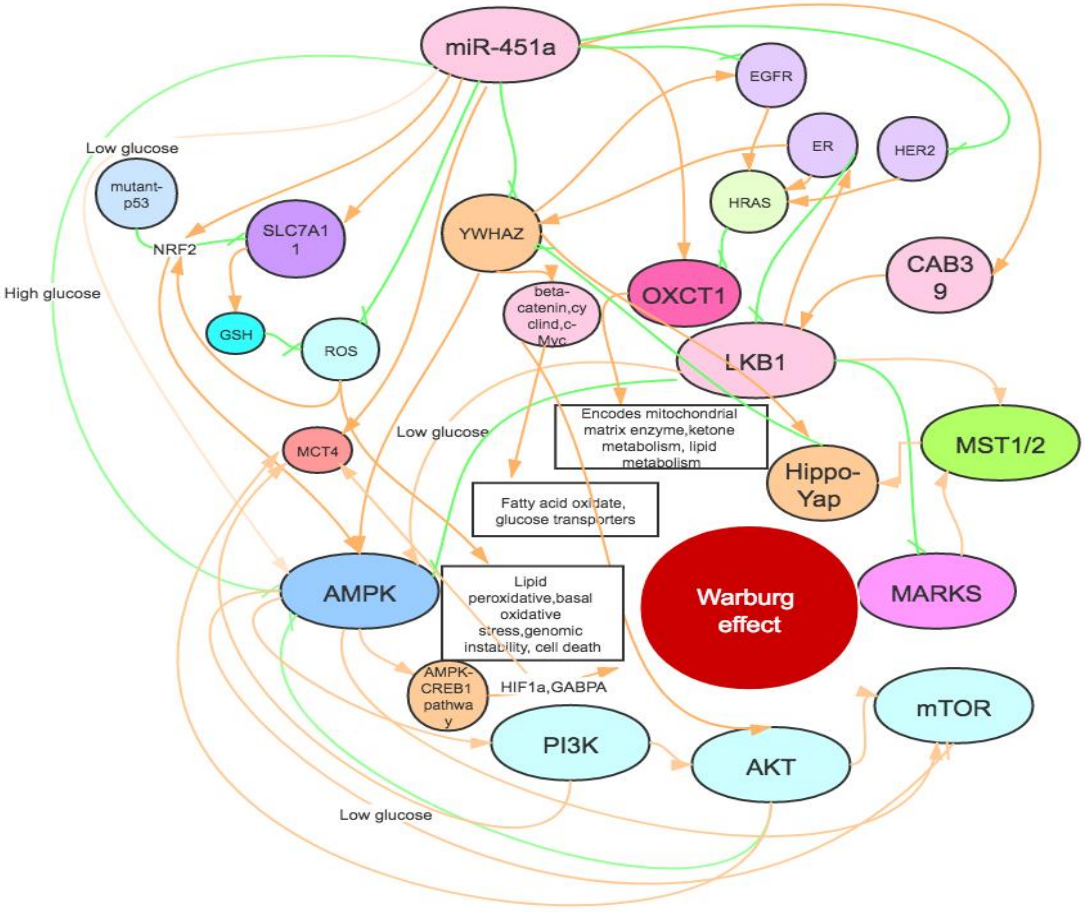

Figure 4.20*: Potential networks associated with the miR-451a-mediated regulation of its targets (Orange: promoting, Green: inhibiting).*

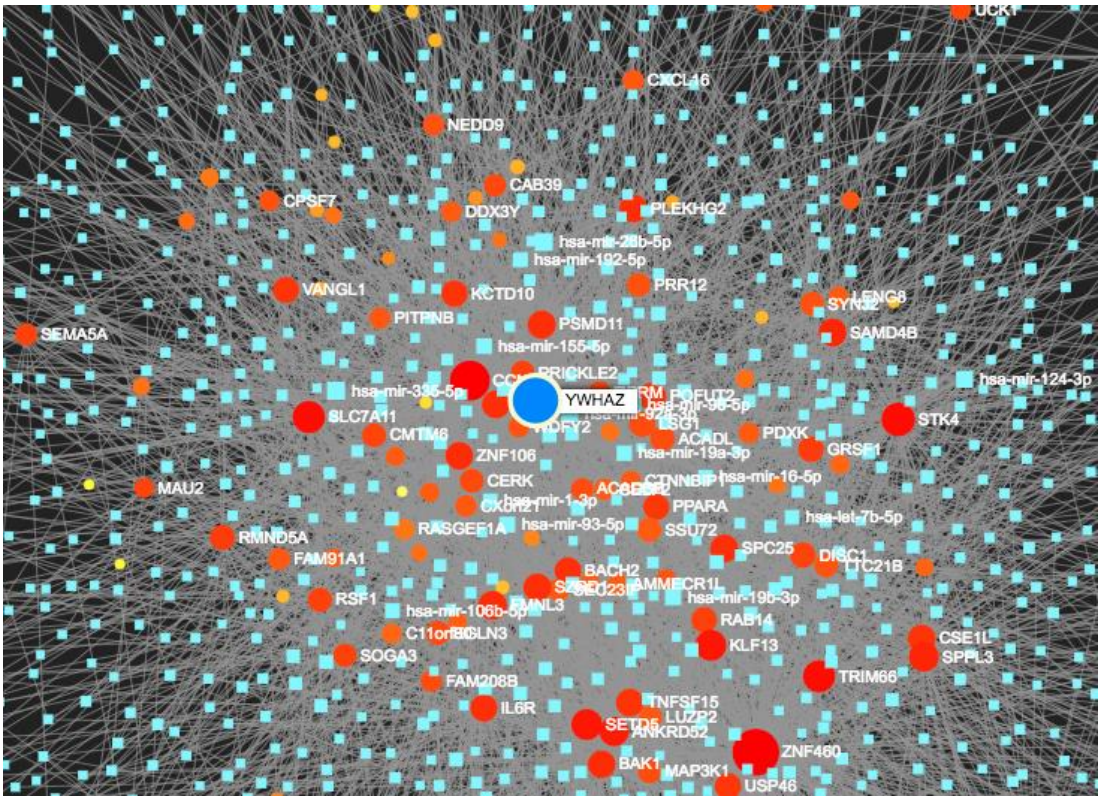

Figure 4-21*: Gene-miRNA interactions of miR-451a showed that YWHAZ was the hub gene of miR-451a (analysis from Innate-DB website)*

4.3.8.2 The relationship between the miR-451a related proteins and miR-451a

We used the eight EAC cell lines for this study: six adherent cell lines (OE19, OE33, JHEsoAd1, SKGT4, FLO1, and OACP4C), one suspension cell line (ESO51), and one semi-adherent cell line (ESO26). The miR-451a level was tested by qRT-PCR while the miR-451a related proteins were assessed by western blotting. The miR-451a related proteins were: YWHAZ (14-3-3 zeta/delta), AKT, OXCT1, SLC7A11, LKB1 (STK11), MST1 (STK4), CAB39, AMPK (pAMPK Thr172), and p53 according to the analysis of bioinformatics and literature study above. Some of them were detecting the phosphorylated form of the protein because protein phosphorylation is the most common and important molecular mechanism associated with the regulation of protein function[382]. For example, the upstream kinases (LKB1) activate AMPK by phosphorylating Thr172[383]. Therefore, this phosphorylated protein was detected in our study. The low cell density (the

equivalent of ~ 22,000 cells per well in a 24-well plate) and high cell density (the equivalent of ~ 60,000 cells per well in a 24-well plate) were used in this analysis and the Spearman rank correlation was used for statistical analysis. The two different densities were set here as well because our previous data showed that cell density might affect the expression of miR-451a and OE19. Prior miR-451a knockdown experiments performed in our lab demonstrated an inconsistent impact upon drug response across independent experiments (drug treatment experiments were done at low cell density), while the impact upon radiation response across independent experiments was consistent (radiation treatment experiments were done at high cell density). Our study showed that the miRNA expression was different between low and high cell density, indicating that the cell density might affect the miRNA expression (Appendix 4.7).

At low cell density, there were associations between expression of YWHAZ (14-3-3 zeta/delta) and miR-451a (rho=0.714, p=0.058), pAkt308, and miR-451a (rho=0.667, p=0.083). However, these did not reach statistical significance. Similarly, at high cell density, the results showed that YWHAZ (14-3-3 zeta/delta) has a correlation with miR-451a expression (rho=0.893, p=0.012). pAkt308 has an association with miR-451a expression at high cell density. However, this did not reach statistical significance (rho=0.750, p=0.066), Table 4-4, and Figure 4-22. There was no clear correlation between the other proteins and miR-451a expression at both low and high cell densities.

The cell lines were divided into resistant and sensitivity groups according to whether the treatment response was above the mean of all samples or not, and then the proteins were compared between the resistant and sensitivity groups. The results showed that YWHAZ (14-3-3 zeta/delta) and pAKT308 have a significant difference between the two groups (Table 4-4, and graphs in Appendix 4.6).

Table 4-4. *The relationship between the miR-451a related proteins and miR-451a*

Proteins	**Low cell density**	**High cell density**
	Spearman	**Spearman**

	rho	*p value*	*rho*	*p value*
YWHAZ (14-3-3 zeta/delta)	0.714	0.058	0.893	0.012
LKB1	-0.286	0.501	0.071	0.906
MST1	-0.048	0.935	-0.071	0.906
AKT	-0.310	0.462	0.036	0.964
pAKT308	0.667	0.083	0.750	0.066
OXCT1	-0.333	0.428	-0.143	0.783
SLC7A11	-0.191	0.665	-0.143	0.783
p53	-0.171	0.652	-0.214	0.665
CAB39	-0.024	0.977	0.071	0.906
pAMPK Thr172	-0.143	0.752	-0.286	0.556

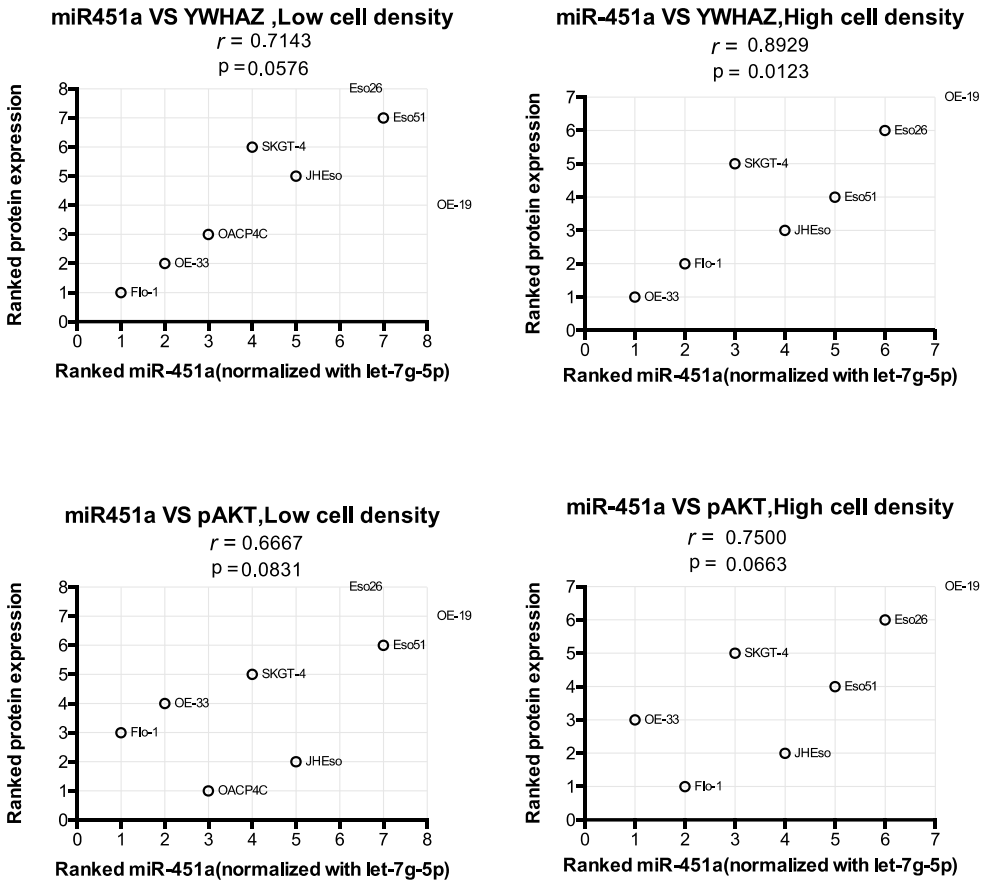

Figure 4-22*: The relationship between the miR-451a related proteins and miR-451a expression. (Only seven cell lines in high cell density, because the radiation response for OACP4C cell line varied markedly across five independent measurements. Therefore, it was excluded from the high-cell-density miR-451a assays performed here).*

4.3.8.3 The relationship between the miR-451a related proteins and treatment response

We used the eight EAC cell lines for this study: OE19, OE33, JHEsoAd1, SKGT4, FLO1, OACP4C, ESO51, and ESO26. These cell lines were treated with 8 μM cisplatin, 50 μM 5-FU, or irradiation (2 Gy, Xrad320, Precision X-Ray). The treatment response was assessed by MTS, flow cytometry, and Clonogenic assays. The miR-451a related proteins, YWHAZ (14-3-3 zeta/delta), AKT, pAKT308, CAB39, OXCT1, SLC7A11, MST1, LKB1, p53, and pAMPK Thr172 were assessed by western blotting.

The results showed that the YWHAZ protein (14-3-3 zeta/delta) was correlated with radiation treatment response (rho=0.929, p=0.007) and pAKT308 was correlated with radiation treatment response as well (rho=0.786, p=0.048) (Table 4-7, Figure 4-23). As for the drug treatment, there were associations between the expression of YWHAZ (14-3-3 zeta/delta) (rho=-0.643, p=0.096), AKT (rho=0.714, p=0.058), and 5-FU treatment response by flow cytometry. However, these did not reach statistical significance (Table 4-6, Figure 4-23). pAKT308 (rho=0.714, p=0.058) and SLC7A11 (rho=0.667, p=0.083) were associated with cisplatin and 5-FU treatment response, respectively by MTS, However, these did not reach statical significance (Table 4-5, 4-6, and Figure 4-23).

Table 4-5. *The relationships between proteins and cisplatin treatment response in eight EAC cell lines (the p value is labeled in red when less than 0.1 and the rho is in bold)*

Proteins	**Cisplatin treatment response**			
	Flow cytometry		**MTS**	
	Spearman		**Spearman**	
	rho	*p value*	*rho*	*p value*
YWHAZ (14-3-3 zeta/delta)	0.619	0.115	0.381	0.360
LKB1	-0.548	0.171	0.048	0.935
MST1	-0.095	0.840	-0.381	0.360
AKT	0.071	0.882	-0.262	0.536
pAKT308	0.405	0.327	**0.714**	0.058

OXCT1	-0.167	0.703	-0.381	0.360
SLC7A11	-0.167	0.703	0.381	0.360
p53	-0.512	0.178	-0.342	0.379
CAB39	0.048	0.935	-0.143	0.752
pAMPK Thr172	-0.405	0.327	0.048	0.935

Table 4-6. *The relationships between proteins and 5-FU treatment response in eight EAC cell lines (the p value is labeled in red when less than 0.1 and the rho is in bold)*

Proteins	**5-FU treatment response**			
	Flow cytometry		**MTS**	
	spearman		**spearman**	
	rho	*p value*	*rho*	*p value*
YWHAZ(14-3-3 zeta/delta)	**-0.643**	0.096	0.095	0.840
LKB1	-0.119	0.793	-0.333	0.428
MST1	-0.167	0.703	0.143	0.752
AKT	**0.714**	0.058	0.238	0.582
pAKT308	-0.167	0.703	0.238	0.582
OXCT1	0.476	0.327	0.071	0.882

SLC7A11	0.048	0.935	**0.667**	0.083
p53	-0.146	0.700	**-0.610**	0.104
CAB39	0.191	0.665	0.405	0.327
pAMPK Thr172	-0.191	0.665	-0.333	0.428

Table 4-7*. The relationships between proteins and irradiation treatment response in eight EAC cell lines (the p value is labeled in red when less than 0.1 and the rho is in bold)*

Proteins	**Radiation treatment response**	
	Clonogenic assay	
	spearman	
	rho	*p value*
YWHAZ(14-3-3 zeta/delta)	**0.929**	0.007
LKB1	0.250	0.595
MST1	-0.179	0.713
AKT	0.107	0.840
pAKT308	**0.786**	0.048
OXCT1	0.000	>0.999

SLC7A11	-0.071	0.906
p53	-0.321	0.498
CAB39	0.357	0.444
pAMPK Thr172	-0.393	0.396

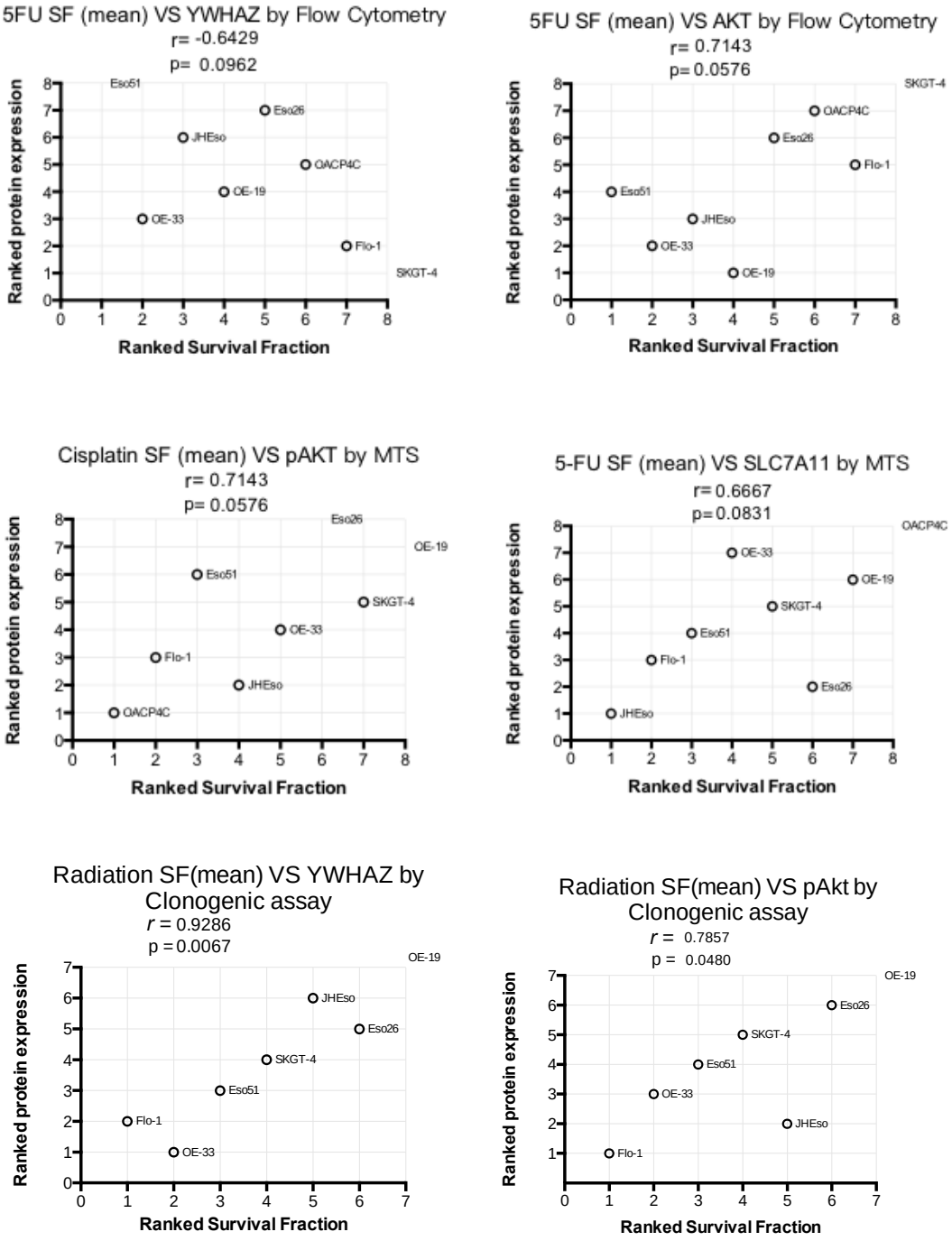

Figure 4-23. *The relationships between proteins and treatment response in eight EAC cell lines. The treatment response was the mean of three independent experiments, as indicated by '(mean)' in the graph titles). OACP4C cells were not included in the radiation experiment as they did not have a consistent response to radiation treatment.*

4.3.8.4 Investigating evidence for specific mechanisms underlying the role of miR-451a in regulating drug/irradiation response

According to the prediction from bioinformatics above, the mechanisms driving the impact of miR-451a on drug/irradiation response may involve the regulation of the expression of key proteins and the signaling pathways they are involved in. Therefore, the proteins YWHAZ (14-3-3 zeta and delta,) AMPK, pAMPK Thr172, HER2, CAB39, EGFR, pEGFR, Akt, pAkt308, STK11/LKB1, STK4/MST1, p53, SCOT1/OXCT1, and SLC7A11 were tested in miR-451a transfected OE33 cells by western blotting. The protein expression was quantified using local background subtraction methods (Chapter 2:2.2.18.10.1), and the data between OE33 cells transfected with miR-451a mimics or the non-targeting mimic control was compared.

The results are shown in Table 4-8; the western blotting bands are shown in Figure 4-24. As discussed in 4.3.8, AMPK, Akt, and YWHAZ were the important proteins or hub genes of miR-451a. The experiment from 10-11-2017 (labeled 171110 in table 4-8) was chosen for the miR-451a drug response mechanism study (labeled as "mechanism study" in Table 4-8) because in this experiment the miR-451a mimic molecule increased cell proliferation (4.3.2) and made the cells more resistant to drugs (4.3.3 and 4.3.4). The 180911 and 181017 experiments were also chosen for this reason, and also chosen to explore the possible reasons for the differences in plating efficiency between these two experiments (labeled as "PE discrepancy study" in Table 4-8).

The results showed that the expression of AMPK was decreased in two independent experiments (171110 and 181017) between miR-451a mimics and non-targeting mimic control after transfection, however in another independent experiment conducted on 180911, there was no clear difference. The expression of pAMPK Thr172 decreased in two independent experiments (180911 and 181017) between miR-451a mimics and non-targeting mimic control after transfection; however, in another independent experiment conducted on 171110, there was an increase in the expression of pAMPK Thr172.

The expression of 14-3-3 zeta/delta increased in two independent experiments (171110 and 180911) between miR-451a mimics and non-targeting mimic control after transfection; however, in another independent experiment conducted on 181017, its expression showed a decrease. Experiments from 171110 and 180911 showed an increase in the levels of 14-3-3 zeta phos Ser58; there was no clear difference in the levels of 14-3-3 zeta phos Ser58 in the experiment from 181017.

The levels of Akt and pAkt were measured in the 171110 experiment. The expression of Akt was increased by the miR-451a mimic. pAkt308 was not detected at the cell density used for the experiment. However, it was detected at higher cell densities (Figure 4-25).

The levels of EGFR and pEGFR were measured in the 171110 experiment. There was no clear difference in the normalized expression value of EGFR between miR-451a mimic and non-targeting mimic control transfected cells. The expression of pEGFR was decreased after transfection with the miR-451a mimic.

In the 171110 experiment, the expression levels of CAB39, STK11/LKB1, SLC7A11, SCOT1/OXCT1, p53, and HER2 were increased after transfection with the miR-451a mimic. STK4/MST1 was not detected at the cell density used for the experiment. However, it was detected at higher cell densities (Figure 4-25).

Table 4-8*. The differential protein expression after miR-451a transfection (the red down arrow indicates that the miR-451a mimics groups have decreased protein expression, while the black up arrow indicates that the miR-451a mimics groups have increased protein expression compared to that in the non-targeting mimic control groups. The arrow is up when miR-451a mimic/NT is above 1, otherwise it is down; - means no clear difference).*

Proteins	Aims		Date of experiment	0.05nM mimics/0.05nM non-binding	↑ , ↓ or _
AMPK	Mechanism study		171110	0.46	↓
		PE discrepancy study	180911	0.99	↓ _
			181017	0.86	↓
pAMPK Thr172	Mechanism study		171110	1.34	↑
		PE discrepancy study	180911	0.72	↓
			181017	0.86	↓
14-3-3 zeta/delta	Mechanism study		171110	1.4	↑
		PE discrepancy study	180911	2.37	↑
			181017	0.86	↓
14-3-3 zeta Ser 58	Mechanism study		171110	1.4	↑
		PE discrepancy study	180911	1.36	↑
			181017	0.99	↓ _
CAB39	Mechanism study		171110	1.44	↑
Akt	Mechanism study		171110	2.15	↑
pAkt308	Mechanism study		171110	Not detected	
STK11/LKB1	Mechanism study		171110	1.91	↑
SLC7A11	Mechanism study		171110	1.64	↑
SCOT1/OXCT1	Mechanism study		171110	1.47	↑
STK4/MST1	Mechanism study		171110	Not detected	
p53	Mechanism study		171110	2.99	↑
HER2	Mechanism study		171110	1.38	↑
EGFR	Mechanism study		171110	1.02	↑_
pEGFR	Mechanism study		171110	0.65	↓

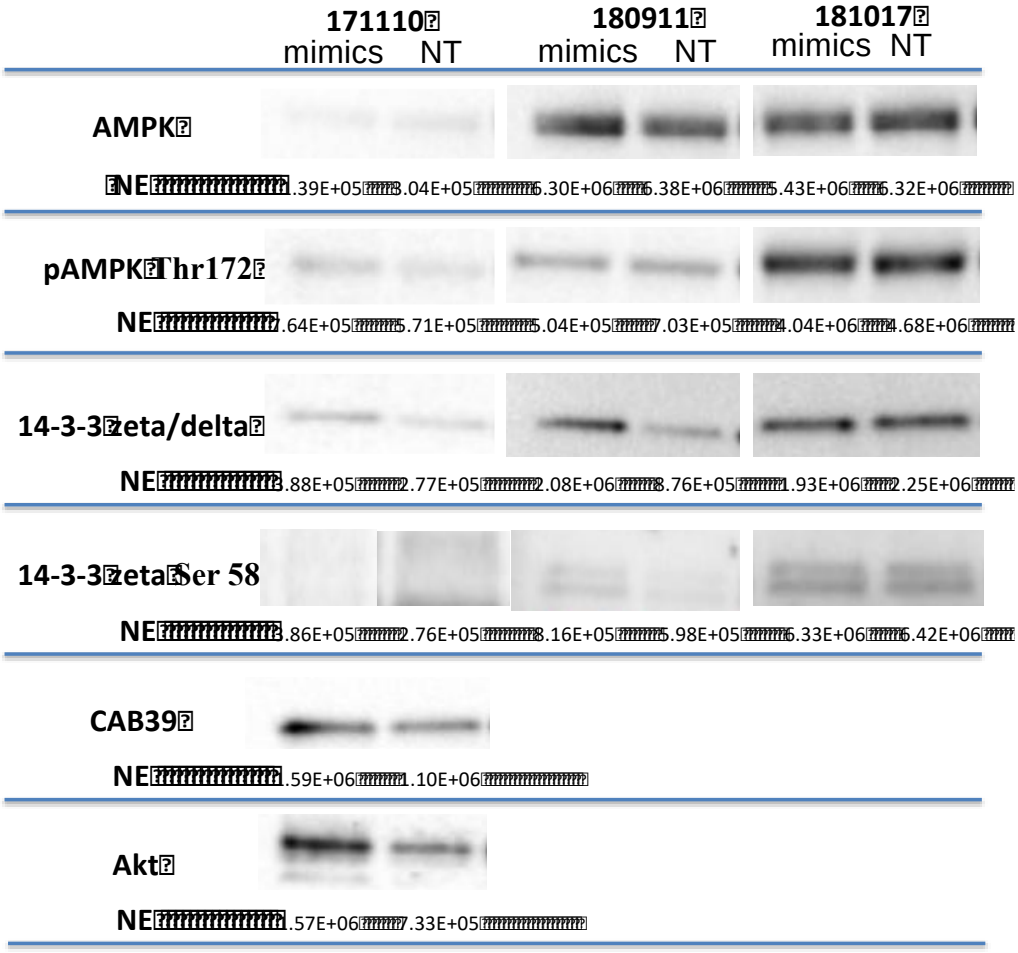
171110
mimics NT
180911
mimics NT
181017
mimics NT
AMPK
NE
pAMPK Thr172
NE
14-3-3 zeta/delta
NE
14-3-3 zeta Ser 58
NE
CAB39
NE
Akt
NE

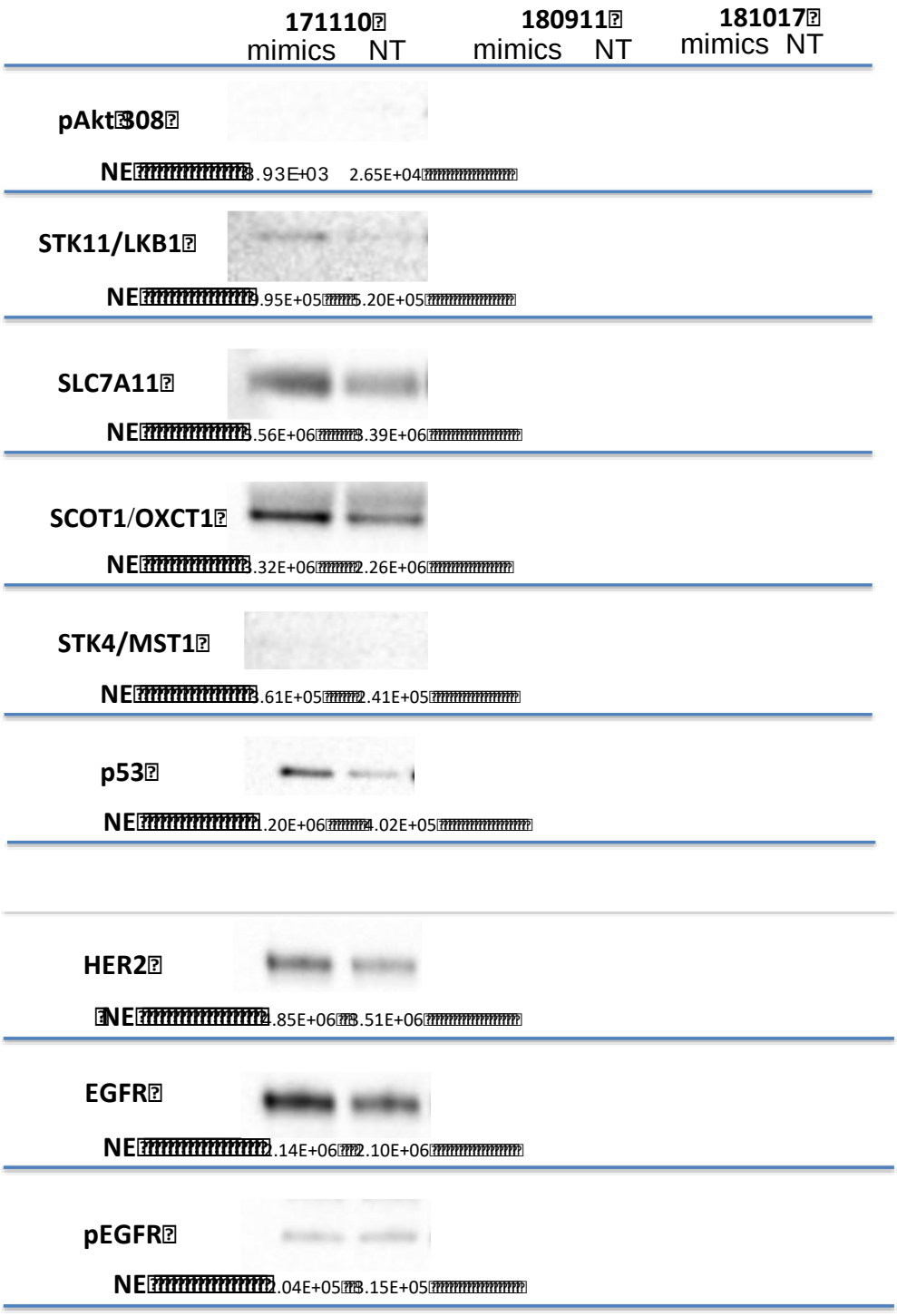

Figure 4-24. *The western blotting images of protein bands (60k cell density, 0.05 nM miR-451a mimic transfection. NE: values for the normalized expression).*

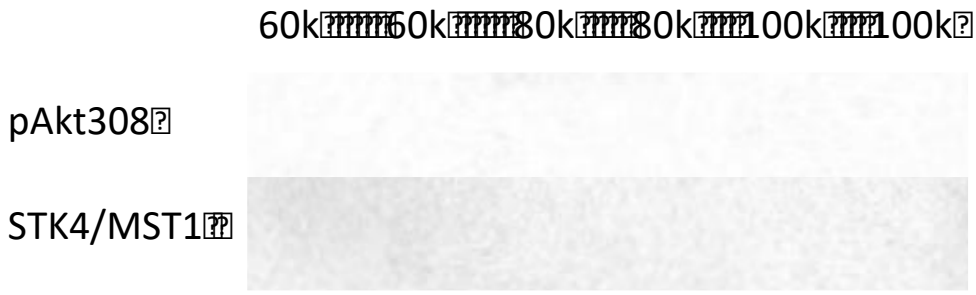

Figure 4-25*. Bands of pAkt308 and STK4/MST1 (60k, 80k, and 100k are the cell densities, i.e., the number of cells seeded in the 24-well plate: for e.g., 60k = 60,000 seeded cells)*

As discussed above, phosphorylation is an important molecular mechanism associated with the regulation of the expression of proteins and the signaling pathways they are involved in. The roles of phosphorylated and unphosphorylated proteins are different, for instance, 14-3-3 zeta delta interacts with TP53 and this interaction enhances p53 transcriptional activity. However, the phosphorylation of Ser 58 inhibits this interaction and p53 transcriptional activity[384]. Therefore, the ratio of phosphorylation was calculated using the normalized expression values from Figure 4-24 (Figure 4-26). The results showed increased pAMPK Thr172/AMPK expression levels in the mimic group in the 171110 experiment compared with non-targeting mimic control group. The 14-3-3 zeta phos Ser58/14-3-3 zeta/delta ratio was similar between the mimic and non-targeting mimic control groups. The 171110 experiment showed that the pEGFR/EGFR levels were decreased in the mimic group compared with non-targeting mimic control group. Therefore, the AMPK and pEGFR signaling pathways might play an important role in regulating chemoradiotherapy response.

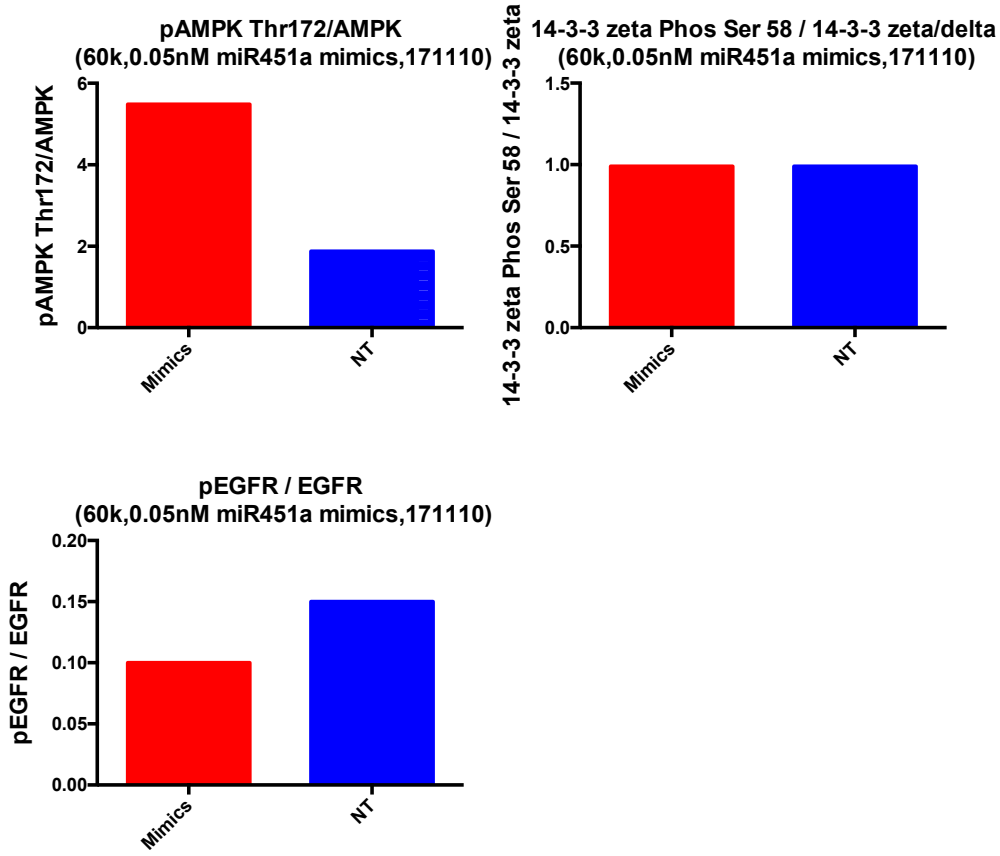

***Figure 4-26**. The ratio of phosphorylation for pAMPK, 14-3-3 zeta phos Ser58, and pEGFR (The title of the graph includes the date of the experiment, cell density, and the mimics concentration used in the experiment).*

4.3.9 The potential mechanisms underlying the discrepancy of PE between two independent experiments

In the 4.3.5 section, the results showed that the miR-451a mimics transfected cells increased the clonogenic potential of OE33 cells in the first two experiments (180501 and 180911), and this phenomenon was seen in their treatment with 5-FU, cisplatin, carboplatin, and paclitaxel. However, the 181017 experiment showed that miR-451a decreased the clonogenic potential of OE33 cells in the treatment of 5-FU, cisplatin, and paclitaxel and no clear difference between the miR-451a mimic and control groups in carboplatin treatment (Figure 4-9, 4-10, 4-11, 4-12). The discrepancy of PE could be due to activation of potential signaling pathways. As discussed above (4.3.9), the AMPK, pAMPK, 14-3-3 zeta/delta, and 14-3-3 zeta

Phos Ser 58 might play an important role in regulation of OE33 cell growth and drug treatment response. Therefore, these proteins were tested in order to explore the potential mechanisms underlying the discrepancy of PE between experiments. AMPK, pAMPK, 14-3-3 zeta/delta, and 14-3-3 zeta Phos Ser 58 were tested between the 180911 and 181017 experiments. The proteins were collected before the cells received drug treatment.

The results showed that the expression levels of 14-3-3 zeta/delta and 14-3-3 zeta Phos Ser 58 were different between 180911 and 181017, especially for 14-3-3 zeta/delta, the fold difference between the two experiments was 2.37 vs 0.86 (Figure 4-24, Table 4-8). Besides, the ratio of phosphorylation (the 14-3-3 zeta phos Ser58/14-3-3 zeta/delta) was opposite between the two experiments (Figure 4-27).

There was not much difference of AMPK and pAMPK between 180911 and 181017 (Figure 4-24, Table 4-8). The ratio of pAMPK Thr172/AMPK showed that there was less phosphorylation of AMPK (mimic vs NT) in 180911 compared with 181017 (Figure 4-27).

These differences could explain the discrepancy of PE between the two independent experiments.

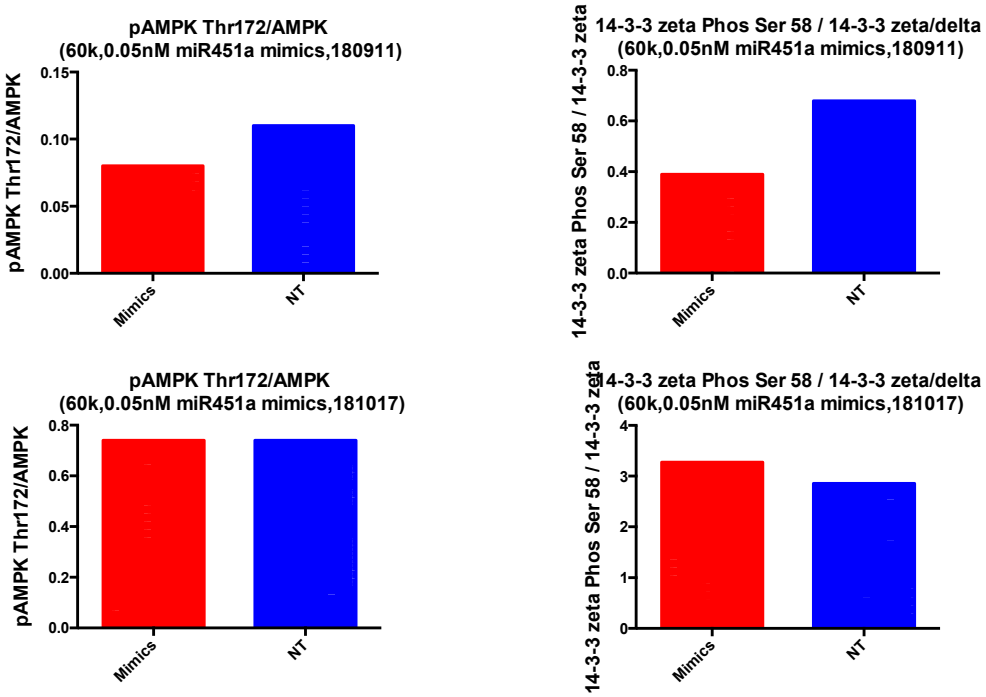

Figure 4-27*. The phosphorylation of AMPK and 14-3-3 zeta/delta was different between 180911 and 181017.*

4.4 Discussion

4.4.1 The optimization of the concentrations of 5-FU, cisplatin, carboplatin, and paclitaxel in OE33 cells

In chapter 3, the chemotherapy drugs used were 5-FU and cisplatin. 5-FU has been identified to inhibit the nucleotide synthetic enzyme, thymidylate synthase by inserting fluoronucleotides into DNA and RNA[385]. cisplatin is a platinum-containing drug, and acts by interacting with the purine bases of DNA, thus interfering with DNA repair and causing DNA damage in cancer cells[386]. Both are regular drugs for the treatment of EAC. In this chapter, we included carboplatin and paclitaxel as well because carboplatin and paclitaxel are the chemotherapy agents currently being used for the treatment of EAC in neoadjuvant settings. The mechanism underlying the action of carboplatin is similar to that for cisplatin, while

the mechanism underlying the action of paclitaxel was thought to be chromosome missegregation on multipolar spindles instead of causing mitotic arrest [387].

In order to study the function of miR-451a, the drug concentration for the treatment response needed to be optimized, that refers to the identification of an effective, but not a lethal dose, so as to allow miRNA modulation to enhance or suppress the drug treatment response. Several concentrations of 5-FU, cisplatin, carboplatin, and paclitaxel were tried according to the literature and previous data from our lab. The results showed that 100 μM carboplatin, 50 μM 5-FU, 8 μM cisplatin, and 10 nM paclitaxel were the optimized doses for the transfection experiments (Appendix 4.1).

The vehicle control was used to compare effect of the drug in order to get the right drug optimization. In our study, we found that the vehicle control of paclitaxel showed cytotoxicity (Appendix 4.2). The vehicle controls of paclitaxel were citric acid and Kolliphor (PEG35 35 castor oil), which were both potentially cytotoxic even at low concentrations, according to a previous study[388]. Additionally, studies indicated that high concentrations (around 0.1%) of the vehicle of paclitaxel may suppress the effects of the drug[389]. Our data showed that there was no cytotoxicity at the paclitaxel vehicle concentration of 0.001% and this concentration could be used for the future experiments.

4.4.2 The relationship between small RNAs expression and drug/radiation treatment response in EAC cell lines

The small RNAs that were selected as candidate biomarkers from tissue (chapter 3) were tested in eight EAC cell lines to investigate the relationship between small RNAs and treatment response. The results showed that several small RNAs had a relationship with treatment response, such as miR-451a, miR-767-5p, and miR-1301-3p, which validated our clinical data in cell lines. These small RNAs were reported to have an important role in the regulation of treatment response in cell lines. For example, miR-451a sensitized lung cancer cells to cisplatin[335] and breast cancer cells to paclitaxel[334], and regulated renal cell cancer drug resistance[343]. The results supported the hypothesis that some of the selected tissue

biomarkers of response to chemoradiotherapy might exert a direct biological role in controlling drug and radiation response in EAC cells.

The piRNAs and snoRNAs were tested in this study as well. During the writing of this thesis, it was noted that the piRNA assays on cell line RNA were done using cDNA generated with the Qiagen miScriptII reverse transcription kit and HiSpec buffer. The first step in this method of reverse transcription is the addition of a polyA tail to the 3′ end of RNA molecules. This is called polyadenylation of the RNA. According to previous advice from Qiagen, obtained at the beginning of this project, this method is unsuitable because piRNA sequences have 2'-O-methylation at their 3′ end which make them refractory to polyA tailing. When asked about this again during the writing of this thesis, the Research and Development team at Qiagen confirmed that based upon their testing, synthetic RNA molecules with 2'-O-methylation at their 3′ end cannot be polyadenylated and therefore cannot be converted into cDNA using the miScript II reverse transcription kit and HiSpec buffer. However, they acknowledged that their testing was more general and not specifically based on expertise with piRNA. They suggested that synthetic piRNA templates bearing the 2'-O-methylation could be ordered from them and used as templates to see if for some reason these specific piRNAs can be poly A-tailed. They also checked the sequences of the piRNAs using genomic databases and noted that they overlap significantly with other genes, thus raising the possibility that the PCR products synthesized in the piRNA PCR assays might have been generated from othe genes, i.e., derived from mRNAs or snoRNAs etc. that are coded for by the same chromosomal DNA sequences as the piRNAs. Further testing was outside the scope of this thesis. Therefore, the piRNA PCR assay results from cell lines require further confirmation.

miR-451a was one of the significant biomarkers that was correlated with treatment response in cell lines. The results showed that there is a positive correlation between miR-451a expression and the treatment response, which is consistent with the clinical data in chapter three. Therefore, miR-451a was selected for further functional studies. However, the relationship between miR-451a expression and drug treatment response was not as potent as the relationship between miR-451a

expression and radiation treatment. The potential reason for this could be that the cell density for drug treatment was considerably lower than the cell density for irradiation treatment. This might affect miR-451a expression, as the cell density affects the miRNA expression[392], and our data confirmed this as well (Appendix 4.7).

Six of 14 small RNAs (14 biomarkers selected from tissue) were not tested in cell lines because the QIAGEN company could not design a functional qRT-PCR assay for some piRNAs and snoRNAs. The function of these piRNAs and snoRNAs would be investigated in the future with further progress in biology technology.

4.4.3 The function of miR-451a in cell proliferation

The first function of miR-451a identified in OE33 cells was the promotion of cell proliferation. The cell confluence in miR-451a mimic group was higher than the corresponding non-targeting mimic control group at the same time point of treatment in Incucyte assay, which showed that miR-451a mimic enhanced cell proliferation. Our results showed that the miR-451a mimics increased cell proliferation after treatment with the vehicles of cisplatin, paclitaxel, carboplatin, and 5-FU. The results were also supported using the caspase3/7 apoptosis assay, and the results from 4-12-2017 showed that the miR-451a mimic molecule decreased the apoptosis of OE33 cells in most situations. However, another experiment on 10-11-2017 showed that the miR-451a mimic increased apoptosis after treatment with the vehicle of carboplatin and decreased the degree of apoptosis after treatment with the vehicle of paclitaxel. The reasons for the discrepancy between experiments could be complex, for example, environmental factors (O_2, CO_2, and pH)[393]. Besides, an increase in proliferation is not always necessarily associated with a decrease in apoptosis and sometimes both proliferation and apoptosis can be simultaneously increased[394].

The data obtained from Incucyte consistently indicate that miR-451a promotes cellular proliferation. However, this effect might make it difficult to isolate the assessment of the effect of miR-451a mimic on drug treatment response. Therefore, the Clonogenic Assay of assessment was performed for further analysis.

The results from the clonogenic assay showed that the miR-451a mimics-transfected cells increased the clonogenic potential of OE33 cells in most experiments, and this phenomenon was also seen in the treatment with 5-FU, cisplatin, carboplatin, and paclitaxel, which was consistent with the results of Incucyte experiments. The experiment conducted on 181017 showed that miR-451a decreased the clonogenic potential of OE33 cells after treatment with 5-FU, cisplatin, and paclitaxel and no clear difference between the miR-451a mimic and control groups in Carboplatin treatment. The discrepancy of PE was found in the experiment conducted on 181017, which was opposite to the other two experiments. Experiments thereafter proved that 14-3-3 zeta/delta and 14-3-3 zeta Phos Ser 58 in cells between two independent experiments were different. Besides, the ratio of phosphorylation (the 14-3-3 zeta phos Ser58/14-3-3 zeta/delta) was opposite between the two experiments as well. The ratio of pAMPK Thr172/AMPK showed that there was reduced phosphorylation of AMPK in the 180911 experiment compared with the 181017 experiment. These observations could explain the discrepancy of PE between two independent experiments.

A previous study showed that 14-3-3 plays an important role in cell division[395], cell growth, cell death, and cell migration[396], therefore it has been referred to as the dynamic and stress-adaptive signaling hub[397]. The AMPK signaling pathway is an energy sensing pathway that modulates cell metabolism[369] and coordinates cell proliferation and autophagy[398, 399]. The localization of AMPK is also important for energy regulation of cells[400]. These functions of the proteins discussed above could also explain the discrepancy of the PE.

The two independent experiments of irradiation showed that the miR-451a mimics-transfected cells decreased the clonogenic potential of OE33 cells in the control irradiation treatment and more independent experiments are needed.

According to the literature study, in esophageal squamous cell carcinoma, the miR-451a increased cell proliferation and contributed to cancer progression[401]. This function can be seen in other cancers as well. Guo et al.[251] reported that miR-451 promoted cell proliferation in pancreatic cancer and this was observed in renal cell

carcinoma as well[402], which was consistent with our findings. Another interesting study reported that the function of miR-451a is different according to the type of cell lines, for example, Liu et al.[345] observed that miR-451a inhibited cell proliferation in breast cancer, and this inhibition was observed in lung cancer as well[403]. Besides, miR-451a inhibited the proliferation, invasion, and migration of hepatocellular cells by targeting YWHAZ[370]. Recently, another study showed that the role of miR-451a is complex, and it suppresses the cell proliferation and also promotes cell infiltration in malignant glioma cells[366].

4.4.4 The function of miR-451a in regulating drug/radiation treatment response

The results of our drug treatment showed that miR-451a in OE33 cells made the cells more resistant to the drugs by Incucyte. We upregulated miR-451a expression in OE33 cells by transfecting the cells with the miR-451a mimics. The results showed that the upregulation of miR-451a increased the drug treatment resistance to 5-FU, cisplatin, carboplatin, and paclitaxel in OE33 cells. These findings were supported by a caspase3/7 experiment, which was used to monitor the apoptosis between miR-451a mimic and non-targeting mimic control groups. The results showed that there was less apoptosis in miR-451a mimic groups compared to the non-targeting mimic control groups after cisplatin, 5-FU, carboplatin, and paclitaxel treatment, which was consistent with the proliferation data. However, another experiment on 4-12-2017 showed that cisplatin, 5-FU, and carboplatin have no differences between the miR-451a mimic group and non-targeting mimic control groups while the results of paclitaxel showed that the miR-451a mimic groups showed increased levels of apoptosis, compared to those in the non-targeting mimic groups; these results were unlike those of the experiment conducted on 10-11-2017 (using the Incucyte assay). The reason for this discrepancy between experiments is complicated, as discussed above, for example, due to environmental factors (O2, CO2, and pH)[393].The clonogenic experiments showed that miR-451a mimics might make the cells more resistant to cisplatin, 5-FU, and carboplatin, but less resistant to paclitaxel.

As for the irradiation experiments, the results showed that the miR-451a mimics decreased the treatment response in one experiment, and more experiments were needed to confirm this. Thus, the function of miR-451a was different between chemotherapy and irradiation treatment.

Previous research has identified that miR-451a has an important role in regulating drug/radiation treatment response. miR-451 was reported to regulate paclitaxel resistance and increase the sensitivity to tamoxifen in a breast cancer cell line[334, 336], and it regulated chemoresistance in renal cell carcinoma[343]. Cheng et al. found that miR-451a increased the chemotherapy response to cisplatin in lung cancer cells[335]. miR-451a also regulated the radiation response, as it increased the sensitivity to radiation treatment in non-small cell lung cancers[342]. Thus, miR-451a might play a pivotal role in modulating the drug/radiation treatment response, and the individual function could vary according to the types of cell line or the types of treatment.

4.4.5 Investigating evidence for specific mechanisms underlying the effects of miR-451a

The target genes of miR-451a, which were predicted by seven or more databases were chosen for further bioinformatics analysis. The results showed that there were 180 signaling pathways identified by InnateDB ($p<0.05$), and the Mitotic G1-G1/S phases, energy dependent regulation of mTOR by LKB1-AMPK, and ErbB1 downstream signaling pathways were at the top of the list.

The relationship between the proteins discussed above and miR-451a treatment response was explored. Our results showed that YWHAZ (14-3-3 zeta/delta) and pAKt308 had a close correlation with miR-451a expression. The results also showed that YWHAZ (14-3-3 zeta/delta) and pAKT had a correlation with treatment response. These findings showed that miR-451a might regulate the treatment response by affecting YWHAZ (14-3-3 zeta/delta) and pAKT, and thus their signaling pathways.

In order to further investigate the regulation of treatment response, OE33 cells were transfected with miR-451a mimics (0.05 nM), and the transfected cells were lysed

for protein studies. The protein expression between miR-451a mimics and the non-targeting mimic control groups was compared. The results showed that AMPK and pEGFR expression levels were decreased to different degrees between the miR-451a mimics and non-targeting mimic control groups after transfection. miRNAs regulate gene expression post-transcriptionally by destabilizing the expression of mRNA and translational silencing the target genes and thus repressing protein production. Moreover, the ratio of phosphorylation showed that pAMPK Thr172/AMPK and pEGFR/EGFR were different in mimic groups compared with non-targeting mimic control groups. Therefore, miR-451a might play an important role in regulating chemoradiotherapy response via AMPK and pEGFR.

4.4.6 Limitations

This study had some limitations. First, we only tested the function of miR-451a mimic in one cell line, OE33. Further studies will transfect other EAC cell lines with the miR-451a mimic and evaluate its function. Besides, more biomarker candidates from chapter 3 should be studied because the mechanism underlying the regulation of chemoradiotherapy response is complicated. Second, the results showed that the data was not always consistent among repeated experiments, therefore, more experiments are needed to make the conclusions more reliable. Besides, this study did not compare the function of miR-451a in other kinds of cancer cell lines, such as the breast cancer cell line, MCF-7. Identifying the function of miR-451a in other types of cell lines helps us to understand the function of miR-451a comprehensively because miR-451a has different functions in cell proliferation and drug/radiation treatment according to different types of cells. Further, the mechanism of miR-451a in regulating chemoradiotherapy response is complicated and could involve several signaling pathways at the same time. Thus, further experiments to explore these mechanisms need to be performed. Future studies could also consider treatment response associations with combinations of biomarkers rather than a single biomarker at a time.

4.4.7 Summary

Several small RNAs that were selected as candidate biomarkers from tissue had a positive correlation with treatment response, especially for miR-451a.

The functional study of miR-451a showed that miR-451a enhances EAC cell proliferation and decreases the degree of apoptosis in most cases. Besides, miR-451a renders EAC cells more resistant to drug treatment.

From the Clonogenic assay, miR-451a increased the plating efficiency in most experiments and the discrepancy of results might result from the differential expression of 14-3-3 zeta/delta and the level of phosphorylation for AMPK and 14-3-3 zeta Phos Ser58. The Clonogenic assay showed that miR-451a made the cells more resistant to cisplatin, 5-FU, carboplatin, but less resistant to paclitaxel. In radiation experiments, the results showed that miR-451a decreased the plating efficiency and made the cells less resistant to irradiation, which indicated that the mechanisms between drug and irradiation may be different.

From the bioinformatical analysis and literature study, miR-451a might regulate treatment response by affecting AMPK, YWHAZ (14-3-3 zeta/delta), AKT, OXCT1, SLC7A11, LKB1 (STK11), MST1 (STK4), CAB39, and p53. The results showed the miR-451a was correlated with YWHAZ (14-3-3 zeta/delta) and pAKT and they were correlated with drug and irradiation treatment response. After transfection with the miR-451a mimics, AMPK expression decreased consistently. Besides, analysis of the ratio of phosphorylation showed that the levels of pAMPK Thr172/AMPK, 14-3-3 zeta phos ser58/14-3-3 zeta/delta, and pEGFR/EGFR were different in the mimic and the control groups, indicating that miR-451a might regulate the treatment response by affecting the levels of these proteins or their signaling pathways. Therefore, it is reasonable to hypothesize that they are the potential targets for EAC treatment in the future to improve chemoradiotherapy response.

CHAPTER 5

IDENTIFICATION OF POTENTIAL SMALL RNA BIOMARKERS OF RESPONSE TO CHEMORADIOTHERAPY IN PRE-TREATMENT BLOOD FROM PATIENTS WITH LOCALLY ADVANCED EAC

5.1 Introduction

Several small RNAs were identified as biomarkers of response to chemoradiotherapy in pre-treatment tissue samples of EAC patients in chapter 3. Cancer cells release small RNAs into the bloodstream or secrete extracellular vesicles that contain small RNAs into the bloodstream[82] and the levels of cancer-derived exosomes in cancer patients are higher than those in healthy controls[404, 405]. The circulating exosomes play an important role in cell-to-cell communication and pathogenesis. A number of studies showed that small RNAs in circulating exosomes were potential biomarkers of pathophysiological conditions[406-409]. Therefore, it was reasonable to study the small RNAs in exosomes of blood circulation as biomarkers of response to chemoradiotherapy.

A few studies have reported on circulating miRNAs as biomarkers of response to chemotherapy in ESCC patients. Tanake et al.[239] found that miR-27a/b was related to chemoresistance in EC, and they observed that miR-27a/b induced the transferring of normal fibroblast into cancer-associated fibroblast and promoted the production of transforming growth factor. Dong et al.[207] reported that miR-7 could be a biomarker for predicting chemotherapy response by interfering with EGFR mRNA translation. Decreased miR-377 expression predicts the poor response to chemoradiotherapy with 5-FU and cisplatin[221], by interfering with CD133 to suppress cancer initiation and progression, and by involving angiogenesis by regulating VEGF. The circulating miRNAs could also predict the radiotherapy response, for example, the ESCC patients who had a high miR-16 expression were

more sensitive to radiotherapy[231]. Lv et al.[198] indicated that the elevated expression of miR-21 increased the resistance to radiotherapy and recurrence frequency in esophageal cancer. However, very few studies have focused on the effects of small RNAs in exosomes from circulation as biomarkers of response to chemoradiotherapy in EAC patients.

The aim of this chapter was to investigate whether the small RNAs in serum exosomes could be useful biomarkers of response to chemoradiotherapy.

5.2 Methods and rationale

5.2.1 The patient cohorts

There were two patient cohorts: one was South Australia (SA) patient cohort (four complete responders, four moderate responders, and three poor-responders) and another was the Netherlands patient cohort (five complete responders and five non-responders), Chapter 2, 2.2.1. The tumor regression grading assessed the treatment response and divided the patients into responders and non-responders, Chapter 2,2.2.2. The blood sample preparation was slightly different between the two patient cohorts (table 5-1), which might impact biomarker expression levels and complicate a combined analysis of both cohorts. Therefore, the small RNAs were analyzed in the two patient cohorts separately.

Table 5-1. *Blood sample preparation between the two patient cohorts (★: initially centrifuged for 15 minutes at 453 g, but the clot separator gel did not resolve properly so they were centrifuged for an additional 5 minutes at 805 g)*

Sample from	Time between collection and centrifugation	Centrifuge force (RCF)	Centrifuge time (min)
SA patient cohort	<=24 hrs	453 or 453+805★	15+5★
Netherlands patient cohort	<=2 hrs	2000	10

5.2.2 Investigating the small RNAs selected from tissue as biomarker of chemoradiotherapy response in serum exosomes of EAC patient cohorts

The first experiment of this chapter was to investigate the small RNAs selected from tissue as biomarker of chemoradiotherapy response in serum exosomes of patient cohorts because the exosomes in blood might derive from the tumor tissues.

The biomarkers selected from the tissues in chapter 3 were as follows: miR-451a, miR-340-5p, DQ598428, DQ576665, miR-767-5p, miR-1301-3p, miR-552-3p, miR-99a-5p, miR-206, DQ598641, piR-hsa-32187, SNORD58B-201, SNORD46-2-201, and SNORD114-17-201. PCR was used for the testing of above small RNA expression. However, only seven of 14 small RNAs were tested because the Qiagen company could not design a functional qRT-PCR assay for some piRNAs and snoRNAs.

The exosome isolation from serum samples was performed by Exoquick assay (Cat No.: EXOQ5A-1, 5 mL), Chapter 2: 2.2.5. The process of RNA extraction from exosomes was described in Chapter 2: 2.2.7.

We tried to perform one reverse transcription reaction that would generate cDNA that could be used for all four (miRNA, piRNA, snoRNA, and snRNA) different classes of small RNAs. piRNAs have a 2'-OMe on their 3' terminal base that renders them significantly refractory to polyadenylation, while the polyadenylation is the rationale for Miscript II RT kit, therefore, the Miscript II system is not suited for detecting piRNAs. While the single cell kit uses the ligation of an adapter to the 3' end of the miRNA/piRNA, which is unaffected by the presence of the 2'-OMe. The miScript Single Cell qPCR Kit is a completely universal kit. Both annotated and non-annotated miRNAs, are selectively converted into cDNA and subsequently amplified. The Miscript single cell kit manual suggested that only a small number of representative samples selected from the total samples need to undergo PCR quality control test. However, in this study all samples underwent the PCR quality control

test to ensure that samples of satisfactory quality were used for assessment of biomarker performance (Chapter 2: 2.2.14.2).

The p-value between responders and non-responders was calculated with Mann-Whitney test and level of significance was $\alpha = 0.05$.

Results are presented in section 5.3.2

5.2.3 Comparison of sequencing data from serum exosomes with the matched OpenArray data

A previous study from Associate Professor Hussey's laboratory used Taqman OpenArray to identify serum exosomal miRNA that could be potential biomarkers for EAC detection [410]. The OpenArray profiling of additional EAC serum exosome patient samples, taken prior to commencement of therapy, was ongoing at the time of commencing my Master's degree (data generated by Dr. Karen Chiam and Mrs. Tingting Wang), and the miRNA data was made available for analysis as part of the work described in this Master's thesis. A sub-selection of these samples was used for the chemoradiotherapy response biomarker studies described herein.

However, the miRNA candidates in Taqman OpenArray are limited, because the Taqman OpenArrays currently used in the lab for serum exosome miRNA screening was based on miRBase v14. The miRBase database is currently at version 21 and many more miRNAs have since been characterized. Besides, the Taqman OpenArray data did not assess the other classes of small RNAs, such as piRNAs, snRNAs, and snoRNAs. The RNA sequencing can capture both known and new miRNAs, piRNA, snoRNA, and snRNA. Therefore, in the second part of chapter 5, we profiled the small RNA by RNA Sequencing serum exosomes of two EAC patients S15 and S17 to investigate the differences of serum exosomal small RNAs between responder and non-responder.

The S17 (RSAB01031) patient was a chemoradiotherapy responder while S15 (RSAB01015) was a non-responder. The assessment of treatment response was based on histological tumor regression assessment with the AJCC (American Joint Cancer Committee) staging manual system (for both samples) and 5-tier

classification (for S15) (Chapter 2:2.2.2). The blood was collected before chemoradiotherapy, and the serum exosomes were isolated (Chapter 2:2.2.4) and RNA was extracted from the exosomes (Chapter 2:2.2.5). The RNA was sequenced, and data analyzed by Dr Shashikanth Marri (Flinders Genomics Facility) and Dr George Mayne using Deseq2. miRBase 21 was used for alignment and miRNA quantification by RPKM counts (not GC normalized), Chapter 2:2.2.8.

The comparison of the sequencing data with the matched Taqman OpenArray data was performed in order to gauge whether the sequencing data was of satisfactory quality for further analysis. The overlapped miRNAs were discovered among fold change >2 in S17/S15 or S15/S17 between sequencing data and Taqman OpenArray data.

Results are presented in section 5.3.3.

5.2.4 Candidate small RNA biomarker selection from serum exosome sequencing data

The small RNA expression from serum exosomes was profiled by RNA sequencing as discussed above. The biomarkers were selected based on the fold change between responder and non-responder. The expression of small RNA in the tissue (Chapter 3, the formalin fixed pre-treatment endoscopy biopsies tissue) and Taqman OpenArray were considered as well for the biomarker selection. Selection criteria for the candidates were:

a) Not in the list of Taqman and RPKM differential expression (DE) above 20 in S15/S17 or S17/S15.

Not in the list of Taqman because the miRNAs in Taqman list have been tested by Taqman. The DE was a common method to pick biomarker, higher DE means a greater possibility as a biomarker[411, 412]. The DE above 20 was set as the criteria because we wanted to identify an effective biomarker, but not too many so that they could not be validated in a patient cohort.

b) RPKM DE above 10 in S15/S17 or S17/S15 and the p value between responder and non-responder in tissue is below 0.1 by Mann-Whitney test.
c) RPKM DE above 3 in S15/S17 or S17/S15 and the p value between responder and non-responder in tissue is below 0.05 by Mann-Whitney test.

In selection criteria b) and c), the expression of miRNAs in tissue was also considered based on the fact that the exosomes in blood might derive from the tumor tissues. There were only a few miRNAs with a DE above 20 with significance in tissue data as well, so the DE was adjusted to 10 and 3 in b) and c), respectively.

d) Some additional small RNAs with a common biological theme were also included.

The small RNAs with a common biological theme might work together to regulate the cells. For example, miR-4728-3p, miR-615-3p, and miR-92b-3p had been reported to regulate the estrogen receptor (ER) in one review[413], which indicated that the potential mechanism underlying the regulation of chemoradiotherapy response may involve the ER. miRNAs play a pivotal role in regulating the chemoradiotherapy response via the ER, such as miR-873 modulates the chemotherapy response to tamoxifen via ERα [278] (Chapter 1:1.6.6). Therefore, these miRNAs were selected as biomarkers because of their common biological theme of ER.

Results are presented in section 5.3.4 and 5.3.5

5.2.5 Testing the small RNAs selected as candidate biomarkers in serum exosomes of EAC patient cohorts

The method is similar to 5.2.3. The selected biomarkers of response to chemoradiotherapy from serum exosomes were tested in the SA and Netherlands patient cohorts separately by qRT-PCR.

As previously mentioned, and justified (footnote on page 2, Chapter 3:3.2), the expression studies described in this thesis were performed using housekeeper

normalized small RNA expression. In order to select a housekeeping miRNA to use for normalization of serum exosome data, Dr Karen Chiam used the available serum exosome OpenArray data and a previously described method [346]. This analysis demonstrated that miR-18a-5p was an appropriate normalizer.

The two patient cohorts are describes above. The p-value between responders and non-responders was calculated using the Mann-Whitney test and the level of significance was $\alpha = 0.05$.

Results are presented in section 5.3.6

5.3 Results

5.3.1 Samples remaining after PCR quality control testing

As described in Chapter 2, 2.1.1, there were 11 patients in the SA cohort. However, only four of them passed the PCR quality control (PCR quality control, see Chapter 2: 2.2.14.2). They were RSAB01031, RSAB 01074, RSAB 01082, and RSAB01015. Their clinical characteristics are shown in table 5-2.

There were 10 patients in the Netherland patient cohort and all of them passed the PCR quality control, and their clinical characteristics are shown in table 5-3.

Table 5-2*. The characteristics of the SA patient cohort. The tumor regression grade of RSAB01015 is written with a question mark because it was graded from a biopsy, not a resection specimen, and therefore could be inaccurate. The '5-tier response classification' for this patient was "poor partial". The accuracy is not clear.*

Patient ID	Age (years)	Gender	AJCC TRG	Treatment	Resection
RSAB 01031 (S17)	64	Male	AJCC 0	2 cycles Cis/5-FU+radiation	Yes

RSAB 01074	64	Male	AJCC 0	Carboplatin + Taxol	Yes
RSAB 01082	71	Male	AJCC 3	Neoadjuvant CRtx + esophagectomy	Yes
RSAB 01015 (S15)	62	Male	AJCC 2?	4 cycles Cis/5-FU	No

***Table 5-3**. The characteristics of the Netherlands patient cohort*

Patient ID	Age (years)	Gender	Mandard TRG	Treatment	Resection
NL 1	64	Male	TRG 1	5 cycles Carboplatin and Taxol +R	Yes
NL 15	72	Male	TRG 1	5 cycles Carboplatin and Taxol +R	Yes
NL 39	64	Male	TRG 1	5 cycles Carboplatin and Taxol +R	Yes
NL 44	56	Female	TRG 1	5 cycles Carboplatin and Taxol +R	Yes
NL 52	66	Male	TRG 1	5 cycles Carboplatin and Taxol +R	Yes
NL 16	50	Female	TRG 5	5 cycles Carboplatin and Taxol +R	Yes
NL 19	64	Male	TRG 5	4 cycles Carboplatin and Taxol +R	Yes
NL 21	82	Male	TRG 5	5 cycles Carboplatin and Taxol +R	Yes
NL 23	73	Male	TRG 5	5 cycles Carboplatin and Taxol +R	Yes
NL 51	66	Male	TRG 5	5 cycles Carboplatin and Taxol +R	Yes

5.3.2 Investigation of the biomarkers selected from tissue in serum exosomes of patient cohorts

The Qiagen company failed to design a functional qRT-PCR assay for some piRNAs and snoRNAs. Thus, only seven small RNAs that were selected from tissue as biomarkers were tested in serum exosomes from patient cohorts. They were miR-451a, miR-340-5p, DQ598428, miR-1301-3p, miR-206, piR-hsa-32187, and

SNORD114. The expression of these small RNAs was compared between responders and non-responders in patient cohorts.

Hemolysis affects small RNA expression[414, 415], which can affect biomarker testing and analysis. One sample for each patient cohort was hemolyzed at collection. These two samples are labeled in pink (Figure 5-1, 5-2).

In the SA patient cohort, the statistical tests could not be performed because the sample size was only two for each group. However, the results in the SA patient cohort showed that miR-340-5p expression was clearly different between the responder and non-responder groups. For miR-1301-3p and miR-206, the non-hemolyzed non-responder sample was clearly different from the two responder samples. The results for the hemolyzed non-responder sample were similar to those for the two responder samples. It is possible that hemolysis obscured serum exosome biomarker discrimination for these small RNAs. Thus, these small RNAs might be worth following up for testing in larger cohorts as possible biomarkers of response to chemoradiotherapy.

In the Netherland patient cohort, the results showed that miR-451a and DQ598428 were promising, though they were not statistically significant by the Mann-Whitney test between responders and non-responders ($p > 0.1$ for all tests; Figure 5-2).

Although some small RNAs were promising in the two patient cohorts, the data in serum exosomes showed the opposite pattern of differential expression between responders and non-responders in tissue *vs* serum exosomes. For example, miR-340-5p was higher in responders while it was lower in responders in tissue samples. The origin of serum exosomes from cancer tissue is complicated and several factors affect the loading of small RNAs, such as the differential and selective sorting of small RNAs from cancer cells into exosomes[416-418].

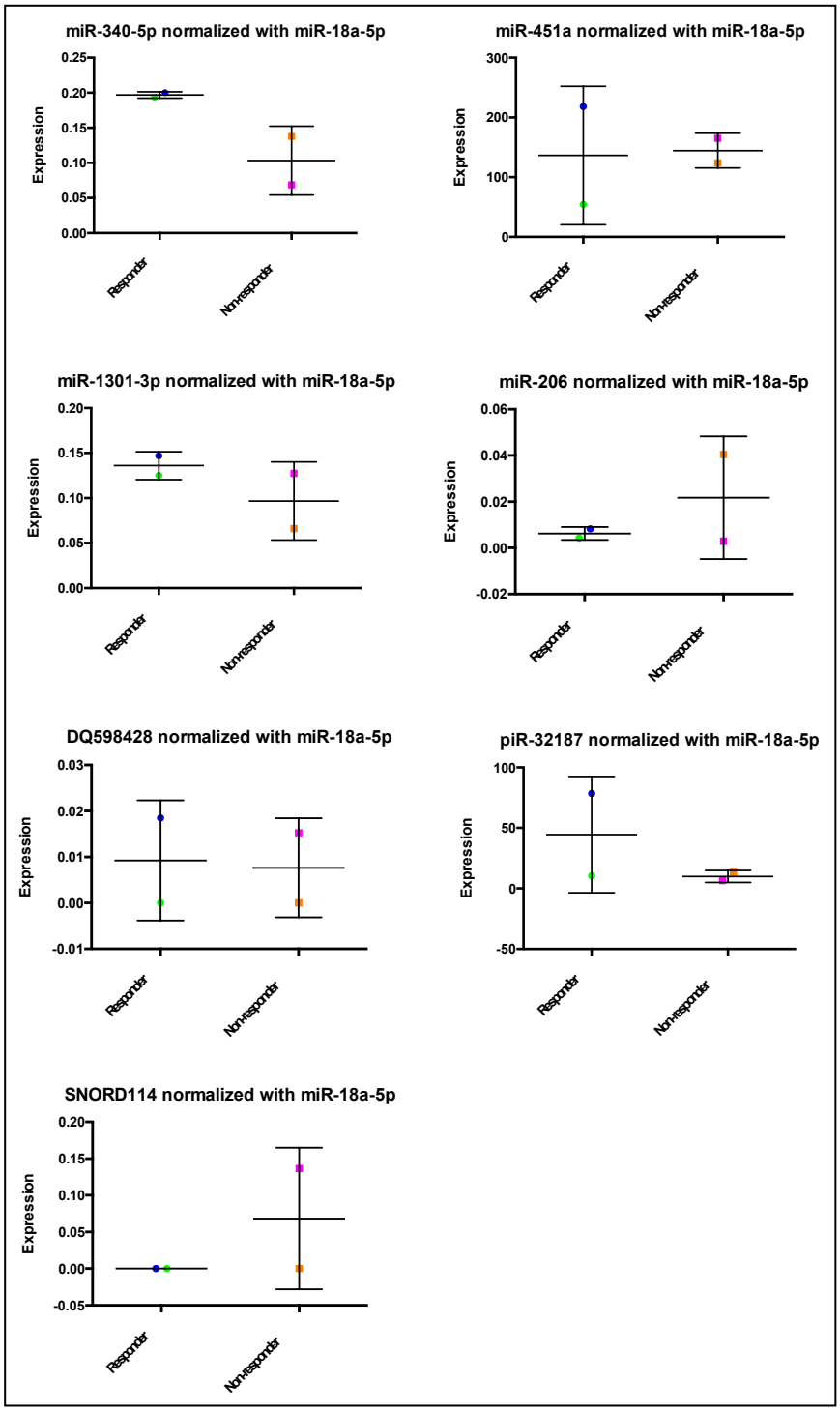

Figure 5-1. *The biomarkers selected from tissue in serum exosomes of SA patient cohorts.* *(Two responders: RSAB01031 (also called S17, blue in the Figure) and RSAB01074 (green in the Figure). Two non-responders: RSAB01082 (pink in the Figure, this sample had hemolysis from collection), RSAB01015 (also called S15, orange in the Figure).*

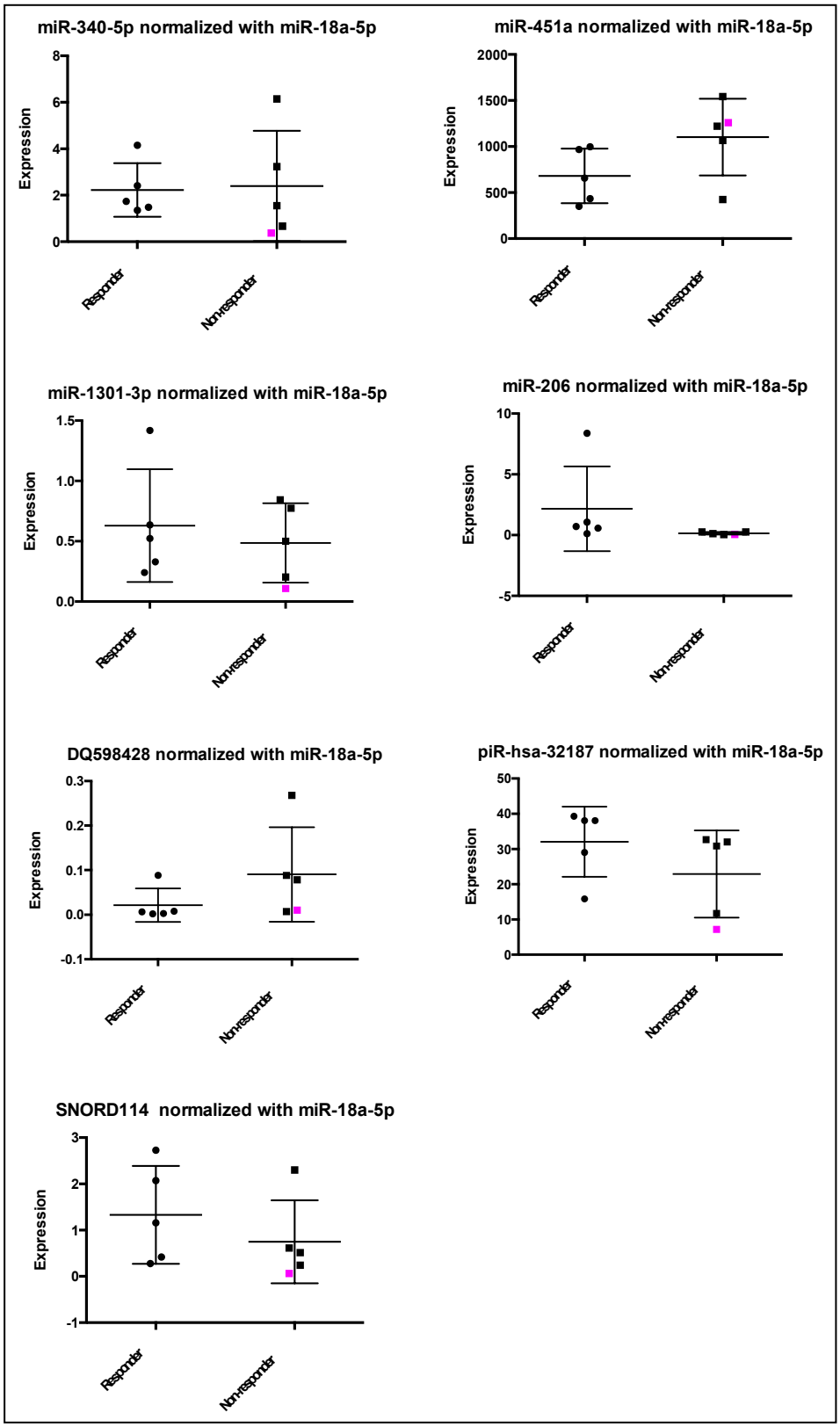

Figure 5-2. *The biomarkers selected from tissue in serum exosomes of Netherlands patient cohorts (Pink: hemolysis).*

5.3.3 Comparison of the serum exosome sequencing data with the matched Taqman OpenArray data

The Taqman OpenArrays used in Associate Professor Hussey's laboratory for serum exosome screening started with about 750 miRNAs from miRBase version14, and for later custom qRT-PCR OpenArrays, they were subsequently reduced to about 100 miRNAs that were found in earlier studies to be detectable in all samples. The miRBase database was currently at version 21 and many more miRNAs had since been characterized, and these were not present in the OpenArrays that the lab used for high throughput screening. Therefore, some potentially useful miRNA biomarkers were not being profiled, and this warranted further investigation using small RNA sequencing.

A preliminary sequencing experiment was undertaken using the RNA samples for S15 and S17 that had previously been profiled on Taqman OpenArray. Then a comparison of the sequencing data with the matched Taqman OpenArray data for these samples was performed in order to gauge whether the sequencing data was of satisfactory quality for further experiments.

The sequencing data results showed that 37 miRNAs were more than two-fold changed between S15/S17, and 11 of them were more than two-fold changed in Taqman OpenArray (18.3% was overlapped). As for the S17/S15, four miRNAs were more than two-fold changed in Taqman OpenArray and in sequencing data as well (Figure 5-3). The overlapping miRNAs included miR-375, hsa-miR-31-5p, hsa-miR-130b-3p, among others (Full list provided in Appendix 5-1, Table 5-5). These three miRNAs are all established as important regulators of chemoradiotherapy response, as described in Chapter 1.

Besides, the data in sequencing, Taqman OpenArray, and PCR (single cell miScript) was consistent in direction of expression (e.g., miR-375 ,Figure 5-4). This indicated that the sequencing data was reliable; therefore, we were confident in picking candidates from these data.

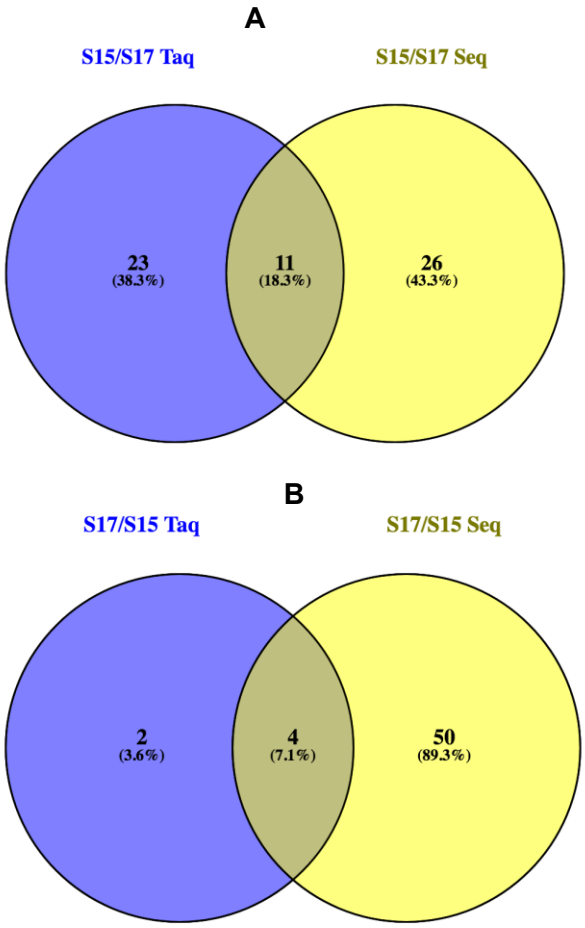

Figure 5-3. *The overlap between the sequencing data (Seq) and the matched Taqman OpenArray data (Taq) (A: S15/S17 data; the blue pie represents the number of miRNAs that have a fold change more than two in Taq and the yellow pie represents the number of miRNAs that have a fold change more than two in Seq. The overlapped pie represents the number of overlapped miRNAs between Taq and Seq. B:S17/S15 data, same as A)*

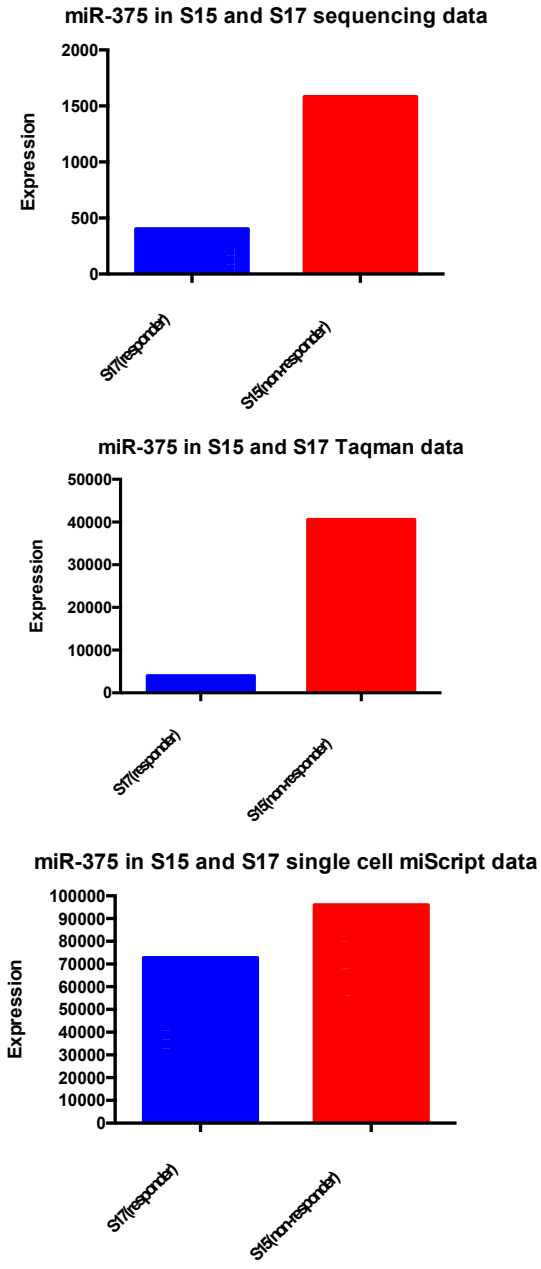

Figure 5-4*. miR-375 expression in the Sequencing data, Taqman OpenArray data, and PCR data (Single Cell miScript)*

The results also showed that there were many additional miRNAs in sequencing data than those presented in the Taqman OpenArrays. Some miRNAs in the sequencing data had potentially very high fold differences between non-responder vs responder

and these miRNAs were not present in the OpenArrays at all or were present in the OpenArrays but not detected strongly and consistently in the PCRs.

5.3.4 Exploring RNA sequencing data from serum exosomes to identify possible small RNAs biomarkers of response to chemoradiotherapy

RNA sequencing profiled a number of small RNAs in serum exosomes as potential candidates for the biomarkers of response to chemoradiotherapy.

In non-responder/responder (S15/S17), the results showed that miR-4728-3p, hsa-miR-3605-3p, hsa-miR-615-3p, hsa-let-7b-3p, hsa-miR-141-3p, hsa-miR-3168, hsa-miR-32-5p, and miR-660-5p all had maximal fold changes. The piRNAs, such as DQ598008, DQ570887, DQ590386, and DQ59711 all had maximal fold change. As for the snoRNAs, the SNORD42A, SNORA71B, SNORD58B, and SNORD123 also had the maximal fold change. RNU11 and RNU2-50P had more than two-fold change (Table 5-4), the entire table is shown in Appendix 5-1, Figure 5-1,5-3,5-5,5-7.

In responder/ non-responder (S17/S15), the results indicated that miR-1226-3p, hsa-miR-3614-5p, hsa-miR-1237-3p, hsa-miR-224-5p, hsa-miR-30e-3p, hsa-miR-1301-3p, and miR-381-3p all had two-fold or more change and were on the top of the list. The piRNAs such as DQ571591, DQ571335, and DQ570339 all had greater than two-fold change. As for the snoRNAs, the levels of SNORD37, SNORD10, SNORA71A, and SNORA64 showed a change greater than two-fol d. Further, the levels of RNU12, RNU4-2, and RNU6-254P showeda two-fold change (Table 5-5), the entire table is shown in Appendix 5-1, Figure 5-2,5-4,5-6,5-8.

All the small RNAs mentioned above have a big fold change between responder and non-responder and they might be potential biomarkers of response to chemoradiotherapy in serum exosomes.

Table 5-4. *The top small RNAs in S15/S17 (The 'dot' in the picture means omitted, because of space constraints).*

S15/S17	S15 (RSAB01015)	S17 (RSAB01031)	RPKM DE
hsa-miR-4728-3p	1623.00	6.64	244.28
hsa-miR-3605-3p	333.00	11.39	29.24
hsa-miR-615-3p	138.00	6.64	20.77
hsa-let-7b-3p	171.00	10.44	16.38
hsa-miR-141-3p	244.00	15.19	16.07
hsa-miR-3168	88.00	6.64	13.24
hsa-miR-32-5p	88.00	6.64	13.24
hsa-miR-660-5p	244.00	18.98	12.85
.	.	.	.
.	.	.	.
.	.	.	.
DQ598008	168.00	9.04	18.59
DQ570687	31.00	9.04	3.43
DQ590386	112.00	41.58	2.69
DQ599711	40.00	17.17	2.33
.	.	.	.
.	.	.	.
.	.	.	.
SNORD42A	38.00	1.04	36.41
SNORA71B	38.00	1.04	36.41
SNORD58B	15.00	0.52	28.74
SNORD123	38.00	1.57	24.27
.	.	.	.
.	.	.	.
.	.	.	.
RNU11	18.00	8.07	2.23
RNU2-50P	18.00	8.07	2.23
.	.	.	.
.	.	.	.
.	.	.	.

***Table 5-5**. The top small RNAs in S17/S15 (The 'dot' in the picture means omitted, because of space constraints).*

S17/S15	RNAS15 (RSAB01015)	RNAS17 (RSAB01031)	RPKM DE
hsa-miR-1226-3p	2.00	503.05	251.53
hsa-miR-3614-5p	2.00	281.90	140.95
hsa-miR-1237-3p	2.00	159.46	79.73
hsa-miR-224-5p	2.00	113.90	56.95
hsa-miR-30e-3p	10.00	537.22	53.72
hsa-miR-1301-3p	5.00	230.65	46.13
hsa-miR-381-3p	2.00	70.24	35.12
hsa-miR-3173-5p	2.00	70.24	35.12
.	.	.	.
.	.	.	.
.	.	.	.
DQ570339	7.00	160.43	22.92
DQ571335	7.00	119.31	17.04
DQ571591	7	53.33	7.62
.	.	.	.
.	.	.	.
.	.	.	.
SNORD37	1.00	41.75	41.75
SNORD10	1.00	41.75	41.75
SNORA71A	2	41.75	20.88
SNORA64	1	15.66	15.66
.	.	.	.
.	.	.	.
.	.	.	.
RNU12	6.00	16.15	2.69
RNU4-2	6.00	16.15	2.69
.	.	.	.
.	.	.	.
.	.	.	.

5.3.5 The selection of biomarkers for chemoradiotherapy response in serum exosomes

Some small RNAs from the biomarkers of response to chemoradiotherapy in serum exosomes were selected for testing in patient cohorts. miR-4728-3p (which was not present in OpenArray) and miR-615-3p (which was present in the original OpenArray but did not demonstrate amplification in many samples, and was not present in custom OpenArray) were chosen as the first candidates for investigation because the sequencing data indicated that they potentially had the largest fold difference between non-responder and responder.

miR-92b–3p was also chosen for investigation as a potential biomarker because it was not present in the OpenArray but had a big fold change in sequencing data. All three miRNAs had been reported to regulate the estrogen Receptor (ER)[413]. The role of ERs in regulating chemoradiotherapy response, with particular attention to these three miRNAs, was described in section 1.6.6 Chapter 1 of this thesis. Therefore, these three miRNAs were selected for further analysis (labeled as red in table 5-6).

miR-1301-3p was selected because of its big fold change (46 in DE of S17/S15) between responder and non-responder and because it was significant in tissue of AJCC0 .V. 3 (p=0.003) and AJCC012. V.3 (p=0.007). Similarly, for miR-32-5p, the fold change is 13.2 in S15/S17, and it was significant in tissue of AJCC0 .V. 3 (p=0.0496) and AJCC012. V.3 (p=0.017; labeled as blue in Table 5-6).

The Qiagen company could not design the functional qRT-PCR assay for some piRNAs and snoRNAs, thus only DQ570339, DQ571335, SNORD42A, and SNORA71B were tested in the patient cohorts because they had a big fold change between responder and non-responder (labeled as green in table 5-6).

The biomarker selection from the candidates was based on the method subsection 5-2-2. The table 5-4 shows the selected biomarkers from serum exosomes. There were

18 miRNAs, four piRNAs, and eight snoRNAs that might be biomarkers of response to chemoradiotherapy in serum exosomes.

***Table 5-6**. The selected biomarkers from serum exosomes (the miRNAs with common biological theme were labeled in red, the blue miRNAs were significant in tissue, the green ones were the other small RNAs that will be tested in patient cohorts)*

Ranked list	miRNA	piRNA	snoRNA	snRNA
1	hsa-miR-1226-3p	DQ570339	SNORD37	No good biomarkers
2	hsa-miR-4728-3p	DQ571335	SNORD10	
3	hsa-miR-3614-5p	DQ571591	SNORD42A	
4	hsa-miR-1237-3p	DQ598008	SNORA71B	
5	hsa-miR-1301-3p		SNORD58B	
6	hsa-miR-381-3p		SNORD123	
7	hsa-miR-3173-5p		SNORA71A	
8	hsa-miR-150-3p		SNORD57	
9	hsa-miR-3605-3p			
10	hsa-miR-615-3p			
11	hsa-miR-141-3p			
12	hsa-miR-769-5p			
13	hsa-miR-32-5p			
14	hsa-miR-431-5p			
15	hsa-miR-424-3p			
16	hsa-miR-7706			
17	hsa-miR-26b-3p			
18	*hsa-miR-92b-3p*			

5.3.6 The expression of small RNAs selected as candidate biomarkers from serum exosomes of chemoradiotherapy response in cohort of EAC patients

In the SA patient cohort, the statistical tests were not performed because the sample size was only two for each group. The results in the SA patient cohort showed that miR-92b-3p and SNORD42A were promising as biomarkers of the treatment response (Figure 5-5).

The one non-responder patient and one responder patient samples used for sequencing were also included in the qRT-PCR test. They were the blue and orange labeled samples, respectively in the SA patient cohort (Figure 5-5). From the Figure 5-5, the sequencing data was consistent with the qRT-PCR data in the direction of expression for four of the eight small RNAs that were tested.

In the Netherland patient cohort, the PCR results showed that miR-32-5p ($p=0.0951$), DQ570339 ($p=0.0499$) and SNORA71B ($p=0.0725$) had higher expression in the responder group and were promising as biomarkers. However, these did not reach statistical significance (p-value between groups calculated with the Mann-Whitney test and level of significance $\alpha = 0,05$; Figure 5-5).

	Sequencing data	SA patient cohort(PCR)	The Netherland patient cohort(PCR)
miR-4728-3P	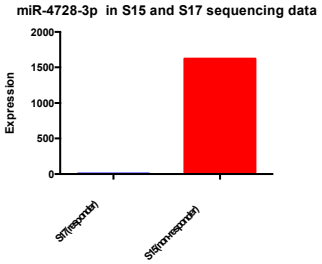	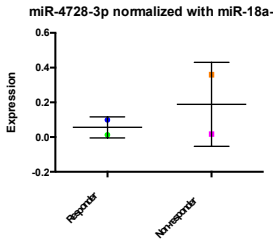	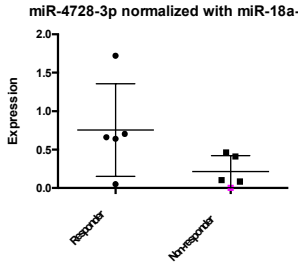
miR-615-3P	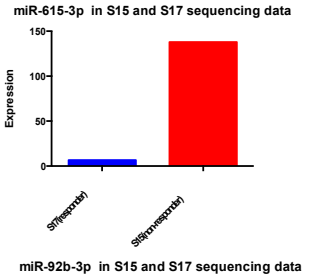	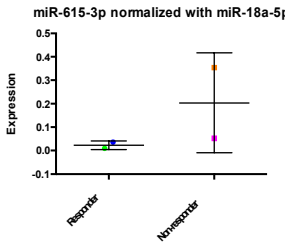	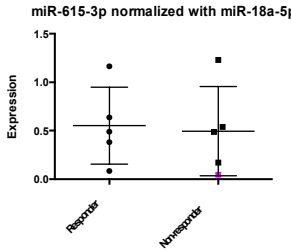
miR-92b-3p	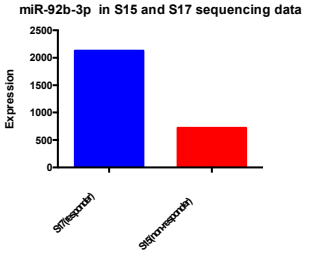	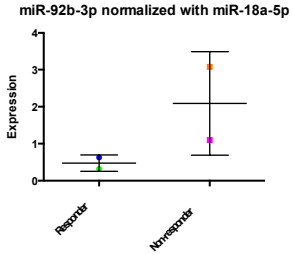	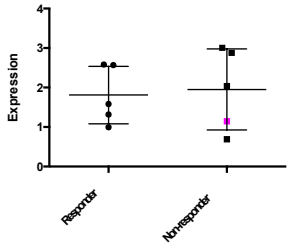
miR-32-5p	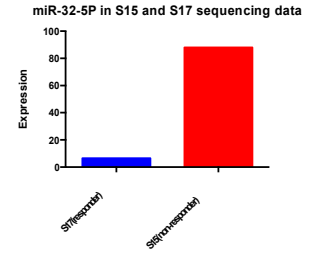	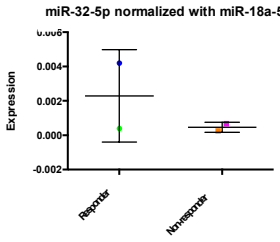	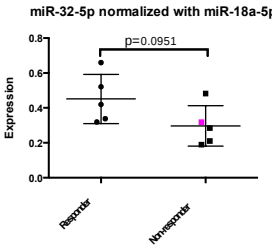

	Sequencing data	SA patient cohort(PCR)	The Netherland patient cohort(PCR)
DQ570339	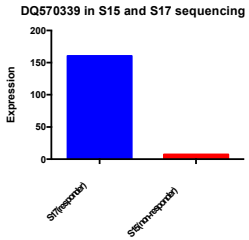	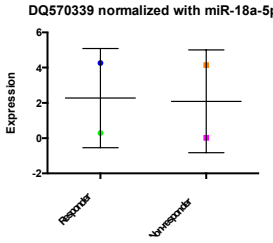	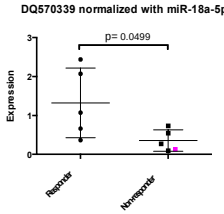
DQ571335	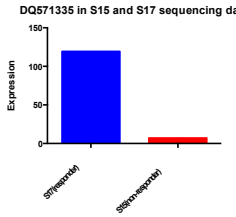	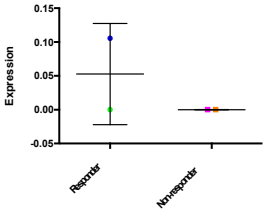	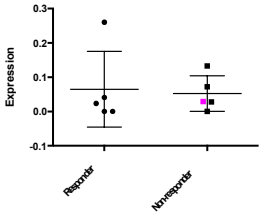
SNORD42A	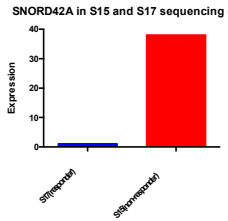	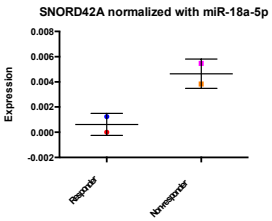	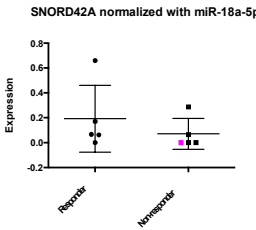
SNORA71B	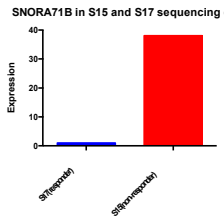	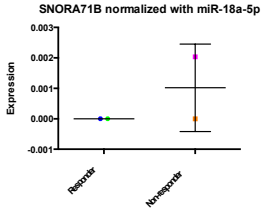	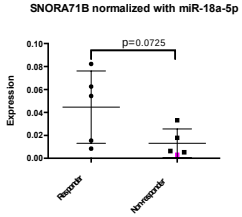

***Figure 5-5**. The biomarkers selected from serum exosomes in the SA and Netherlands patient cohorts (Blue: RSAB01031 (also called S17), Orange: RSAB01015 (also called S15), Pink: sample was labeled hemolysis).*

5.4 Discussion

5.4.1 The discrepancy of the small RNAs in tissue and the serum exosomes

The biomarkers selected from tissue in Chapter 3 were tested in two patient cohorts. Although no firm conclusions could be drawn, due to the small numbers of samples tested and the possible impact of hemolysis on the data, the results showed that some of them were promising in serum exosomes. However, the results showed that the expression of small RNAs in serum exosomes was not the same or even opposite to the expression in tissue. For example, in the SA cohort the expression of miR-340-5p in serum exosomes was higher in responders while it was lower in responders in tissue samples. The mechanism underlying this phenomenon may be related to the loading of small RNA into exosomes.

The origin of serum exosomes from cancer tissue is complicated and several factors could affect the loading of small RNAs including RNA packaging into exosomes, including secondary configuration and RNA sequence motifs[418-420], the differential affinity for membrane lipids[421], and RNA-binding proteins, like AGO2[422], ALIX[423], YBX1[424], and HuR[425], and major vault proteins[426]. The heterogeneous nuclear ribonucleoprotein K and scaffold-attachment factor B1 regulated the content of small RNAs in exosomes by secretory autophagy[427]. Several studies have reported that these mechanisms that could affect the packaging of RNAs into exosomes, but the exact mechanisms underlying the cellular regulation of cargo loading remains unclear[428]. These factors mean indicate that it is not a straightforward translation from expression pattern of miRNAs in tissues to their expression pattern in the corresponding exosomes.

5.4.2 The small RNA-based biomarkers selected from serum exosome sequencing data and tested by qRT-PCR

The SA patient cohort had a few promising small RNAs, such as miR-92b-3p and SNORD42A. The Netherland patient cohort showed that miR-32-5p, DQ570339, and SNORA71B were promising as biomarkers.

miR-32-5p was reported to involve cancer proliferation and chemotherapy response as well. miR-32-5p increased the proliferation and metastasis in ovarian cancer[429], and was the diagnostic biomarker of prostate cancer[430]. Serum miR-32-5p had a higher expression in oral squamous cell carcinoma patients compared to healthy patients[431]. Moreover, exosomal miR-32-5p induced multidrug resistance in hepatocellular cancer by targeting PTEN and affecting the PI3K/Akt signaling pathway by enhancing angiogenesis and epithelial to mesenchymal transition (EMT)[432]. Besides, downregulation of miR-32-5p was found to increase the chemosensitivity of prostate cancer to cisplatin[433]. The downregulation of miR-32-5p promoted the radiosensitization and suppressed the migration and invasion abilities of colorectal cancer cells[434].

There are only a few studies on snoRNA. A recent study reported that SNORA71B had a high expression in breast cancer tissues and it might be a biomarker of breast cancer, and SNORA71B induced the EMT process of brain metastasis breast cancer cells[435]. There are very few studies about exosomal piRNAs in cancer. DQ570339 was reported to have a higher expression in cardiosphere-derived cells, suggesting that it was responsible for cardiac regeneration and this regenerative potential might play an important role in cancer[436].

Some biomarkers of response to chemoradiotherapy selected from the sequencing discovery study were promising in serum exosomes of patient cohorts when tested with qRT-PCR. These small RNAs from the serum exosomes might be potential biomarkers of response to chemoradiotherapy. They might play an important role in regulation of treatment response and more independent patient cohorts are needed to confirm this.

5.4.3 Limitations

This study had some major limitations. More patients should be included into the patient cohorts to fully explore the selected biomarkers. The current sample size was only four in the SA patient cohort and 10 in the Netherlands patient cohort. Besides, one sample in each patient cohort was hemolyzed, which might affect the expression of the small RNAs. Further, there were differences in the methods for processing of blood to serum between the South Australian and the Netherlands cohorts and these add an additional confounding factor to the study.

We only tested some biomarkers in patient cohorts because the Qiagen company could not design the functional qRT-PCR assay for some piRNAs and snoRNAs, and the PCR could not detect some small RNAs effectively. Future studies should validate more candidate biomarkers, and should investigate using combinations of biomarkers for discriminating responders from non-responders.

Comprehensive sequencing studies might identify biomarkers that are not identified by qRT-PCR due to technical differences between the two methods. For example, the full set of samples in the Netherlands cohort was sequenced after I finished my study, and miR-451a was identified as a differentially expressed biomarker [346], even though it did not demonstrate this in the qRT-PCR data in this chapter.

CHAPTER 6

INVESTIGATION OF THE POSSIBLE INVOLVEMENT OF BLOOD SMALL RNAS IN REGULATING CHEMORADIOTHERAPY RESPONSE IN EAC CELLS

6.1 Introduction

In chapter 5, several small RNAs were identified as potential biomarkers of response to chemoradiotherapy in serum exosomes of EAC patients, and some of these showed promise when tested by PCR in the patient cohorts. These small RNAs from serum exosomes might play an important role in regulating chemoradiotherapy response. For example, the exosomal miR-32-5p which we selected as the biomarker of chemoradiotherapy response in chapter 5 was reported to induce multidrug resistance in hepatocellular carcinoma by promoting angiogenesis and EMT (epithelial-mesenchymal transition)[432].

Blood exosomes include numerous small RNAs, and these blood exosomes can modulate the local tumor environment so as to influence tumor response to chemoradiotherapy. The exosomes from non-responders of breast

cancer could transmit chemoresistance by delivering miRNAs[437, 438]. Secreted miR-221/222 from exosomes served as signaling molecules to regulate communication of tamoxifen resistance in breast cancer[439].

Therefore, we hypothesized that the small RNAs which were enriched in serum exosomes in non-responder cells might deliver small RNAs to cancer cells or distant areas in the body, and that these small RNAs might be responsible for influencing the proliferation and/or drug or radiation response behavior of these cells.

The aim of this chapter was to investigate the possible involvement of blood small RNAs in regulating chemoradiotherapy response in EAC cells. As a first step towards investigating this, we looked at whether the baseline cellular levels of these miRNAs are associated with drug and radiation response in EAC cell lines. We then investigated the role of serum exosomes in controlling cell proliferation and drug/radiation response in EAC cells.

6.2 Methods

6.2.1 Investigation of the small RNAs and their association with treatment response in cells

The first experiment of this chapter was to investigate the baseline cellular levels of small RNAs selected from serum exosomes of EAC patients as biomarkers of response to chemoradiotherapy (*miR-4728-3p, miR-615-3p, miR-32-5p, miR-92b-3p, DQ570339, DQ571335, SNORD37, SNORD42A,* and *SNORA71B*) and their association with drug or radiation response. We used eight EAC cell lines for this study: OE19, OE33, JHEsoAd1, SKGT4, FLO1, OACP4C, ESO51, and ESO26. The miScript II qPCR System was used for the detection and quantification of small RNAs (Chapter 2:2.2.14.3). The small RNAs in cells were normalized by let-7g-5p. Let-7g-5p was selected as the housekeeping miRNA for normalization. This selection was based on analyses performed by Dr Karen Chiam from Associate Professor Hussey's laboratory. Dr Chiam used the method of house-keeping gene selection that was described in a previous study [440]. Using this method, Dr Chiam identified let-7g-5p as a suitable housekeeper in the cohort of pre-neoadjuvant tissue samples (described in Chapter 3); let-7g-5p was also identified as a suitable

housekeeper in control and chemotherapy treated samples from an OE-33 cell line experiment that was being used for other work in the laboratory. The choice of let-7g-5p is also supported by a previous study on the identification of housekeeping miRNAs in human cancer tissues using sequencing data from TCGA database[351]

The treatment response was assessed by the flow cytometry - Annexin V-FITC / PI apoptosis assay, MTS, and Clonogenic Assay (Chapter 2:2.2.13). The cells were divided into resistant and sensitivity groups according to the treatment response. Differences in the mean of small RNA expression between sensitive and resistant group cell lines were analyzed using the t-test. Direct correlations between the quantity of small RNA expressed and the degree of drug or radiation response were analyzed using Spearman correlation test.

6.2.2 Investigation of the role of serum exosomes in controlling cell proliferation

The second part of this Chapter studied the effect of exosomes in controlling cell proliferation in EAC cells. OE33 cells were used for this study. The exosomes were extracted from one responder patient (RSAB01031) and one non-responder patient (RSAB01015). We isolated the exosomes using Exoquick and then counted the exosome number using Nanosight (Chapter2: 2.2.5,2.2.6).

The OE33 cells were subcultured to 70% confluency on the day of exosome exposure and the exosomes of responder and non-responder patients were added respectively to the cells (3333 exosomes/cell, 48 hours of treatment). The next day, (24 hours of the treatment) after the first exosome exposure, cells were replated at 1.07×10^5 cells/mL and then the exosomes were re-added at 3333 exosomes/cell. The cells were treated with the vehicle of 5-FU and cisplatin (0 hour of treatment) (Cell culture: Chapter 2:2.2.9, drug treatment: Chapter 2:2.2.11); the diagram is shown in Figure 6-1.

The cells in the vehicle of drugs were assessed by the MTS assay (Chapter 2: 2.2.13.1), Crystal violet (CV) assay (Chapter 2:2.2.13.6), and xCelligence (Chapter 2:2.2.13.7) to identify the role of serum exosomes in controlling cell proliferation. p-

value between groups was calculated using an unpaired t-test and the level of significance $\alpha = 0.05$.

The MTS assay is a popular test to assess cell proliferation. The basis of the MTS assay is the reduction of tetrazolium salt to formazan that occurs in the mitochondria of living cells due to the activity of mitochondrial dehydrogenases. The metabolic activity measured by the assay is used as an indicator of cellular proliferation (or viability or toxicity). Some researcher found that rottlerin (uncouples the mitochondrial respiratory chain) might increase the production of formazan crystals and thus, yield a negative result[441]. Besides, the level of MTT tetrazolium salt decreases not only in mitochondria but also on the cell surface, endosome and lysosome membranes, and the cytoplasm [442]. CV assay is used to test viable adherent cells and colonies. The xCelligence measures the net cellular adhesion within the cells. The cells that adhere on the plate surface will affect the impedance values, and the impedance values were converted into the cell index (CI)[443]. Because of the possible shortcomings, using one kind of assay might give erroneous results[444]. Therefore, we used the MTS assay, CV assay, and xCelligence in this study.

Background subtraction: For the exosome experiments all background wells contained medium with the respective drug or vehicle. The background wells did not contain any exosomes. For the MTS and the CV assays the background subtraction of each well was done by subtracting the value from one background well.

6.2.3 Investigation of the role of serum exosomes in controlling drug/irradiation response

The third part of this chapter studied the effect of exosomes in controlling drug / radiation response in EAC cells. OE33 cells were used in this study. The exosomes were precipitated from the serum of one responder patient (RSAB01031), and one non-responder patient (RSAB01015), Chapter 2: 2.2.5. Two batches of exosome aliquots were prepared for this experiment. The first batch of exosomes was prepared by Exoquick precipitation on 05/03/2018. The second batch of exosomes was prepared by Exoquick precipitation on 07/06/2018, using the same serum samples as

the 05/03/2018 precipitation. The four independent drug treatment experiments were performed on 180306, 180327, 180522, and 181023. The first batch of exosomes was used for the 180306, 180327, and 180522 experiments while the second batch of exosomes was used for the 181023 experiment.

The cells were exposed to exosomes at -48 hours, -24 hours of treatment, and then treated by 5-FU (50 μM) or cisplatin (8 μM) or irradiation (2 Gy) separately (Chapter 2:2.2.11 and 2.2.12). The treatment response of drug was assessed by xCelligence, MTS, and Crystal violet (Chapter 2:2.2.13). The cells received the irradiation by Xrad320, precision X-Ray, at 2 Gy. The treatment response of irradiation was assessed by Clonogenic assay (Chapter 2:2.2.13.5), for experimental design, see Figure 6-1.

The Background subtraction was the same as 6.2.2. The MTS and Crystal violet data was normalized by dividing with the vehicle controls. The Xcelligence data was normalized by subtracting the vehicle control. The Survival Fraction (SF), obtained by dividing the number of viable cells of one treated sample by the number of viable cells of the respective untreated vehicle controls, was used for the irradiation response.

The p-values for the data from the different groups was calculated using the unpaired t-test and the following level of significance $\alpha = 0.05$.

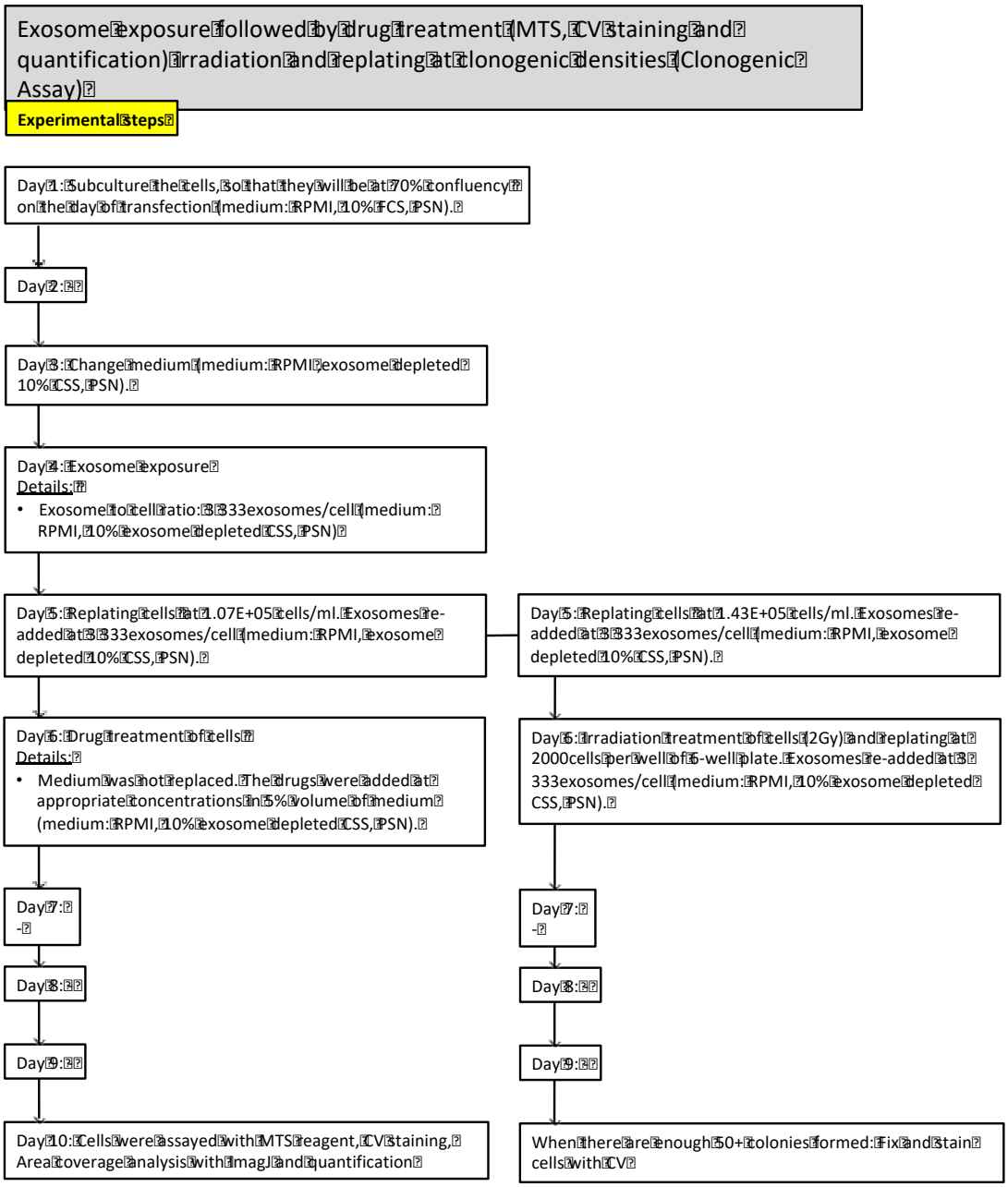

Figure 6-1. *The diagram of exosome exposure followed by drug and irradiation treatment.*

6.3 Results

6.3.1 Investigation of the baseline cellular levels of small RNAs between resistant and sensitive cells by t-test

We analyzed the expression of small RNAs in resistant and sensitive cell lines and compared the expression level between the two groups. The further study aimed to examine the role of the exosomes in regulating the treatment response. The possible mechanism underlying this process was the delivery of small RNAs by exosomes. Therefore, the expression level was investigated between resistant and sensitive cell lines in this part. In the next part (6.3.2) the correlation was analyzed to see whether these miRNAs had a linear relationship with treatment response.

The small RNAs that were selected as candidate biomarkers from serum exosomes were tested in eight EAC cell lines and those cell lines were treated by drug (5-FU or cisplatin) or radiation. Flow Cytometry and MTS were used for the testing of treatment response in the drug experiment, while Clonogenic assay was used for the testing of treatment response in the radiation experiment. The treatment response was tested by three independent experiments[346]. The cell lines were divided into resistant and sensitive groups by determining the mean surviving fraction across all cell lines and then defining ‘resistant’ cell lines as those above the mean, and ‘sensitive’ cell lines as those below the mean, Figure 6-2.

A

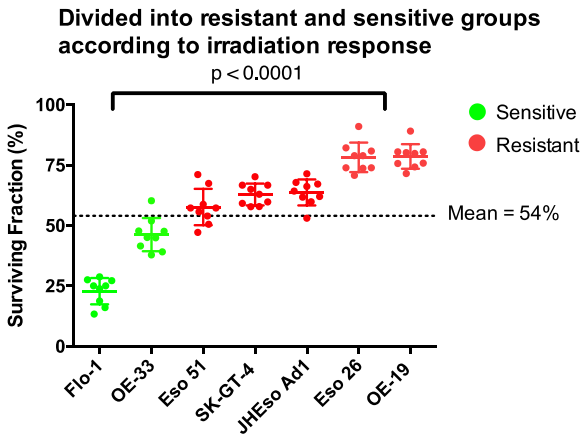

B

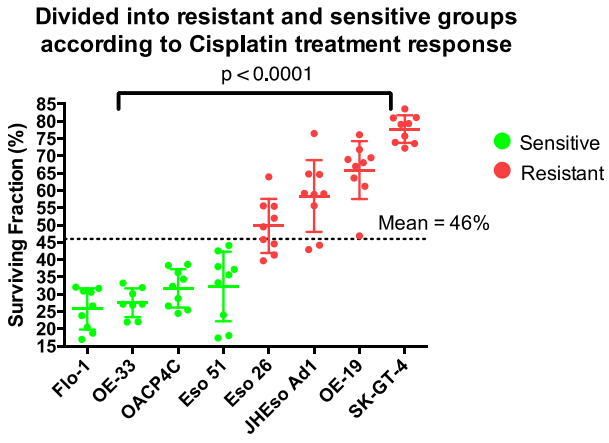

C

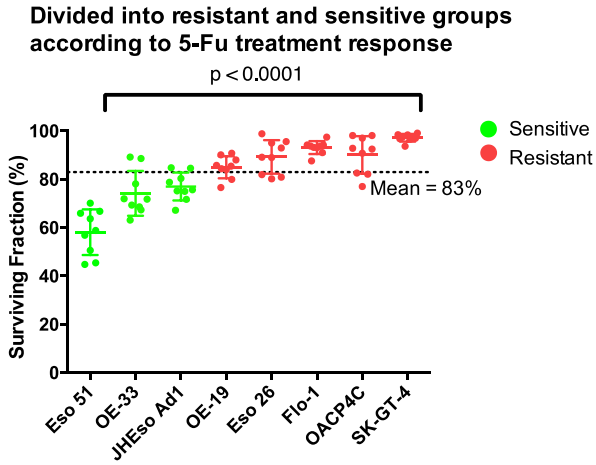

Figure 6-2. *The cell lines were divided into the resistant and sensitive groups according to the treatment response. A: seven EAC cell lines-irradiated with 2 Gy vs. mock-irradiated controls, Surviving Fraction calculated from*

Clonogenic Assay. OACP4C cells were not included as they did not have a consistent response to radiation treatment. B: Surviving Fractions of eight EAC cell lines, 20 μM cisplatin vs. vehicle control, flow cytometry after the 72-hour treatment, n = 3 independent experiments. C: Survival Fractions of eight EAC cell lines 50 μM 5-FU vs. vehicle control, flow cytometry after 72 hours of treatment, n = 3 independent experiments. p-value between group means was calculated with unpaired t-test with level of significance α = 0.05.

According to the cisplatin treatment results from flow cytometry, the resistant groups were SKGT4 (survival fraction: 77.76%), OE19 (survival fraction: 65.93%), JHEsoAd1 (survival fraction: 58.43%), and Eso26 (survival fraction: 49.79%) while the sensitive groups were Eso51 (survival fraction: 32.25%), OACP4C (survival fraction: 31.71%), OE33 (survival fraction: 27.57%), and Flo-1 (survival fraction: 25.78%).

The results showed that the expression of SNORD37 (p=0.04) had a significant difference between cisplatin-resistant and -sensitive cell lines (Figure 6-3).

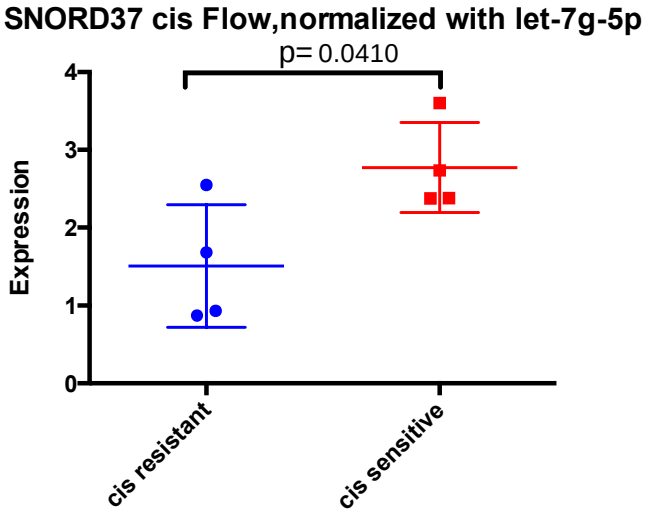

***Figure 6-3**. SNORD37 expression measured by PCR in cisplatin (cis) resistant and sensitive cell lines. Cisplatin sensitivity was measured using flow cytometry (Flow)*

According to the 5-FU treatment results from flow cytometry, the resistant groups were SKGT4 (survival fractions: 97.23%), OE19 (survival fractions: 85.01%), Flo-1 (survival fractions: 90.13%), OACP4C (survival fractions: 93.15%), and Eso26 (survival fractions: 89.31%), while the sensitive groups were Eso51 (survival fractions: 58.14%), OE33 (survival fractions: 74.25%), and JHEsoAd1 (survival fractions: 77.05%). The small RNAs between the two groups were compared and there were no small RNAs showing significantly different expression between the 5-FU resistant and sensitive groups.

According to the cisplatin treatment results from MTS, the resistant groups were SKGT4 (survival fractions: 30.00%), OE19 (survival fractions: 49.19%) and Eso26 (survival fractions: 25.96%) while the sensitive groups were Eso51 (survival fractions: 10.35%), OACP4C (survival fractions: 7.13%), OE33 (survival fractions: 20.88%), JHEsoAd1 (survival fractions: 15.38%), and Flo-1 (survival fractions: 12.11%). The MTS results showed that miR-4728-3p ($p=0.0843$), miR-615-3p ($p=0.0841$), and miR-32-5p ($p=0.0945$) had differential expression between the cisplatin resistant and sensitive groups, however it did not meet statistical significance (Figure 6-4).

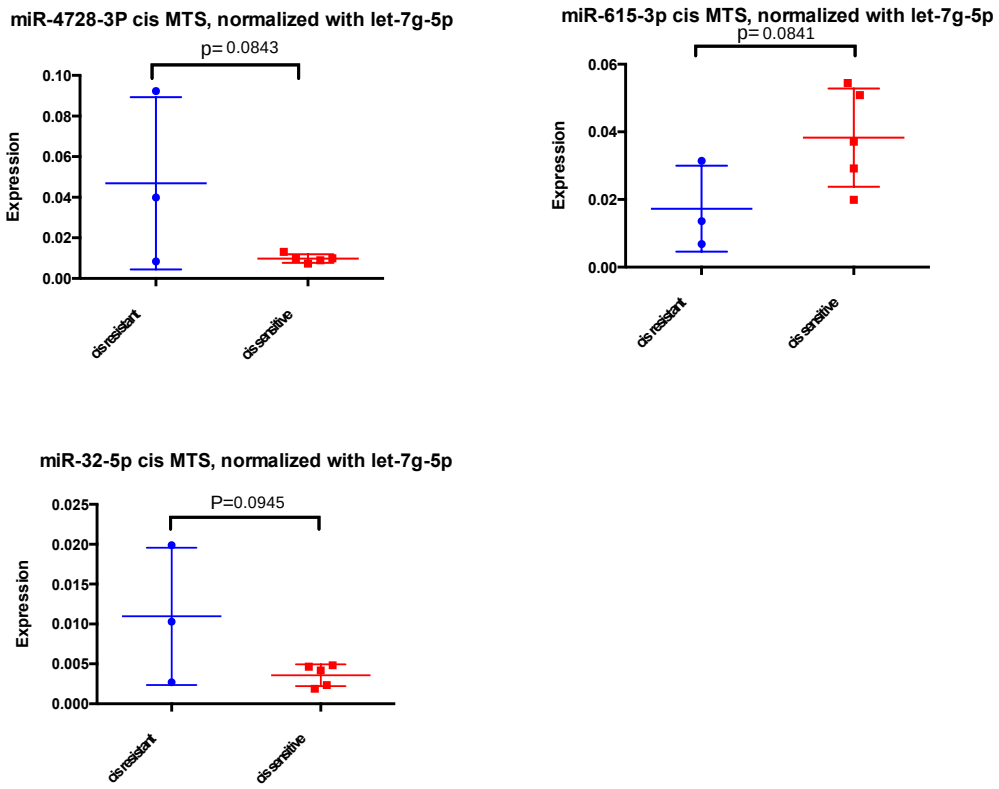

Figure 6-4*. The small RNA expression measured by PCR in cisplatin (cis)-resistant and sensitive cell lines. Cisplatin sensitivity was measured using MTS assay.*

According to the 5-FU treatment results from MTS, the resistant groups were OACP4C (survival fractions: 75.98%), OE19 (survival fractions: 53.71%), and Eso26 (survival fractions: 49.51%) while the sensitive groups were Eso51 (survival fractions: 40.78%), SKGT4 (survival fractions: 39.51%), OE33 (survival fractions: 43.85%), JHEsoAd1 (survival fractions: 20.61%), and Flo-1 (survival fractions: 32.80%). The small RNAs between the two groups were compared. The results showed that miR-32-5p (p=0.041) and DQ570339 (p=0.026) were significantly different between the two groups (DQ570339 was done with miScript II and therefore require further confirmation – see Chapter 4, section 4.4.2 for further explanation). miR-4728-3p (p=0.075) and SNORD37 (p=0.072) had different expression between 5-FU resistant and sensitive groups however it did not reach statistical significance (Figure 6-5).

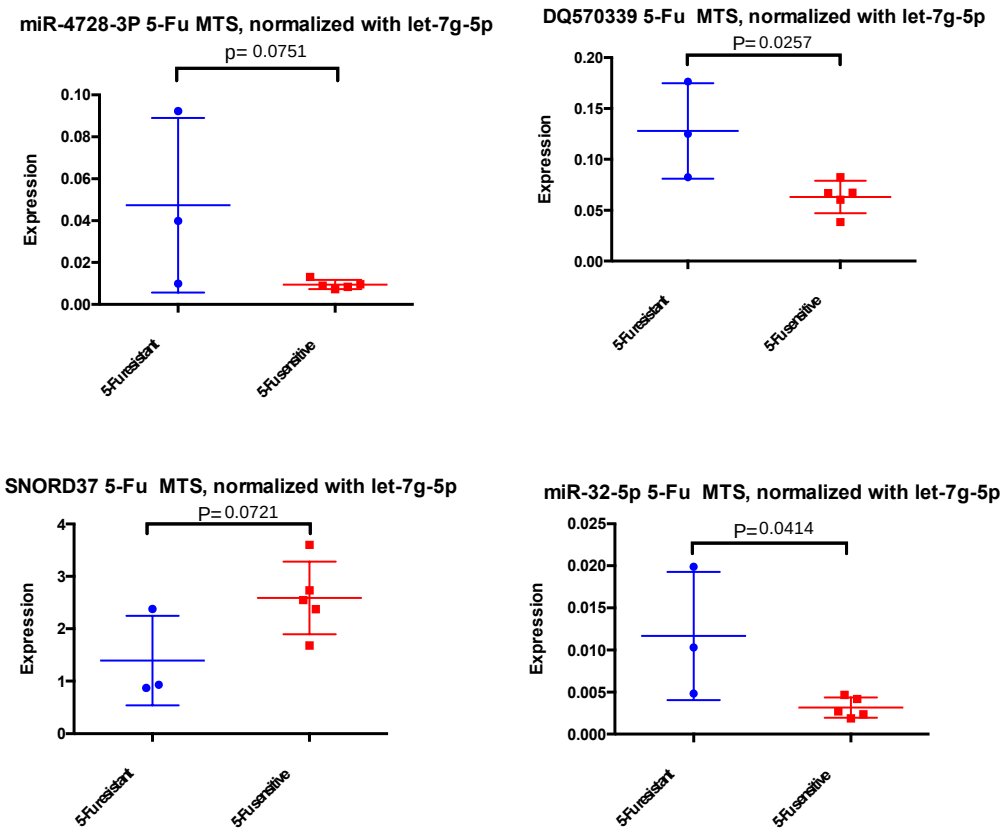

Figure 6-5*. The small RNA expression measured by PCR in 5-FU resistant and sensitive cell lines. 5-FU sensitivity was measured using MTS. DQ570339 was done with miScript II and therefore require further confirmation.*

As for the irradiation treatment response, the resistant groups were SKGT4 (survival fractions: 62.9%), OE19 (survival fractions: 78.6%), JHEsoAd1 (survival fractions: 63.7%), and Eso26 (survival fractions: 78.3%), while the sensitive groups were Eso51 (survival fractions: 57.7%), OE33 (survival fractions: 46.2%), and Flo-1 (survival fractions: 22.8%). miR-615-3p had differential expression between radiation resistant and sensitive groups, however it did not reach statistical significance (p=0.075; Figure 6-6). See the complete Figures in appendix 6.1.

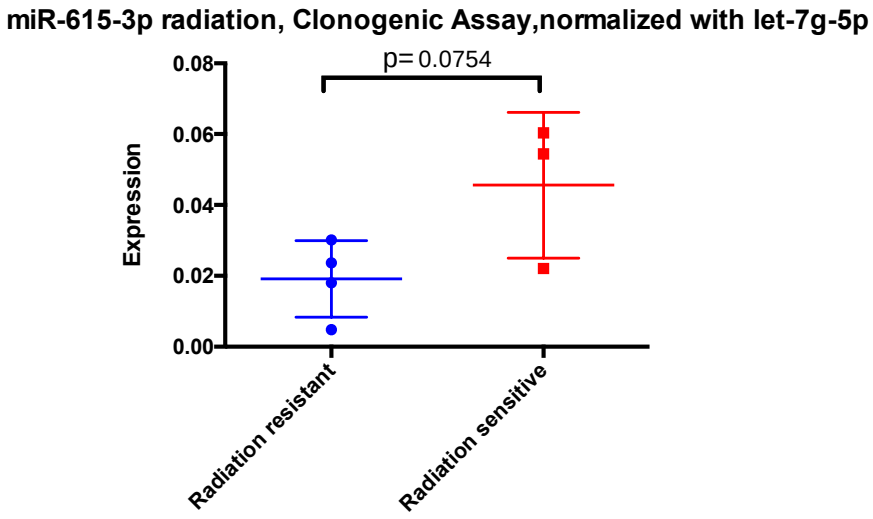

***Figure 6-6**. miR-615-3p expression measured by PCR in irradiation resistant and sensitive cell lines. Irradiation sensitivity was measured using Clonogenic Assay.*

6.3.2 Investigation of the baseline cellular levels of small RNAs and testing their association with drug or radiation response using Spearman correlation test

The correlation between the quantity of small RNA expressed and the degree of drug or radiation response was analyzed using the Spearman correlation test.

The flow cytometry results did not reveal an association between the expression of small RNAs and drug treatment response. The MTS was also used to investigate the relationship between treatment response and the expression of small RNAs. The results showed that miR-32-5p (rho=0.762, p=0.037) and DQ570339 (rho=0.898, p=0.005) had a positive correlation with 5-FU treatment response (DQ570339 was done with miScript II and therefore require further confirmation). There was an association between expression of miR-4728-3p and 5-FU treatment response (rho = 0.714, p=0.058), however it did not reach statistical significance (Figure 6-7, table 6-1). See the complete Figures in appendix 6.2.

There were no small RNAs associated with irradiation treatment using the Spearman correlation test.

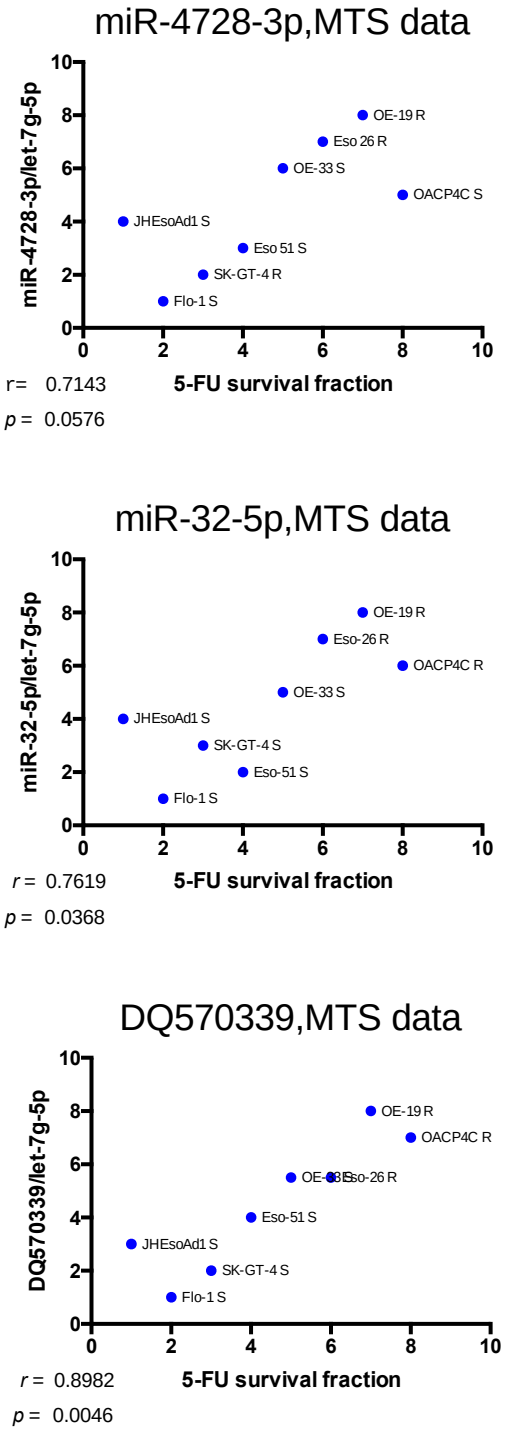

Figure 6-7*. The relationship between small RNA and treatment response, as assessed by Spearman correlation test (the data were normalized with let-7g-5p,*

DQ570339 was done with miScript II; therefore, its results require further validation).

Table 6-1. *Summary table showing the relationship between small RNA and treatment response via t-test, and via Spearman correlation (the p value is labeled in red when it is less than 0.1 and the according small RNAs are labeled in bold, DQ570339 was done with miScript II and therefore require further confirmation).*

small RNAs	CISPLATIN						5-FU						RADIATION		
	Flow cytometry			MTS			Flow cytometry			MTS			Clonogenic assay		
	group	Spearman		group	Spearman		group	Spearman		group	Spearman		group	Spearman	
	p val	*rho*	*p val*	*p val*	*rho*	*p val*	*p val*	rho	p val	*p val*	*rho*	*p val*	*p val*	*rho*	*p val*
miR-4728-3p	0.209	0.214	0.619	0.084	0.333	0.428	0.374	-0.357	0.389	0.075	**0.714**	0.058	0.316	0.393	0.396
miR-615-3p	0.188	**-0.524**	0.197	0.084	-0.167	0.703	0.226	-0.381	0.360	0.166	-0.357	0.389	0.075	**-0.607**	0.167
miR-32-5p	0.192	0.333	0.428	0.095	0.333	0.428	0.385	-0.095	0.840	**0.041**	**0.762**	**0.037**	0.353	**0.643**	0.139
miR-92b-3p	0.386	-0.167	0.703	0.704	-0.357	0.389	0.398	0.333	0.428	0.561	0.238	0.582	0.999	0.179	0.713
DQ570339	0.594	0.108	0.808	0.380	0.132	0.761	0.489	-0.323	0.414	**0.026**	**0.898**	**0.005**	0.488	-0.357	0.444
DQ571335	0.381	0.333	0.428	0.776	0.238	0.582	0.200	-0.024	0.977	0.206	-0.405	0.327	0.435	-0.143	0.783
SNORD37	**0.041**	-0.286	0.501	0.105	-0.286	0.501	0.235	-0.286	0.501	0.072	-0.143	0.752	0.505	**-0.643**	0.139
SNORD42A	0.408	-0.084	0.825	0.283	-0.276	0.487	0.205	-0.084	0.825	0.480	-0.012	0.965	0.459	-0.143	0.783
SNORA71B	0.718	-0.132	0.735	0.827	-0.072	0.849	0.407	-0.024	0.944	0.827	0.180	0.673	0.427	0.286	0.556
miR-1301-3p	**0.013**	**0.667**	0.083	**0.034**	**0.595**	0.132	0.453	0.095	0.840	0.189	0.214	0.619	0.402	0.393	0.396

6.3.3 The role of serum exosomes in controlling cell proliferation and response to drug treatment in EAC cells

The four independent experiments were analyzed: 180306, 180327, 180522, and 181023.

In cells treated with the vehicle for cisplatin, the MTS data suggested that the exosomes from non-responder (RSAB01015) caused a small but significant increase in the cell number compared to exosomes from the responder (RSAB01031). This was seen in all four independent experiments (Table 6-2, Figure 6-8). The CV data showed no significant differences between non-responder exosome- and responder exosome-treated cells, although the mean value was slightly higher for non-responder-treated cells in the 180522 experiment (Table 6-2, Figure 6-9). The xCelligence data showed similar results and in one experiment (180522), the exosomes from the non-responder increased the cell number significantly ($p=0.019$) (Table 6-2, Figure 6-10). Overall, these results suggested that the non-responder exosomes might increase cell proliferation.

In cells treated with cisplatin, the MTS data suggested that cells exposed to exosomes from the non-responder were more sensitive to cisplatin than cells exposed to exosomes from the responder. This result was statistically significant in three out of the four experiments (1803606, 180327, and 181023; Table 6-2, Figure 6-11). There were no significant differences observed in the CV data (Figure 6-12). The xCelligence data indicated that cells exposed to exosomes from the non-responder were more sensitive to cisplatin than cells exposed to exosomes from the responder, and the difference was significant in both experiments (180522 ($p<0.001$) and 181023 ($p=0.003$); Figure 6-13). Overall, the results suggested that the non-responder exosomes might result in increased sensitivity to cisplatin compared to the responder exosomes.

***Table 6-2**. The role of serum exosomes in controlling cell proliferation and cisplatin treatment response (vehicle control of cisplatin, ↑ : there are more viable cells in RSAB01015 exosome (Non-responder) exposure group compared to RSAB01031 exosome (responder) exposure group. ↓: there are less viable cells in RSAB01015 exosome (Non-responder) exposure group compared to RSAB01031 exosome (responder) exposure group. NT: condition not tested. The cells were lost during washing in the CV experiment of 180306. The p-value is labeled in red when p<0.1.*

Vehicle control of Cisplatin				Cisplatin 8 uM			
Date	MTS (NON-RESP / RESP)	CV (NON-RESP / RESP)	xCelligence 96h	Date	MTS (NON-RESP / RESP)	CV (NON-RESP / RESP)	xCelligence 96h
180306	1.176 ↑ (p<0.0001)	CELLS LOST IN WASH	NT	180306	0.871 ↓ (p<0.0001)	CELLS LOST IN WASH	NT
180327	1.128 ↑ (p=0.008)	1.020 (p=0.791)	NT	180327	0.904 ↓ (p=0.006)	0.925 (p=0.147)	NT
180522	1.192 ↑ (p=0.030)	1.237 (p=0.176)	2.449 ↑ (p=0.019)	180522	0.948 (p=0.326)	1.056 (p=0.938)	0.502 ↓ (p<0.0001)
181023	1.126 ↑ (p=0.045)	1.060 (p=0.444)	1.343 (p=0.196)	181023	0.875 ↓ (p=0.003)	1.018 (p=0.923)	0.795 ↓ (p=0.003)

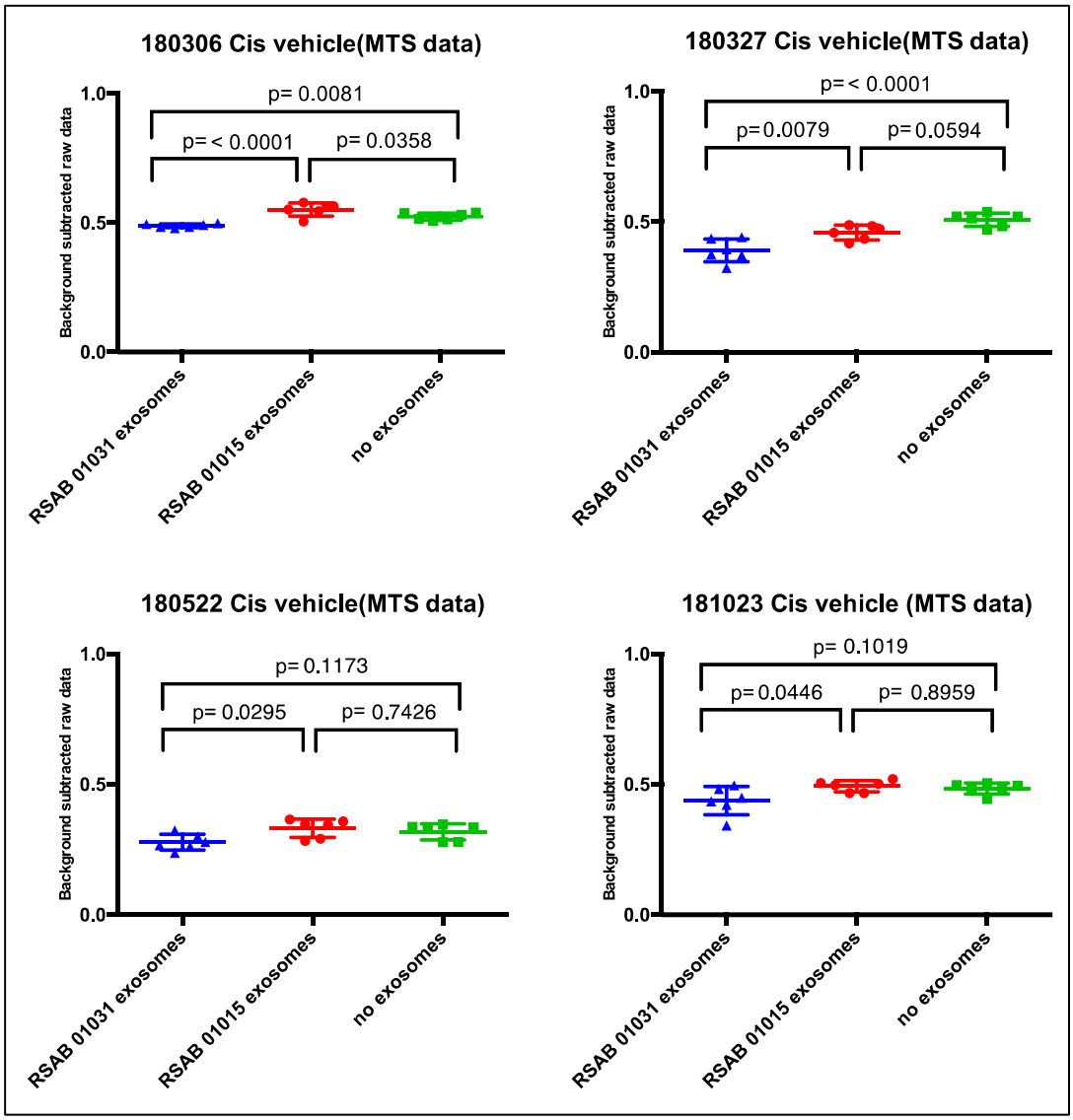

Figure 6-8. *The role of serum exosomes in controlling cell proliferation (vehicle control for cisplatin treatment; MTS data; the MTS data normalized by background subtraction).*

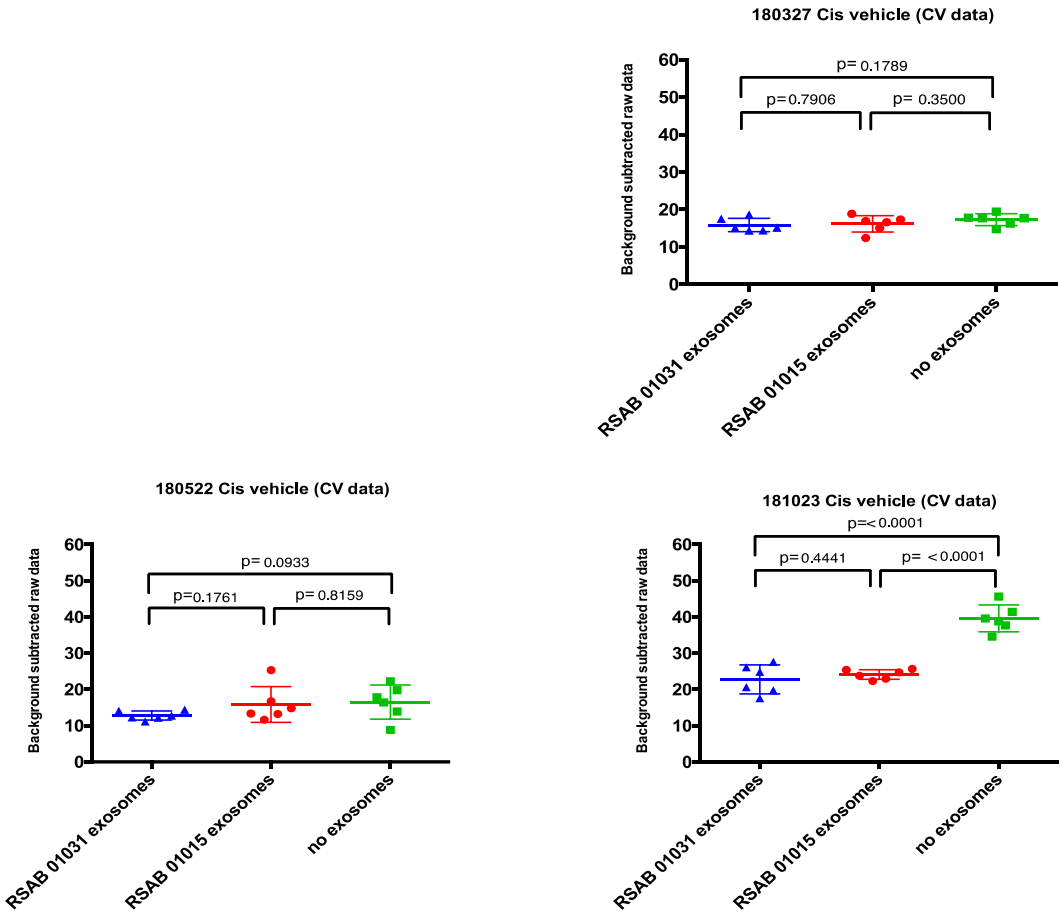

Figure 6-9. *The role of serum exosomes in controlling cell proliferation (vehicle control for cisplatin treatment; CV data; the CV data were normalized by background subtraction).*

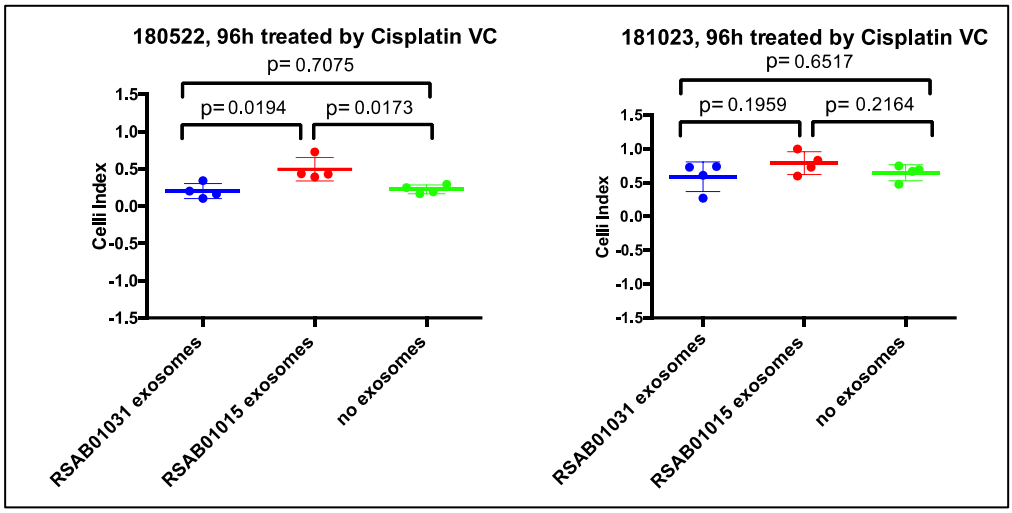

Figure 6-10. *The role of serum exosomes in controlling cell proliferation (vehicle control for cisplatin treatment; xCelligence data; the xCelligence data were normalized by cell index. Cell Index: the Xcelligence data normalized by subtracting the data of VC).*

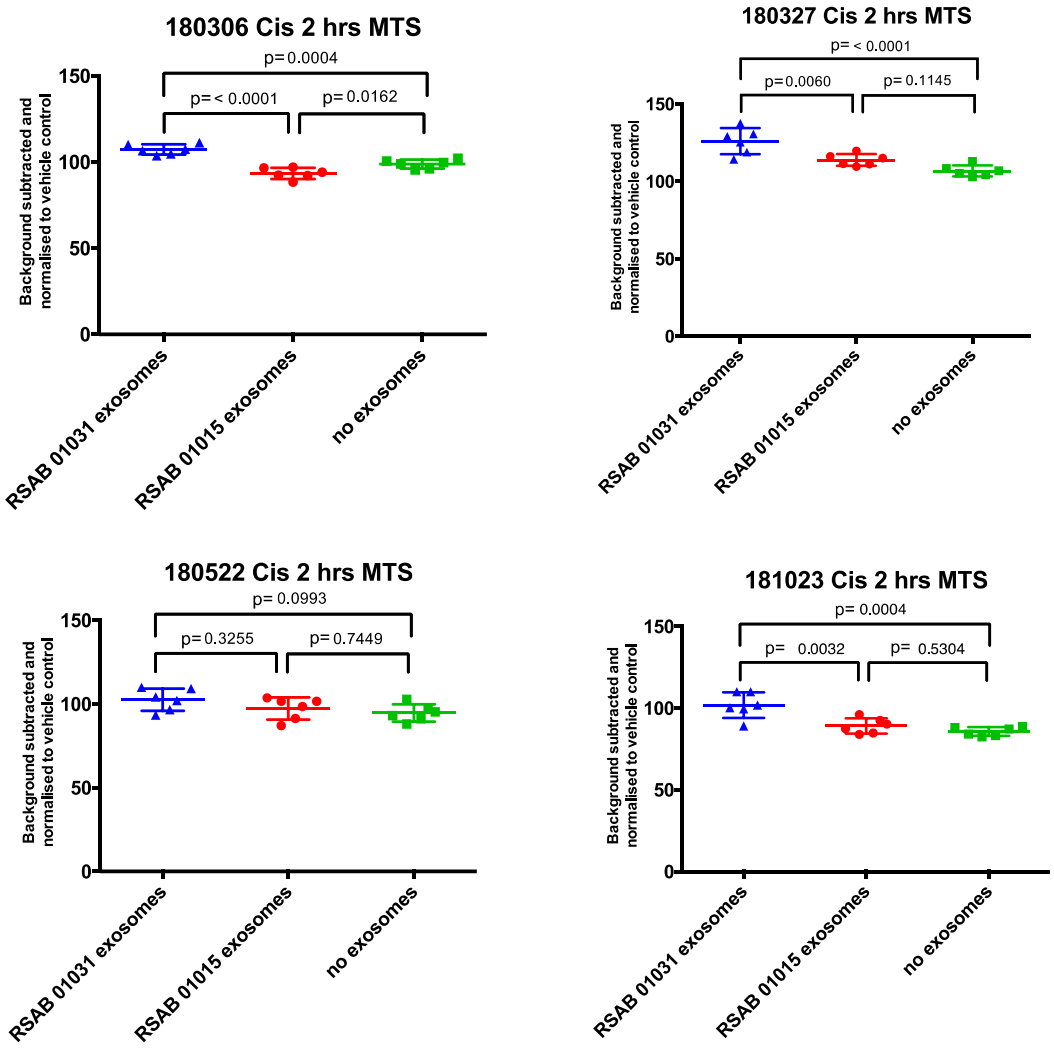

Figure 6-11. *The effect of exosomes on cisplatin response, as assessed by MTS data analysis (the exosome-treated cells were treated with 8 μM cisplatin, and the MTS data were measured after 2 hours of adding the MTS regents. All the data were normalized with regard to the data for the vehicle control).*

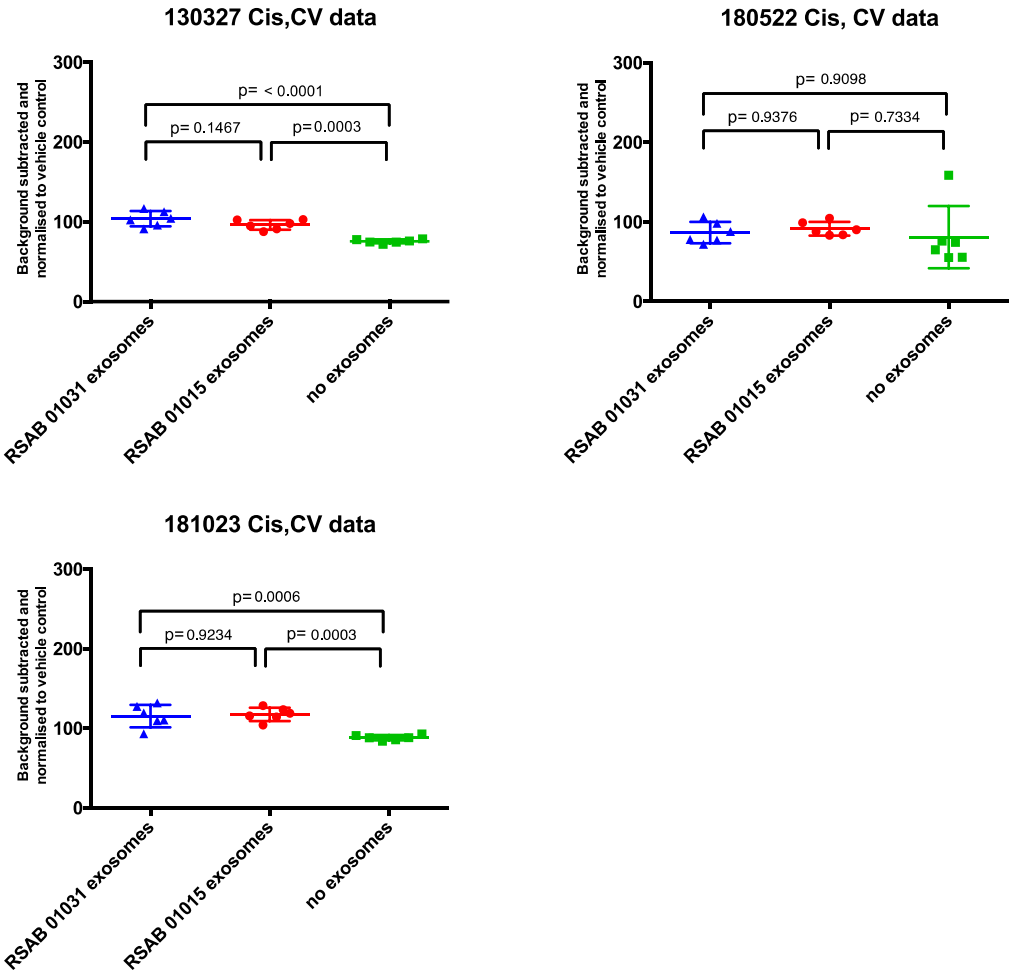

Figure 6-12. *The effect of exosomes on cisplatin response, as assessed by CV data analysis (Background subtracted and normalized to vehicle control, large circle area analysis).*

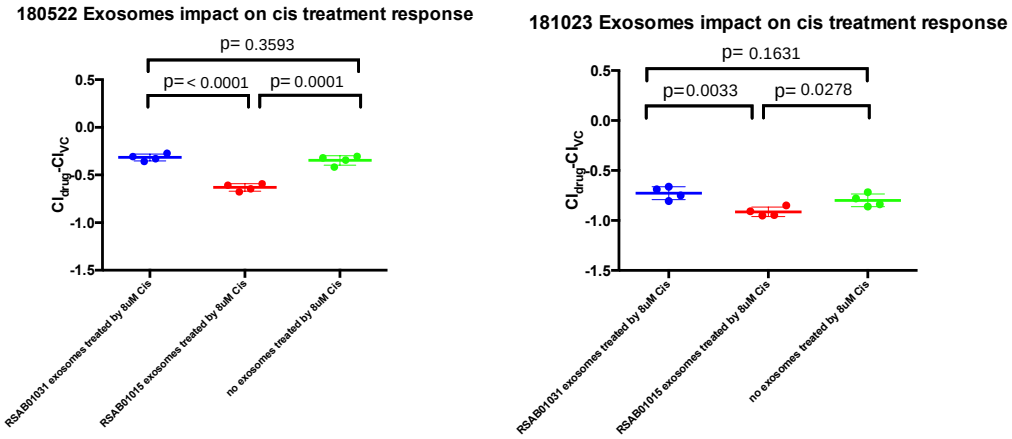

***Figure 6-13**. The effect of exosomes on cisplatin response, as assessed by xCelligence data analysis (the exosome-treated cells were treated with cisplatin, and the xCelligence data were normalized by subtracting vehicle control, CI drug: cell index of drug treatment, CI VC: cell index of vehicle control).*

In cells treated with the vehicle control for 5-FU, the exosomes showed no reproducible effects across the four independent experiments (Table 6-3, Appendix 6.3).

Similarly, in cells treated with 5-FU, the exosomes showed no reproducible effects across the four independent experiments (Table 6.3, Appendix 6.3).

While no consistent effects were observed across the four independent experiments, there were some inverse associations between the direction of effect of the exosomes on cell number in the vehicle-treated cultures compared to the direction of effect of the exosomes on cell number in the drug-treated cultures. These are described below, and shown in Table 6-3 and Figures 6-14 and 6-15. All other Figures for the vehicle of 5-FU and 5-FU treatment data are presented in Appendix section 6.3 and 6.4.

- In the 180306 experiment vehicle cultures, the MTS assay suggested that non-responder exosomes (RSAB01015) resulted in a small but statistically significant decrease in the number of cells, compared to the case after treatment with responder exosomes. In the same experiment in 5-FU-treated cultures, the MTS assay suggested that non-responder exosomes resulted in a

small but statistically significant increase in resistance to 5-FU treatment compared to the responder exosomes (Figure 6-14).

- In the 180522 experiment vehicle cultures, the xCelligence assay suggested that non-responder exosomes resulted in a statistically significant increase in the number of cells, compared to the case for the treatment with the responder exosomes. In the same experiment in 5-FU-treated cultures, the xCelligence assay suggested that non-responder exosomes resulted in a statistically significant decrease in resistance to 5-FU treatment compared to the responder exosomes (Figure 6-15).

***Table 6-3**. The role of serum exosomes in controlling cell proliferation and 5-FU treatment response (vehicle control of 5-FU, ↑: there are more viable cells in RSAB01015 exosome (Non-responder) exposure group compared to RSAB01031 exosome (responder) exposure group. ↓: there are less viable cells in RSAB01015 exosome (Non-responder) exposure group compared to RSAB01031 exosome (responder) exposure group. NT: condition not tested. The p-value is labeled in red when p<0.1. The cells were lost during washing in CV experiment of 180306.*

Vehicle control of 5-FU				5-FU 50 uM			
Date	MTS (NON-RESP / RESP)	CV (NON-RESP / RESP)	xCelligence 96h	Date	MTS (NON-RESP / RESP)	CV (NON-RESP / RESP)	xCelligence 96h
180306	0.946 ↓ (p=0.010)	CELLS LOST IN WASH	NT	180306	1.104 ↑ (p=0.000)	CELLS LOST IN WASH	NT
180327	1.036 (p=0.5798)	0.917 ↓ (p=0.084)	NT	180327	0.963 (p=0.770)	1.124 (p=0.418)	NT
180522	0.971 (p=0.887)	1.064 (p=0.610)	1.894 ↑ (p=0.021)	180522	0.986 (p=0.916)	0.959 (p=0.979)	0.623 ↓ (p<0.000)
181023	1.026 (p=0.779)	0.978 (p=0.764)	0.809 (p=0.5561)	181023	0.981 (p=0.704)	1.488 ↑ (p=0.014)	1.105 ↑ (p=0.0114)

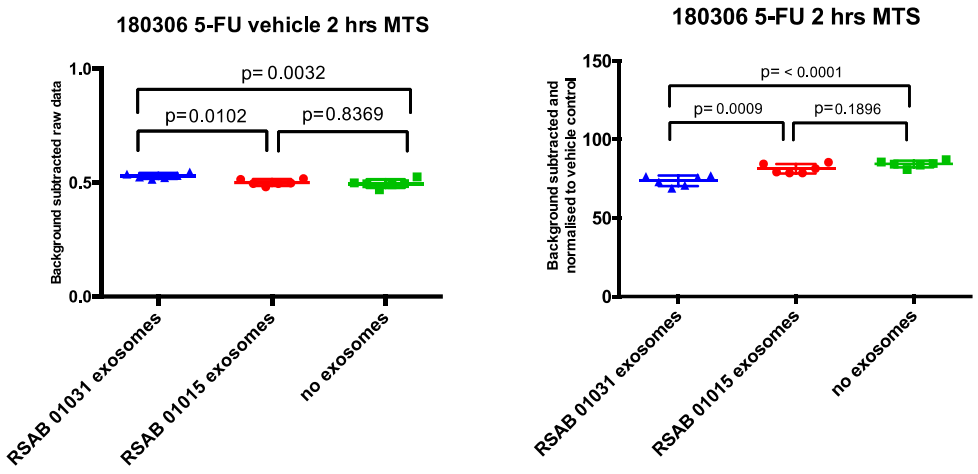

Figure 6-14. *The role of serum exosomes in controlling cell proliferation and response to 5-FU treatment in the 180306 experiment. The exosome-treated cells were treated with 5-FU vehicle (left) or 50 μM 5-FU (right) and MTS assay data were obtained; the MTS data were normalized using background subtraction.*

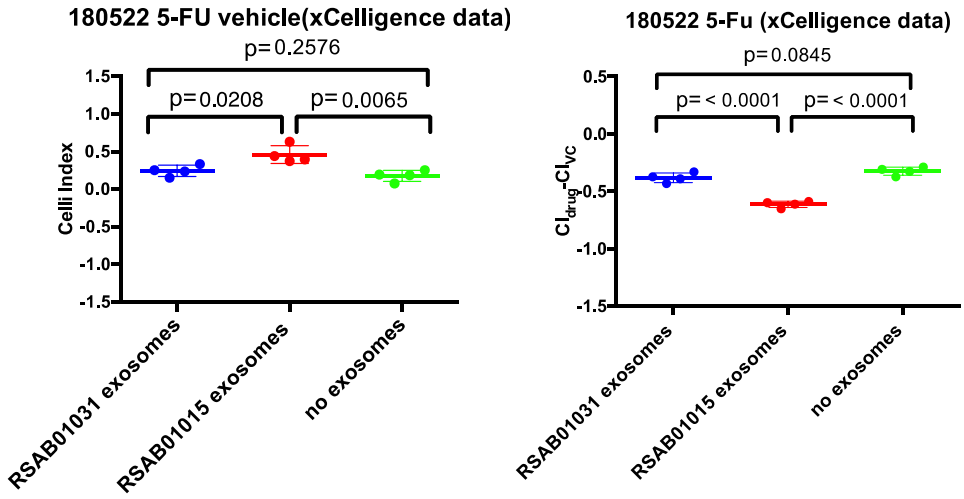

Figure 6-15. *The role of serum exosomes in controlling cell proliferation and 5-FU treatment response in the 180522 experiment. The exosome-treated cells were treated with 5-FU vehicle (left) or 50 μM 5-FU (right). The xCelligence data were*

normalized by subtracting the vehicle control data, CI drug: cell index of drug treatment, CI VC: cell index of vehicle control.

6.3.4 The role of serum exosomes in controlling cell viability and response to radiation treatment in EAC cells

The effect of exosomes was tested in the irradiation experiments. Two plating efficiencies were measured to determine the impact of exosomes on cell viability: one in the non-irradiated group and another one in the irradiated group. The effects on plating efficiencies across the three experiments were not consistent. There were no statistically significant effects in the first experiment (180327). In the second experiment, in the non-irradiated controls, there were less colonies formed in the cells treated with the non-responder exosomes compared with the cells treated with the responder exosomes (180606, p=0.009). There were no significant observations in irradiated cells in this experiment. In the third experiment (180828), in the non-irradiated controls, there were more colonies formed in the cells treated with the non-responder exosomes compared with the cells treated with the responder exosomes however it did not reach statistical significance (p=0.085). In the irradiated cells, there were more colonies formed in the cells treated with the non-responder exosomes compared to the responder exosomes (p=0.018; Table 6-4, Figure 6-16).

The impact of exosomes on radiation response was also measured in these three experiments by calculating the survival fraction (Table 6-4). There were no statistically significant observations in the 180327 and 180606 experiments. In the 180828 experiment, the exosomes from the non-responders made the cells more resistant to irradiation (p=0.0022; Table 6-4, Figure 6-17). All other Figures are shown in Appendix section 6-3 and 6-4.

Table 6-4*. The role of serum exosomes in controlling cell viability (plating efficiency; PE) and irradiation treatment response (survival fraction; SF).*

↑: there are more viable cells in the RSAB01015 exosome (Non-responder) exposure group than in the RSAB01031 exosome (responder) exposure group. ↓: there are less viable cells in the RSAB01015 exosome (Non-responder) exposure

group than in the RSAB01031 exosome (responder) exposure group. The p-value is labeled in red when p<0.1.

	Radiation		
Date	PE NO RADIATION (NON-RESPONDER/RESPONDER	PE IRRADIATION (NON-RESPONDER/RESPONDER)	SF (NON-RESPONDER/RESPONDER)
180327	0.686 (p=0.130)	0.905 (p=0.749)	1.319 (p=0.684)
180606	0.730 ↓ **(p=0.009)**	0.757 (p=0.214)	1.037 (p=0.9852)
180828	1.290 ↑ **(p=0.085)**	2.47 ↑ **(p=0.018)**	1.914 ↑ **(p=0.0450)**

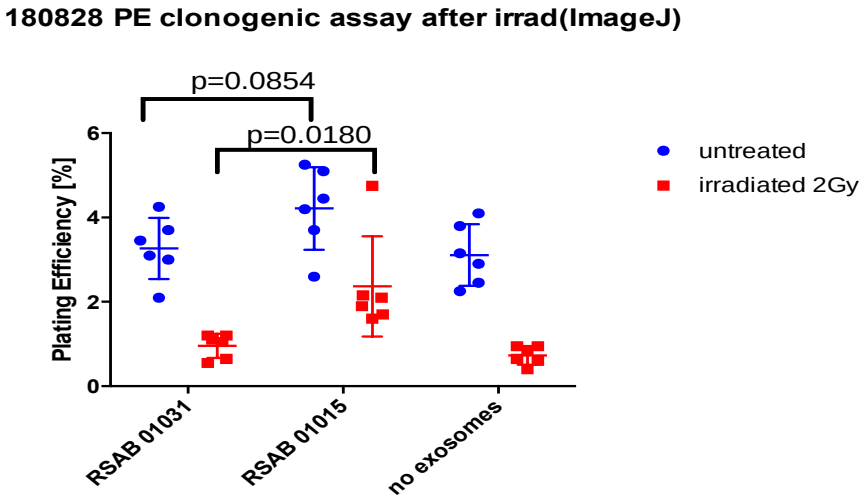

***Figure 6-16**. The exosomes showed no reproducible effects on cell viability across the three independent irradiation experiments.*

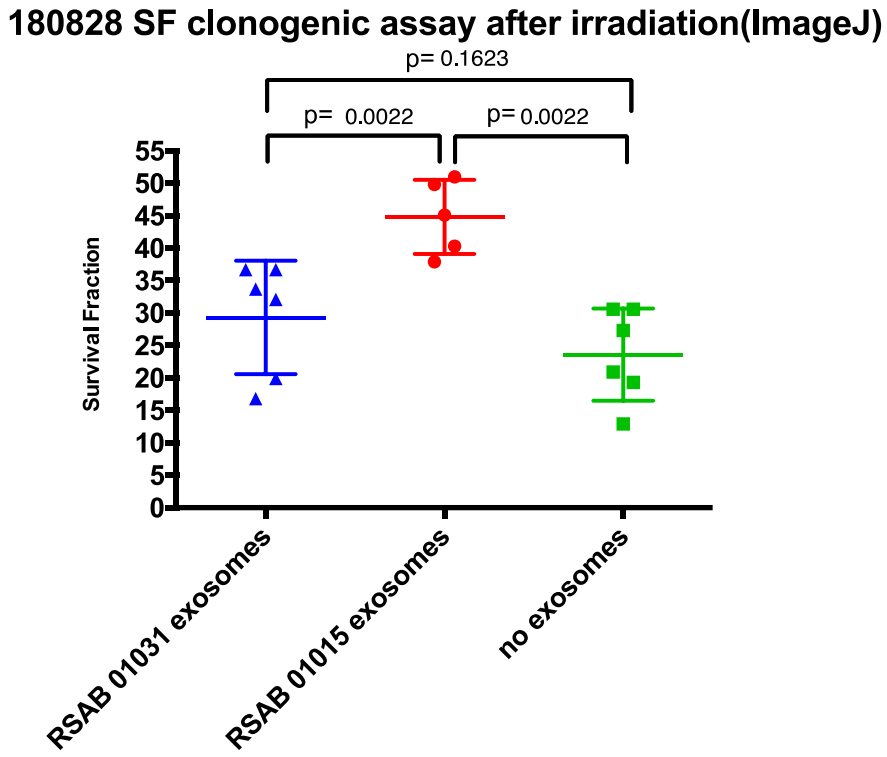

Figure 6-17*. The effects of exosomes on irradiation response, as assessed using the Clonogenic assay (the data was analyzed using Image J software; one outlier datapoint (Survival Fraction = 112.6) from the RSAB01015 group was removed for the statistical tests shown in this figure. When the outlier was included, the p-values were p=0.045 for RSAB 01031 exosomes vs RSAB 01015 exosomes; p=0.0149 for RSAB01015 exosomes vs no exosomes; p=0.8400 for RSAB01031 vs no exosomes.*

6.4 Discussion

6.4.1 The relationship between small RNAs expression and drug/radiation treatment response in EAC cell lines

The small RNAs studied in this chapter were significant in the serum study between therapy responders and non-responders (Chapter 5.3.6), and thus, they may be important in the regulation of treatment response in cells. The aim of this chapter was to investigate the possible involvement of blood small RNAs in regulating chemoradiotherapy response in EAC cells. As a first step towards investigating this, we examined whether the baseline cellular levels of these miRNAs are associated with drug and radiation response in EAC cell lines.

The results showed that miR-4728-3p, miR-615-3p, miR-32-5p, DQ570339, miR-1301-3p, and SNORD37 are associated with drug/radiation treatment response. However, the piRNA results require further clarification. This is because during the writing of this thesis, it was noted that the piRNA assays on cell line RNA were done using cDNA generated with the Qiagen miScriptII reverse transcription kit and HiSpec buffer. The first step in this method of reverse transcription is addition of a polyA tail to the 3' end of RNA molecules. This is called polyadenylation of the RNA. According to previous advice from Qiagen, obtained at the beginning of this project, this method is unsuitable because piRNA sequences have 2'-O-methylation at their 3' end; this makes them refractory to polyA tailing. They also checked the sequences of the piRNAs using genomic databases and noted that they 'overlap significantly with other genes,' thus raising the possibility that the PCR products synthesized in the piRNA PCR assays may have been generated from other genes,

i.e., derived from mRNAs or snoRNAs etc. that are coded for by the same chromosomal DNA sequences as the piRNAs (more discussion details in the part of the discussion: Chapter 4:4.4.2). DQ570339 was performed with miScript II; therefore, these results require further confirmation. Further testing was outside the scope of this thesis. Therefore, the piRNA PCR assay results from cell lines require further confirmation.

These small RNAs have an important role in regulating treatment response. Wang et al.[290] used microarray profiling and reported that miR-4728-3p was downregulated in the 5-FU-resistant gastric cancer cell line, and may serve as a biomarker for multidrug resistance. miR-615-3p has also been pointed out as a potential biomarker of chemotherapy response. miR-615-3p regulated bortezomib resistance in patients with multiple myeloma[291]. In lung cancer, exosomal H19 facilitated erlotinib resistance by the miR-615-3p/ATG7 axis, and may thus, serve as a potential target for the diagnosis and treatment of lung cancer[292]. Mukai et al.[293] used miRNA microarray analysis to show that miR-615-3p is related to the malignant proliferation of hepatocellular carcinoma cells, and induced chemoresistance, indicating that miR-615-3p is a potential biomarker of chemotherapy response. Another biomarker, miR-32-5p, which is selected from serum exosomes, was reported to be involved in chemotherapy response as well. Exosomal miR-32-5p induced multidrug resistance in hepatocellular carcinoma by promoting angiogenesis and EMT (epithelial-mesenchymal transition)[432]. Besides, downregulation of miR-32-5p increased the chemosensitivity of prostate cancer to cisplatin[433]. The downregulation of miR-32-5p promoted radiosensitization and decreased the migration and invasion abilities of colorectal cancer cells[434]. Very

few studies have reported the association between piRNAs, snoRNAs, and treatment response in cancers.

Thus, these small RNAs are associated with drug/radiation treatment response, and might play an important role in the regulation of treatment response.

6.4.2 The role of serum exosomes in controlling cell proliferation/ viability and response in EAC cells

Exosomes are membrane-bound carriers and their cargos include proteins, nucleic acids, and small RNAs[445]. Exosomes play an important role in cancer growth and metastasis by acting as communication vehicles between cells. There are numerous proteins and small RNAs in exosomes, and the exosomes could carry the miRNAs to circulation. Previous research has demonstrated that exosomal small RNAs transmitted as the 'correspondent' between cells are involved in cell proliferation, apoptosis, and invasion. The serum exosomal miR-1247-3p moves between cancer cells and fibroblasts that correlated with lung metastasis in liver cancer[446]. The exosomes as the miRNA cargo were demonstrated to promote osteoclast differentiation and bone resorption activities[447].

The results showed that the exosomes from the non-responders increased the cell viability in most of the cisplatin vehicle experiments. The reason might be that exosomes transmit the small RNAs that affect cell proliferation. However, the results in 5-FU vehicle were less clear and appeared to differ between experiments. The apparent differences between exosome effects on OE-33 cells cultured in cisplatin vehicle *vs* OE-33 cells cultured in the presence of the 5-FU vehicle might be due to different chemical contents of the drug vehicles. The chemicals in the 5-FU vehicle might disrupt the function of exosomes more than the chemicals in the cisplatin

vehicle. A previous study showed that many factors affect exosome targeting, such as the phosphatidylethanolamine enriched glioblastoma-derived exosomes target glioblastoma cells and breast cancer cells[448]. Microenvironmental pH was another important factor that affected exosome transmission in cancer cells[449]. Besides, several factors affect exosome transmission, and some factors are harder to control during experiments that might affect the transfer of small RNAs in exosomes, such as temperature, resulting in discrepancy in results. All these factors might result in the differences observed between the effects of exosomes on cells cultured in the presence of the 5-FU vehicle and cisplatin vehicle.

As for the role of serum exosomes in controlling treatment response, three of four MTS experiments and two of two xCelligence experiments suggested that exosomes from non-responder made the cells less resistant to cisplatin. However, the CV data did not show the difference between different exosomes in affecting drug response. CV acts when the cells that undergo cell death lose their adherence and are subsequently lost from the population of cells, reducing the amount of crystal violet staining in a culture due to some cells that are still alive but have lost their adherence. Therefore, the CV data is not very reliable to test cell death. In the future, flow cytometry might be better to test cell death. The xCelligence measures the net cellular adhesion within the cells. The cells adhering on the plate surface will affect the impedance values, and the impedance values are converted into the cell index (CI)[443]. The CV and xCelligence test different things; therefore, their results are not always consistent with each other.

Similar to the case for the cells cultured with the vehicle for 5-FU, there were no consistent effects of exosomes observed in the cells treated with the drug 5-FU. The

reasons are complicated, such as temperature, pH, and the chemical compositions of 5-FU vehicle; this might affect the transport of exosomes.

The results of the three independent clonogenic assays did not show a consistent impact of non-responders/ responder exosomes on the survival potential of OE-33 cells. Likewise, no consistent impact on radiation response was observed.

6.4.3 Limitations

This study has some limitations. First, we only tested the relationship between a sub-set of small RNAs with drug or radiation response in cells. This was because the Qiagen company could not design the functional qRT-PCR assay for some piRNAs and snoRNAs. Second, the serum exosomes are only from one patient each, which might result in bias. In the future, more exosomes from a large sample could be collected and tested to strengthen the study of the function of exosomes in regulating the chemoradiotherapy response. Besides, the exosomal preparations might contain serum factors, such as serum proteins or cell free non-exosome bound small RNAs that could impact the cellular response. Third, more independent experiments should be performed in order to validate the function of exosomes. Fourth, to improve the significance of the findings additional cell lines should be tested. Co-culturing with cancer-associated fibroblasts or the use of organoid models might also provide valuable information. Lastly, the mechanisms underlying the effects of exosomes on the recipient cells should be explored, such as the expression of the small RNAs and related proteins after exosome exposure should be analyzed in detail.

6.4.4 Summary

In summary, this study has shown that the expression of some small RNAs in serum exosomes are associated with drug or radiation response. These include miR-4728-3p, miR-615-3p, miR-32-5p, DQ570339, and SNORD37, indicating that they might play a pivotal role in the cell proliferation and treatment response. The exosomes from non-responder and responders have different effects on proliferation of recipient cells and their response to antineoplastic agents. This effect was consistent for cisplatin across independent experiments but not for 5-FU or radiation. The effects of the exosomes might be in part due to the small RNAs that they deliver. These might be potential targets for the treatment of EAC to improve chemoradiotherapy response in the future.

CHAPTER 7
SUMMARY, CONCLUSIONS AND FUTURE STUDIES

The aim of this study described in this thesis was to identify the small RNAs as potential biomarkers of response to chemoradiotherapy in EAC and study the potential roles of significant miRNAs in regulating chemoradiotherapy response and the mechanisms underlying these roles.

7.1 Identification of potential small RNA-based biomarkers of response to chemoradiotherapy in pre-treatment tumor tissues from patients with locally advanced EAC.

Prediction of responders: The results showed that miR-451a and miR-340-5p might be potential biomarkers for the prediction of responders. As for the piRNA, DQ576665 and DQ598428 were adequate as biomarkers of responders according to the ROC curve and the lower bound of the false positive rate. There were four snoRNAs selected as biomarkers for the prediction of responders, which were SNORD58B.201, SNORD123.201, SNORA2B.201, and SNORD18A.201. SNORD58B.201, SNORD123.201, SNORA2B.201, and SNORD18A.201 were significant in AJCC-0 vs. AJCC-3. However, all of them were unacceptable according to the lower bound of the false positive rate and the lower bound of the sensitivity. As for the snRNAs, RNU1.148P.201 was identified as a potential biomarker for the prediction of responders, but this snRNA was not significant in the extreme situation of AJCC-0 vs. AJCC-3. Furthermore, the lower bound of the false positive rate was as high as 90% when the lower bound of the sensitivity was 75%. Therefore, there were no suitable snRNAs as biomarker of treatment response.

Prediction of non-responders: The results showed that there were 12 miRNAs that could be potential biomarkers for the prediction of non-responders, and nine of them were significant in AJCC-0 vs. AJCC-3. However, only five of them were selected according to the lower bound of the false positive rate and the lower bound of the sensitivity, that were miR-767-5p, miR-1301-3p, miR-552-3p, miR-99a-5p, and miR-206. Five piRNAs were identified as potential biomarkers for the prediction of non-responders, that were piR-hsa-32187, DQ598641, DQ599147, DQ582265, and DQ599822 and two of them were significant in AJCC-0 vs. AJCC-3. However, only piR-hsa-32187, DQ598641, and DQ599147 were picked as biomarkers of responders according to the lower bound of the false positive rate. There were six snoRNAs picked as biomarkers for the prediction of non-responders, which were SNORD114-17-201, SNORD14A-201, SNORD92-201, SNORD58B-201, SNORD15A-201, and SNORD46-201 and four of them were significant between AJCC-0 and AJCC-3. However, only SNORD58B-201, SNORD46-201, and SNORD114-17-201 were chosen as the potential biomarkers for the prediction of non-responders according to the lower bound of the false positive rate and the lower bound of the sensitivity. As for the snRNAs, RNU5E-4P-201, RNU5E-6P-201, and RNU6ATAC25P-201 were identified as potential biomarkers for the prediction of non-responders, and all of them were significant in the extreme situation of AJCC-0 vs. AJCC-3. However, the lower bound of the false positive rate was too high when the lower bound of the sensitivity was over 80%, therefore, they were not valid biomarkers.

The biomarkers with the potential for predicting chemoradiotherapy response prior to commencing therapy were as follows: Prediction of responders: miR-340-5p, miR-451a, DQ598428, and DQ576665. Prediction of non-responders: miR-767-5p,

miR-1301-3p, miR-552-3p, miR-99a-5p, miR-206, DQ598641, piR-hsa-32187, SNORD58B-201, SNORD46-2-201, and SNORD114-17-201.

The top miRNA biomarkers were tested by qRT-PCR. The results showed that the expression of miR-451a was significant between responders and non-responders (p=0.0018). miRNA levels gradually decrease over time in FFPE tissue blocks[325]. Therefore, we suspected that the age of FFPE tissue block might significantly impact the results of qRT-PCR and our data analysis supported this hypothesis. Therefore, the remaining small RNAs were not tested by qRT-PCR. Our data showed that there is no correlation between the age of FFPE and NGS data. Therefore, the data from the sequencing analysis in this study was reliable.

7.2 Investigation of the role of cellular small RNAs in regulating chemoradiotherapy response in EAC cells

The results showed that there was a positive correlation between small RNA expression and drug response, such as for miR-451a, miR-1301-3p, and miR-767-5p. Besides, the results showed that there was a positive correlation between expression of miR-451a (p=0.024) and radiation treatment response. Although only eight of 14 selected biomarkers from chapter 3 were tested in cell lines because the Qiagen company could not design a functional qRT-PCR assay for some piRNAs and snoRNAs, the results supported the hypothesis that some of the selected tissue biomarkers of response to chemoradiotherapy might have a direct biological role in controlling drug and or radiation response in EAC cells, especially for miR-451a.

From the bioinformatical analysis and literature study, miR-451a might regulate treatment response by affecting AMPK, YWHAZ (14-3-3 zeta/delta), AKT, OXCT1, SLC7A11, LKB1 (STK11), MST1 (STK4), CAB39, and p53. The results showed

that miR-451a was correlated with YWHAZ and pAKT. Further, YWHAZ and pAKT had a correlation with drug and irradiation treatment response. Therefore, miR-451a was selected for the functional study.

The functional study of miR-451a showed that miR-451a enhanced EAC cell proliferation and decreased the degree of apoptosis in these cells. Besides, miR-451a renders the EAC cells more resistant to drug treatment.

From the clonogenic assay, miR-451a increased the plating efficiency in most experiments. Some discrepancy of results might result from the differential expression of 14-3-3 zeta/delta, 14-3-3 zeta Phos Ser 58, AMPK, and pAMPK Thr172. These proteins or their related signaling pathways might be activated due to technical variables in cell culture, such as hypoxia from a longer time in transferring of the cell suspension. The clonogenic assay showed that miR-451a made the cells more resistant to cisplatin, 5-FU, and carboplatin, but less resistant to paclitaxel. In radiation experiments, the results showed that miR-451a decreased the plating efficiency (in two out of two independent experiments) and made the cells slightly less resistant to irradiation (in one out of two independent experiments; there was no effect on radiation observed in the second experiment), indicated that the mechanisms underlying the responses to drugs and irradiation may differ.

After transfection with the miR-451a mimics, the level of AMPK was decreased. Besides, the ratio of phosphorylation showed that pAMPK Thr172/AMPK, 14-3-3 zeta phos Ser58/14-3-3 zeta/delta, pEGFR/EGFR were different in mimic groups compared with non-targeting control mimic groups. This indicates that miR-451a might regulate the treatment response by affecting these proteins. Therefore, it is

reasonable to hypothesize that they could be potential targets for EAC treatment in the future to improve chemoradiotherapy response.

7.3 To identify potential small RNA biomarkers of response to chemoradiotherapy in pre-treatment blood from locally advanced EAC patients

From the RNA sequencing of serum exosomes, the results showed that the miRNAs, miR-4728-3p, miR-615-3p, miR-92b–3p, and miR-32-5p, the piRNAs, DQ571335, DQ571591, DQ598008, and DQ570339, and the snoRNAs, SNORD37, SNORD42A, SNORA71B, SNORD58B, and SNORD123 could be potential biomarkers of response to chemoradiotherapy in serum exosomes.

These small RNAs selected as candidate biomarkers from serum exosomes of chemoradiotherapy response were tested in cohorts of EAC patients. The results in SA patient cohort showed that the selected small RNAs in serum exosomes were promising as biomarkers of the treatment response, such as miR-92b-3p and SNORD42A. In the Netherland patient cohort, the results showed that miR-32-5p ($p=0.0951$), DQ570339 ($p=0.0499$), and SNORA71B ($p=0.0725$) had more expression in the responder group and were promising as biomarkers.

Thus, some biomarkers of response to chemoradiotherapy selected from the sequencing discovery study were promising in serum exosomes of patient cohorts. These small RNAs from the exosomes of the serum might be potential biomarkers of response to chemoradiotherapy. More independent patient cohorts are needed to confirm this.

7.4 Investigation of the possible involvement of blood small RNAs in regulating chemoradiotherapy response in EAC cells

The aim of this chapter was to investigate the possible involvement of blood small RNAs in regulating chemoradiotherapy response in EAC cells. First, we investigated whether the baseline cellular levels of these miRNAs are associated with drug and radiation response in EAC cell lines. The flow cytometry results did not show an association between expression of small RNAs and drug treatment response. The MTS was also used to investigate the relationship between treatment response and the expression of small RNAs. The results showed that miR-32-5p ($p=0.037$) and DQ570339 ($p=0.005$) had a positive correlation with 5-FU treatment response. There was an association between expression of miR-4728-3p and 5-FU treatment response ($p=0.058$), however it did not reach statistical significance.

The role of serum exosomes and their small RNAs in controlling cell growth and drug/radiation response in EAC cells was investigated using two kinds of drug vehicles. In the cisplatin vehicle experiment, the data showed that in the vehicle control without cisplatin, the exosomes from non-responder (RSAB01015) resulted in an increased cell viability, compared to the case for the treatment with the exosomes from the responder (RSAB01031). As for the 5-FU vehicle and irradiation experiment, the data showed no reproducible effects.

The results of the cisplatin treatment showed that the exosomes from non-responders made the cells less resistant to cisplatin. As for the 5-FU treatment, the data showed that exosomes from non-responders made the cells more resistant to 5-FU in most experiments. The results of irradiation treatment showed that exosomes from the non-responders made the cells more resistant to irradiation in one experiment.

7.5 Future directions

The knowledge gained from this study can be built upon to further understand the role of small RNAs in biomarkers and regulators of chemoradiotherapy response in EAC.

7.5.1 Validating more small RNA candidates as biomarkers for chemoradiotherapy response in EAC

In chapter 3, RNA sequencing was used to profile the potential small RNAs as biomarkers for chemoradiotherapy response by DESeq2. However, only the top two miRNAs were validated by qRT-PCR. More candidates need to be validated in the future. Future studies could look at treatment response and all the markers combined rather than 1 marker at a time.

7.5.2 Studying the functions of piRNAs, SnoRNAs, and snRNAs

Some piRNAs, snoRNAs, and snRNAs have been identified as biomarkers of response to chemoradiotherapy. However, there is very little knowledge of their roles in regulating chemoradiotherapy treatment, and requires further research.

7.5.3 Testing the functions of miR-451a *in vivo*

We observed that miR-451a could affect cell proliferation and treatment response. However, these need to be tested further *in vivo* because *in vivo* studies have the potential to offer conclusive insights about the nature of medicine and disease. Besides, the body might react to the drug to some extent, which is different from *in vitro* conditions. The mechanism underlying the regulation of the responses to chemoradiotherapy in the human body is much more complicated than that in simple

cell lines. In order to more appropriately mimic the human body, the function of miR-451a should be tested *in vivo* in the future. For example, using the miR-451a knockout mouse model to test the drug/irradiation response.

7.5.4 Validating the mechanism underlying the regulation of the responses to chemoradiotherapy

In chapter 4, we found that miR-451a might play an important role in regulating chemoradiotherapy response by affecting AMPK, 14-3-3 zeta phos Ser58, and pAKT. However, the regulation network was complicated and many of them affected each other. For example, AMPK-Akt feedback loop could produce multi-stability and cause phenotypic switching in cancer cell proliferation[450]. Besides, activated AMPK phosphorylates many 14-3-3 zeta targets[397]. Thus, further experiment should be done to validate the signaling pathways and more complicated regulatory networks.

7.5.5 More patient cohorts are needed

The small RNAs selected as candidate biomarkers from serum exosomes of chemoradiotherapy response were tested in cohorts of EAC patients. However, the sample size was too small. Larger patient cohorts are needed to confirm these findings further.

7.5.6 Studying the effects of exosomes on the recipient cells and the mechanisms underlying these effects

In chapter 6, we found that the serum exosomes from responders and non-responders affected the treatment response of recipient cells differently. However, the results were not very repeatable, and more experiments were needed to study the function of

exosomes. Besides, the mechanisms whereby the exosomes affect the treatment response of recipient cells should be explored. Furthermore, testing the small RNAs and their related proteins in recipient cells should also be performed in the future.

7.6 Conclusion

Many small RNAs from tissue and serum exosomes could be biomarkers of response to chemoradiotherapy for the prediction of responders and non-responders. miR-451a was at the top of the list and was significant between responders and non-responders. Besides, this miRNA shows a positive correlation with radiation treatment response in EAC cell lines.

Functional studies regarding miR-451a using miRNA mimics showed that it enhanced EAC cell proliferation and increased the plating efficiency in most experiments. Some experiments indicated that miR-451a made cells more resistant to chemotherapy drugs. Inconsistent results between independent experiments were associated with differential expression of 14-3-3 zeta/delta, 14-3-3 zeta Phos Ser 58, AMPK, and pAMPK Thr172. This indicates that miR-451a may regulate the treatment response by affecting these proteins or related signaling pathways.

Some selected biomarkers of response to chemoradiotherapy were promising in serum exosomes of patient cohorts. These small RNAs from the serum exosomes of the serum may serve as potential biomarkers of responses to chemoradiotherapy. They might play an important role in regulating treatment response. The role of serum exosomes in controlling cell growth and drug/radiation response in EAC cells was investigated. The results showed that the exosomes from non-responder made the cells less resistant to cisplatin. As for the 5-FU vehicle experiment and irradiation experiment, the data showed no reproducible effects.

This study identified small RNAs as biomarkers of response to chemoradiotherapy in EAC and the potential roles of significant miRNAs in regulating the response to chemoradiotherapy and the mechanisms underlying these roles. In the future, these small RNAs may serve as treatment targets for patients showing chemoradioresistance.

REFERENCES

1. Pennathur, A., et al., *Oesophageal carcinoma.* Lancet, 2013. **381**(9864): p. 400-12.
2. Arnold, M., et al., *Global incidence of oesophageal cancer by histological subtype in 2012.* Gut, 2015. **64**(3): p. 381-7.
3. Xie, S.H. and J. Lagergren, *Time trends in the incidence of oesophageal cancer in Asia: Variations across populations and histological types.* Cancer Epidemiol, 2016. **44**: p. 71-76.
4. Corley, D.A. and P.A. Buffler, *Oesophageal and gastric cardia adenocarcinomas: analysis of regional variation using the Cancer Incidence in Five Continents database.* Int J Epidemiol, 2001. **30**(6): p. 1415-25.
5. Sewram, V., et al., *Tobacco and alcohol as risk factors for oesophageal cancer in a high incidence area in South Africa.* Cancer Epidemiol, 2016. **41**: p. 113-21.
6. Skeie, G., et al., *Intake of whole grains and incidence of oesophageal cancer in the HELGA Cohort.* Eur J Epidemiol, 2016. **31**(4): p. 405-14.
7. Lu, Y., et al., *Diet-related inflammation and oesophageal cancer by histological type: a nationwide case-control study in Sweden.* Eur J Nutr, 2016. **55**(4): p. 1683-94.

8. Zhu, Y., et al., *Reproductive factors are associated with oesophageal cancer risk: results from a meta-analysis of observational studies.* Eur J Cancer Prev, 2016.
9. Pohl, H., et al., *Length of Barrett's oesophagus and cancer risk: implications from a large sample of patients with early oesophageal adenocarcinoma.* Gut, 2016. **65**(2): p. 196-201.
10. Tan, C., et al., *Potential biomarkers for esophageal cancer.* Springerplus, 2016. **5**: p. 467.
11. Hoeben, A., et al., *Cervical esophageal cancer: a gap in cancer knowledge.* Ann Oncol, 2016. **27**(9): p. 1664-74.
12. Yamamoto, M., et al., *Minimally invasive surgery for esophageal cancer: review of the literature and institutional experience.* Cancer Control, 2013. **20**(2): p. 130-7.
13. Enzinger, P.C. and R.J. Mayer, *Esophageal cancer.* N Engl J Med, 2003. **349**(23): p. 2241-52.
14. Portale, G., et al., *Modern 5-year survival of resectable esophageal adenocarcinoma: single institution experience with 263 patients.* J Am Coll Surg, 2006. **202**(4): p. 588-96; discussion 596-8.
15. Schuchert, M.J., J.D. Luketich, and R.J. Landreneau, *Management of Esophageal Cancer.* Current Problems in Surgery, 2010. **47**(11): p. 845-946.
16. Molena, D., et al., *Esophageal Cancer Treatment Is Underutilized Among Elderly Patients in the USA.* J Gastrointest Surg, 2016.
17. Hopper, A.D. and J.A. Campbell, *Early diagnosis of oesophageal cancer improves outcomes.* Practitioner, 2016. **260**(1791): p. 23-8, 3.
18. Shah, P.M. and H. Gerdes, *Endoscopic options for early stage esophageal cancer.* J Gastrointest Oncol, 2015. **6**(1): p. 20-30.
19. Patel, V. and R.A. Burbridge, *Endoscopic approaches for early-stage esophageal cancer: current options.* Curr Oncol Rep, 2015. **17**(1): p. 421.
20. Kleinberg, L., M.K. Gibson, and A.A. Forastiere, *Chemoradiotherapy for localized esophageal cancer: regimen selection and molecular mechanisms of radiosensitization.* Nature Clinical Practice Oncology, 2007. **4**(5): p. 282-294.
21. Klevebro, F., et al., *A randomized clinical trial of neoadjuvant chemotherapy versus neoadjuvant chemoradiotherapy for cancer of the oesophagus or gastro-oesophageal junction.* Ann Oncol, 2016. **27**(4): p. 660-7.

22. Markar, S.R., et al., *Role of neoadjuvant treatment in clinical T2N0M0 oesophageal cancer: results from a retrospective multi-center European study.* Eur J Cancer, 2016. **56**: p. 59-68.
23. Wang, Q.F., et al., *Expression of epidermal growth factor receptor is an independent prognostic factor for esophageal squamous cell carcinoma.* World Journal of Surgical Oncology, 2013. **11**.
24. Dong, J., et al., *Expression of estrogen receptor alpha and beta in esophageal squamous cell carcinoma.* Oncol Rep, 2013. **30**(6): p. 2771-6.
25. Bird-Lieberman, E.L., et al., *Population-based study reveals new risk-stratification biomarker panel for Barrett's esophagus.* Gastroenterology, 2012. **143**(4): p. 927-35 e3.
26. Chen, M., et al., *Prognostic value of vascular endothelial growth factor expression in patients with esophageal cancer: a systematic review and meta-analysis.* Cancer Epidemiol Biomarkers Prev, 2012. **21**(7): p. 1126-34.
27. Fitzgerald, R.C., et al., *British Society of Gastroenterology guidelines on the diagnosis and management of Barrett's oesophagus.* Gut, 2014. **63**(1): p. 7-42.
28. Chan, D.S., C.P. Twine, and W.G. Lewis, *Systematic review and meta-analysis of the influence of HER2 expression and amplification in operable oesophageal cancer.* J Gastrointest Surg, 2012. **16**(10): p. 1821-9.
29. Cui, X.B., et al., *SLC39A6: a potential target for diagnosis and therapy of esophageal carcinoma.* J Transl Med, 2015. **13**: p. 321.
30. Tan, H.T., et al., *Serum autoantibodies as biomarkers for early cancer detection.* FEBS J, 2009. **276**(23): p. 6880-904.
31. Qin, J.J., et al., *Mini-array of multiple tumor-associated antigens (TAAs) in the immunodiagnosis of esophageal cancer.* Asian Pac J Cancer Prev, 2014. **15**(6): p. 2635-40.
32. Kilic, A., et al., *Use of novel autoantibody and cancer-related protein arrays for the detection of esophageal adenocarcinoma in serum.* J Thorac Cardiovasc Surg, 2008. **136**(1): p. 199-204.
33. Shimada, H., et al., *Serological identification of tumor antigens of esophageal squamous cell carcinoma.* Int J Oncol, 2005. **26**(1): p. 77-86.
34. Bagaria, B., et al., *Comparative study of CEA and CA19-9 in esophageal, gastric and colon cancers individually and in combination (ROC curve analysis).* Cancer Biol Med, 2013. **10**(3): p. 148-57.
35. Zhang, H., et al., *Serum autoantibodies in the early detection of esophageal cancer: a systematic review.* Tumour Biol, 2015. **36**(1): p. 95-109.

36. Marzancola, M.G., A. Sedighi, and P.C. Li, *DNA Microarray-Based Diagnostics.* Methods Mol Biol, 2016. **1368**: p. 161-78.
37. Patel, A. and S.W. Cheung, *Application of DNA Microarray to Clinical Diagnostics.* Methods Mol Biol, 2016. **1368**: p. 111-32.
38. Schauer, M., et al., *Microarray-based response prediction in esophageal adenocarcinoma.* Clin Cancer Res, 2010. **16**(1): p. 330-7.
39. Xie, J.J., et al., *Integrin alpha5 promotes tumor progression and is an independent unfavorable prognostic factor in esophageal squamous cell carcinoma.* Hum Pathol, 2016. **48**: p. 69-75.
40. De Bruijn, K., et al., *Absence or low IGF-1R-expression in esophageal adenocarcinoma is associated with tumor invasiveness and radicality of surgical resection.* J Surg Oncol, 2015. **111**(8): p. 1047-53.
41. Ziegler, A., et al., *Personalized medicine using DNA biomarkers: a review.* Human Genetics, 2012. **131**(10): p. 1627-1638.
42. Funaki, N.O., et al., *Identification of carcinoembryonic antigen mRNA in circulating peripheral blood of pancreatic carcinoma and gastric carcinoma patients.* Life Sci, 1996. **59**(25-26): p. 2187-99.
43. Kopreski, M.S., et al., *Detection of tumor messenger RNA in the serum of patients with malignant melanoma.* Clin Cancer Res, 1999. **5**(8): p. 1961-5.
44. Lo, K.W., et al., *Analysis of cell-free Epstein-Barr virus associated RNA in the plasma of patients with nasopharyngeal carcinoma.* Clin Chem, 1999. **45**(8 Pt 1): p. 1292-4.
45. Shi, J., et al., *Circulating lncRNAs associated with occurrence of colorectal cancer progression.* Am J Cancer Res, 2015. **5**(7): p. 2258-65.
46. Yuan, T., et al., *Plasma extracellular RNA profiles in healthy and cancer patients.* Sci Rep, 2016. **6**: p. 19413.
47. Etheridge, A., et al., *Extracellular microRNA: a new source of biomarkers.* Mutat Res, 2011. **717**(1-2): p. 85-90.
48. Chim, S.S., et al., *Detection and characterization of placental microRNAs in maternal plasma.* Clin Chem, 2008. **54**(3): p. 482-90.
49. Cui, L., et al., *Detection of circulating tumor cells in peripheral blood from patients with gastric cancer using piRNAs as markers.* Clin Biochem, 2011. **44**(13): p. 1050-7.
50. Yang, X., et al., *Detection of stably expressed piRNAs in human blood.* Int J Clin Exp Med, 2015. **8**(8): p. 13353-8.
51. Freedman, J.E., et al., *Diverse human extracellular RNAs are widely detected in human plasma.* Nature Communications, 2016. **7**.

52. Unger, L., et al., *Optimized methods for extracting circulating small RNAs from long-term stored equine samples.* Acta Vet Scand, 2016. **58**(1): p. 44.
53. Bononi, I., et al., *Circulating microRNAs found dysregulated in ex-exposed asbestos workers and pleural mesothelioma patients as potential new biomarkers.* Oncotarget, 2016.
54. Park, N.J., et al., *Salivary microRNA: discovery, characterization, and clinical utility for oral cancer detection.* Clin Cancer Res, 2009. **15**(17): p. 5473-7.
55. Weber, J.A., et al., *The microRNA spectrum in 12 body fluids.* Clin Chem, 2010. **56**(11): p. 1733-41.
56. Zubakov, D., et al., *MicroRNA markers for forensic body fluid identification obtained from microarray screening and quantitative RT-PCR confirmation.* Int J Legal Med, 2010. **124**(3): p. 217-26.
57. Xie, Z.J., et al., *Salivary MicroRNAs as Promising Biomarkers for Detection of Esophageal Cancer.* Plos One, 2013. **8**(4).
58. Correa-Gallego, C., et al., *Circulating Plasma Levels of MicroRNA-21 and MicroRNA-221 Are Potential Diagnostic Markers for Primary Intrahepatic Cholangiocarcinoma.* PLoS One, 2016. **11**(9): p. e0163699.
59. Mayeux, R., *Biomarkers: potential uses and limitations.* NeuroRx, 2004. **1**(2): p. 182-8.
60. Debey-Pascher, S., et al., *Blood-based miRNA preparation for noninvasive biomarker development.* Methods Mol Biol, 2012. **822**: p. 307-38.
61. Farina, N.H., et al., *Standardizing analysis of circulating microRNA: clinical and biological relevance.* J Cell Biochem, 2014. **115**(5): p. 805-11.
62. Komabayashi, Y., et al., *Circulating Epstein-Barr virus-encoded micro-RNAs as potential biomarkers for nasal natural killer/T-cell lymphoma.* Hematol Oncol, 2016.
63. Zheng, J. and J. Li, *Serum miRNA-203 expression, a potential biomarker for recurrence and prognosis in papillary thyroid carcinoma.* Cancer Biomark, 2016.
64. Zhou, X., et al., *A panel of 13-miRNA signature as a potential biomarker for predicting survival in pancreatic cancer.* Oncotarget, 2016.
65. Liang, S., et al., *Increased Serum Level of MicroRNA-663 Is Correlated with Poor Prognosis of Patients with Nasopharyngeal Carcinoma.* Dis Markers, 2016. **2016**: p. 7648215.
66. Ren, C., et al., *High expression of miR-16 and miR-451 predicating better prognosis in patients with gastric cancer.* J Cancer Res Clin Oncol, 2016.

67. Zhang, B., et al., *miR-489 acts as a tumor suppressor in human gastric cancer by targeting PROX1.* Am J Cancer Res, 2016. **6**(9): p. 2021-2030.
68. Yan, L.H., et al., *miR-135a promotes gastric cancer progression and resistance to oxaliplatin.* Oncotarget, 2016.
69. Song, D.K., Y.A. Sung, and H. Lee, *The Role of Serum MicroRNA-6767-5p as a Biomarker for the Diagnosis of Polycystic Ovary Syndrome.* PLoS One, 2016. **11**(9): p. e0163756.
70. Nallar, S.C. and D.V. Kalvakolanu, *Regulation of snoRNAs in cancer: close encounters with interferon.* J Interferon Cytokine Res, 2013. **33**(4): p. 189-98.
71. Freedman, J.E., et al., *Diverse human extracellular RNAs are widely detected in human plasma (vol 7, 11106, 2016).* Nature Communications, 2016. **7**.
72. Chu, H., et al., *Identification of novel piRNAs in bladder cancer.* Cancer Lett, 2015. **356**(2 Pt B): p. 561-7.
73. Ng, K.W., et al., *Piwi-interacting RNAs in cancer: emerging functions and clinical utility.* Mol Cancer, 2016. **15**: p. 5.
74. Li, Y., et al., *Piwi-Interacting RNAs (piRNAs) Are Dysregulated in Renal Cell Carcinoma and Associated with Tumor Metastasis and Cancer-Specific Survival.* Mol Med, 2015. **21**: p. 381-8.
75. Macfarlane, L.A. and P.R. Murphy, *MicroRNA: Biogenesis, Function and Role in Cancer.* Curr Genomics, 2010. **11**(7): p. 537-61.
76. Assumpcao, C.B., et al., *The role of piRNA and its potential clinical implications in cancer.* Epigenomics, 2015. **7**(6): p. 975-84.
77. Weick, E.M. and E.A. Miska, *piRNAs: from biogenesis to function.* Development, 2014. **141**(18): p. 3458-3471.
78. Brase, J.C., et al., *Circulating miRNAs are correlated with tumor progression in prostate cancer.* Int J Cancer, 2011. **128**(3): p. 608-16.
79. Ng, E.K.O., et al., *Differential expression of microRNAs in plasma of patients with colorectal cancer: a potential marker for colorectal cancer screening.* Gut, 2009. **58**(10): p. 1375-1381.
80. Wulfken, L.M., et al., *MicroRNAs in Renal Cell Carcinoma: Diagnostic Implications of Serum miR-1233 Levels.* Plos One, 2011. **6**(9).
81. Fritz, J.V., et al., *Sources and Functions of Extracellular Small RNAs in Human Circulation.* Annual Review of Nutrition, Vol 36, 2016. **36**: p. 301-336.
82. Singh, R., et al., *Circulating microRNAs in cancer: Hope or hype?* Cancer Lett, 2016. **381**(1): p. 113-21.

83. Pigati, L., et al., *Selective release of microRNA species from normal and malignant mammary epithelial cells.* PLoS One, 2010. **5**(10): p. e13515.
84. Witwer, K.W., *Circulating microRNA biomarker studies: pitfalls and potential solutions.* Clin Chem, 2015. **61**(1): p. 56-63.
85. Duttagupta, R., et al., *Impact of cellular miRNAs on circulating miRNA biomarker signatures.* PLoS One, 2011. **6**(6): p. e20769.
86. Pritchard, C.C., et al., *Blood cell origin of circulating microRNAs: a cautionary note for cancer biomarker studies.* Cancer Prev Res (Phila), 2012. **5**(3): p. 492-7.
87. Thery, C., M. Ostrowski, and E. Segura, *Membrane vesicles as conveyors of immune responses.* Nature Reviews Immunology, 2009. **9**(8): p. 581-593.
88. Taylor, D.D. and C. Gercel-Taylor, *The origin, function, and diagnostic potential of RNA within extracellular vesicles present in human biological fluids.* Front Genet, 2013. **4**: p. 142.
89. Yáñez-Mó, M., et al., *Biological properties of extracellular vesicles and their physiological functions.* J Extracell Vesicles, 2015. **4**: p. 27066.
90. Valadi, H., et al., *Exosome-mediated transfer of mRNAs and microRNAs is a novel mechanism of genetic exchange between cells.* Nature Cell Biology, 2007. **9**(6): p. 654-U72.
91. Lima, L.G., et al., *Tumor-derived microvesicles modulate the establishment of metastatic melanoma in a phosphatidylserine-dependent manner.* Cancer Lett, 2009. **283**(2): p. 168-75.
92. Gurung, S., et al., *The exosome journey: from biogenesis to uptake and intracellular signalling.* Cell Commun Signal, 2021. **19**(1): p. 47.
93. Gyorgy, B., et al., *Membrane vesicles, current state-of-the-art: emerging role of extracellular vesicles.* Cell Mol Life Sci, 2011. **68**(16): p. 2667-88.
94. Janas, T., et al., *Mechanisms of RNA loading into exosomes.* Febs Letters, 2015. **589**(13): p. 1391-1398.
95. Fabbri, M., et al., *MicroRNAs bind to Toll-like receptors to induce prometastatic inflammatory response.* Proc Natl Acad Sci U S A, 2012. **109**(31): p. E2110-6.
96. Groot, M. and H. Lee, *Sorting Mechanisms for MicroRNAs into Extracellular Vesicles and Their Associated Diseases.* Cells, 2020. **9**(4).
97. Liu, C.M., et al., *Exosomes from the tumor microenvironment as reciprocal regulators that enhance prostate cancer progression.* Int J Urol, 2016. **23**(9): p. 734-44.
98. Jahagirdar, D., et al., *Export of microRNAs: A Bridge between Breast Carcinoma and Their Neighboring Cells.* Front Oncol, 2016. **6**: p. 147.

99. Taverna, S., et al., *Exosomes isolation and characterization in serum is feasible in non-small cell lung cancer patients: critical analysis of evidence and potential role in clinical practice.* Oncotarget, 2016. **7**(19): p. 28748-28760.
100. Khalyfa, A., et al., *Extracellular microvesicle microRNAs in children with sickle cell anaemia with divergent clinical phenotypes.* Br J Haematol, 2016. **174**(5): p. 786-98.
101. Kumar, S. and P.H. Reddy, *Are circulating microRNAs peripheral biomarkers for Alzheimer's disease?* Biochim Biophys Acta, 2016. **1862**(9): p. 1617-27.
102. Turchinovich, A., et al., *Characterization of extracellular circulating microRNA.* Nucleic Acids Research, 2011. **39**(16): p. 7223-7233.
103. Khalyfa, A. and D. Gozal, *Exosomal miRNAs as potential biomarkers of cardiovascular risk in children.* Journal of Translational Medicine, 2014. **12**.
104. Wang, K., et al., *Export of microRNAs and microRNA-protective protein by mammalian cells.* Nucleic Acids Research, 2010. **38**(20): p. 7248-7259.
105. Vickers, K.C. and A.T. Remaley, *Lipid-based carriers of microRNAs and intercellular communication.* Current Opinion in Lipidology, 2012. **23**(2): p. 91-97.
106. Wagner, J., et al., *Characterization of Levels and Cellular Transfer of Circulating Lipoprotein-Bound MicroRNAs.* Arteriosclerosis Thrombosis and Vascular Biology, 2013. **33**(6): p. 1392-+.
107. Desgagne, V., et al., *Variations in HDL-carried miR-223 and miR-135a concentrations after consumption of dietary trans fat are associated with changes in blood lipid and inflammatory markers in healthy men - an exploratory study.* Epigenetics, 2016. **11**(6): p. 438-48.
108. Assumpcao, C.B., et al., *The role of piRNA and its potential clinical implications in cancer.* Epigenomics, 2015. **7**(6): p. 975-984.
109. Wang, K., et al., *The Complex Exogenous RNA Spectra in Human Plasma: An Interface with Human Gut Biota?* Plos One, 2012. **7**(12).
110. Wang, K., et al., *The Spectrum of Circulating RNA: A Window into Systems Toxicology.* Toxicological Sciences, 2013. **132**(2): p. 478-492.
111. Zhang, L., et al., *Exogenous plant MIR168a specifically targets mammalian LDLRAP1: evidence of cross-kingdom regulation by microRNA.* Cell Res, 2012. **22**(1): p. 107-26.
112. Pastrello, C., et al., *Circulating plant miRNAs can regulate human gene expression in vitro.* Scientific Reports, 2016. **6**.

113. Zhang, H., et al., *Role of plant MicroRNA in cross-species regulatory networks of humans.* Bmc Systems Biology, 2016. **10**.
114. Pirro, S., et al., *MicroRNA from Moringa oleifera: Identification by High Throughput Sequencing and Their Potential Contribution to Plant Medicinal Value.* Plos One, 2016. **11**(3).
115. Chin, A.R., et al., *Cross-kingdom inhibition of breast cancer growth by plant miR159.* Cell Research, 2016. **26**(2): p. 217-228.
116. Mico, V., et al., *Unsuccessful Detection of Plant MicroRNAs in Beer, Extra Virgin Olive Oil and Human Plasma After an Acute Ingestion of Extra Virgin Olive Oil.* Plant Foods for Human Nutrition, 2016. **71**(1): p. 102-108.
117. Bagci, C. and J. Allmer, *One Step Forward, Two Steps Back; Xeno-MicroRNAs Reported in Breast Milk Are Artifacts.* Plos One, 2016. **11**(1).
118. Fu, Q., et al., *An oncogenic role of miR-592 in tumorigenesis of human colorectal cancer by targeting Forkhead Box O3A (FoxO3A).* Expert Opin Ther Targets, 2016. **20**(7): p. 771-82.
119. Shen, Z.L., et al., *Downregulation of miR-199b is associated with distant metastasis in colorectal cancer via activation of SIRT1 and inhibition of CREB/KISS1 signaling.* Oncotarget, 2016. **7**(23): p. 35092-105.
120. Sun, S.F., et al., *MicroRNA-544a Regulates Migration and Invasion in Colorectal Cancer Cells via Regulation of Homeobox A10.* Digestive Diseases and Sciences, 2016. **61**(9): p. 2535-2544.
121. Wu, K., L. Ma, and J. Zhu, *miR4835p promotes growth, invasion and selfrenewal of gastric cancer stem cells by Wnt/betacatenin signaling.* Mol Med Rep, 2016. **14**(4): p. 3421-8.
122. Xu, K. and Y.C. Zhao, *MEF2D/Wnt/beta-catenin pathway regulates the proliferation of gastric cancer cells and is regulated by microRNA-19.* Tumor Biology, 2016. **37**(7): p. 9059-9069.
123. Xie, M., et al., *Insights into roles of the miR-1,-133 and-206 family in gastric cancer (Review).* Oncology Reports, 2016. **36**(3): p. 1191-1198.
124. Zheng, L., et al., *miRNA-558 promotes gastric cancer progression through attenuating Smad4-mediated repression of heparanase expression.* Cell Death Dis, 2016. **7**(9): p. e2382.
125. Zhou, Q., et al., *Smad2/3/4 Pathway Contributes to TGF-beta-Induced MiRNA-181b Expression to Promote Gastric Cancer Metastasis by Targeting Timp3.* Cell Physiol Biochem, 2016. **39**(2): p. 453-66.

126. Tang, B., et al., *MicroRNA-155-3p promotes hepatocellular carcinoma formation by suppressing FBXW7 expression.* Journal of Experimental & Clinical Cancer Research, 2016. **35**.
127. Zhao, G., et al., *MicroRNA-548a-5p promotes proliferation and inhibits apoptosis in hepatocellular carcinoma cells by targeting Tg737.* World Journal of Gastroenterology, 2016. **22**(23): p. 5364-5373.
128. Kang, J., et al., *TFAP2C promotes lung tumorigenesis and aggressiveness through miR-183- and miR-33a-mediated cell cycle regulation.* Oncogene, 2016.
129. Zhu, D.Y., et al., *MiR-454 promotes the progression of human non-small cell lung cancer and directly targets PTEN.* Biomedicine & Pharmacotherapy, 2016. **81**: p. 79-85.
130. Li, G., et al., *The microRNA-182-PDK4 axis regulates lung tumorigenesis by modulating pyruvate dehydrogenase and lipogenesis.* Oncogene, 2016.
131. Xiao, P., W. Liu, and H. Zhou, *miR-429 promotes the proliferation of non-small cell lung cancer cells via targeting DLC-1.* Oncol Lett, 2016. **12**(3): p. 2163-2168.
132. Chen, Y.F., et al., *MicroRNA-211 Enhances the Oncogenicity of Carcinogen-Induced Oral Carcinoma by Repressing TCF12 and Increasing Antioxidant Activity.* Cancer Res, 2016. **76**(16): p. 4872-86.
133. Cheng, Y., et al., *MiR-200c promotes bladder cancer cell migration and invasion by directly targeting RECK.* Onco Targets Ther, 2016. **9**: p. 5091-9.
134. Liang, T., et al., *MicroRNA-194 promotes the growth, migration, and invasion of ovarian carcinoma cells by targeting protein tyrosine phosphatase nonreceptor type 12.* Onco Targets Ther, 2016. **9**: p. 4307-15.
135. Xiaohong, Z., et al., *MiR-203 promotes the growth and migration of ovarian cancer cells by enhancing glycolytic pathway.* Tumour Biol, 2016.
136. Wang, B., J. Yang, and B. Xiao, *MicroRNA-20b (miR-20b) Promotes the Proliferation, Migration, Invasion, and Tumorigenicity in Esophageal Cancer Cells via the Regulation of Phosphatase and Tensin Homologue Expression.* PLoS One, 2016. **11**(10): p. e0164105.
137. Cheng, J., et al., *piRNA, the new non-coding RNA, is aberrantly expressed in human cancer cells.* Clin Chim Acta, 2011. **412**(17-18): p. 1621-5.
138. Yan, H., et al., *piRNA-823 contributes to tumorigenesis by regulating de novo DNA methylation and angiogenesis in multiple myeloma.* Leukemia, 2015. **29**(1): p. 196-206.

139. Nallar, S.C. and D.V. Kalvakolanu, *Regulation of snoRNAs in Cancer: Close Encounters with Interferon.* Journal of Interferon and Cytokine Research, 2013. **33**(4): p. 189-198.
140. Siprashvili, Z., et al., *The noncoding RNAs SNORD50A and SNORD50B bind K-Ras and are recurrently deleted in human cancer.* Nat Genet, 2016. **48**(1): p. 53-8.
141. Liao, J., et al., *Small nucleolar RNA signatures as biomarkers for non-small-cell lung cancer.* Mol Cancer, 2010. **9**: p. 198.
142. Mei, Y.P., et al., *Small nucleolar RNA 42 acts as an oncogene in lung tumorigenesis.* Oncogene, 2012. **31**(22): p. 2794-2804.
143. Okugawa, Y., et al., *Clinical significance of SNORA42 as an oncogene and a prognostic biomarker in colorectal cancer.* Gut, 2017. **66**(1): p. 107-117.
144. Ma, P., et al., *Up-regulation of small nucleolar RNA 78 is correlated with aggressive phenotype and poor prognosis of hepatocellular carcinoma.* Tumour Biol, 2016.
145. Dong, X.Y., et al., *Implication of snoRNA U50 in human breast cancer.* J Genet Genomics, 2009. **36**(8): p. 447-54.
146. Cheng, Z., et al., *Gene expression profiling reveals U1 snRNA regulates cancer gene expression.* Oncotarget, 2017. **8**(68): p. 112867-112874.
147. Kohler, J., et al., *Circulating U2 small nuclear RNA fragments as a diagnostic and prognostic biomarker in lung cancer patients.* Journal of Cancer Research and Clinical Oncology, 2016. **142**(4): p. 795-805.
148. Kano, M., et al., *miR-145, miR-133a and miR-133b: tumor-suppressive miRNAs target FSCN1 in esophageal squamous cell carcinoma.* International Journal of Cancer, 2010. **127**(12): p. 2804-2814.
149. Xiao, B., et al., *Expression of microRNA-133 inhibits epithelial-mesenchymal transition in lung cancer cells by directly targeting FOXQ1.* Arch Bronconeumol, 2016. **52**(10): p. 505-11.
150. Jiang, X.K., et al., *GATA3-driven expression of miR-503 inhibits prostate cancer progression by repressing ZNF217 expression.* Cellular Signalling, 2016. **28**(9): p. 1216-1224.
151. Hua, K.Y., et al., *MicroRNA-7 inhibits proliferation, migration and invasion of thyroid papillary cancer-cells via targeting CKS2.* International Journal of Oncology, 2016. **49**(4): p. 1531-1540.
152. Zhou, W., et al., *MicroRNA-98 acts as a tumor suppressor in hepatocellular carcinoma via targeting SALL4.* Oncotarget, 2016.

153. Yang, Z.Q., et al., *MicroRNA-143 targets CD44 to inhibit breast cancer progression and stem cell-like properties.* Molecular Medicine Reports, 2016. **13**(6): p. 5193-5199.
154. Chang, W., et al., *MiR-377 inhibits the proliferation of pancreatic cancer by targeting Pim-3.* Tumour Biol, 2016.
155. Shin, S.S., et al., *MicroRNA-106a suppresses proliferation, migration, and invasion of bladder cancer cells by modulating MAPK signaling, cell cycle regulators, and Ets-1-mediated MMP-2 expression.* Oncol Rep, 2016. **36**(4): p. 2421-9.
156. Qian, K., et al., *MicroRNA-561 inhibits gastric cancercell proliferation and invasion by downregulating c-Myc expression.* Am J Transl Res, 2016. **8**(9): p. 3802-3811.
157. Chen, W., et al., *MicroRNA-155 promotes apoptosis in SKOV3, A2780, and primary cultured ovarian cancer cells.* Tumour Biol, 2016. **37**(7): p. 9289-99.
158. Xi, Y., et al., *The novel miR-9501 inhibits cell proliferation, migration and activates apoptosis in non-small cell lung cancer.* Med Oncol, 2016. **33**(11): p. 124.
159. An, H.J., et al., *Novel miR-5582-5p functions as a tumor suppressor by inducing apoptosis and cell cycle arrest in cancer cells through direct targeting of GAB1, SHC1, and CDK2.* Biochimica Et Biophysica Acta-Molecular Basis of Disease, 2016. **1862**(10): p. 1926-1937.
160. Cheng, J., et al., *piR-823, a novel non-coding small RNA, demonstrates in vitro and in vivo tumor suppressive activity in human gastric cancer cells.* Cancer Lett, 2012. **315**(1): p. 12-7.
161. Hashim, A., et al., *RNA sequencing identifies specific PIWI-interacting small non-coding RNA expression patterns in breast cancer.* Oncotarget, 2014. **5**(20): p. 9901-10.
162. Peng, L., et al., *piR-55490 inhibits the growth of lung carcinoma by suppressing mTOR signaling.* Tumour Biol, 2016. **37**(2): p. 2749-56.
163. Dong, X.Y., et al., *SnoRNA U50 is a candidate tumor suppressor gene at 6q14.3 with a mutation associated with clinically significant prostate cancer.* Hum Mol Genet, 2008. **17**(7): p. 1031-42.
164. Chen, L., et al., *SNORD76, a box C/D snoRNA, acts as a tumor suppressor in glioblastoma.* Sci Rep, 2015. **5**: p. 8588.
165. Su, H., et al., *Elevated snoRNA biogenesis is essential in breast cancer.* Oncogene, 2014. **33**(11): p. 1348-58.

166. Langhendries, J.L., et al., *The human box C/D snoRNAs U3 and U8 are required for pre-rRNA processing and tumorigenesis.* Oncotarget, 2016.
167. Spraggon, L. and L. Cartegni, *U1 snRNP-Dependent Suppression of Polyadenylation: Physiological Role and Therapeutic Opportunities in Cancer.* Int J Cell Biol, 2013. **2013**: p. 846510.
168. Zhao, L., et al., *MiRNA-221-3p desensitizes pancreatic cancer cells to 5-fluorouracil by targeting RB1.* Tumour Biol, 2016.
169. Zhu, M., et al., *miR-20a induces cisplatin resistance of a human gastric cancer cell line via targeting CYLD.* Mol Med Rep, 2016. **14**(2): p. 1742-50.
170. Wu, L., et al., *miR-96 induces cisplatin chemoresistance in non-small cell lung cancer cells by downregulating SAMD9.* Oncol Lett, 2016. **11**(2): p. 945-952.
171. Zhou, N., et al., *Upregulation of microRNA-375 increases the cisplatin-sensitivity of human gastric cancer cells by regulating ERBB2.* Exp Ther Med, 2016. **11**(2): p. 625-630.
172. Wang, L.L., et al., *MiR-30a increases cisplatin sensitivity of gastric cancer cells through suppressing epithelial-to-mesenchymal transition (EMT).* Eur Rev Med Pharmacol Sci, 2016. **20**(9): p. 1733-9.
173. Zhao, H., et al., *MiR-770-5p inhibits cisplatin chemoresistance in human ovarian cancer by targeting ERCC2.* Oncotarget, 2016.
174. Xue, J., et al., *MiRNA-621 sensitizes breast cancer to chemotherapy by suppressing FBXO11 and enhancing p53 activity.* Oncogene, 2016. **35**(4): p. 448-58.
175. Tang, Y., et al., *Radiation-induced miR-208a increases the proliferation and radioresistance by targeting p21 in human lung cancer cells.* J Exp Clin Cancer Res, 2016. **35**: p. 7.
176. Ma, W., et al., *Up- regulation of miR-328-3p sensitizes non-small cell lung cancer to radiotherapy.* Sci Rep, 2016. **6**: p. 31651.
177. Ma, W., et al., *Examining the effect of gene reduction in miR-95 and enhanced radiosensitivity in non-small cell lung cancer.* Cancer Gene Ther, 2016. **23**(2-3): p. 66-71.
178. Egeli, U., et al., *miR-216b Targets FGFR1 and Confers Sensitivity to Radiotherapy in Pancreatic Ductal Adenocarcinoma Patients Without EGFR or KRAS Mutation.* Pancreas, 2016. **45**(9): p. 1294-302.
179. Chu, L., et al., *Multiple myeloma-associated chromosomal translocation activates orphan snoRNA ACA11 to suppress oxidative stress.* J Clin Invest, 2012. **122**(8): p. 2793-806.

180. Wang, Y.Y., et al., *A piRNA-like Small RNA Induces Chemoresistance to Cisplatin-Based Therapy by Inhibiting Apoptosis in Lung Squamous Cell Carcinoma.* Molecular Therapy-Nucleic Acids, 2017. **6**: p. 269-278.
181. Kuhlmann, J.D., et al., *Circulating U2 Small Nuclear RNA Fragments as a Novel Diagnostic Tool for Patients with Epithelial Ovarian Cancer.* Clinical Chemistry, 2014. **60**(1): p. 206-213.
182. van Soest, E.M., et al., *Increasing incidence of Barrett's oesophagus in the general population.* Gut, 2005. **54**(8): p. 1062-1066.
183. Zhang, C.N., et al., *Expression Profile of MicroRNAs in Serum: A Fingerprint for Esophageal Squamous Cell Carcinoma.* Clinical Chemistry, 2010. **56**(12): p. 1871-1879.
184. Kang, M., et al., *miR-129-2 suppresses proliferation and migration of esophageal carcinoma cells through downregulation of SOX4 expression.* Int J Mol Med, 2013. **32**(1): p. 51-8.
185. Chen, X., et al., *CpG island methylation status of miRNAs in esophageal squamous cell carcinoma.* Int J Cancer, 2012. **130**(7): p. 1607-13.
186. Ogawa, R., et al., *Expression profiling of micro-RNAs in human esophageal squamous cell carcinoma using RT-PCR.* Med Mol Morphol, 2009. **42**(2): p. 102-9.
187. Dharmawardana, N., et al., *Circulating microRNAs in head and neck cancer: a scoping review of methods.* Clin Exp Metastasis, 2019. **36**(3): p. 291-302.
188. Zhang, K., et al., *Circulating miRNA profile in esophageal adenocarcinoma.* Am J Cancer Res, 2016. **6**(11): p. 2713-2721.
189. Bus, P., et al., *Profiling of circulating microRNAs in patients with Barrett's esophagus and esophageal adenocarcinoma.* Journal of Gastroenterology, 2016. **51**(6): p. 560-570.
190. Chiam, K., et al., *Circulating Serum Exosomal miRNAs As Potential Biomarkers for Esophageal Adenocarcinoma.* Journal of Gastrointestinal Surgery, 2015. **19**(7): p. 1208-1215.
191. Zhang, T.F., et al., *The oncogenetic role of microRNA-31 as a potential biomarker in oesophageal squamous cell carcinoma.* Clinical Science, 2011. **121**(9-10): p. 437-447.
192. Hirajima, S., et al., *Clinical impact of circulating miR-18a in plasma of patients with oesophageal squamous cell carcinoma.* Br J Cancer, 2013. **108**(9): p. 1822-9.
193. Wu, C.Y., et al., *Diagnostic and Prognostic Implications of a Serum miRNA Panel in Oesophageal Squamous Cell Carcinoma.* Plos One, 2014. **9**(3).

194. Komatsu, S., et al., *Plasma microRNA profiles: identification of miR-25 as a novel diagnostic and monitoring biomarker in oesophageal squamous cell carcinoma.* British Journal of Cancer, 2014. **111**(8): p. 1614-1624.
195. Wang, C., et al., *Prognostic and diagnostic potential of miR-146a in oesophageal squamous cell carcinoma.* British Journal of Cancer, 2016. **114**(3): p. 290-297.
196. Sun, L., et al., *Predictive value of plasma miRNA-718 for esophageal squamous cell carcinoma.* Cancer Biomarkers, 2016. **16**(2): p. 265-273.
197. Xu, H., et al., *Predictive Value of Serum miR-10b, miR-29c, and miR-205 as Promising Biomarkers in Esophageal Squamous Cell Carcinoma Screening.* Medicine, 2015. **94**(44).
198. Lv, H.B., et al., *Differential expression of miR-21 and miR-75 in esophageal carcinoma patients and its clinical implication.* American Journal of Translational Research, 2016. **8**(7): p. 3288-3298.
199. Komatsu, S., et al., *Circulating microRNAs in plasma of patients with oesophageal squamous cell carcinoma.* Br J Cancer, 2011. **105**(1): p. 104-11.
200. Li, B.X., et al., *Circulating microRNAs in esophageal squamous cell carcinoma: association with locoregional staging and survival.* International Journal of Clinical and Experimental Medicine, 2015. **8**(5): p. 7241-7250.
201. Jiang, Z.J., et al., *Serum microRNA-218 is a potential biomarker for esophageal cancer.* Cancer Biomarkers, 2015. **15**(4): p. 381-389.
202. Hui, B.N., et al., *Serum miRNA expression in patients with esophageal squamous cell carcinoma.* Oncology Letters, 2015. **10**(5): p. 3008-3012.
203. Zhang, T.F., et al., *MicroRNA-1322 Regulates ECRG2 Allele Specifically and Acts as a Potential Biomarker in Patients With Esophageal Squamous Cell Carcinoma.* Molecular Carcinogenesis, 2013. **52**(8): p. 581-590.
204. Sharma, P., et al., *Decreased levels of circulating and tissue miR-107 in human esophageal cancer.* Biomarkers, 2013. **18**(4): p. 322-330.
205. Li, S.P., et al., *Plasma miRNA-506 as a Prognostic Biomarker for Esophageal Squamous Cell Carcinoma.* Medical Science Monitor, 2016. **22**: p. 2195-2201.
206. Takeshita, N., et al., *Serum microRNA expression profile: miR-1246 as a novel diagnostic and prognostic biomarker for oesophageal squamous cell carcinoma.* British Journal of Cancer, 2013. **108**(3): p. 644-652.

207. Dong, W., et al., *Diagnostic and predictive significance of serum microRNA-7 in esophageal squamous cell carcinoma.* Oncol Rep, 2016. **35**(3): p. 1449-56.
208. Liu, R., et al., *Circulating miR-155 expression in plasma: a potential biomarker for early diagnosis of esophageal cancer in humans.* J Toxicol Environ Health A, 2012. **75**(18): p. 1154-62.
209. Cai, E.H., et al., *Serum miR-21 expression in human esophageal squamous cell carcinomas.* Asian Pac J Cancer Prev, 2012. **13**(4): p. 1563-7.
210. Wang, B. and Q. Zhang, *The expression and clinical significance of circulating microRNA-21 in serum of five solid tumors.* J Cancer Res Clin Oncol, 2012. **138**(10): p. 1659-66.
211. Kurashige, J., et al., *Serum microRNA-21 is a novel biomarker in patients with esophageal squamous cell carcinoma.* J Surg Oncol, 2012. **106**(2): p. 188-92.
212. Warnecke-Eberz, U., et al., *Exosomal onco-miRs from serum of patients with adenocarcinoma of the esophagus: comparison of miRNA profiles of exosomes and matching tumor.* Tumour Biol, 2015. **36**(6): p. 4643-53.
213. Dong, S., et al., *Predictive Value of Plasma MicroRNA-216a/b in the Diagnosis of Esophageal Squamous Cell Carcinoma.* Dis Markers, 2016. **2016**: p. 1857067.
214. Guan, S., et al., *MiR-613: a novel diagnostic and prognostic biomarker for patients with esophageal squamous cell carcinoma.* Tumour Biol, 2016. **37**(4): p. 4383-91.
215. Liu, W., et al., *MicroRNA-373 promotes migration and invasion in human esophageal squamous cell carcinoma by inhibiting TIMP3 expression.* Am J Cancer Res, 2016. **6**(1): p. 1-14.
216. Sharma, P., A. Saraya, and R. Sharma, *Potential diagnostic implications of miR-144 overexpression in human oesophageal cancer.* Indian J Med Res, 2016. **143**(Supplement): p. S91-s103.
217. Wang, C., et al., *Serum miR-1297: a promising diagnostic biomarker in esophageal squamous cell carcinoma.* Biomarkers, 2016. **21**(6): p. 517-22.
218. Cui, Y., et al., *Plasma microRNA-9 as a diagnostic and prognostic biomarker in patients with esophageal squamous cell carcinoma.* J Int Med Res, 2017: p. 300060517709370.
219. Fassan, M., et al., *Early miR-223 Upregulation in Gastroesophageal Carcinogenesis.* Am J Clin Pathol, 2017. **147**(3): p. 301-308.

220. Huang, Z., et al., *A novel serum microRNA signature to screen esophageal squamous cell carcinoma.* Cancer Med, 2017. **6**(1): p. 109-119.
221. Li, B., et al., *MicroRNA-377 suppresses initiation and progression of esophageal cancer by inhibiting CD133 and VEGF.* Oncogene, 2017. **36**(28): p. 3986-4000.
222. Li, J., et al., *Serum microRNA-15a level acts as a potential diagnostic and prognostic biomarker for human esophageal squamous cell carcinoma.* Cancer Biomark, 2017. **18**(1): p. 11-17.
223. Zhou, X., et al., *A six-microRNA signature in plasma was identified as a potential biomarker in diagnosis of esophageal squamous cell carcinoma.* Oncotarget, 2017. **8**(21): p. 34468-34480.
224. Sun, J.T., et al., *MicroRNA-367 is a potential diagnostic biomarker for patients with esophageal squamous cell carcinoma.* Biochemical and Biophysical Research Communications, 2016. **473**(2): p. 363-369.
225. Liu, K., et al., *Down-Regulation of MiR-1294 is Related to Dismal Prognosis of Patients with Esophageal Squamous Cell Carcinoma through Elevating C-MYC Expression.* Cellular Physiology and Biochemistry, 2015. **36**(1): p. 100-110.
226. Song, Y., et al., *MicroRNA-9 promotes tumor metastasis via repressing E-cadherin in esophageal squamous cell carcinoma.* Oncotarget, 2014. **5**(22): p. 11669-11680.
227. Li, W.L., et al., *Down-Regulation of miR-140 Induces EMT and Promotes Invasion by Targeting Slug in Esophageal Cancer.* Cellular Physiology and Biochemistry, 2014. **34**(5): p. 1466-1476.
228. Sun, N.N., et al., *microRNA-195-Cdc42 axis acts as a prognostic factor of esophageal squamous cell carcinoma.* International Journal of Clinical and Experimental Pathology, 2014. **7**(10): p. 6871-6879.
229. Okumura, T., et al., *MicroRNA Profiles to Predict Postoperative Prognosis in Patients with Small Cell Carcinoma of the Esophagus.* Anticancer Research, 2015. **35**(2): p. 719-727.
230. Fu, C., et al., *The expression of miR-21 and miR-375 predict prognosis of esophageal cancer.* Biochem Biophys Res Commun, 2014. **446**(4): p. 1197-203.
231. Yu, Q., et al., *Plasma microRNAs to predict the response of radiotherapy in esophageal squamous cell carcinoma patients.* Am J Transl Res, 2015. **7**(10): p. 2060-71.
232. Odenthal, M., et al., *Serum microRNA profiles as prognostic/predictive markers in the multimodality therapy of locally advanced*

adenocarcinomas of the gastroesophageal junction. International Journal of Cancer, 2015. **137**(1): p. 230-237.
233. Tanaka, K., et al., *Circulating miR-200c levels significantly predict response to chemotherapy and prognosis of patients undergoing neoadjuvant chemotherapy for esophageal cancer.* Ann Surg Oncol, 2013. **20 Suppl 3**: p. S607-15.
234. Yu, H., et al., *Serum miR-200c and clinical outcome of patients with advanced esophageal squamous cancer receiving platinum-based chemotherapy.* Am J Transl Res, 2013. **6**(1): p. 71-7.
235. Holscher, A.H., et al., *Prognostic impact of neoadjuvant chemoradiation in cT3 oesophageal cancer - A propensity score matched analysis.* Eur J Cancer, 2014. **50**(17): p. 2950-7.
236. Ronellenfitsch, U., et al., *Perioperative chemo(radio)therapy versus primary surgery for resectable adenocarcinoma of the stomach, gastroesophageal junction, and lower esophagus.* Cochrane Database Syst Rev, 2013(5): p. CD008107.
237. Bollschweiler, E., et al., *Neoadjuvant treatment for advanced esophageal cancer: response assessment before surgery and how to predict response to chemoradiation before starting treatment.* Chinese Journal of Cancer Research, 2015. **27**(3): p. 221-230.
238. Bollschweiler, E., et al., *Histological type of esophageal cancer might affect response to neo-adjuvant radiochemotherapy and subsequent prognosis.* Annals of Oncology, 2009. **20**(2): p. 231-238.
239. Tanaka, K., et al., *miR-27 is associated with chemoresistance in esophageal cancer through transformation of normal fibroblasts to cancer-associated fibroblasts.* Carcinogenesis, 2015. **36**(8): p. 894-903.
240. Komatsu, S., et al., *Circulating miR-21 as an independent predictive biomarker for chemoresistance in esophageal squamous cell carcinoma.* Am J Cancer Res, 2016. **6**(7): p. 1511-23.
241. Qian, L., et al., *Piwi-Interacting RNAs: A New Class of Regulator in Human Breast Cancer.* Front Oncol, 2021. **11**: p. 695077.
242. Mai, D., et al., *PIWI-interacting RNA-54265 is oncogenic and a potential therapeutic target in colorectal adenocarcinoma.* Theranostics, 2018. **8**(19): p. 5213-5230.
243. Muz, B., et al., *The role of hypoxia in cancer progression, angiogenesis, metastasis, and resistance to therapy.* Hypoxia (Auckl), 2015. **3**: p. 83-92.

244. Cosse, J.P. and C. Michiels, *Tumour hypoxia affects the responsiveness of cancer cells to chemotherapy and promotes cancer progression.* Anticancer Agents Med Chem, 2008. **8**(7): p. 790-7.
245. Doktorova, H., et al., *Hypoxia-induced chemoresistance in cancer cells: The role of not only HIF-1.* Biomed Pap Med Fac Univ Palacky Olomouc Czech Repub, 2015. **159**(2): p. 166-77.
246. Jiang, S.M., et al., *MicroRNA-21 modulates radiation resistance through upregulation of hypoxia-inducible factor-1 alpha-promoted glycolysis in non-small cell lung cancer cells.* Molecular Medicine Reports, 2016. **13**(5): p. 4101-4107.
247. Roscigno, G., et al., *MiR-24 induces chemotherapy resistance and hypoxic advantage in breast cancer.* Oncotarget, 2017. **8**(12): p. 19507-19521.
248. Long, Y.C. and J.R. Zierath, *AMP-activated protein kinase signaling in metabolic regulation.* J Clin Invest, 2006. **116**(7): p. 1776-83.
249. Zhang, Y., G. Duan, and S. Feng, *MicroRNA-301a modulates doxorubicin resistance in osteosarcoma cells by targeting AMP-activated protein kinase alpha 1.* Biochem Biophys Res Commun, 2015. **459**(3): p. 367-73.
250. He, Q., et al., *LKB1 promotes radioresistance in esophageal cancer cells exposed to radiation, by suppression of apoptosis and activation of autophagy via the AMPK pathway.* Mol Med Rep, 2017.
251. Guo, R., et al., *MiR-451 Promotes Cell Proliferation and Metastasis in Pancreatic Cancer through Targeting CAB39.* Biomed Res Int, 2017. **2017**: p. 2381482.
252. Godlewski, J., et al., *MicroRNA-451 regulates LKB1/AMPK signaling and allows adaptation to metabolic stress in glioma cells.* Mol Cell, 2010. **37**(5): p. 620-32.
253. Zhang, S., et al., *Silencing protein kinase C ζ by microRNA-25-5p activates AMPK signaling and inhibits colorectal cancer cell proliferation.* Oncotarget, 2017. **8**(39): p. 65329-65338.
254. Nagashima, S., Y. Bao, and Y. Hata, *The Hippo Pathway as Drug Targets in Cancer Therapy and Regenerative Medicine.* Curr Drug Targets, 2017. **18**(4): p. 447-454.
255. Pfleger, C.M., *The Hippo Pathway: A Master Regulatory Network Important in Development and Dysregulated in Disease.* Curr Top Dev Biol, 2017. **123**: p. 181-228.
256. Wang, Y., A. Yu, and F.X. Yu, *The Hippo pathway in tissue homeostasis and regeneration.* Protein Cell, 2017.

257. Zhao, Y. and X. Yang, *The Hippo pathway in chemotherapeutic drug resistance.* Int J Cancer, 2015. **137**(12): p. 2767-73.
258. Ren, A., et al., *Down-regulation of mammalian sterile 20-like kinase 1 by heat shock protein 70 mediates cisplatin resistance in prostate cancer cells.* Cancer Res, 2008. **68**(7): p. 2266-74.
259. Lit, L.C., et al., *LATS2 Is a Modulator of Estrogen Receptor Alpha.* Anticancer Research, 2013. **33**(1): p. 53-63.
260. Xia, Y., et al., *YAP Promotes Ovarian Cancer Cell Tumorigenesis and Is Indicative of a Poor Prognosis for Ovarian Cancer Patients (vol 9, e91770, 2014).* Plos One, 2016. **11**(3).
261. Touil, Y., et al., *Colon cancer cells escape 5FU chemotherapy-induced cell death by entering stemness and quiescence associated with the c-Yes/YAP axis.* Clin Cancer Res, 2014. **20**(4): p. 837-46.
262. Lee, K.W., et al., *Activation of yap1 is significantly associated with poor prognosis and cetuximab resistance in colorectal cancer patients.* Cancer Research, 2014. **74**(19).
263. Cordenonsi, M., et al., *The Hippo transducer TAZ confers cancer stem cell-related traits on breast cancer cells.* Cell, 2011. **147**(4): p. 759-72.
264. Tsujiura, M., et al., *Yes-associated protein (YAP) modulates oncogenic features and radiation sensitivity in endometrial cancer.* PLoS One, 2014. **9**(6): p. e100974.
265. Ting Zhan, X.H., Xia Tian,Xiaoli Chen, YuDing, HeshengLuo, YadongZ hang, *Downregulation of MicroRNA-455-3p Links to Proliferation and Drug Resistance of Pancreatic Cancer Cells via Targeting TAZ.* Molecular Therapy-Nucleic Acids, 2018. **10**: p. 215-226.
266. Que, K., et al., *Downregulation of miR-874-3p promotes chemotherapeutic resistance in colorectal cancer via inactivation of the Hippo signaling pathway.* Oncology Reports, 2017. **38**(6): p. 3376-3386.
267. He, Y., et al., *MicroRNA-135b regulates apoptosis and chemoresistance in colorectal cancer by targeting large tumor suppressor kinase 2.* Am J Cancer Res, 2015. **5**(4): p. 1382-95.
268. Miao, Y., et al., *MicroRNA-130b targets PTEN to mediate drug resistance and proliferation of breast cancer cells via the PI3K/Akt signaling pathway.* Sci Rep, 2017. **7**: p. 41942.
269. Yang, S.M., et al., *miR-21 confers cisplatin resistance in gastric cancer cells by regulating PTEN.* Toxicology, 2013. **306**: p. 162-168.

270. Zheng, P., et al., *Exosomal transfer of tumor-associated macrophage-derived miR-21 confers cisplatin resistance in gastric cancer cells.* J Exp Clin Cancer Res, 2017. **36**(1): p. 53.
271. Zhou, X., et al., *Downregulation of miR-21 inhibits EGFR pathway and suppresses the growth of human glioblastoma cells independent of PTEN status.* Lab Invest, 2010. **90**(2): p. 144-55.
272. Tung, S.L., et al., *miRNA-34c-5p inhibits amphiregulin-induced ovarian cancer stemness and drug resistance via downregulation of the AREG-EGFR-ERK pathway.* Oncogenesis, 2017. **6**(5): p. e326.
273. Li, Y., et al., *MicroRNA-27a functions as a tumor suppressor in renal cell carcinoma by targeting epidermal growth factor receptor.* Oncol Lett, 2016. **11**(6): p. 4217-4223.
274. Zhen, Q., et al., *MicroRNA-200a Targets EGFR and c-Met to Inhibit Migration, Invasion, and Gefitinib Resistance in Non-Small Cell Lung Cancer.* Cytogenet Genome Res, 2015. **146**(1): p. 1-8.
275. Wang, L.K., et al., *MicroRNA-133a suppresses multiple oncogenic membrane receptors and cell invasion in non-small cell lung carcinoma.* PLoS One, 2014. **9**(5): p. e96765.
276. Chiyomaru, T., et al., *Dual regulation of receptor tyrosine kinase genes EGFR and c-Met by the tumor-suppressive microRNA-23b/27b cluster in bladder cancer.* Int J Oncol, 2015. **46**(2): p. 487-96.
277. Matsumura, S., et al., *Activation of estrogen receptor alpha by estradiol and cisplatin induces platinum-resistance in ovarian cancer cells.* Cancer Biol Ther, 2016: p. 0.
278. Cui, J., et al., *MiR-873 regulates ER alpha transcriptional activity and tamoxifen resistance via targeting CDK3 in breast cancer cells.* Oncogene, 2015. **34**(30): p. 3895-3907.
279. Luo, H.L., et al., *Expression of Estrogen Receptor Beta Predicts Oncologic Outcome of pT3 Upper Urinary Tract Urothelial Carcinoma Better Than Aggressive Pathological Features.* Sci Rep, 2016. **6**: p. 24263.
280. Pinton, G., et al., *Agonist activation of estrogen receptor beta (ERbeta) sensitizes malignant pleural mesothelioma cells to cisplatin cytotoxicity.* Mol Cancer, 2014. **13**: p. 227.
281. Wilk, A., et al., *Inhibition of ERbeta induces resistance to cisplatin by enhancing Rad51-mediated DNA repair in human medulloblastoma cell lines.* PLoS One, 2012. **7**(3): p. e33867.

282. Pandey, D.P. and D. Picard, *miR-22 Inhibits Estrogen Signaling by Directly Targeting the Estrogen Receptor alpha mRNA (vol 29, pg 3783, 2009).* Molecular and Cellular Biology, 2009. **29**(17): p. 4873-4873.
283. Adams, B.D., H. Furneaux, and B.A. White, *The micro-ribonucleic acid (miRNA) miR-206 targets the human estrogen receptor-alpha (ER alpha) and represses ER alpha messenger RNA and protein expression in breast cancer cell lines.* Molecular Endocrinology, 2007. **21**(5): p. 1132-1147.
284. Liu, B., et al., *Elevated MiR-222-3p promotes proliferation and invasion of endometrial carcinoma via targeting ERalpha.* PLoS One, 2014. **9**(1): p. e87563.
285. Eichelser, C., et al., *Increased serum levels of circulating exosomal microRNA-373 in receptor-negative breast cancer patients.* Oncotarget, 2014. **5**(20): p. 9650-9663.
286. Newie, I., et al., *The HER2-Encoded miR-4728-3p Regulates ESR1 through a Non-Canonical Internal Seed Interaction.* Plos One, 2014. **9**(5).
287. Jiang, A., et al., *miR-615-3p promotes the phagocytic capacity of splenic macrophages by targeting ligand-dependent nuclear receptor corepressor in cirrhosis-related portal hypertension.* Exp Biol Med (Maywood), 2011. **236**(6): p. 672-80.
288. Al-Nakhle, H., et al., *Estrogen Receptor beta 1 Expression Is Regulated by miR-92 in Breast Cancer.* Cancer Research, 2010. **70**(11): p. 4778-4784.
289. Newie, I., et al., *The HER2-encoded miR-4728-3p regulates ESR1 through a non-canonical internal seed interaction.* PLoS One, 2014. **9**(5): p. e97200.
290. Wang, Y., et al., *microRNA expression profiling in multidrug resistance of the 5Fuinduced SGC7901 human gastric cancer cell line.* Mol Med Rep, 2013. **7**(5): p. 1506-10.
291. Liu, J., et al., *CircRNA ITCH increases bortezomib sensitivity through regulating the miR-615-3p/PRKCD axis in multiple myeloma.* Life Sci, 2020. **262**: p. 118506.
292. Pan, R. and H. Zhou, *Exosomal Transfer of lncRNA H19 Promotes Erlotinib Resistance in Non-Small Cell Lung Cancer via miR-615-3p/ATG7 Axis.* Cancer Manag Res, 2020. **12**: p. 4283-4297.
293. Mukai, R., et al., *miR-615-3p expression level in bone marrow is associated with tumor recurrence in hepatocellular carcinoma.* Mol Clin Oncol, 2015. **3**(3): p. 487-494.
294. Zhuang, L.K., et al., *MicroRNA-92b promotes hepatocellular carcinoma progression by targeting Smad7 and is mediated by long non-coding RNA XIST.* Cell Death Dis, 2016. **7**: p. e2203.

295. Poel, D., et al., *A specific microRNA profile as predictive biomarker for systemic treatment in patients with metastatic colorectal cancer.* Cancer Med, 2020. **9**(20): p. 7558-7571.
296. Li, Y., et al., *MiR-92b regulates the cell growth, cisplatin chemosensitivity of A549 non small cell lung cancer cell line and target PTEN.* Biochem Biophys Res Commun, 2013. **440**(4): p. 604-10.
297. Le, M.T.N., et al., *MicroRNA-125b is a novel negative regulator of p53.* Genes & Development, 2009. **23**(7): p. 862-876.
298. Zhang, Y., et al., *MicroRNA-520g confers drug resistance by regulating p21 expression in colorectal cancer.* J Biol Chem, 2015. **290**(10): p. 6215-25.
299. Alam, F., et al., *The role of p53-microRNA 200-Moesin axis in invasion and drug resistance of breast cancer cells.* Tumour Biol, 2017. **39**(9): p. 1010428317714634.
300. Eichelmann, A.K., et al., *Mutant p53 Mediates Sensitivity to Cancer Treatment Agents in Oesophageal Adenocarcinoma Associated with MicroRNA and SLC7A11 Expression.* Int J Mol Sci, 2021. **22**(11).
301. Bhattacharya, B., M.F. Mohd Omar, and R. Soong, *The Warburg effect and drug resistance.* Br J Pharmacol, 2016. **173**(6): p. 970-9.
302. Liu, Q., X. Liu, and G. Song, *The Hippo Pathway: A Master Regulatory Network Important in Cancer.* Cells, 2021. **10**(6).
303. Edge, S.B. and C.C. Compton, *The American Joint Committee on Cancer: the 7th edition of the AJCC cancer staging manual and the future of TNM.* Ann Surg Oncol, 2010. **17**(6): p. 1471-4.
304. Kim, S.H., et al., *What Is the Ideal Tumor Regression Grading System in Rectal Cancer Patients after Preoperative Chemoradiotherapy?* Cancer Res Treat, 2016. **48**(3): p. 998-1009.
305. Ding, M., et al., *Comparison of commercial exosome isolation kits for circulating exosomal microRNA profiling.* Anal Bioanal Chem, 2018.
306. Martin, M., *Cutadapt removes adapter sequences from high-throughput sequencing reads.* EMBnet, 2011. **17**(1): p. 10-12.
307. Andrews, S., *FastQC: A Quality Control Tool for High Throughput Sequence Data.* http://www.bioinformatics.babraham.ac.uk/projects/fastqc/, 2010. **Online**.
308. Li, H. and R. Durbin, *Fast and accurate short read alignment with Burrows-Wheeler transform.* Bioinformatics, 2009. **25**(14): p. 1754-60.
309. Anders, S., P.T. Pyl, and W. Huber, *HTSeq--a Python framework to work with high-throughput sequencing data.* Bioinformatics, 2015. **31**(2): p. 166-9.

310. Kozomara, A. and S. Griffiths-Jones, *miRBase: annotating high confidence microRNAs using deep sequencing data.* Nucleic Acids Res, 2014. **42**(Database issue): p. D68-73.
311. Zhang, P., et al., *piRBase: a web resource assisting piRNA functional study.* Database (Oxford), 2014. **2014**: p. bau110.
312. Risso, D., et al., *GC-content normalization for RNA-Seq data.* BMC Bioinformatics, 2011. **12**: p. 480.
313. Love, M.I., W. Huber, and S. Anders, *Moderated estimation of fold change and dispersion for RNA-seq data with DESeq2.* Genome Biol, 2014. **15**(12): p. 550.
314. Robinson, M.D., D.J. McCarthy, and G.K. Smyth, *edgeR: a Bioconductor package for differential expression analysis of digital gene expression data.* Bioinformatics, 2010. **26**(1): p. 139-40.
315. Ajani, J.A., et al., *Phase II randomized trial of two nonoperative regimens of induction chemotherapy followed by chemoradiation in patients with localized carcinoma of the esophagus: RTOG 0113.* J Clin Oncol, 2008. **26**(28): p. 4551-6.
316. Wen, J., et al., *MiRNA Expression Analysis of Pretreatment Biopsies Predicts the Pathological Response of Esophageal Squamous Cell Carcinomas to Neoadjuvant Chemoradiotherapy.* Annals of Surgery, 2016. **263**(5): p. 942-948.
317. Jin, Y.Y., et al., *Upregulation of microRNA-98 increases radiosensitivity in esophageal squamous cell carcinoma.* J Radiat Res, 2016. **57**(5): p. 468-476.
318. Koduru, S.V., et al., *Exploration of small RNA-seq data for small non-coding RNAs in Human Colorectal Cancer.* J Genomics, 2017. **5**: p. 16-31.
319. Koduru, S.V., et al., *A Comprehensive NGS Data Analysis of Differentially Regulated miRNAs, piRNAs, lncRNAs and sn/snoRNAs in Triple Negative Breast Cancer.* J Cancer, 2017. **8**(4): p. 578-596.
320. Y, W., *A piRNA-like Small RNA Induces Chemoresistance to Cisplatin-Based Therapy by Inhibiting Apoptosis in Lung Squamous Cell Carcinoma.* Nucleic Acids Res, 2017. **2017.01.003**.
321. Chiam, K., et al., *Identification of microRNA Biomarkers of Response to Neoadjuvant Chemoradiotherapy in Esophageal Adenocarcinoma Using Next Generation Sequencing.* Ann Surg Oncol, 2018. **25**(9): p. 2731-2738.
322. Metz, C.E., *Basic principles of ROC analysis.* Semin Nucl Med, 1978. **8**(4): p. 283-98.

323. El Khouli, R.H., et al., *Relationship of temporal resolution to diagnostic performance for dynamic contrast enhanced MRI of the breast.* J Magn Reson Imaging, 2009. **30**(5): p. 999-1004.
324. Youngstrom, E.A., *A primer on receiver operating characteristic analysis and diagnostic efficiency statistics for pediatric psychology: we are ready to ROC.* J Pediatr Psychol, 2014. **39**(2): p. 204-21.
325. Peskoe, S.B., et al., *Differential long-term stability of microRNAs and RNU6B snRNA in 12-20 year old archived formalin-fixed paraffin-embedded specimens.* Bmc Cancer, 2017. **17**.
326. Jin, H.L., et al., *Neoadjuvant chemoradiotherapy for resectable esophageal carcinoma: a meta-analysis.* World J Gastroenterol, 2009. **15**(47): p. 5983-91.
327. Sugimura, K., et al., *Let-7 Expression Is a Significant Determinant of Response to Chemotherapy through the Regulation of IL-6/STAT3 Pathway in Esophageal Squamous Cell Carcinoma.* Clinical Cancer Research, 2012. **18**(18): p. 5144-5153.
328. Chen, G.M., et al., *Combined downregulation of microRNA-133a and microRNA-133b predicts chemosensitivity of patients with esophageal squamous cell carcinoma undergoing paclitaxel-based chemotherapy.* Medical Oncology, 2014. **31**(11).
329. Wang, Y., et al., *miR-221 Mediates Chemoresistance of Esophageal Adenocarcinoma by Direct Targeting of DKK2 Expression.* Ann Surg, 2016. **264**(5): p. 804-814.
330. Song, L., et al., *MicroRNA-340-5p modulates cisplatin resistance by targeting LPAATbeta in osteosarcoma.* Braz J Med Biol Res, 2017. **50**(5): p. e6359.
331. Wozniak, M., M. Sztiller-Sikorska, and M. Czyz, *Diminution of miR-340-5p levels is responsible for increased expression of ABCB5 in melanoma cells under oxygen-deprived conditions.* Experimental and Molecular Pathology, 2015. **99**(3): p. 707-716.
332. Pan, X., R. Wang, and Z.X. Wang, *The potential role of miR-451 in cancer diagnosis, prognosis, and therapy.* Mol Cancer Ther, 2013. **12**(7): p. 1153-62.
333. Wang, W., et al., *Involvement of miR-451 in resistance to paclitaxel by regulating YWHAZ in breast cancer.* Cell Death Dis, 2017. **8**(10): p. e3071.
334. Gu, X., et al., *Influence of MiR-451 on Drug Resistances of Paclitaxel-Resistant Breast Cancer Cell Line.* Med Sci Monit, 2015. **21**: p. 3291-7.

335. Cheng, D., et al., *MicroRNA-451 sensitizes lung cancer cells to cisplatin through regulation of Mcl-1.* Mol Cell Biochem, 2016. **423**(1-2): p. 85-91.
336. Liu, Z.R., et al., *Over-expression of miR-451a can enhance the sensitivity of breast cancer cells to tamoxifen by regulating 14-3-3zeta, estrogen receptor alpha, and autophagy.* Life Sci, 2016. **149**: p. 104-13.
337. Zhang, Y.J., et al., *MiR-99a and MiR-491 Regulate Cisplatin Resistance in Human Gastric Cancer Cells by Targeting CAPNS1.* International Journal of Biological Sciences, 2016. **12**(12): p. 1437-1447.
338. Ding, Y., X. Zhang, and S. Cui, *Role of Mir-206 in Cisplatin Resistance of Ovarian Serous Carcinoma.* International Journal of Gynecological Cancer, 2014. **24**(9): p. 88-88.
339. Chen, Q.Y., et al., *miR-206 regulates cisplatin resistance and EMT in human lung adenocarcinoma cells partly by targeting MET.* Oncotarget, 2016. **7**(17): p. 24510-26.
340. Meng, X.M. and R. Fu, *miR-206 regulates 5-FU resistance by targeting Bcl-2 in colon cancer cells.* Oncotargets and Therapy, 2018. **11**: p. 1757-1765.
341. Loudig, O., et al., *Evaluation and Adaptation of a Laboratory-Based cDNA Library Preparation Protocol for Retrospective Sequencing of Archived MicroRNAs from up to 35-Year-Old Clinical FFPE Specimens.* International Journal of Molecular Sciences, 2017. **18**(3).
342. Tian, F., et al., *Upregulation of microrna-451 increases the sensitivity of A549 cells to radiotherapy through enhancement of apoptosis.* Thorac Cancer, 2016. **7**(2): p. 226-31.
343. Sun, X., et al., *MicroRNA-451 regulates chemoresistance in renal cell carcinoma by targeting ATF-2 gene.* Exp Biol Med (Maywood), 2017: p. 1535370217701625.
344. Soltani, I., et al., *Downregulation of miR-451 in Tunisian chronic myeloid leukemia patients: potential implication in imatinib resistance.* Hematology, 2017. **22**(4): p. 201-207.
345. Liu, Z., et al., *miR-451a Inhibited Cell Proliferation and Enhanced Tamoxifen Sensitive in Breast Cancer via Macrophage Migration Inhibitory Factor.* Biomed Res Int, 2015. **2015**: p. 207684.
346. Butz, F., et al., *MicroRNA Profiling in Oesophageal Adenocarcinoma Cell Lines and Patient Serum Samples Reveals a Role for miR-451a in Radiation Resistance.* Int J Mol Sci, 2020. **21**(23).
347. Liu, X., et al., *microRNAs expression profile related with response to preoperative radiochemotherapy in patients with locally advanced gastric cancer.* BMC Cancer, 2018. **18**(1): p. 1048.

348. Shi, S., et al., *LGR5 acts as a target of miR-340-5p in the suppression of cell progression and drug resistance in breast cancer via Wnt/beta-catenin pathway.* Gene, 2019. **683**: p. 47-53.
349. Yang, L., et al., *MiR-340-5p is a potential prognostic indicator of colorectal cancer and modulates ANXA3.* Eur Rev Med Pharmacol Sci, 2018. **22**(15): p. 4837-4845.
350. Wu, L.L., et al., *NRAL mediates cisplatin resistance in hepatocellular carcinoma via miR-340-5p/Nrf2 axis.* J Cell Commun Signal, 2018.
351. Zhan, C., et al., *Identification of reference miRNAs in human tumors by TCGA miRNA-seq data.* Biochem Biophys Res Commun, 2014. **453**(3): p. 375-8.
352. Ajani, J.A., et al., *Esophageal and Esophagogastric Junction Cancers, Version 2.2019, NCCN Clinical Practice Guidelines in Oncology.* J Natl Compr Canc Netw, 2019. **17**(7): p. 855-883.
353. Dweep, H. and N. Gretz, *miRWalk2.0: a comprehensive atlas of microRNA-target interactions.* Nat Methods, 2015. **12**(8): p. 697.
354. Dweep, H., et al., *miRWalk--database: prediction of possible miRNA binding sites by "walking" the genes of three genomes.* J Biomed Inform, 2011. **44**(5): p. 839-47.
355. Breuer, K., et al., *InnateDB: systems biology of innate immunity and beyond--recent updates and continuing curation.* Nucleic Acids Res, 2013. **41**(Database issue): p. D1228-33.
356. Franken, N.A., et al., *Clonogenic assay of cells in vitro.* Nat Protoc, 2006. **1**(5): p. 2315-9.
357. Andriani, F., et al., *Increased sensitivity to cisplatin in non-small cell lung cancer cell lines after FHIT gene transfer.* Neoplasia, 2006. **8**(1): p. 9-17.
358. Dasari, V.R., D.J. Carey, and R. Gogoi, *Synergistic enhancement of efficacy of platinum drugs with verteporfin in ovarian cancer cells.* BMC Cancer, 2020. **20**(1): p. 273.
359. Fath, M.A., et al., *Enhancement of carboplatin-mediated lung cancer cell killing by simultaneous disruption of glutathione and thioredoxin metabolism.* Clin Cancer Res, 2011. **17**(19): p. 6206-17.
360. Khoei, S., et al., *Methoxyamine Enhances 5-Fluorouracil-Induced Radiosensitization in Colon Cancer Cell Line HT29.* Cell J, 2017. **19**(2): p. 283-291.
361. Kuittinen, T., et al., *Paclitaxel, Carboplatin and 1,25-D3 Inhibit Proliferation of Ovarian Cancer Cells In Vitro.* Anticancer Res, 2020. **40**(6): p. 3129-3138.

362. Riaz, M.A., et al., *Metformin enhances the radiosensitizing effect of cisplatin in non-small cell lung cancer cell lines with different cisplatin sensitivities.* Sci Rep, 2019. **9**(1): p. 1282.
363. Ciccarese, F., E. Zulato, and S. Indraccolo, *LKB1/AMPK Pathway and Drug Response in Cancer: A Therapeutic Perspective.* Oxid Med Cell Longev, 2019. **2019**: p. 8730816.
364. Mi, L., et al., *ACSS2/AMPK/PCNA pathway-driven proliferation and chemoresistance of esophageal squamous carcinoma cells under nutrient stress.* Mol Med Rep, 2019. **20**(6): p. 5286-5296.
365. Park, J.B., et al., *Corosolic acid reduces 5-FU chemoresistance in human gastric cancer cells by activating AMPK.* Mol Med Rep, 2018. **18**(3): p. 2880-2888.
366. Zhao, K., et al., *The role of miR-451 in the switching between proliferation and migration in malignant glioma cells: AMPK signaling, mTOR modulation and Rac1 activation required.* Int J Oncol, 2017. **50**(6): p. 1989-1999.
367. He, Q., et al., *LKB1 promotes radioresistance in esophageal cancer cells exposed to radiation, by suppression of apoptosis and activation of autophagy via the AMPK pathway.* Mol Med Rep, 2017. **16**(2): p. 2205-2210.
368. Weerasekara, V.K., et al., *Metabolic-stress-induced rearrangement of the 14-3-3 ζ interactome promotes autophagy via a ULK1- and AMPK-regulated 14-3-3 ζ interaction with phosphorylated Atg9.* Mol Cell Biol, 2014. **34**(24): p. 4379-88.
369. Gwinn, D.M., et al., *AMPK phosphorylation of raptor mediates a metabolic checkpoint.* Mol Cell, 2008. **30**(2): p. 214-26.
370. Wei, G.Y., et al., *MiR-451a suppresses cell proliferation, metastasis and EMT via targeting YWHAZ in hepatocellular carcinoma.* Eur Rev Med Pharmacol Sci, 2019. **23**(12): p. 5158-5167.
371. Minna, E., et al., *miR-451a is underexpressed and targets AKT/mTOR pathway in papillary thyroid carcinoma.* Oncotarget, 2016. **7**(11): p. 12731-47.
372. Streleckiene, G., et al., *miR-20b and miR-451a Are Involved in Gastric Carcinogenesis through the PI3K/AKT/mTOR Signaling Pathway: Data from Gastric Cancer Patients, Cell Lines and Ins-Gas Mouse Model.* Int J Mol Sci, 2020. **21**(3).

373. Riquelme, I., et al., *miR-101-2, miR-125b-2 and miR-451a act as potential tumor suppressors in gastric cancer through regulation of the PI3K/AKT/mTOR pathway.* Cell Oncol (Dordr), 2016. **39**(1): p. 23-33.
374. Ji, X., et al., *xCT (SLC7A11)-mediated metabolic reprogramming promotes non-small cell lung cancer progression.* Oncogene, 2018. **37**(36): p. 5007-5019.
375. Zhang, S. and C. Xie, *The role of OXCT1 in the pathogenesis of cancer as a rate-limiting enzyme of ketone body metabolism.* Life Sci, 2017. **183**: p. 110-115.
376. Ardestani, A., B. Lupse, and K. Maedler, *Hippo Signaling: Key Emerging Pathway in Cellular and Whole-Body Metabolism.* Trends Endocrinol Metab, 2018. **29**(7): p. 492-509.
377. Liu, D.S., et al., *Inhibiting the system xC(-)/glutathione axis selectively targets cancers with mutant-p53 accumulation.* Nat Commun, 2017. **8**: p. 14844.
378. Clemons, N.J., et al., *Inhibiting system xC(-) and glutathione biosynthesis - a potential Achilles' heel in mutant-p53 cancers.* Mol Cell Oncol, 2017. **4**(5): p. e1344757.
379. Liu, Y., et al., *Identification of Hub Genes and Key Pathways Associated With Bipolar Disorder Based on Weighted Gene Co-expression Network Analysis.* Front Physiol, 2019. **10**: p. 1081.
380. Liu, Z.R., et al., *Over-expression of miR-451a can enhance the sensitivity of breast cancer cells to tamoxifen by regulating 14-3-3 zeta, estrogen receptor alpha, and autophagy.* Life Sciences, 2016. **149**: p. 104-113.
381. Li, Y., et al., *miR-451 regulates FoxO3 nuclear accumulation through Ywhaz in human colorectal cancer.* Am J Transl Res, 2015. **7**(12): p. 2775-85.
382. Ardito, F., et al., *The crucial role of protein phosphorylation in cell signaling and its use as targeted therapy (Review).* Int J Mol Med, 2017. **40**(2): p. 271-280.
383. Kim, I. and Y.Y. He, *Targeting the AMP-Activated Protein Kinase for Cancer Prevention and Therapy.* Front Oncol, 2013. **3**: p. 175.
384. Falcicchio, M., et al., *Regulation of p53 by the 14-3-3 protein interaction network: new opportunities for drug discovery in cancer.* Cell Death Discov, 2020. **6**(1): p. 126.
385. Longley, D.B., D.P. Harkin, and P.G. Johnston, *5-fluorouracil: mechanisms of action and clinical strategies.* Nat Rev Cancer, 2003. **3**(5): p. 330-8.

386. Dasari, S. and P.B. Tchounwou, *Cisplatin in cancer therapy: molecular mechanisms of action.* Eur J Pharmacol, 2014. **740**: p. 364-78.
387. Weaver, B.A., *How Taxol/paclitaxel kills cancer cells.* Molecular Biology of the Cell, 2014. **25**(18): p. 2677-2681.
388. Kiss, L., et al., *Kinetic analysis of the toxicity of pharmaceutical excipients Cremophor EL and RH40 on endothelial and epithelial cells.* J Pharm Sci, 2013. **102**(4): p. 1173-81.
389. Liebmann, J.E., et al., *Cytotoxic studies of paclitaxel (Taxol) in human tumour cell lines.* Br J Cancer, 1993. **68**(6): p. 1104-9.
390. Della Bella, E., et al., *Differential Regulation of circRNA, miRNA, and piRNA during Early Osteogenic and Chondrogenic Differentiation of Human Mesenchymal Stromal Cells.* Cells, 2020. **9**(2).
391. Chen, S., et al., *The biogenesis and biological function of PIWI-interacting RNA in cancer.* J Hematol Oncol, 2021. **14**(1): p. 93.
392. Ikari, J., et al., *Effect of culture conditions on microRNA expression in primary adult control and COPD lung fibroblasts in vitro.* In Vitro Cell Dev Biol Anim, 2015. **51**(4): p. 390-9.
393. Klein, S.G., et al., *In situ monitoring reveals cellular environmental instabilities in human pluripotent stem cell culture.* Commun Biol, 2022. **5**(1): p. 119.
394. Ping, S., et al., *Simultaneous Increases in Proliferation and Apoptosis of Vascular Smooth Muscle Cells Accelerate Diabetic Mouse Venous Atherosclerosis.* PLoS One, 2015. **10**(10): p. e0141375.
395. Hermeking, H. and A. Benzinger, *14-3-3 proteins in cell cycle regulation.* Semin Cancer Biol, 2006. **16**(3): p. 183-92.
396. Khorrami, A., et al., *The functional significance of 14-3-3 proteins in cancer: focus on lung cancer.* Horm Mol Biol Clin Investig, 2017. **32**(3).
397. Pennington, K.L., et al., *The dynamic and stress-adaptive signaling hub of 14-3-3: emerging mechanisms of regulation and context-dependent protein-protein interactions.* Oncogene, 2018. **37**(42): p. 5587-5604.
398. Mihaylova, M.M. and R.J. Shaw, *The AMPK signalling pathway coordinates cell growth, autophagy and metabolism.* Nat Cell Biol, 2011. **13**(9): p. 1016-23.
399. Hu, Y., et al., *The AMPK-MFN2 axis regulates MAM dynamics and autophagy induced by energy stresses.* Autophagy, 2021. **17**(5): p. 1142-1156.
400. Afinanisa, Q., M.K. Cho, and H.A. Seong, *AMPK Localization: A Key to Differential Energy Regulation.* Int J Mol Sci, 2021. **22**(20).

401. Khazaei, S., et al., *A novel signaling role for miR-451 in esophageal tumor microenvironment and its contribution to tumor progression.* Clin Transl Oncol, 2017. **19**(5): p. 633-640.
402. Su, Z., et al., *MicroRNA-451a is associated with cell proliferation, migration and apoptosis in renal cell carcinoma.* Mol Med Rep, 2015. **11**(3): p. 2248-54.
403. Yin, P., et al., *MiR-451 suppresses cell proliferation and metastasis in A549 lung cancer cells.* Mol Biotechnol, 2015. **57**(1): p. 1-11.
404. Szczepanski, M.J., et al., *Blast-derived microvesicles in sera from patients with acute myeloid leukemia suppress natural killer cell function via membrane-associated transforming growth factor-beta1.* Haematologica, 2011. **96**(9): p. 1302-9.
405. Taverna, S., et al., *Exosomes isolation and characterization in serum is feasible in non-small cell lung cancer patients: critical analysis of evidence and potential role in clinical practice.* Oncotarget, 2016. **7**(19): p. 28748-60.
406. Ashby, J., et al., *Distribution profiling of circulating microRNAs in serum.* Anal Chem, 2014. **86**(18): p. 9343-9.
407. Bansal, A., V. Gupta, and K. Wang, *MicroRNA Expression Signatures During Malignant Progression From Barrett's Esophagus.* J Cell Biochem, 2016. **117**(6): p. 1288-95.
408. Bus, P., et al., *Profiling of circulating microRNAs in patients with Barrett's esophagus and esophageal adenocarcinoma.* J Gastroenterol, 2016. **51**(6): p. 560-70.
409. Joyce, D.P., M.J. Kerin, and R.M. Dwyer, *Exosome-encapsulated microRNAs as circulating biomarkers for breast cancer.* Int J Cancer, 2016. **139**(7): p. 1443-8.
410. Chiam, K., et al., *Circulating Serum Exosomal miRNAs As Potential Biomarkers for Esophageal Adenocarcinoma.* J Gastrointest Surg, 2015. **19**(7): p. 1208-15.
411. McWilliam, S.J., et al., *Urinary Biomarkers of Aminoglycoside-Induced Nephrotoxicity in Cystic Fibrosis: Kidney Injury Molecule-1 and Neutrophil Gelatinase-Associated Lipocalin.* Sci Rep, 2018. **8**(1): p. 5094.
412. Makhijani, R.K., S.A. Raut, and H.J. Purohit, *Fold change based approach for identification of significant network markers in breast, lung and prostate cancer.* IET Syst Biol, 2018. **12**(5): p. 213-218.

413. Klinge, C.M., *miRNAs regulated by estrogens, tamoxifen, and endocrine disruptors and their downstream gene targets.* Molecular and Cellular Endocrinology, 2015. **418**: p. 273-297.
414. Kirschner, M.B., et al., *The Impact of Hemolysis on Cell-Free microRNA Biomarkers.* Front Genet, 2013. **4**: p. 94.
415. Kirschner, M.B., et al., *Haemolysis during sample preparation alters microRNA content of plasma.* PLoS One, 2011. **6**(9): p. e24145.
416. Luo, X., et al., *Differential RNA packaging into small extracellular vesicles by neurons and astrocytes.* Cell Commun Signal, 2021. **19**(1): p. 75.
417. Temoche-Diaz, M.M., et al., *Distinct mechanisms of microRNA sorting into cancer cell-derived extracellular vesicle subtypes.* Elife, 2019. **8**.
418. Garcia-Martin, R., et al., *MicroRNA sequence codes for small extracellular vesicle release and cellular retention.* Nature, 2022. **601**(7893): p. 446-451.
419. Mateescu, B., et al., *Obstacles and opportunities in the functional analysis of extracellular vesicle RNA - an ISEV position paper.* J Extracell Vesicles, 2017. **6**(1): p. 1286095.
420. Ragusa, M., et al., *Asymmetric RNA Distribution among Cells and Their Secreted Exosomes: Biomedical Meaning and Considerations on Diagnostic Applications.* Front Mol Biosci, 2017. **4**: p. 66.
421. Janas, T., et al., *Mechanisms of RNA loading into exosomes.* FEBS Lett, 2015. **589**(13): p. 1391-8.
422. McKenzie, A.J., et al., *KRAS-MEK Signaling Controls Ago2 Sorting into Exosomes.* Cell Rep, 2016. **15**(5): p. 978-987.
423. Iavello, A., et al., *Role of Alix in miRNA packaging during extracellular vesicle biogenesis.* Int J Mol Med, 2016. **37**(4): p. 958-66.
424. Yanshina, D.D., et al., *Structural features of the interaction of the 3'-untranslated region of mRNA containing exosomal RNA-specific motifs with YB-1, a potential mediator of mRNA sorting.* Biochimie, 2018. **144**: p. 134-143.
425. Mukherjee, K., et al., *Reversible HuR-microRNA binding controls extracellular export of miR-122 and augments stress response.* EMBO Rep, 2016. **17**(8): p. 1184-203.
426. Statello, L., et al., *Identification of RNA-binding proteins in exosomes capable of interacting with different types of RNA: RBP-facilitated transport of RNAs into exosomes.* PLoS One, 2018. **13**(4): p. e0195969.

427. Leidal, A.M., et al., *The LC3-conjugation machinery specifies the loading of RNA-binding proteins into extracellular vesicles.* Nat Cell Biol, 2020. **22**(2): p. 187-199.
428. O'Brien, K., et al., *RNA delivery by extracellular vesicles in mammalian cells and its applications.* Nat Rev Mol Cell Biol, 2020. **21**(10): p. 585-606.
429. Zeng, S., et al., *MicroRNA-32 promotes ovarian cancer cell proliferation and motility by targeting SMG1.* Oncol Lett, 2020. **20**(1): p. 733-741.
430. Paziewska, A., et al., *Candidate diagnostic miRNAs that can detect cancer in prostate biopsy.* Prostate, 2018. **78**(3): p. 178-185.
431. Schneider, A., et al., *Tissue and serum microRNA profile of oral squamous cell carcinoma patients.* Sci Rep, 2018. **8**(1): p. 675.
432. Fu, X., et al., *Exosomal microRNA-32-5p induces multidrug resistance in hepatocellular carcinoma via the PI3K/Akt pathway.* J Exp Clin Cancer Res, 2018. **37**(1): p. 52.
433. Zhang, L., et al., *KLF4, a miR-32-5p targeted gene, promotes cisplatin-induced apoptosis by upregulating BIK expression in prostate cancer.* Cell Commun Signal, 2018. **16**(1): p. 53.
434. Liang, H., et al., *MiR-32-5p Regulates Radiosensitization, Migration And Invasion Of Colorectal Cancer Cells By Targeting TOB1 Gene.* Onco Targets Ther, 2019. **12**: p. 9651-9661.
435. Duan, S., et al., *SNORA71B promotes breast cancer cells across blood-brain barrier by inducing epithelial-mesenchymal transition.* Breast Cancer, 2020. **27**(6): p. 1072-1081.
436. Vella, S., et al., *PIWI-interacting RNA (piRNA) signatures in human cardiac progenitor cells.* Int J Biochem Cell Biol, 2016. **76**: p. 1-11.
437. Chen, W.X., et al., *Exosomes from docetaxel-resistant breast cancer cells alter chemosensitivity by delivering microRNAs.* Tumour Biol, 2014. **35**(10): p. 9649-59.
438. Chen, W.X., et al., *Exosomes from drug-resistant breast cancer cells transmit chemoresistance by a horizontal transfer of microRNAs.* PLoS One, 2014. **9**(4): p. e95240.
439. Wei, Y., et al., *Exosomal miR-221/222 enhances tamoxifen resistance in recipient ER-positive breast cancer cells.* Breast Cancer Res Treat, 2014. **147**(2): p. 423-31.
440. Sreedharan, L., et al., *MicroRNA profile in neosquamous esophageal mucosa following ablation of Barrett's esophagus.* World J Gastroenterol, 2017. **23**(30): p. 5508-5518.

441. Maioli, E., et al., *Critical appraisal of the MTT assay in the presence of rottlerin and uncouplers.* Biol Proced Online, 2009. **11**: p. 227-40.
442. Wang, P., S.M. Henning, and D. Heber, *Limitations of MTT and MTS-based assays for measurement of antiproliferative activity of green tea polyphenols.* PLoS One, 2010. **5**(4): p. e10202.
443. Kho, D., et al., *Application of xCELLigence RTCA Biosensor Technology for Revealing the Profile and Window of Drug Responsiveness in Real Time.* Biosensors (Basel), 2015. **5**(2): p. 199-222.
444. Śliwka, L., et al., *The Comparison of MTT and CVS Assays for the Assessment of Anticancer Agent Interactions.* PLoS One, 2016. **11**(5): p. e0155772.
445. Bobrie, A., et al., *Exosome secretion: molecular mechanisms and roles in immune responses.* Traffic, 2011. **12**(12): p. 1659-68.
446. Fang, T., et al., *Tumor-derived exosomal miR-1247-3p induces cancer-associated fibroblast activation to foster lung metastasis of liver cancer.* Nat Commun, 2018. **9**(1): p. 191.
447. Raimondi, L., et al., *Osteosarcoma cell-derived exosomes affect tumor microenvironment by specific packaging of microRNAs.* Carcinogenesis, 2020. **41**(5): p. 666-677.
448. Toda, Y., et al., *Effective internalization of U251-MG-secreted exosomes into cancer cells and characterization of their lipid components.* Biochem Biophys Res Commun, 2015. **456**(3): p. 768-73.
449. Parolini, I., et al., *Microenvironmental pH is a key factor for exosome traffic in tumor cells.* J Biol Chem, 2009. **284**(49): p. 34211-22.
450. Chedere, A., et al., *Multi-Stability and Consequent Phenotypic Plasticity in AMPK-Akt Double Negative Feedback Loop in Cancer Cells.* J Clin Med, 2021. **10**(3).

APPENDICES

4 INVESTIGATING THE ROLE OF CELLULAR SMALL RNAS IN REGULATING CHEMORADIOTHERAPY RESPONSE IN EAC CELLS

4.1 The drug concentration optimization in OE33 to 5-Fu, Cisplatin, Carboplatin and Paclitaxel

The drug concentration was optimized before the transfection work. The optimized concentration would be the concentration of chemotherapy drugs to identify an effective, but not 100% lethal dose so that to allow miRNA modulation to increase or decrease the chemotherapy response. Several concentrations of the 5-Fu, Cisplatin, Carboplatin and Paclitaxel were tried. The reason for including Carboplatin and Paclitaxel was, as described above, that both of them were common drugs for the treatment of EAC in the neoadjuvant setting. Incucyte and Flow Cytometry were used to assess the drug treatment response. The results showed the 100μM Carboplatin, 50μM 5-Fu, 8μM Cisplatin, and 10nM Paclitaxel would be the candidates for the transfection work , 4 independent experiment performed and 3 replicates for each experiment, the detailed information was in methods section. (Figure 4-2, 4-3,4-4,4-5).

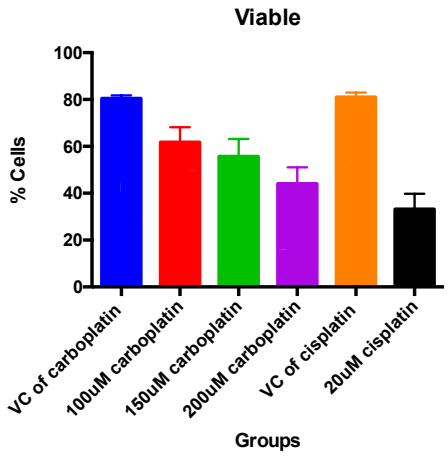

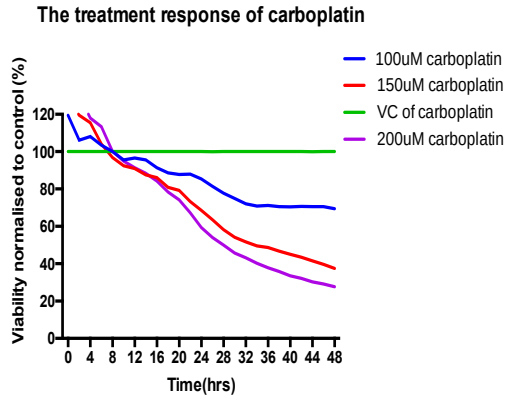

A

B

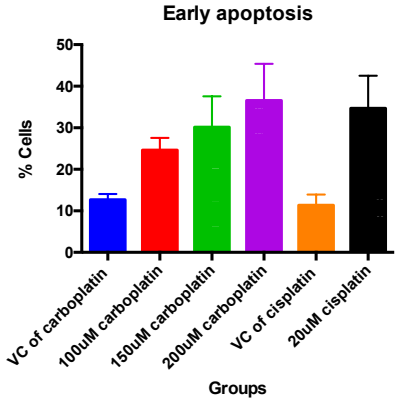

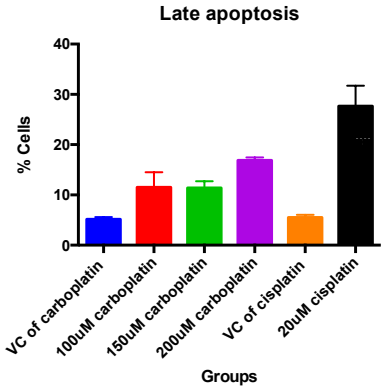

C

D

Figure 4-1. *The treatment response in OE33 to carboplatin: A: the results of Incucyte: the X-axis was duration of treatment while the Y-axis was viability normalized to control, B: the viable percentage from Flow Cytometry(72h timepoint), C: the early apoptosis from Flow Cytometry, D: the late apoptosis from Flow Cytometry.*

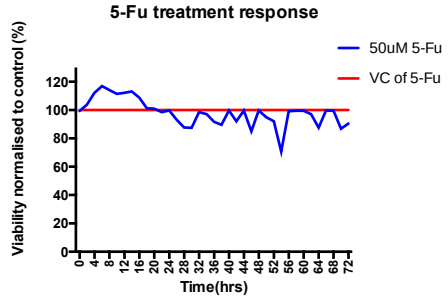

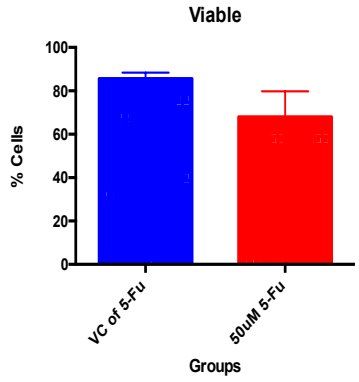

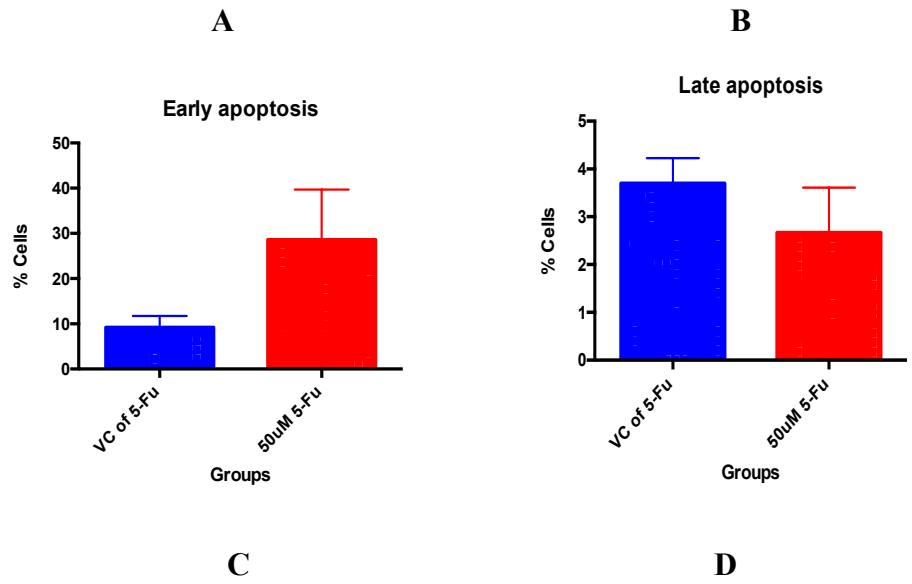

Figure 4-2. *The treatment response in OE33 to 5-Fu: A: the results of Incucyte: the X-axis was time of treatment while the Y-axis was viability normalized to control. The incucyte data did not show very well in this experiment, but experiments from other lab members supported use of 50uM[7]. B: the viable percentage from Flow Cytometry, C: the early apoptosis from Flow Cytometry, D: the late apoptosis from Flow Cytometry.*

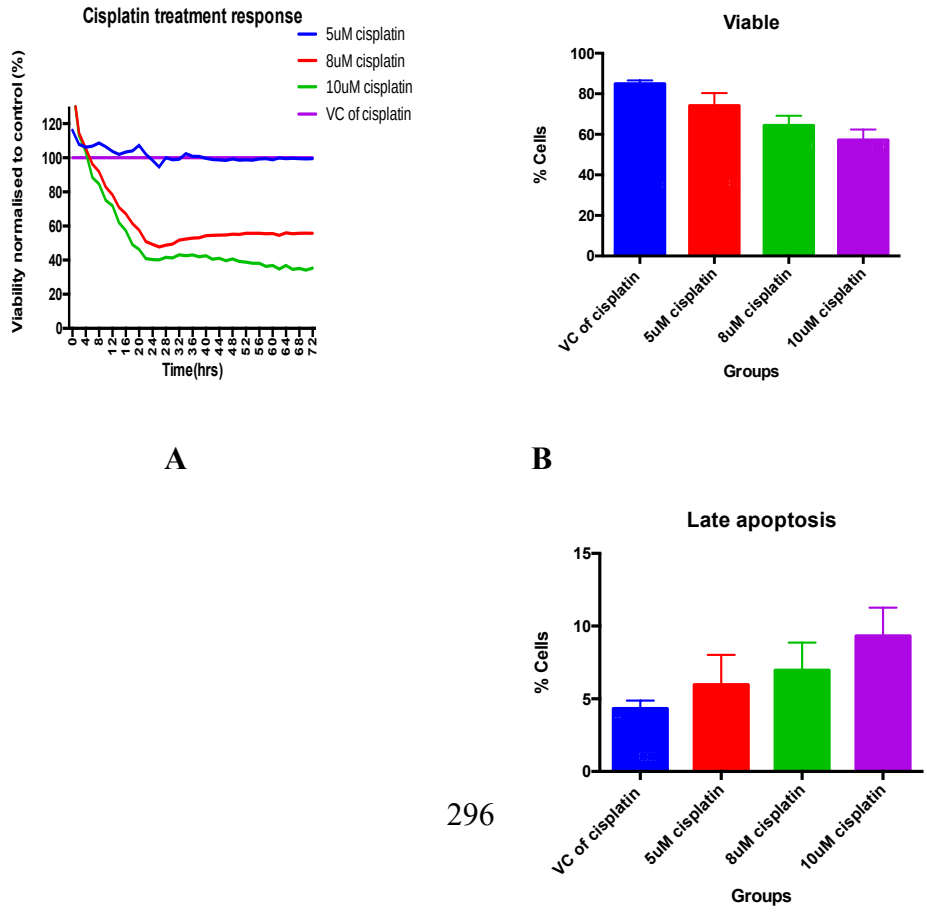

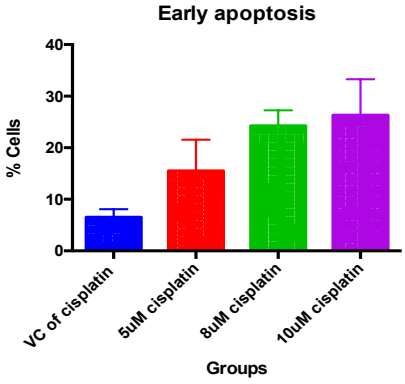

C D

Figure 4-3. *The treatment response in OE33 to Cisplatin: A: the results of Incucyte: the X-axis was time of treatment while the Y-axis was viability normalized to control. B: the viable percentage from flow cytometry, C: the early apoptosis from flow cytometry, D: the late apoptosis from flow cytometry.*

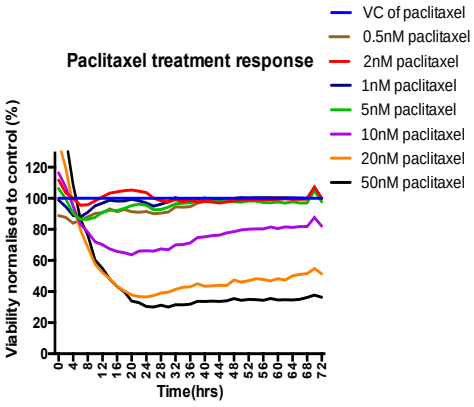

A

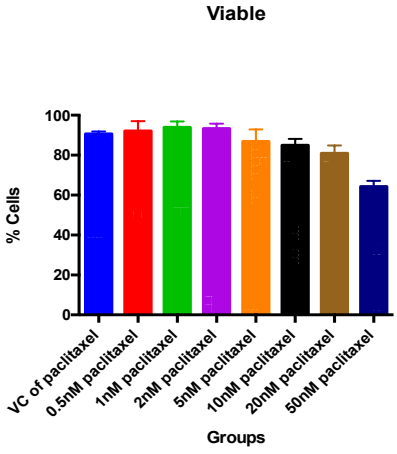

B

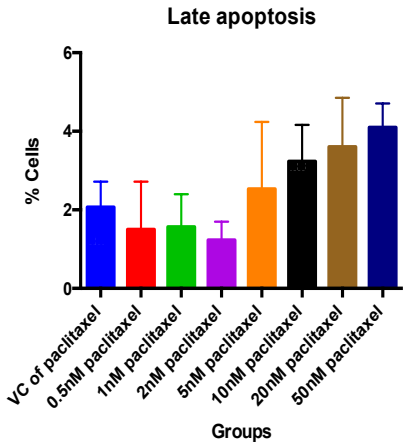

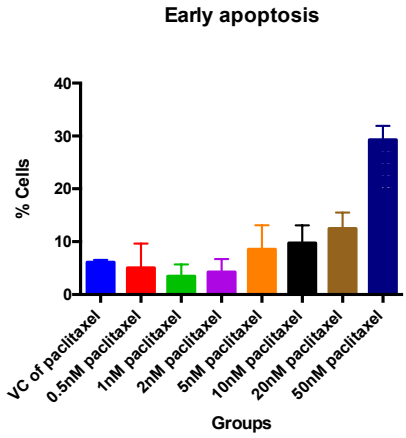

C **D**

Figure 4-4*. The treatment response in OE33 to Paclitaxel: A: the results of Incucyte: the X-axis was time of treatment while the Y-axis was viability normalized to control. B: the viable percentage from Flow Cytometry, C: the early apoptosis from Flow Cytometry, D: the late apoptosis from Flow Cytometry. The vehicle concentration was 0.001% (V/V) , which was previously experimentally optimised (see Appendix 4.2).*

4.2 The cytotoxic activity in vehicle control of Paclitaxel

During the drug concentration optimization, the vehicle control of Paclitaxel showed the cytotoxicity. The vehicle control of Paclitaxel were citric acid and Kolliphor (PEG35 35 castor oil), which were all potential cytotoxic according to the literature even at low concentration(PMID: 17962450, 191594, 24123010,17403041). Our experiment found the concentration of vehicle control of Paclitaxel with the cytotoxicity at 0.1%(V/V) compared to the other vehicle controls (Figure 4-5). However, the cytotoxicity was very weak at 0.001% (Figure 4-6). Therefore, the vehicle control of Paclitaxel at 0.001% or lower was used as for the following experiments.

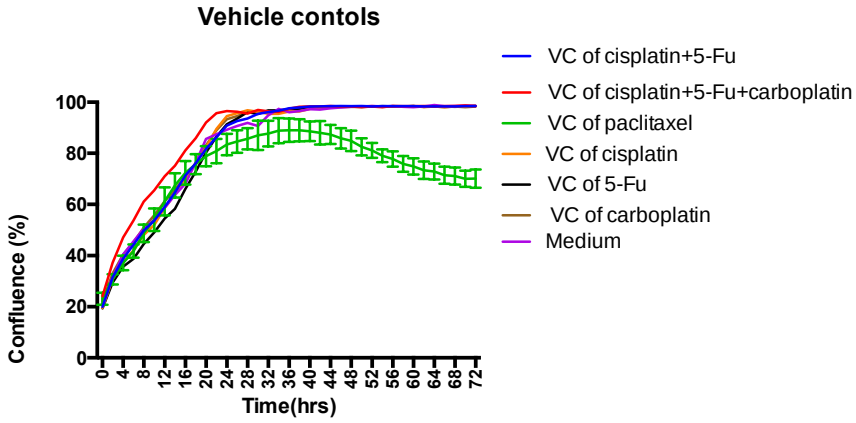

Figure 4-5. *The confluence of OE33 in different kinds of vehicle controls, the vehicle control of Paclitaxel showed cytotoxicity at the concentration of 0.1%(V/V).*

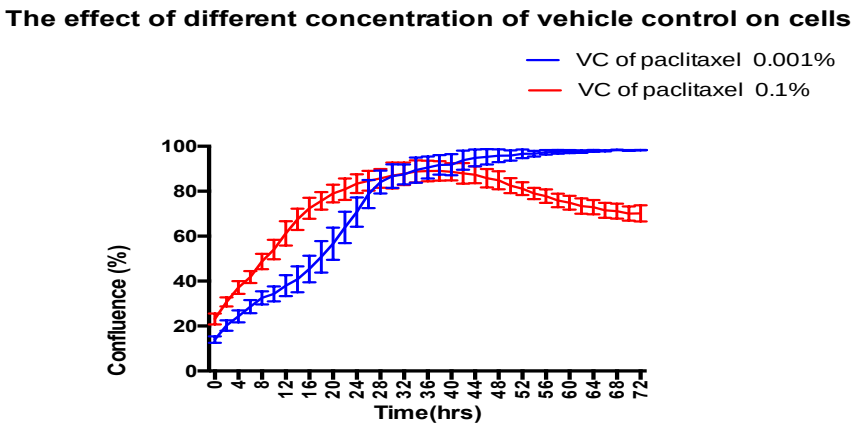

Figure 4-6. *The effect of different concentration of vehicle control of Paclitaxel on OE33 cells (0.001% V/V vs 0.1% V/V).*

4.3 The relationship between small RNAs expression and drug/radiation treatment response in EAC cell lines

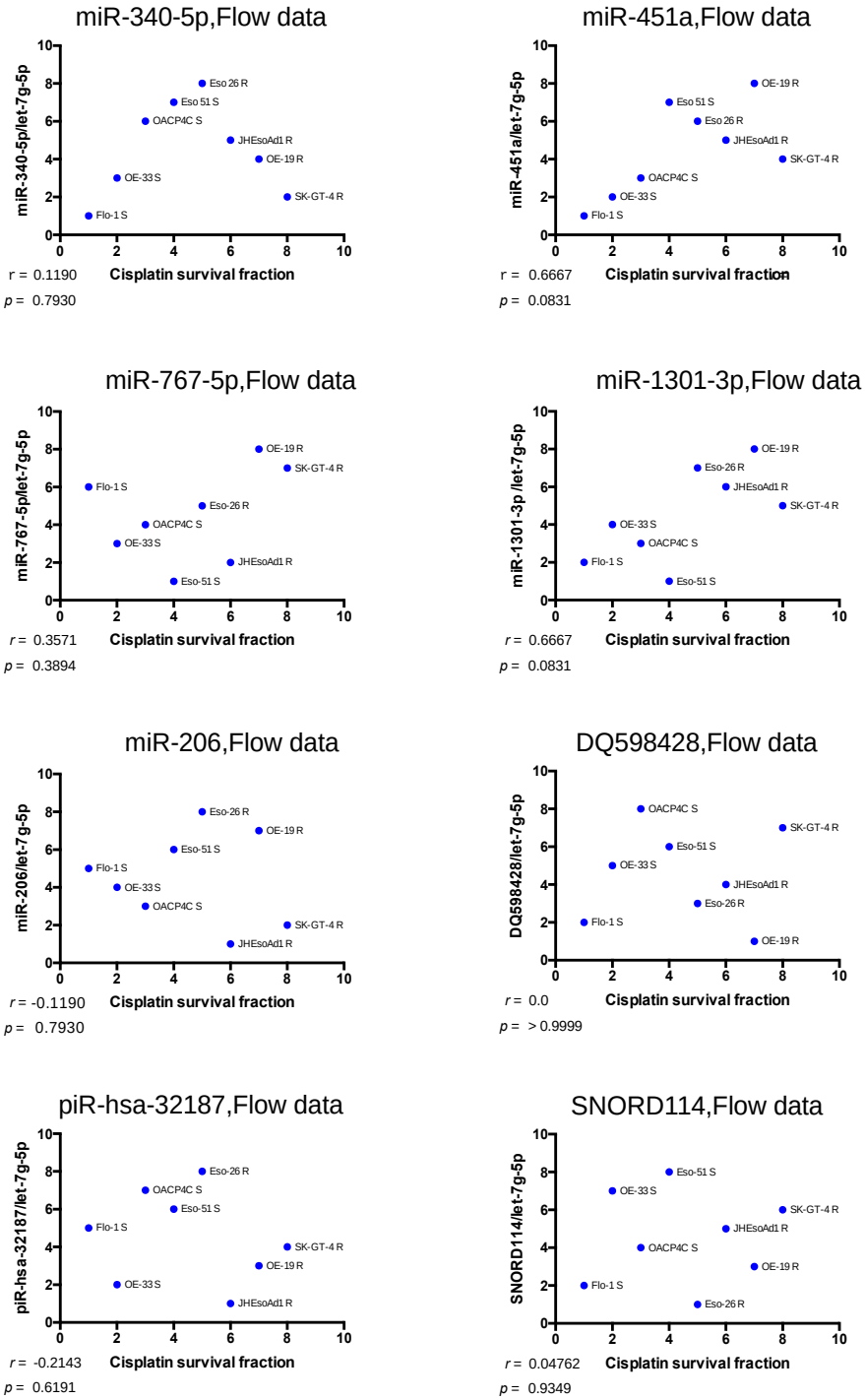

Figure 4-7*. The relationship between cisplatin treatment response and the expression of small RNAs by Flow Cytometry (Y-axis shows the expression of small RNAs*

normalized by let-7g-5p. X-axis shows the Survival Fraction (SF), obtained by dividing the amount of viable cells of one treated sample by the mean of viable cells of the respective untreated vehicle controls).

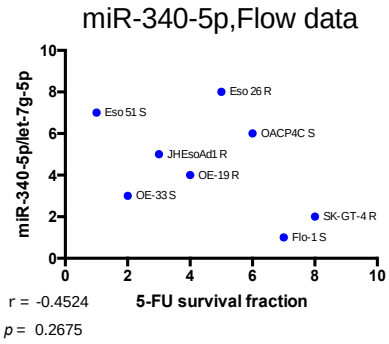

r = -0.4524
p = 0.2675

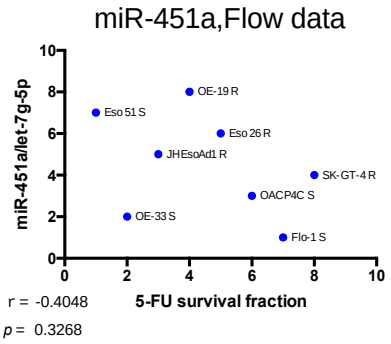

r = -0.4048
p = 0.3268

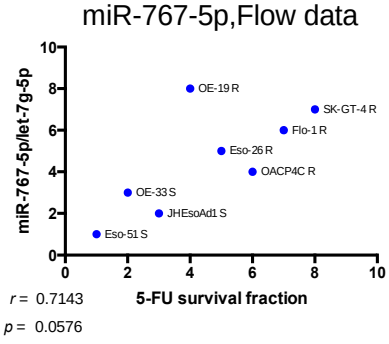

r = 0.7143
p = 0.0576

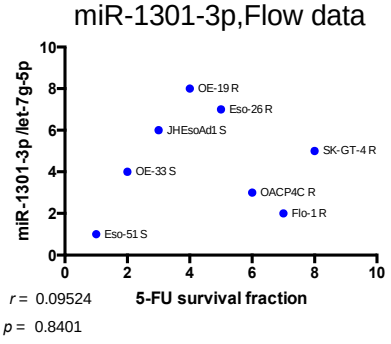

r = 0.09524
p = 0.8401

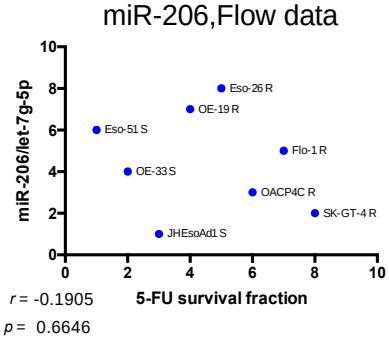

r = -0.1905
p = 0.6646

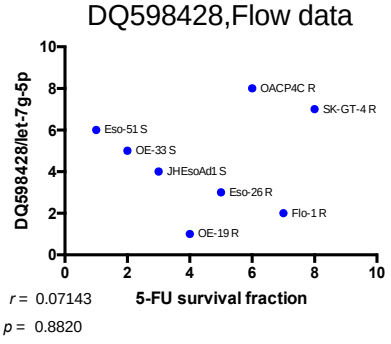

r = 0.07143
p = 0.8820

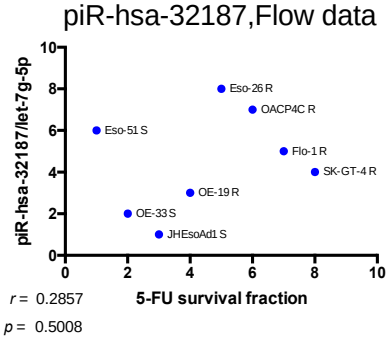

r = 0.2857
p = 0.5008

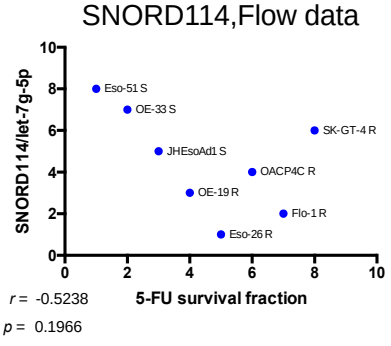

r = -0.5238
p = 0.1966

***Figure 4-8**. The relationship between 5-Fu treatment response and the expression of small RNAs by Flow cytometry (Y-axis shows the expression of small RNAs normalized by let-7g-5p. X-axis shows the Survival Fraction (SF), obtained by dividing the amount of viable cells of one treated sample by the mean of viable cells of the respective untreated vehicle controls).*

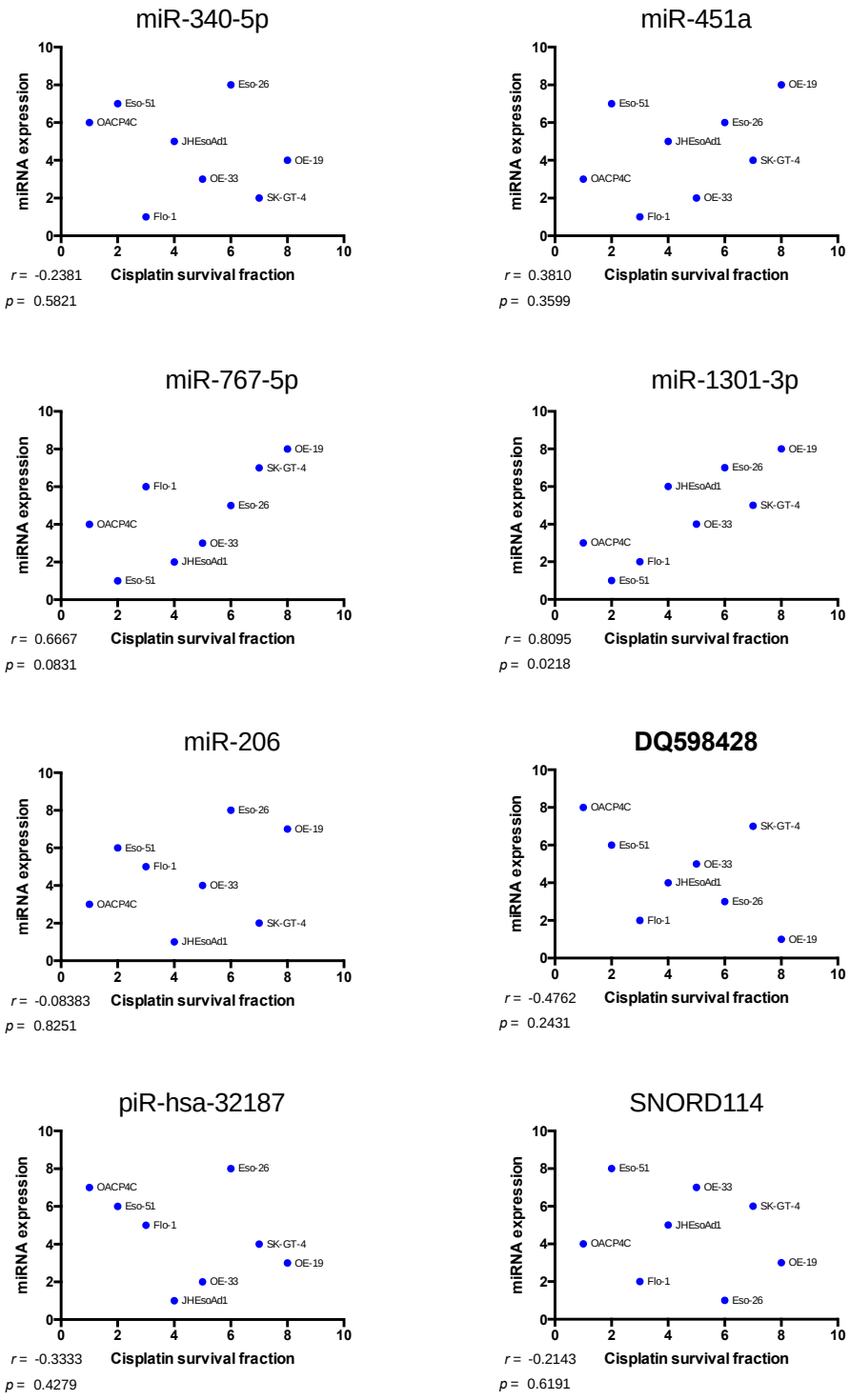

Figure 4-9. *The relationship between Cisplatin treatment response and the expression of small RNAs by MTS (Y-axis shows the expression of small RNAs normalized by let-7g-5p. X-axis shows the Survival Fraction (SF), obtained by dividing the amount of viable cells of one treated sample by the mean of viable cells of the respective untreated vehicle controls).*

.

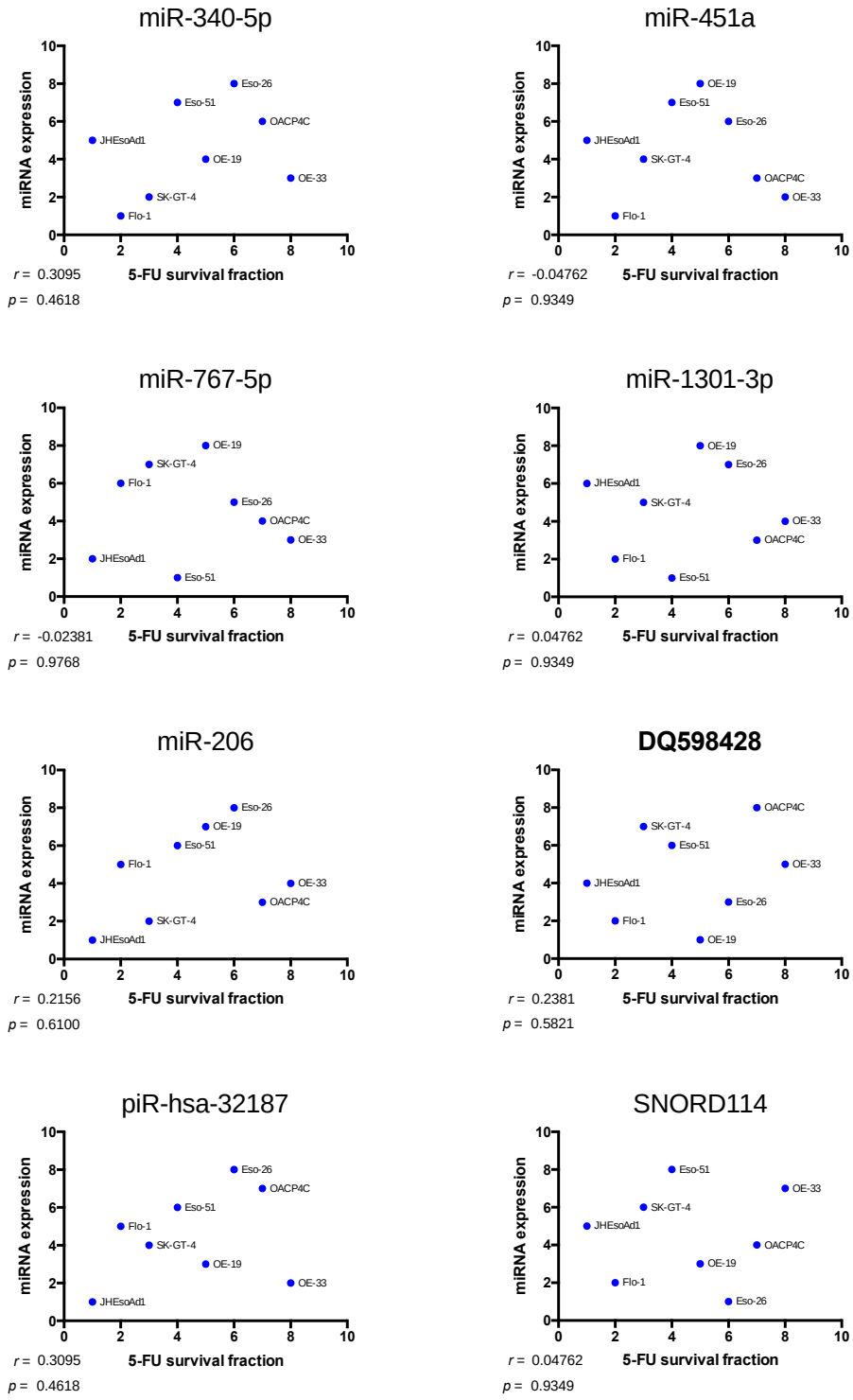

Figure 4-10. *The relationship between 5-Fu treatment response and the expression of small RNAs by MTS (Y-axis shows the expression of small RNAs normalized by let-7g-5p. X-axis shows*

the Survival Fraction (SF), obtained by dividing the amount of viable cells of one treated sample by the mean of viable cells of the respective untreated vehicle controls).

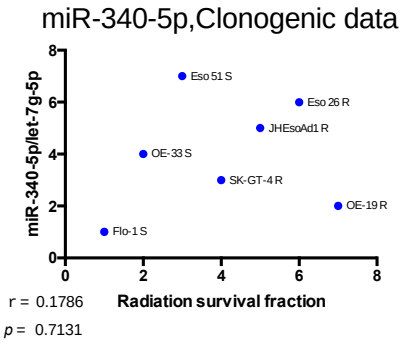

r = 0.1786
p = 0.7131

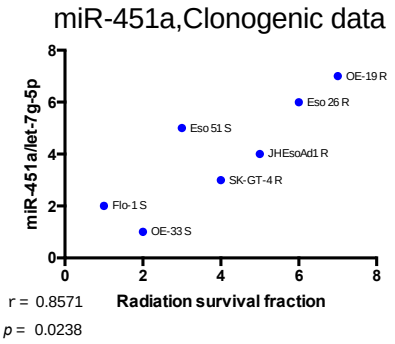

r = 0.8571
p = 0.0238

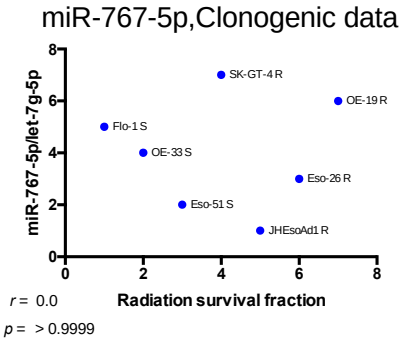

r = 0.0
p = > 0.9999

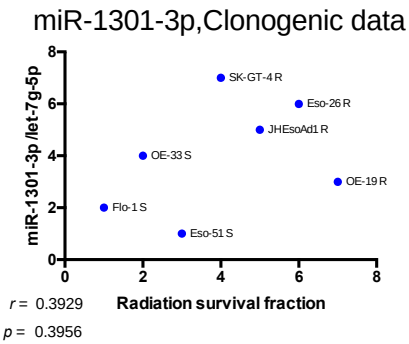

r = 0.3929
p = 0.3956

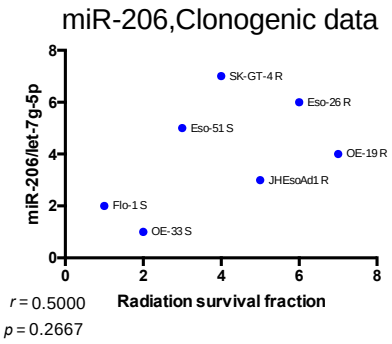

r = 0.5000
p = 0.2667

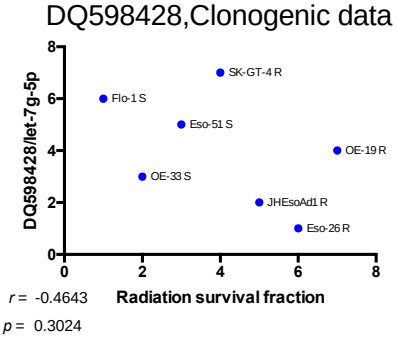

r = -0.4643
p = 0.3024

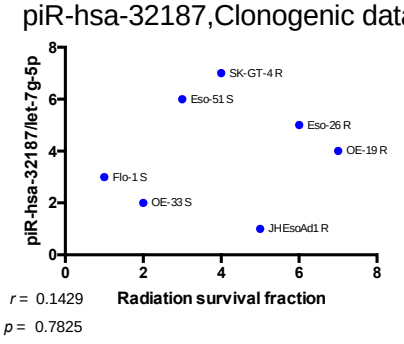

r = 0.1429
p = 0.7825

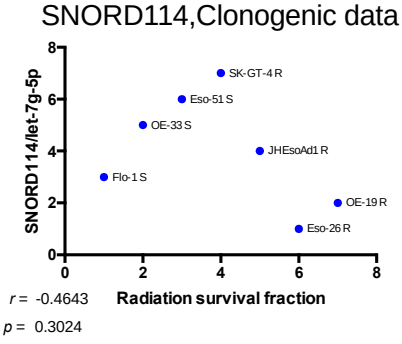

r = -0.4643
p = 0.3024

Figure 4-11*.The relationships between small RNAs expression and radiation response in EAC cell lines by Clonogenic assay (Y-axis shows the expression of small RNAs normalized by let-7g-5p. X-axis shows the Survival Fraction (SF), obtained by dividing the amount of viable cells of one treated sample by the mean of viable cells of the respective untreated vehicle controls).*

4.4 The impact of miR-451a mimic molecule on cell proliferation of OE33 as measured by Incucyte assay

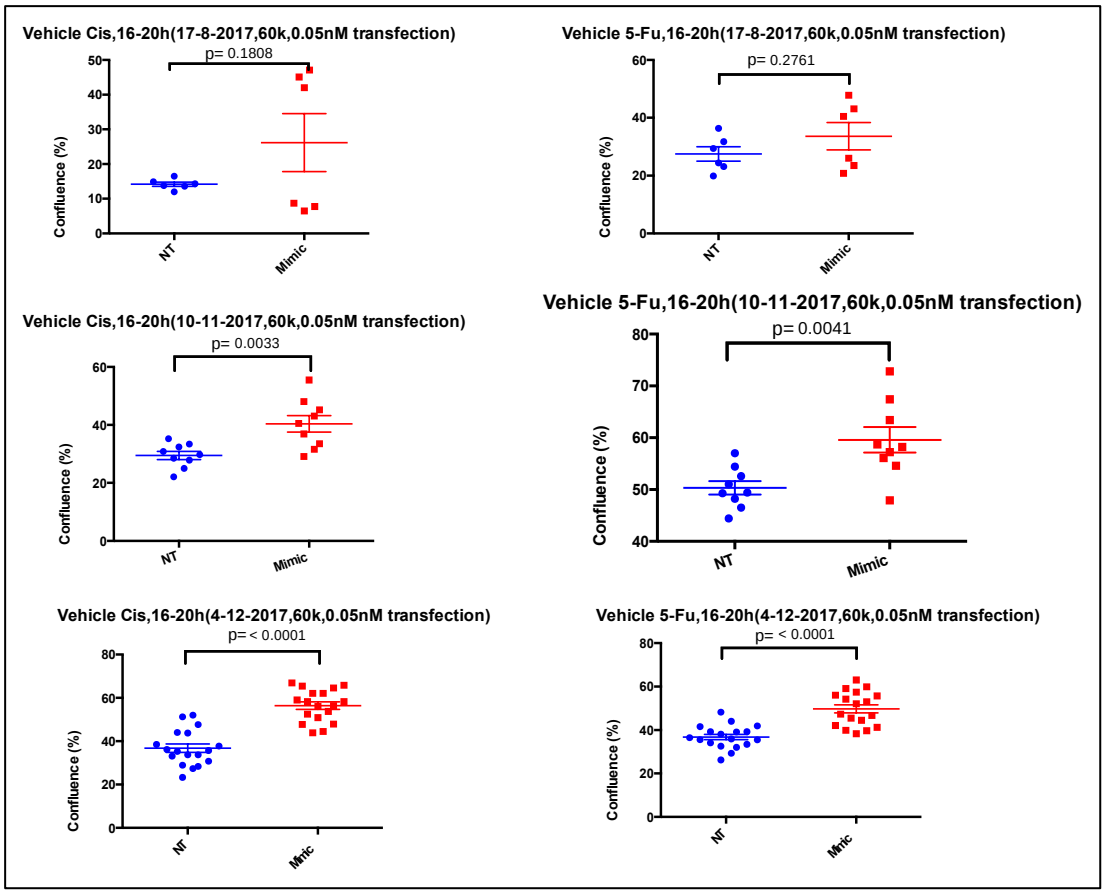

Figure 4-12*. The miR-451a mimic molecule increased the cell proliferation of OE33 at 0.05nM in 60k cell density after 16-20h treated with the vehicle of Cisplatin (Cis) and 5-Fu. NT: non-targeting molecule. The title of the graph includes the date of the experiment.*

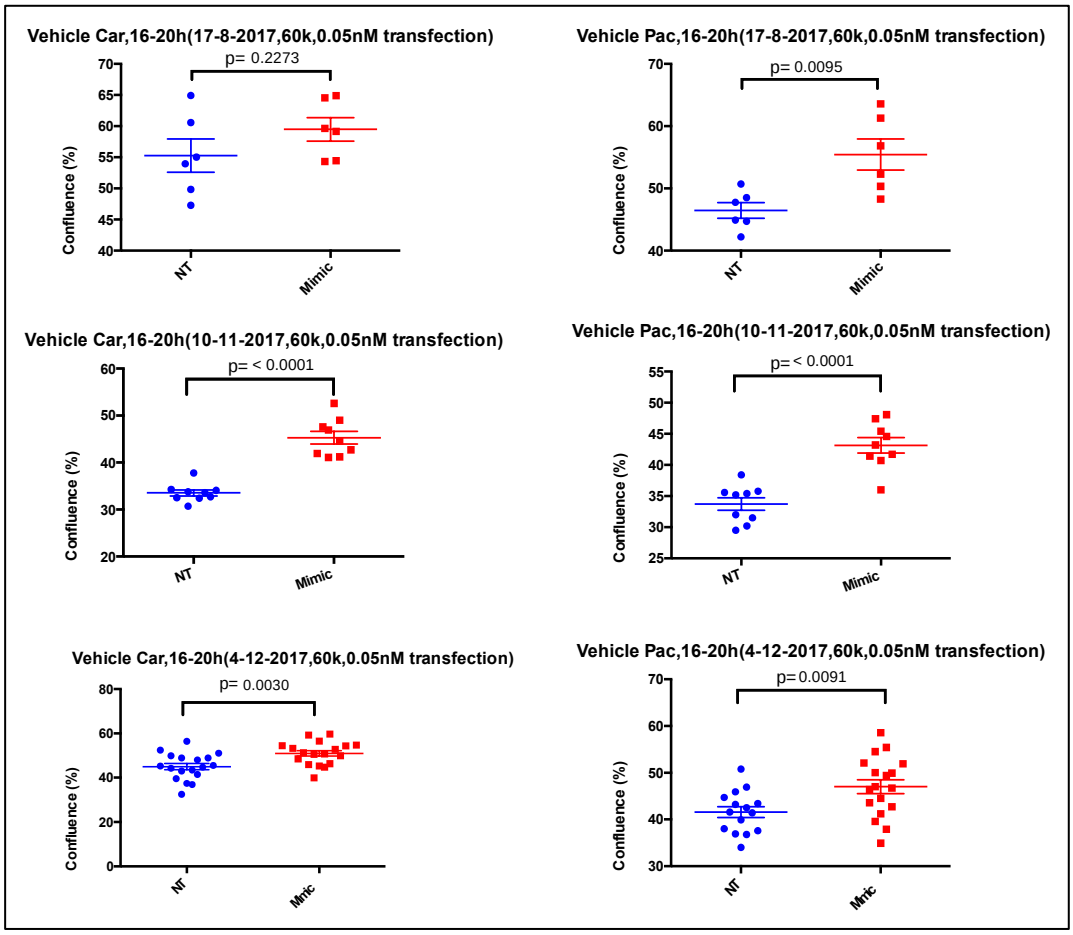

Figure 4-13. *The miR-451a mimic molecule increased the cell proliferation of OE33 at 0.05nM in 60k cell density after 16-20h treated with the vehicle of Carboplatin (Car) and Paclitaxel (Pac). NT: non-targeting molecule. The title of the graph includes the date of the experiment.*

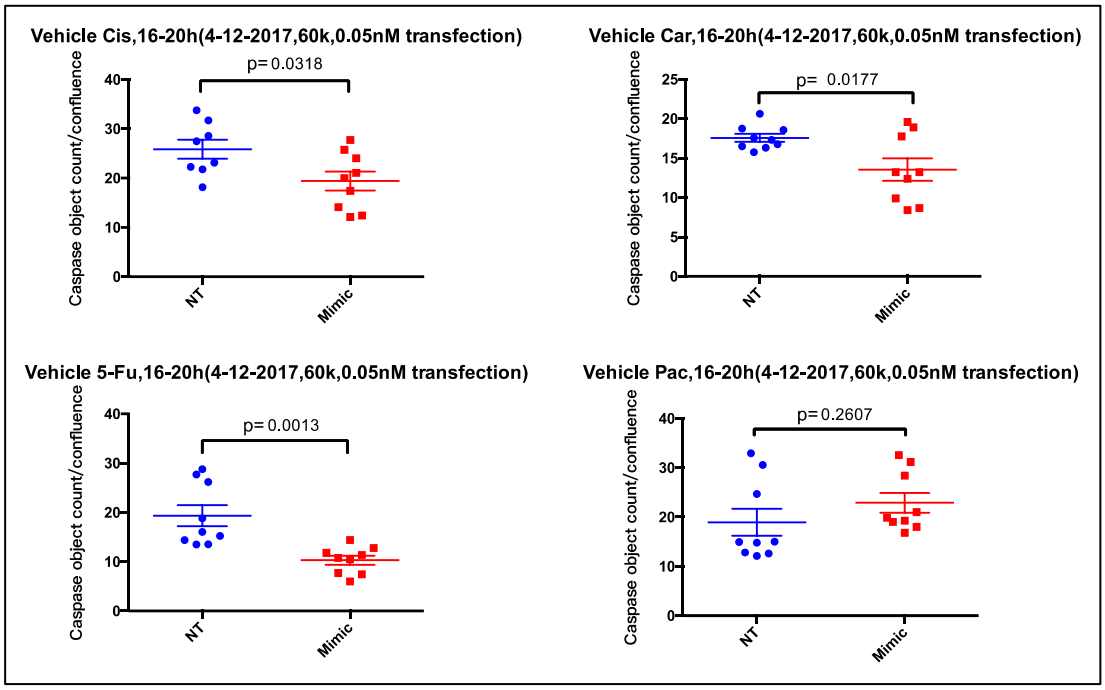

Figure 4-14. *The miR-451a mimic molecule decreased the apoptosis of OE33 at 0.05nM in 60k cell density after 16-20h treated with the vehicle control of Cisplatin(Cis), Carboplatin(Car), 5-Fu and Paclitaxel(Pac). NT: non-targeting molecule. The title of the graph includes the date of the experiment. The apoptosis experiment was only performed on 4-12-2017, not on the 17-8-2017 and 10-11-2017.*

4.5 The miR-451a increases the drug treatment resistance in OE33 as measured by Incucyte assay

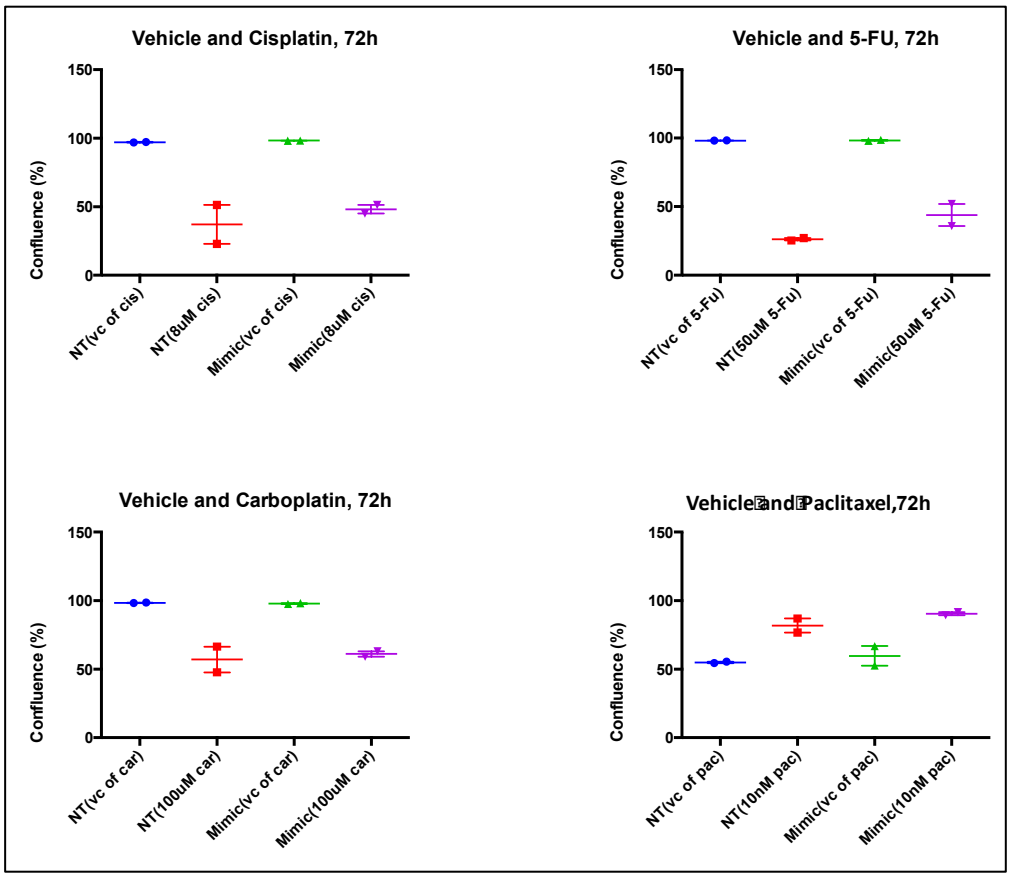

Figure 4-15. *The miR-451a affected the drug treatment response to Cisplatin, 5-Fu, Carboplatin and Paclitaxel after 72h treatment (17-8-2017,60k cell density,0.05nM miR-451a mimic transfection,72h treatment, there was something wrong in the Paclitaxel experiment because the cells were less after treated by the VC of Paclitaxel than treated by the Paclitaxel).*

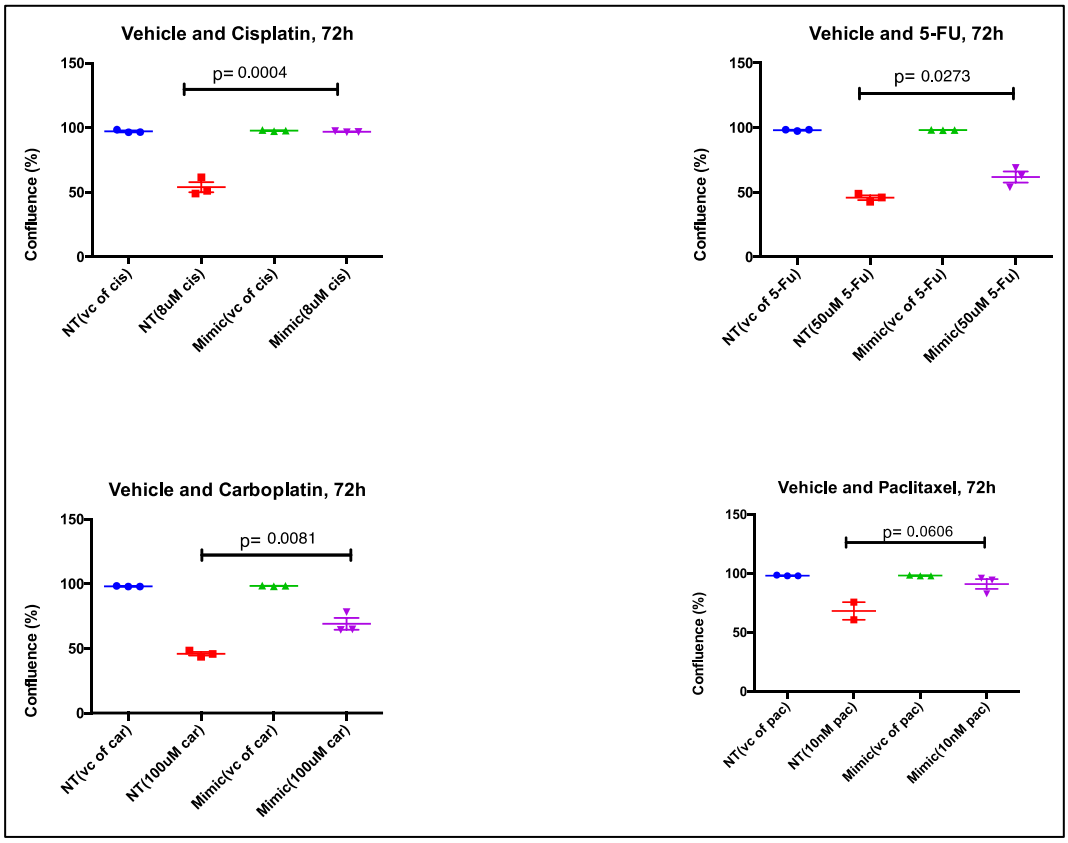

Figure 4-16. *The miR-451a increased the drug treatment response to Cisplatin, 5-Fu, Carboplatin and Paclitaxel (10-11-2017, 60k cell density,0.05nM miR-451a mimic transfection,72h treatment).*

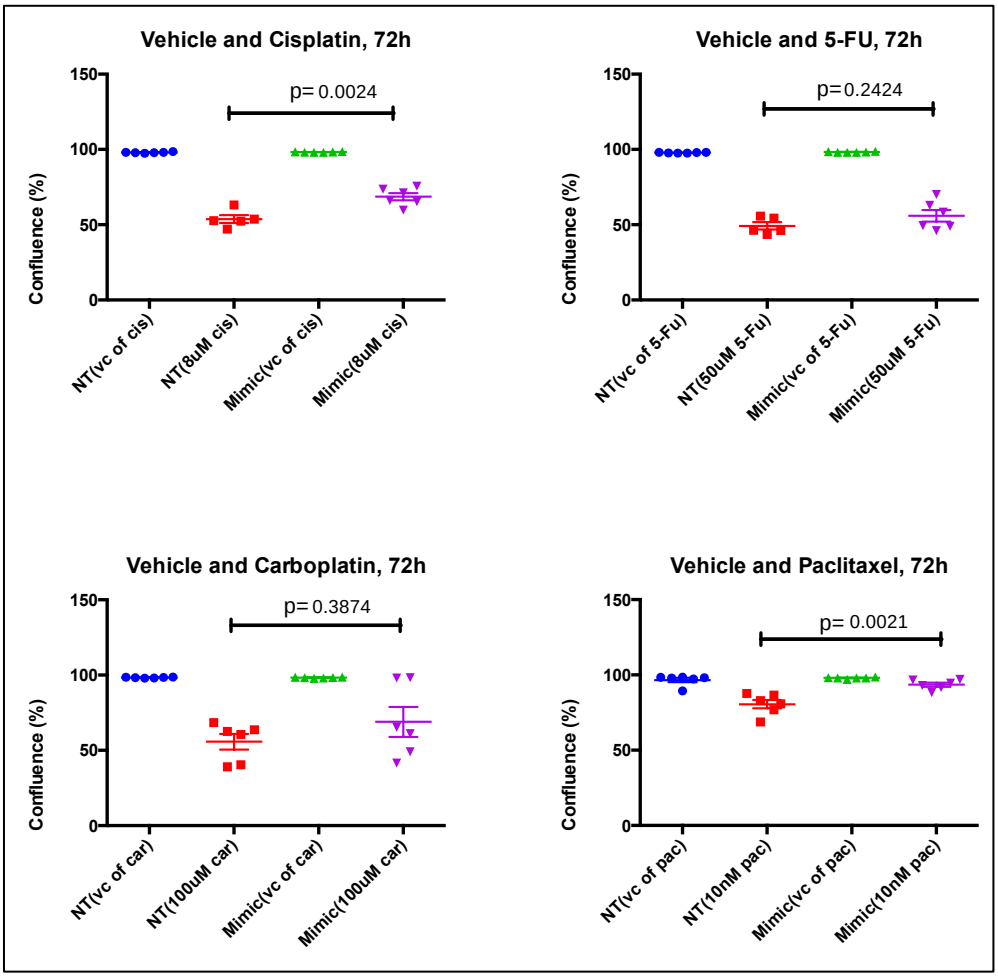

Figure 4-17*. The miR-451a increased the drug treatment response to Cisplatin, 5-Fu, Carboplatin and Paclitaxel after 72h treatment in trend (4-12-2017,60k cell density,0.05nM miR-451a mimic transfection,72h treatment).*

4.6 The expression of miR-451a related proteins in resistant and sensitive cell lines

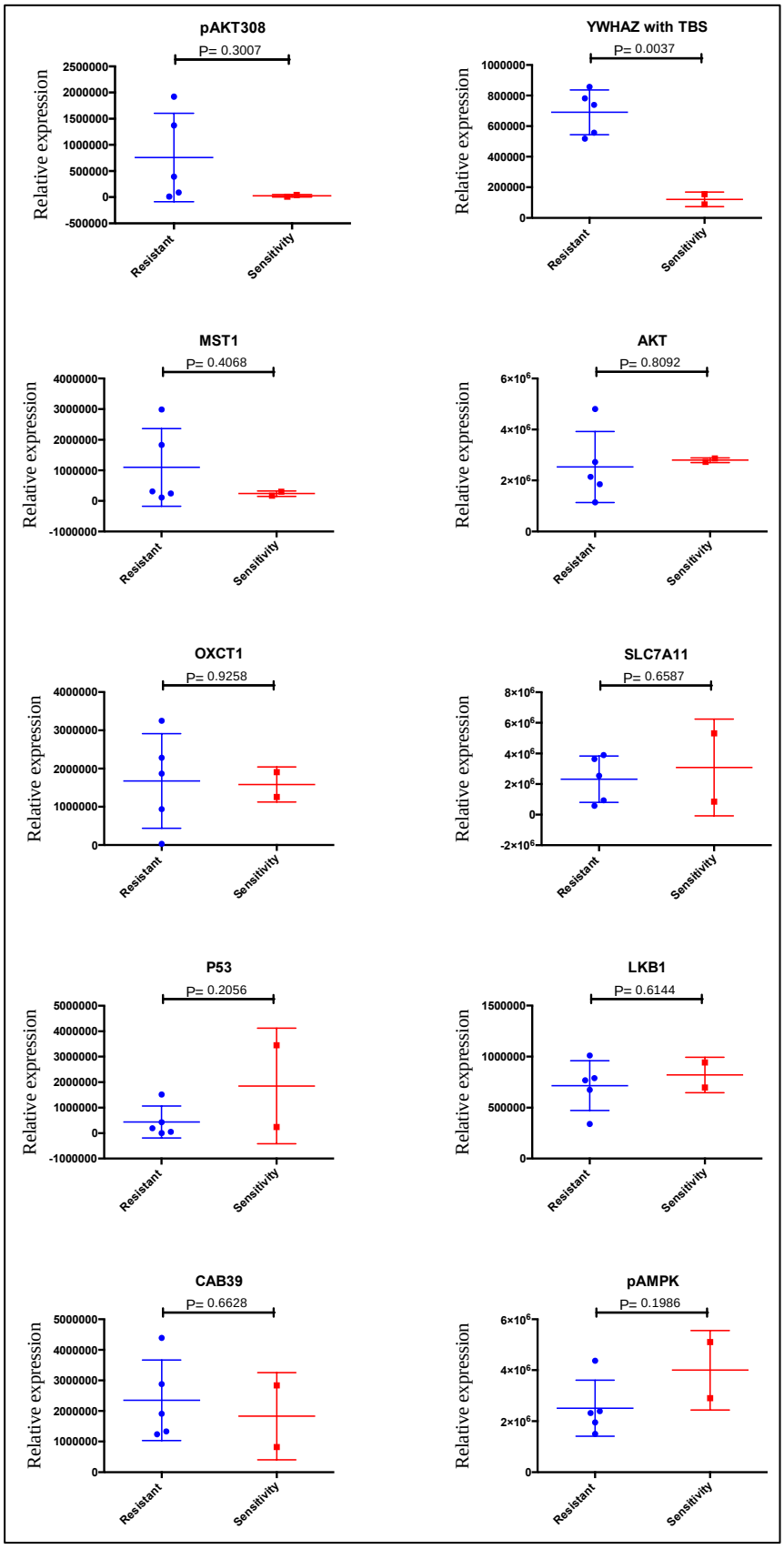

Figure 4-18. *The expression of miR-451a related proteins between resistant and*

sensitivity groups according to SF after irradiation.

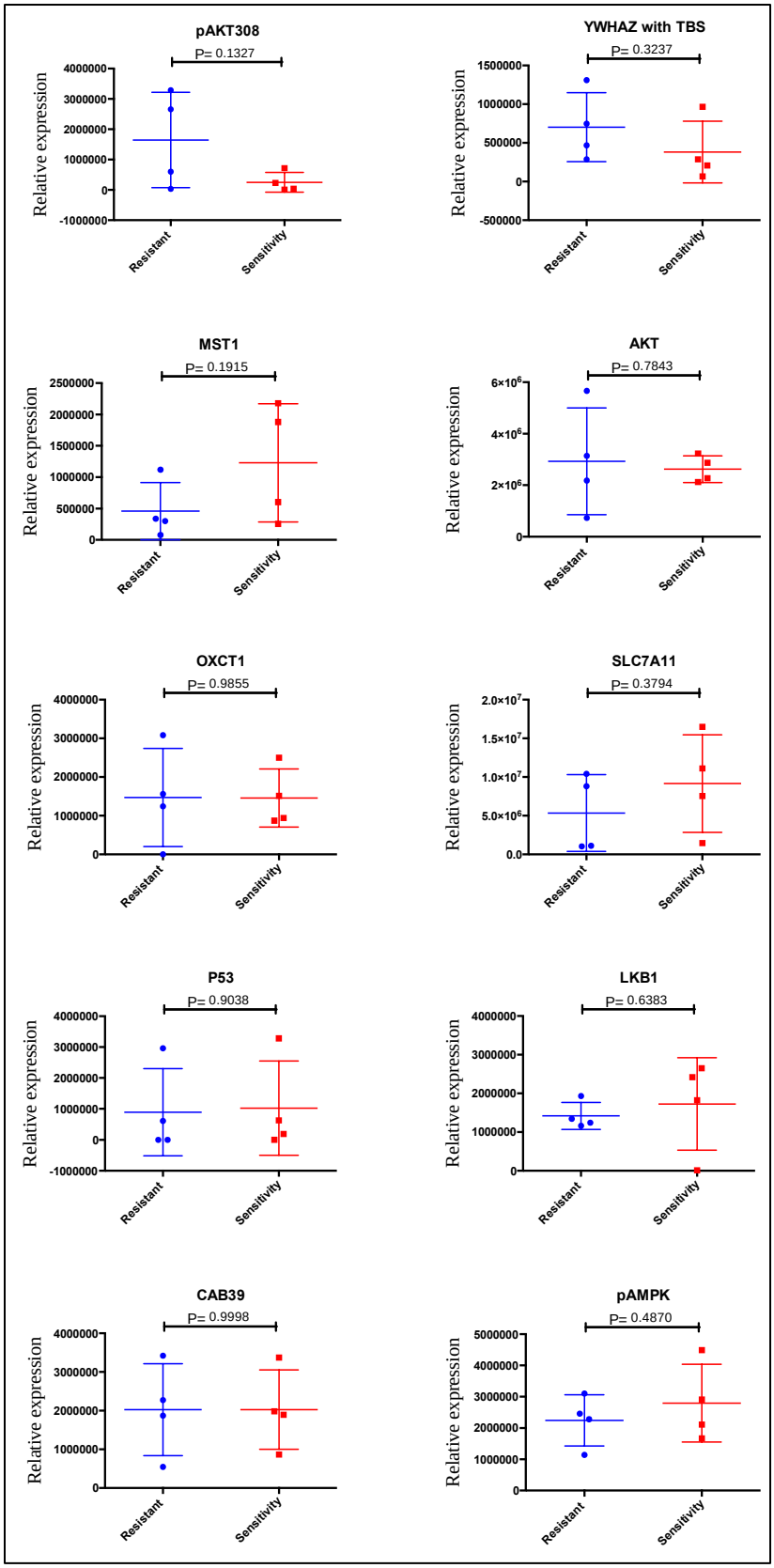

Figure 4-19. *The expression of miR-451a related proteins between resistant and sensitivity groups according to SF from Flow Cytometry after Cisplatin treatment.*

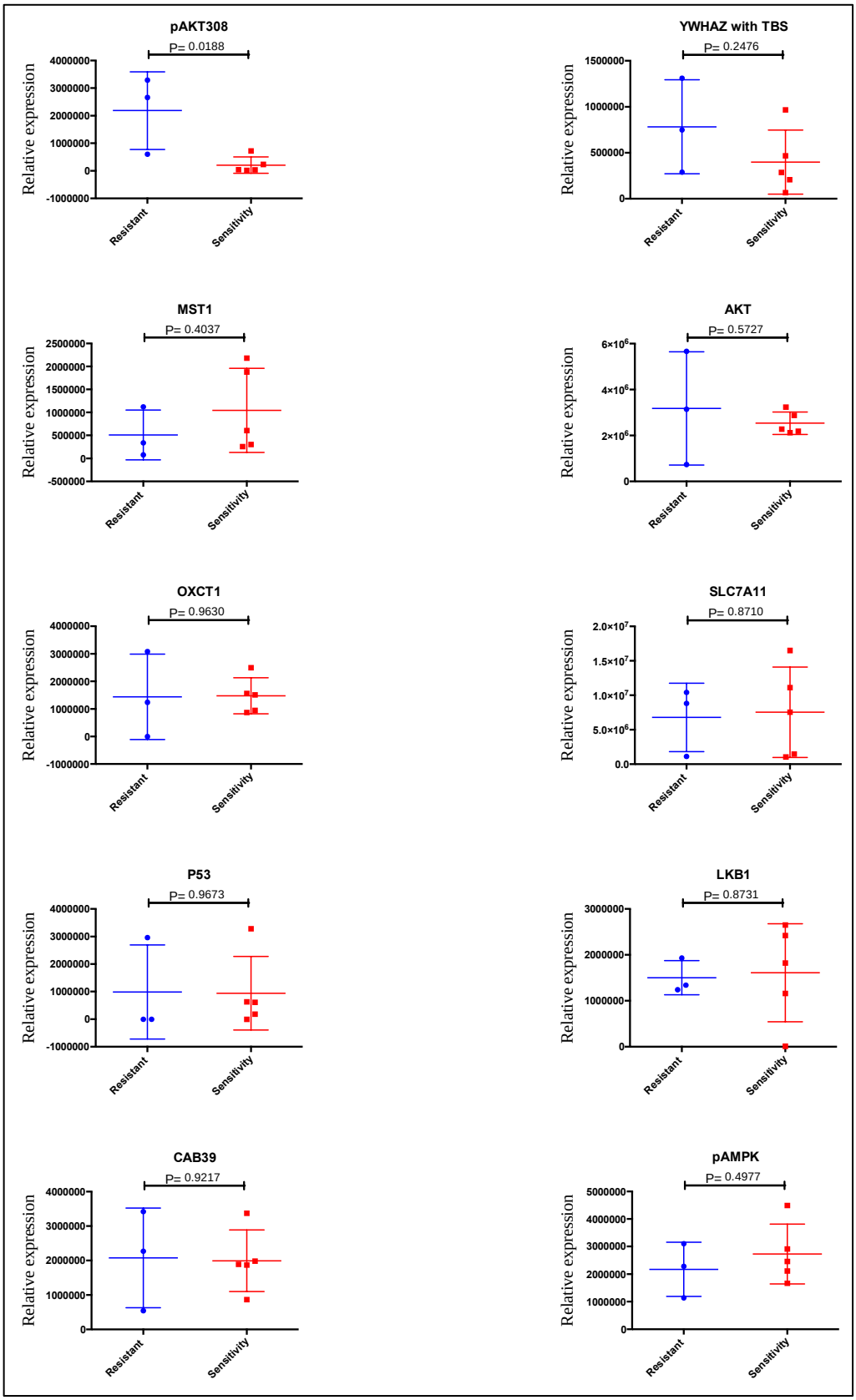

Figure 4-20. *The expression of miR-451a related proteins between resistant and sensitivity groups according to SF from MTS after Cisplatin treatment.*

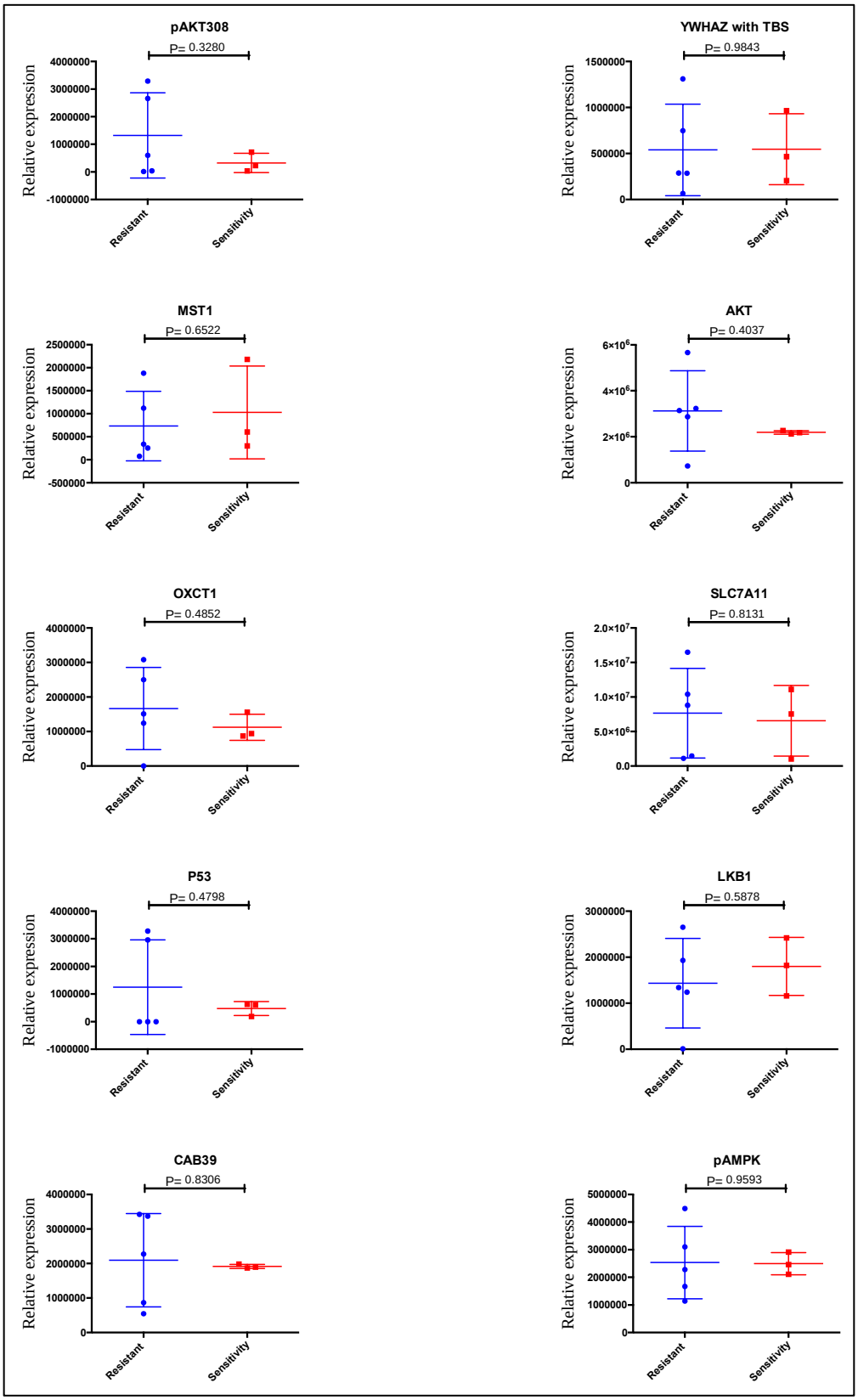
pAKT308
P= 0.3280
Relative expression
4000000
3000000
2000000
1000000
0
-1000000
Resistant
Sensitivity
YWHAZ with TBS
P= 0.9843
Relative expression
1500000
1000000
500000
0
Resistant
Sensitivity
MST1
P= 0.6522
Relative expression
2500000
2000000
1500000
1000000
500000
0
-500000
Resistant
Sensitivity
AKT
P= 0.4037
Relative expression
6×10^6
4×10^6
2×10^6
0
Resistant
Sensitivity
OXCT1
P= 0.4852
Relative expression
4000000
3000000
2000000
1000000
0
Resistant
Sensitivity
SLC7A11
P= 0.8131
Relative expression
2.0×10^7
1.5×10^7
1.0×10^7
5.0×10^6
0.0
Resistant
Sensitivity
P53
P= 0.4798
Relative expression
4000000
3000000
2000000
1000000
0
-1000000
Resistant
Sensitivity
LKB1
P= 0.5878
Relative expression
3000000
2000000
1000000
0
Resistant
Sensitivity
CAB39
P= 0.8306
Relative expression
4000000
3000000
2000000
1000000
0
Resistant
Sensitivity
pAMPK
P= 0.9593
Relative expression
5000000
4000000
3000000
2000000
1000000
0
Resistant
Sensitivity

***Figure 4-21**. The expression of miR-451a related proteins between resistant and sensitivity groups according to SF from Flow Cytometry after 5-Fu treatment.*

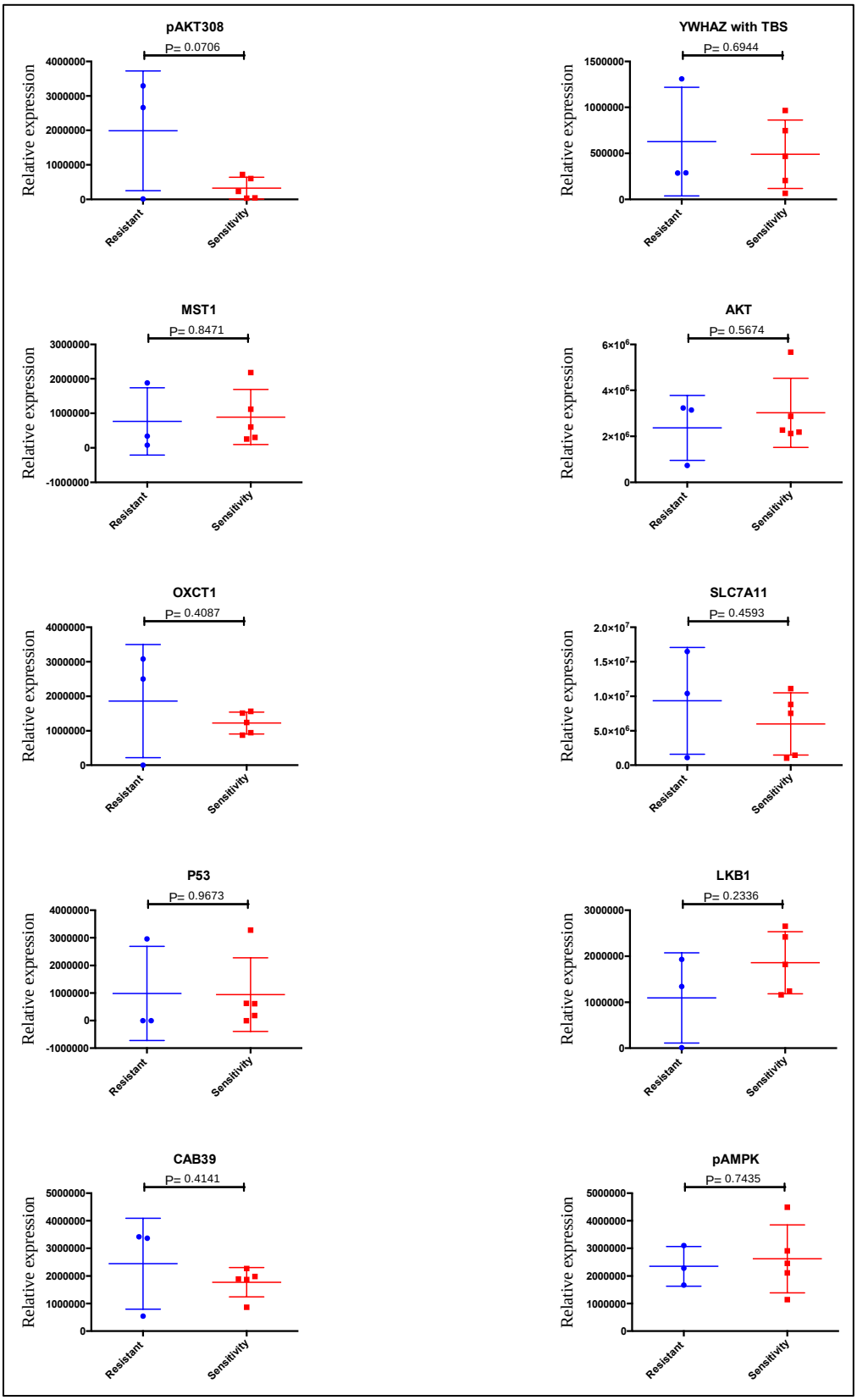
pAKT308
P= 0.0706
Relative expression
4000000
3000000
2000000
1000000
0
Resistant
Sensitivity
YWHAZ with TBS
P= 0.6944
Relative expression
1500000
1000000
500000
0
Resistant
Sensitivity
MST1
P= 0.8471
Relative expression
3000000
2000000
1000000
0
-1000000
Resistant
Sensitivity
AKT
P= 0.5674
Relative expression
6×10^6
4×10^6
2×10^6
0
Resistant
Sensitivity
OXCT1
P= 0.4087
Relative expression
4000000
3000000
2000000
1000000
0
Resistant
Sensitivity
SLC7A11
P= 0.4593
Relative expression
2.0×10^7
1.5×10^7
1.0×10^7
5.0×10^6
0.0
Resistant
Sensitivity
P53
P= 0.9673
Relative expression
4000000
3000000
2000000
1000000
0
-1000000
Resistant
Sensitivity
LKB1
P= 0.2336
Relative expression
3000000
2000000
1000000
0
Resistant
Sensitivity
CAB39
P= 0.4141
Relative expression
5000000
4000000
3000000
2000000
1000000
0
Resistant
Sensitivity
pAMPK
P= 0.7435
Relative expression
5000000
4000000
3000000
2000000
1000000
0
Resistant
Sensitivity

***Figure 4-22**. The expression of miR-451a related proteins between resistant and sensitivity groups according to SF from MTS after 5-Fu treatment.*

4.7 The cell density and the miRNA expression

The cell culture conditions such as the cell density might affect the expression of the miRNAs [27]. Therefore, the miRNA level was detected at low and high cell density separately to find out whether the miRNA expression was different or not. The RNA was extracted from 8 EAC cell lines with low cell density (45000 cells/ml) or high cell density (SKGT4 is 166667 cells/ml, OE19 is 250000 cells/ml, the other cell lines are 222222 cells/ml) separately. Then the qRT-PCR was performed for the miRNA expression. Four specific miRNAs were tested in the samples with two kinds of cell density. The let-7g-5p was chosen as the house keeping and all the miRNAs were normalized with let-7g-5p. Use of Let-7g-5p as a housekeeper is supported in[28] and has been confirmed by our other lab members in their experiments before I started this work. ~~lab~~.

The results indicated the miRNA expression was different in some cells lines between low and high cell density (Figure4-23), which means the cell density might affect the miRNA expression. Based on this finding, several cell densities were set in the following experiments.

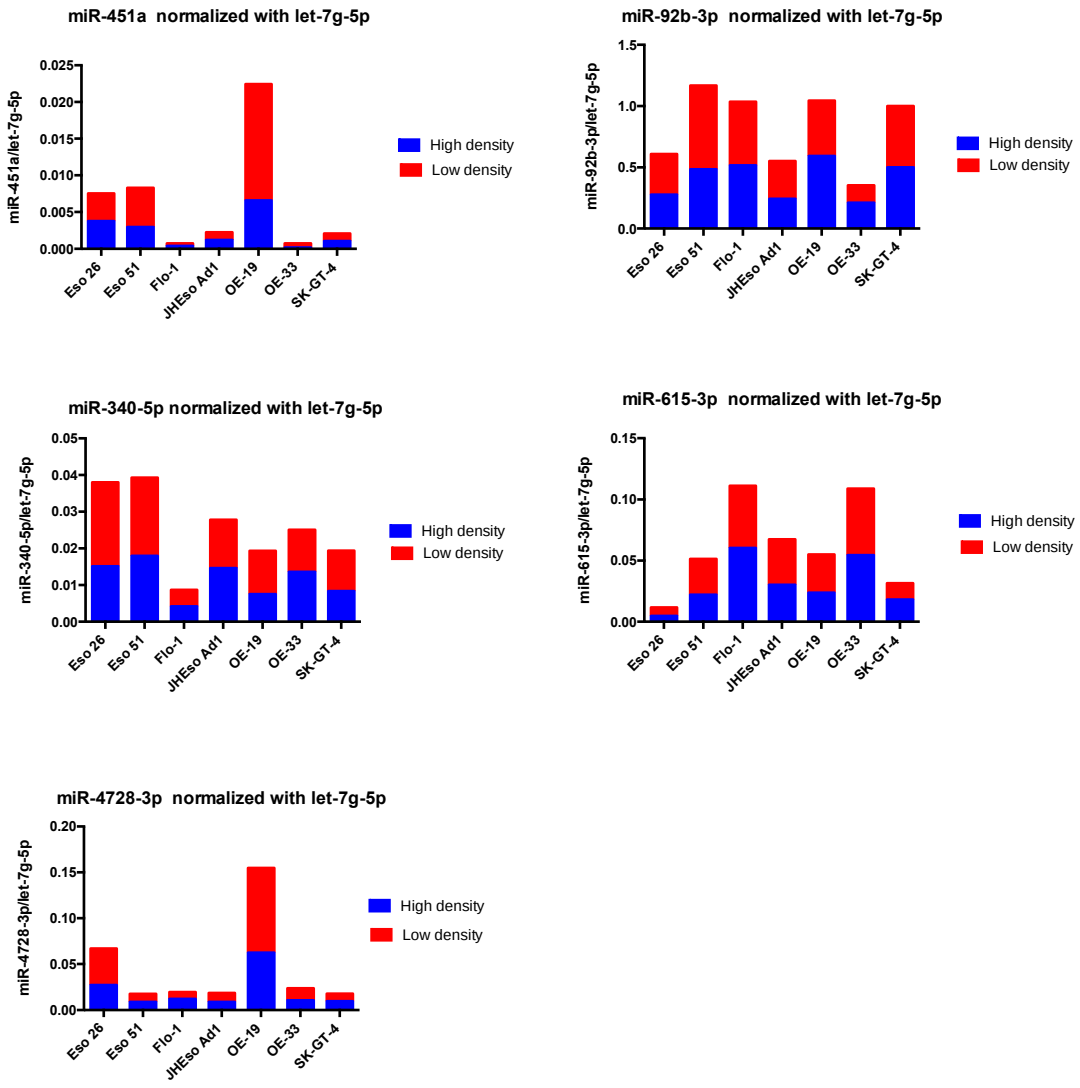

Figure 4-23. *The miRNA expression in high cell density(blue bar) and low cell density(red bar) in 7 EAC cell lines, all the data was normalized with let-7g-5p.*

4.8 Investigating evidence for specific mechanisms underlying the role of miR-451a in regulating drug/irradiation response

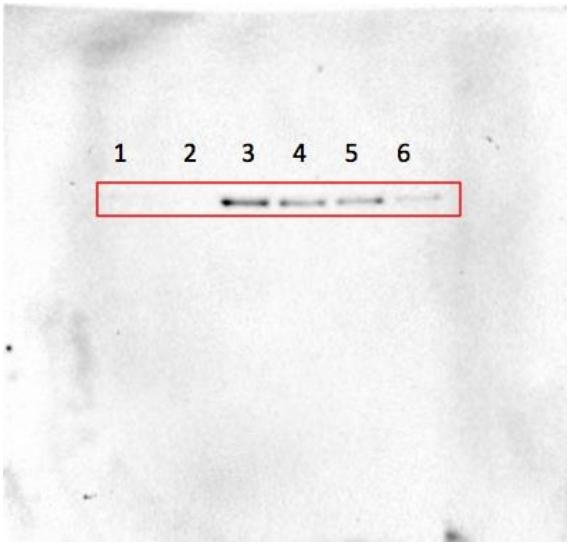

1. 171111, 60k, 0.05 mimics, OE33, untreated, at time of treatment, Drug, 13.11.2017
2. 171111, 60k, 0.05 non-binding, OE33, untreated, at time of treatment, Drug, 13.11.2017
3. 171111, 80k, 0.05 mimics, OE33, untreated, at time of treatment, Rad, 13.11.2017
4. 171111, 80k, 0.05 non-binding, OE33, untreated, at time of treatment, Rad, 13.11.17
5. 171111, 100k, 0.05 mimics, OE33, untreated, at time of treatment, Drug, 13.11.2017
6. 171111, 100k, 0.05 non-binding, OE33, untreated, at time of treatment, Drug, 13.11.2017

Figure 4-24. Bands of STK4/MST1 (60k, 80k, and 100k are the cell densities, i.e., the number of cells seeded in the 24-well plate: for e.g., 60k = 60,000 seeded cells)

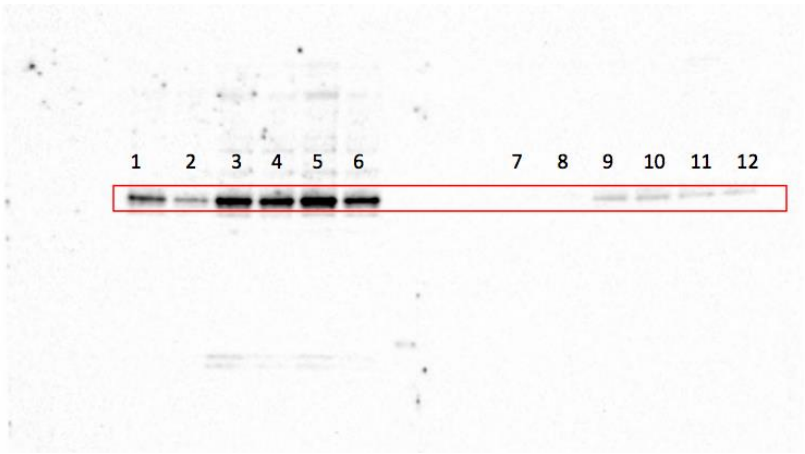

AKt:

1. 171111, 60k, 0.05 mimics, OE33, untreated, at time of treatment, Drug, 13.11.2017
2. 171111, 60k, 0.05 non-binding, OE33, untreated, at time of treatment, Drug, 13.11.2017
3. 171111, 80k, 0.05 mimics, OE33, untreated, at time of treatment, Rad, 13.11.2017
4. 171111, 80k, 0.05 non-binding, OE33, untreated, at time of treatment, Rad, 13.11.217
5. 171111, 100k, 0.05 mimics, OE33, untreated, at time of treatment, Drug, 13.11.2017
6. 171111, 100k, 0.05 non-binding, OE33, untreated, at time of treatment, Drug, 13.11.2017

pAKt:

7. 171111, 60k, 0.05 mimics, OE33, untreated, at time of treatment, Drug, 13.11.2017
8. 171111, 60k, 0.05 non-binding, OE33, untreated, at time of treatment, Drug, 13.11.2017
9. 171111, 80k, 0.05 mimics, OE33, untreated, at time of treatment, Rad, 13.11.2017
10. 171111, 80k, 0.05 non-binding, OE33, untreated, at time of treatment, Rad, 13.11.217
11. 171111, 100k, 0.05 mimics, OE33, untreated, at time of treatment, Drug, 13.11.2017
12. 171111, 100k, 0.05 non-binding, OE33, untreated, at time of treatment, Drug, 13.11.2017

Figure 4-25. Bands of pAkt308 and Akt (60k, 80k, and 100k are the cell densities, i.e., the number of cells seeded in the 24-well plate: for e.g., 60k = 60,000 seeded cells)

CHAPTER 5

IDENTIFICATION OF POTENTIAL SMALL RNA BIOMARKERS OF RESPONSE TO CHEMORADIOTHERAPY IN PRE-TREATMENT BLOOD FROM PATIENTS WITH LOCALLY ADVANCED EAC

5.1 Exploring small RNAs as biomarkers of response to chemoradiotherapy from serum exosomes by RNA Sequencing

S15/S17	S15 (RSAB01015)	S17 (RSAB01031)	RPKM DE	Taqman	direction in tissue	p value in tissue(AJCC0.V.123)	DE in tissue(AJCC0.V.123)	AUC in tissue(AJCC0.V.123)	p value in tissue(AJCC0.V.3)	DE in tissue(AJCC0.V.3)	AUC in tissue(AJCC0.V.3)	p value in tissue(AJCC012.V.3)	DE in tissue(AJCC012.V.3)	AUC in tissue(AJCC012.V.3)
hsa-miR-4728-3p	1623.000	6.644	244.277	this miRNA is not in the list of Taqman	Yes	0.915	0.811	0.515	0.456	1.459	0.630	0.143	1.954	0.700
hsa-miR-3605-3p	333.000	11.390	29.236	this miRNA is not in the list of Taqman	Yes	0.632	0.837	0.558	0.906	0.959	0.528	0.783	1.168	0.540
hsa-miR-615-3p	138.000	6.644	20.770	in the list of Taqman, but the data is empty	Yes	0.103	0.206	0.692	0.224	0.187	0.704	0.364	0.334	0.627
hsa-let-7b-3p	171.000	10.441	16.378	in the list of Taqman, but the data is empty	Yes	0.254	0.429	0.636	0.328	0.429	0.667	0.679	0.659	0.560
hsa-miR-141-3p	244.000	15.187	16.067	in the list of Taqman, but the data in S17 is empty	No	0.041	1.313	0.737	0.088	1.358	0.778	0.575	1.120	0.580
hsa-miR-3168	88.000	6.644	13.245	this miRNA is not in the list of Taqman	There is no this miRNA in tissue									
hsa-miR-32-5p	88.000	6.644	13.245	in the list of Taqman, but the data is empty	Yes	0.654	0.774	0.556	0.050	0.476	0.815	0.017	0.589	0.813
hsa-miR-660-5p	244.000	18.983	12.853	in the list of Taqman,the fold change in Taqman is 16.2	No	0.685	1.205	0.551	0.607	0.957	0.593	0.339	0.710	0.633
hsa-miR-10a-3p	48.000	6.644	7.224	in the list of Taqman, but the data is empty	No	0.334	1.475	0.616	0.607	1.346	0.593	0.942	1.100	0.487
hsa-miR-4732-5p	48.000	6.644	7.224	this miRNA is not in the list of Taqman	There is no this miRNA in tissue									
hsa-miR-31-5p	43.000	6.644	6.472	in the list of Taqman,the fold change in Taqman is 3.67	Yes	0.254	0.791	0.636	0.036	0.722	0.833	0.190	0.731	0.680
hsa-miR-200a-3p	38.000	6.644	5.719	in the list of Taqman, but the data is empty	Yes	0.848	0.682	0.525	0.529	0.654	0.611	0.679	0.844	0.560
hsa-miR-10a-5p	2936.000	537.224	5.465	in the list of Taqman,the fold change in Taqman is 1.31	Yes	0.020	0.801	0.768	0.026	0.724	0.852	0.117	0.756	0.713

S15/S17	S15 (RSAB01015)	S17 (RSAB01031)	RPKM DE	Taqman	direction in tissue	p value in tissue(AJCC0.V.123)	DE in tissue(AJCC0.V.123)	AUC in tissue(AJCC0.V.123)	p value in tissue(AJCC0.V.3)	DE in tissue(AJCC0.V.3)	AUC in tissue(AJCC0.V.3)	p value in tissue(AJCC012.V.3)	DE in tissue(AJCC012.V.3)	AUC in tissue(AJCC012.V.3)
hsa-miR-130b-3p	1522.000	281.900	5.399	in the list of Taqman,the fold change in Taqman is 10.24	Yes	0.915	0.711	0.515	0.864	0.830	0.463	0.532	1.368	0.587
hsa-miR-19a-3p	158.000	29.424	5.370	in the list of Taqman,the fold change in Taqman is 2.46	No	0.428	1.342	0.596	0.776	0.736	0.556	0.391	0.503	0.620
hsa-miR-29c-3p	158.000	29.424	5.370	in the list of Taqman,the fold change in Taqman is 1.92	Yes	0.453	0.781	0.409	0.864	0.561	0.537	0.339	0.542	0.633
hsa-miR-193b-5p	88.000	17.085	5.151	in the list of Taqman, but the data in S17 is empty	No	0.372	1.380	0.606	0.607	0.947	0.407	0.745	0.768	0.547
hsa-miR-7706	55.000	12.339	4.457	this miRNA is not in the list of Taqman	Yes	0.915	0.785	0.485	0.181	2.410	0.722	0.035	3.332	0.780
hsa-miR-204-5p	55.000	15.187	3.622	in the list of Taqman,the fold change in Taqman is 1.46	No	0.380	1.481	0.604	0.515	1.065	0.611	0.900	0.857	0.480
hsa-miR-375	1784.000	503.054	3.546	in the list of Taqman,the fold change in Taqman is 10.06	No	0.881	1.041	0.480	0.689	0.908	0.574	0.510	0.837	0.593
hsa-miR-27a-3p	1273.000	380.613	3.345	in the list of Taqman,the fold change in Taqman is 2.58	Yes	0.749	0.536	0.540	0.689	0.536	0.426	0.419	0.867	0.387
hsa-miR-181a-3p	43.000	13.288	3.236	in the list of Taqman, but the data is empty	No	0.535	1.327	0.576	0.145	1.795	0.741	0.190	1.486	0.680
hsa-miR-874-3p	177.000	55.051	3.215	in the list of Taqman, but the data is empty	No	0.881	1.287	0.520	0.776	1.168	0.556	0.643	1.038	0.567
hsa-miR-125b-2-3p	88.000	29.424	2.991	in the list of Taqman, but the data is empty	Yes	0.273	0.676	0.631	0.328	0.696	0.667	0.608	0.779	0.573
hsa-miR-21-3p	2936.000	983.328	2.986	in the list of Taqman, but the data is empty	No	0.103	0.615	0.692	0.113	0.579	0.759	0.339	1.434	0.633

S15/S17	S15 (RSAB01015)	S17 (RSAB01031)	RPKM DE	Taqman	direction in tissue	p value in tissue(AJCC0.V.123)	DE in tissue(AJCC0.V.123)	AUC in tissue(AJCC0.V.123)	p value in tissue(AJCC0.V.3)	DE in tissue(AJCC0.V.3)	AUC in tissue(AJCC0.V.3)	p value in tissue(AJCC012.V.3)	DE in tissue(AJCC012.V.3)	AUC in tissue(AJCC012.V.3)
hsa-miR-320a	2936.000	983.328	2.986	in the list of Taqman,the fold change in Taqman is 6.19	Yes	0.480	0.598	0.586	0.529	0.422	0.611	0.865	0.693	0.527
hsa-miR-148a-3p	2936.000	1026.040	2.861	in the list of Taqman,the fold change in Taqman is 3.53	No	0.654	1.454	0.556	0.456	0.743	0.630	0.208	0.662	0.673
hsa-miR-500a-3p	48.000	17.085	2.810	in the list of Taqman, but the data is empty	No	0.428	1.058	0.596	0.529	1.076	0.611	0.981	1.011	0.507
hsa-miR-100-5p	1273.000	479.325	2.656	in the list of Taqman,the fold change in Taqman is 23.59	No	0.848	1.020	0.475	0.113	2.074	0.759	0.060	1.935	0.753
hsa-miR-130a-3p	1148.000	450.850	2.546	in the list of Taqman,the fold change in Taqman is 3.05	No	0.273	1.554	0.631	0.036	2.767	0.833	0.009	2.692	0.840
hsa-miR-589-5p	36.000	14.237	2.529	in the list of Taqman, but the data is empty	Yes	0.113	0.643	0.687	0.529	0.824	0.611	0.510	1.235	0.593
hsa-miR-345-5p	855.000	380.613	2.246	in the list of Taqman,the fold change in Taqman is 2.62	Yes	0.848	0.845	0.475	0.607	1.166	0.593	0.478	1.594	0.600
hsa-miR-5189-5p	33.000	15.187	2.173	this miRNA is not in the list of Taqman	There is no this miRNA in tissue									
hsa-miR-148a-5p	14.000	6.644	2.107	in the list of Taqman, but the data is empty	Yes	1.000	0.990	0.500	0.272	0.839	0.685	0.158	0.672	0.693
hsa-miR-15b-3p	36.000	17.085	2.107	in the list of Taqman, but the data is empty	No	0.403	1.186	0.601	0.012	1.457	0.889	0.010	1.480	0.833
hsa-miR-15a-5p	584.000	281.900	2.072	in the list of Taqman, but the data is empty	No	0.094	1.717	0.697	0.456	1.228	0.630	0.827	0.752	0.467
hsa-miR-28-5p	25.000	12.339	2.026	in the list of Taqman,the fold change in Taqman is 0.62	Yes	0.254	0.899	0.636	0.328	0.783	0.667	0.789	0.824	0.540

Figure 5-1*, the miRNAs more than 2 times change in S15/S17 (the blue cells means the direction of fold change was same between Taqman and*

DESeq2, the orange cells means there was no this small RNA in tissue detected, the dark pink means the small RNA was significant in tissue data while the light pink means with a trend)

S17/S15	RNAS15 (RSAB01015)	RNAS17 (RSAB01031)	RPKM DE	Taqman	direction in tissue	p value in tissue(AJCC0.V.123)	DE in tissue(AJCC0.V.123)	AUC in tissue(AJCC0.V.123)	p value in tissue(AJCC0.V.3)	DE in tissue(AJCC0.V.3)	AUC in tissue(AJCC0.V.3)	p value in tissue(AJCC012.V.3)	DE in tissue(AJCC012.V.3)	AUC in tissue(AJCC012.V.3)
hsa-miR-186-5p	357.000	1313.635	3.680	in the list of Taqman,the fold change in Taqman is less 2	No	0.949	0.817	0.490	0.864	0.793	0.463	0.903	1.006	0.480
hsa-let-7d-5p	138.000	537.224	3.893	in the list of Taqman,the fold change in Taqman is less 2	Yes	0.685	1.325	0.551	1.000	1.175	0.500	0.575	1.093	0.420
hsa-miR-26b-3p	34.000	146.170	4.299	in the list of Taqman, but the data is empty	Yes	0.711	1.615	0.545	0.034	3.964	0.843	0.018	3.273	0.820
hsa-miR-409-3p	158.000	685.292	4.337	in the list of Taqman,the fold change in Taqman is less 2	No	0.564	0.723	0.571	0.955	0.950	0.481	0.314	1.403	0.640
hsa-miR-181a-2-3p	25.000	113.899	4.556	in the list of Taqman, but the data is empty in S17	No	0.716	0.933	0.545	1.000	0.930	0.500	0.789	0.994	0.460
hsa-miR-143-3p	333.000	1517.704	4.558	in the list of Taqman,the fold change in Taqman is less 2	No	0.623	0.895	0.561	0.456	0.810	0.630	0.715	0.835	0.553
hsa-miR-23b-3p	36.000	164.204	4.561	in the list of Taqman, but the data is empty	No	0.188	0.798	0.657	0.328	0.760	0.667	0.291	0.888	0.647
hsa-let-7e-5p	46.000	240.137	5.220	in the list of Taqman,the fold change in Taqman is less 2	No	0.356	0.903	0.611	0.955	1.037	0.481	0.643	1.205	0.567
hsa-miR-30b-3p	55.000	311.324	5.660	in the list of Taqman,the	There is no this miRNA in tissue									
hsa-miR-374a-5p	2.000	11.390	5.695	in the list of Taqman,the	Yes	0.428	1.162	0.596	0.456	1.259	0.630	0.679	1.255	0.560

hsa-miR-485-5p	2.000	11.390	5.695	in the list of Taqman, but the data is empty	No	0.313	0.784	0.621	0.776	0.900	0.556	0.575	1.114	0.580
hsa-miR-342-3p	25.000	146.170	5.847	in the list of Taqman,the fold change in Taqman is less 2	No	0.915	0.937	0.485	0.689	0.970	0.426	0.679	1.045	0.560
hsa-miR-15b-5p	12.000	70.238	5.853	in the list of Taqman,the fold change in Taqman is 0.39	Yes	0.654	1.091	0.556	0.272	1.347	0.685	0.117	1.432	0.713
hsa-miR-424-3p	12.000	70.238	5.853	in the list of Taqman, but the data is empty	No	0.046	0.757	0.732	0.607	0.830	0.593	0.679	1.094	0.560
hsa-miR-30b-5p	32.000	191.730	5.992	in the list of Taqman,the fold change in Taqman is less 2	Yes	0.716	1.120	0.455	0.388	0.869	0.648	0.268	0.725	0.653
hsa-miR-342-5p	48.000	299.934	6.249	in the list of Taqman, but the data is empty	Yes	0.949	1.361	0.510	0.456	2.267	0.630	0.208	1.789	0.673
hsa-miR-340-3p	2.000	13.288	6.644	in the list of Taqman,the fold change in Taqman is less 2	No	0.480	0.888	0.586	1.000	1.117	0.500	0.608	1.139	0.573
hsa-miR-10b-5p	357.000	2414.659	6.764	in the list of Taqman,the fold change in Taqman is less 2	No	0.046	0.659	0.732	0.066	0.590	0.796	0.789	0.924	0.540
hsa-miR-223-3p	96.000	653.970	6.812	in the list of Taqman,the fold change in Taqman is 0.66	No	0.292	0.289	0.626	0.689	1.054	0.574	0.143	4.787	0.700
hsa-miR-335-3p	2.000	14.237	7.119	in the list of Taqman, but the data is empty	Yes	0.564	1.134	0.571	0.864	1.031	0.537	0.827	1.005	0.533

S17/S15	RNAS15 (RSAB01015)	RNAS17 (RSAB01031)	RPKM DE	Taqman	direction in tissue	p value in tissue(AJCC0.V.123)	DE in tissue(AJCC0.V.123)	AUC in tissue(AJCC0.V.123)	p value in tissue(AJCC0.V.3)	DE in tissue(AJCC0.V.3)	AUC in tissue(AJCC0.V.3)	p value in tissue(AJCC012.V.3)	DE in tissue(AJCC012.V.3)	AUC in tissue(AJCC012.V.3)
hsa-miR-132-3p	5.000	36.068	7.214	in the list of Taqman, but the data is empty in s15	No	0.103	0.877	0.692	0.388	0.901	0.648	0.789	0.877	0.540
hsa-miR-6852-5p	25.000	191.730	7.669	this miRNA is not in the list of Taqman	There is no this miRNA in tissue									
hsa-miR-541-3p	9.000	70.238	7.804	in the list of Taqman,the fold change in Taqman is less 2	There is no this miRNA in tissue									
hsa-miR-183-5p	20.000	156.611	7.831	in the list of Taqman, but the data is empty	No	0.453	0.693	0.591	0.864	1.035	0.463	0.715	1.828	0.553
hsa-miR-142-3p	36.000	299.934	8.332	in the list of Taqman,the fold change in Taqman is 0.45	No	0.881	0.923	0.480	0.607	1.118	0.593	0.542	1.068	0.587
hsa-miR-4446-3p	14.000	124.340	8.881	this miRNA is not in the list of Taqman	There is no this miRNA in tissue									
hsa-miR-139-5p	2.000	18.034	9.017	in the list of Taqman,the fold change in Taqman is less 2	Yes	0.428	1.104	0.596	0.864	1.018	0.537	0.903	1.016	0.480
hsa-miR-671-3p	47.000	424.274	9.027	in the list of Taqman,the fold change in Taqman is less 2	Yes	0.071	2.965	0.712	0.088	5.784	0.778	0.261	2.860	0.653
hsa-miR-654-3p	38.000	380.613	10.016	in the list of Taqman, but the data is empty	No	0.814	0.814	0.530	0.607	1.085	0.593	0.190	1.450	0.680
hsa-miR-483-3p	11.000	113.899	10.354	in the list of Taqman, but the data is empty	Yes	0.348	1.781	0.611	0.262	1.819	0.685	0.497	1.567	0.593

S17/S15	RNAS15 (RSAB01015)	RNAS17 (RSAB01031)	RPKM DE	Taqman	direction in tissue	p value in tissue(AJCC0.V.123)	DE in tissue(AJCC0.V.123)	AUC in tissue(AJCC0.V.123)	p value in tissue(AJCC0.V.3)	DE in tissue(AJCC0.V.3)	AUC in tissue(AJCC0.V.3)	p value in tissue(AJCC012.V.3)	DE in tissue(AJCC012.V.3)	AUC in tissue(AJCC012.V.3)
hsa-miR-132-3p	5.000	36.068	7.214	in the list of Taqman, but the data is empty in s15	No	0.103	0.877	0.692	0.388	0.901	0.648	0.789	0.877	0.540
hsa-miR-6852-5p	25.000	191.730	7.669	this miRNA is not in the list of Taqman	There is no this miRNA in tissue									
hsa-let-7f-5p	48.000	503.054	10.480	in the list of Taqman, but the data is empty in s15	No	0.593	0.991	0.566	0.224	0.943	0.704	0.542	0.901	0.587
hsa-miR-301a-3p	25.000	299.934	11.997	in the list of Taqman,the fold change in Taqman is less 2	There is no this miRNA in tissue									
hsa-miR-431-5p	25.000	299.934	11.997	in the list of Taqman, but the data is empty	No	0.100	0.286	0.692	0.670	0.533	0.574	0.527	1.555	0.587
hsa-miR-20a-5p	9.000	113.899	12.655	in the list of Taqman,the fold change in Taqman is 2.99	Yes	0.428	1.824	0.596	0.689	2.313	0.574	0.827	1.823	0.533
hsa-miR-148b-3p	25.000	326.511	13.060	in the list of Taqman,the fold change in Taqman is less 2	No	0.507	0.731	0.581	0.145	0.624	0.741	0.227	0.587	0.667
hsa-miR-5010-5p	8.000	106.306	13.288	this miRNA is not in the list of Taqman	There is no this miRNA in tissue									
hsa-let-7a-5p	5.000	70.238	14.048	in the list of Taqman, but the data is empty	No	0.654	0.850	0.444	0.529	0.967	0.389	0.715	1.003	0.553
hsa-miR-769-5p	16.000	230.646	14.415	in the list of Taqman, but the data is empty	Yes	0.033	1.263	0.747	0.388	1.052	0.648	0.608	0.907	0.573

S17/S15	RNAS15 (RSAB01015)	RNAS17 (RSAB01031)	RPKM DE	Taqman	direction in tissue	p value in tissue(AJCC0.V.123)	DE in tissue(AJCC0.V.123)	AUC in tissue(AJCC0.V.123)	p value in tissue(AJCC0.V.3)	DE in tissue(AJCC0.V.3)	AUC in tissue(AJCC0.V.3)	p value in tissue(AJCC012.V.3)	DE in tissue(AJCC012.V.3)	AUC in tissue(AJCC012.V.3)
hsa-miR-98-5p	16.000	230.646	14.415	in the list of Taqman, but the data is empty in s15	No	0.356	0.599	0.611	0.181	0.556	0.722	0.227	0.667	0.667
hsa-miR-323b-3p	11.000	164.204	14.928	this miRNA is not in the list of Taqman	There is no this miRNA in tissue									
hsa-miR-30a-3p	12.000	191.730	15.978	in the list of Taqman,the fold change in Taqman is less 2	Yes	0.749	1.090	0.460	0.388	0.869	0.648	0.510	0.805	0.593
hsa-miR-326	13.000	236.340	18.180	in the list of Taqman, but the data is empty	No	0.349	0.497	0.611	0.595	2.797	0.593	0.240	5.391	0.660
hsa-miR-155-5p	11.000	230.646	20.968	in the list of Taqman,the fold change in Taqman is 4.76	No	0.915	0.907	0.485	0.607	0.865	0.407	0.542	0.859	0.413
hsa-miR-101-3p	5.000	113.899	22.780	in the list of Taqman,the fold change in Taqman is less 2	Yes	0.781	1.014	0.535	0.776	1.167	0.556	0.715	1.270	0.553
hsa-miR-150-3p	10.000	316.070	31.607	this miRNA is not in the list of Taqman	There is no this miRNA in tissue									
hsa-miR-181c-5p	6.000	191.730	31.955	in the list of Taqman,the fold change in Taqman is less 2	Yes	0.983	1.096	0.505	0.955	1.098	0.519	0.920	0.998	0.517
hsa-miR-3173-5p	2.000	70.238	35.119	this miRNA is not in the list of Taqman	There is no this miRNA in tissue									
hsa-miR-381-3p	2.000	70.238	35.119	in the list of Taqman, but the data is empty in S17	No	0.356	0.600	0.611	0.955	0.768	0.519	0.391	1.027	0.620
hsa-miR-1301-3p	5.000	230.646	46.129	in the list of Taqman, but the data is empty	Yes	0.103	1.455	0.692	0.003	1.754	0.944	0.007	1.772	0.847
hsa-miR-30e-3p	10.000	537.224	53.722	in the list of Taqman,the fold change in Taqman is 10	No	0.915	0.931	0.515	0.776	0.850	0.556	0.981	0.975	0.493
hsa-miR-224-5p	2.000	113.899	56.950	in the list of Taqman,the fold change in Taqman is less 2	No	0.188	0.764	0.657	0.181	0.403	0.722	0.158	0.452	0.693
hsa-miR-1237-3p	2.000	159.459	79.729	this miRNA is not in the list of Taqman	There is no this miRNA in tissue									
hsa-miR-3614-5p	2.000	281.900	140.950	this miRNA is not in the list of Taqman	There is no this miRNA in tissue									
hsa-miR-1226-3p	2.000	503.054	251.527	this miRNA is not in the list of Taqman	There is no this miRNA in tissue									

***Figure 5-2**, the miRNAs more than 2 times change in S17/S15 (the blue cells means the direction was same between Taqman and Dseq2, the orange cells means there was no this small RNA in tissue detected, the dark pink means the small RNA was significant in tissue data while the light pink means with a trend).*

GC.length.norm	RNAS15	RNAS17	DE	direction in tissue	p value in tissue(AJCC0.V.123)	DE in tissue(AJCC0.V.123)	AUC in tissue(AJCC0.V.123)	p value in tissue(AJCC0.V.3)	DE in tissue(AJCC0.V.3)	AUC in tissue(AJCC0.V.3)	p value in tissue(AJCC012.V.3)	DE in tissue(AJCC012.V.3)	AUC in tissue(AJCC012.V.3)
DQ598008	168.000	9.039	18.587	No	0.236	1.403	0.641	0.272	1.835	0.685	0.518	1.199	0.587
DQ570687	31.000	9.039	3.430	Yes	0.814	0.984	0.470	0.776	0.751	0.556	0.291	0.817	0.647
DQ590386	112.000	41.577	2.694	There is no this piRNA in tissue									
DQ599711	40.000	17.173	2.329	There is no this piRNA in tissue									

***Figure 5-3**, the piRNAs more than 2 times change in S15/S17(the 'Yes' means the direction was same between data in tissue and Dseq2 data in serum, while 'No' means the direction was opposite between tissue and DESeq2, the dark pink means the small RNA was significant in tissue data while the light pink means with a trend).*

GC.length.norm	RNAS15	RNAS17	DE	direction in tissue	p value in tissue(AJC C0.V.123)	DE in tissue(AJC C0.V.123)	AUC in tissue(AJC C0.V.123)	p value in tissue(AJC C0.V.3)	DE in tissue(AJC C0.V.3)	AUC in tissue(AJC C0.V.3)	p value in tissue(AJC C012.V.3)	DE in tissue(AJC C012.V.3)	AUC in tissue(AJCC012.V.3)
DQ571591	7.000	53.328	7.618	No	0.135	0.824	0.677	0.018	0.764	0.870	0.158	0.890	0.693
DQ571335	7.000	119.309	17.044	No	0.135	0.855	0.677	0.026	0.773	0.852	0.085	0.872	0.733
DQ570339	7.000	160.435	22.919	Yes	0.623	1.174	0.439	0.529	0.991	0.611	0.364	0.852	0.627

***Figure 5-4**, the piRNAs more than 2 times change in S17/S15 (the 'Yes' means the direction was same between data in tissue and Dseq2 data in serum, while 'No' means the direction was opposite between tissue and DESeq2, the dark pink means the small RNA was significant in tissue data while the light pink means with a trend).*

GC- & length-normalised	RNAS15	RNAS17	RPKM-method DE	DESeq DE	direction in tissue	p value in tissue(AJCC0.V.123)	DE in tissue(AJCC0.V.123)	AUC in tissue(AJCC0.V.123)	p value in tissue(AJCC0.V.3)	DE in tissue(AJCC0.V.3)	AUC in tissue(AJCC0.V.3)	p value in tissue(AJCC012.V.3)	DE in tissue(AJCC012.V.3)	AUC in tissue(AJCC012.V.3)
SNORD42A	38.000	1.044	36.406	5.532	Yes	0.356	0.645	0.611	0.529	0.694	0.611	0.902	0.976	0.520
SNORA71B	38.000	1.044	36.406	5.532	There is no this snoRNA in tissue									
SNORD58B	15.000	0.522	28.741	5.625	No	0.006	1.210	0.813	0.003	1.263	0.944	0.012	1.149	0.827
SNORD123	38.000	1.566	24.271	4.821	No	0.006	1.268	0.813	0.036	1.231	0.833	0.428	1.285	0.607
SNORD102	38.000	2.088	18.203	4.301	No	0.236	1.077	0.641	0.456	0.940	0.630	0.174	0.914	0.687
SNORA76A	15.000	1.566	9.580	3.280	There is no this snoRNA in tissue									
SNORD97	4.000	0.522	7.664	3.148	Yes	0.078	0.540	0.707	0.456	0.762	0.630	0.949	0.965	0.507
SNORD28	4.000	0.522	7.664	3.148	No	0.949	0.990	0.490	0.776	0.969	0.556	0.509	0.889	0.593
SNORD105B	4.000	0.522	7.664	3.148	Yes	0.564	0.836	0.571	0.224	0.717	0.704	0.190	0.876	0.680
SNORA5C	10.000	1.566	6.387	2.889	No	0.254	1.310	0.636	0.224	1.511	0.704	0.197	1.250	0.673
SNORD118	3.000	0.522	5.748	2.590	No	0.446	1.063	0.591	0.776	1.075	0.556	0.865	1.067	0.527
SNORD41	3.000	0.522	5.748	2.590	Yes	0.379	0.587	0.606	0.328	0.626	0.667	0.478	0.952	0.600
SNORD95	5.000	1.044	4.790	2.419	No	1.000	1.007	0.500	0.456	0.971	0.630	0.247	0.943	0.660
SNORD12B	10.000	2.088	4.790	2.364	No	0.094	1.051	0.697	0.328	1.070	0.667	0.542	1.016	0.587

***Figure 5-5**, the snoRNAs more than 2 times change in S15/S17 (the 'Yes' means the direction was same between data in tissue and Dseq2 data in serum, while 'No' means the direction was opposite between tissue and DESeq2, the dark pink means the small RNA was significant in tissue data while the light pink means with a trend).*

GC- & length-normalised	RNAS15	RNAS17	RPKM-method DE	DESeq DE	direction in tissue	p value in tissue(AJCC0.V.123)	DE in tissue(AJCC0.V.123)	AUC in tissue(AJCC0.V.123)	p value in tissue(AJCC0.V.3)	DE in tissue(AJCC0.V.3)	AUC in tissue(AJCC0.V.3)	p value in tissue(AJCC012.V.3)	DE in tissue(AJCC012.V.3)	AUC in tissue(AJCC012.V.3)
SNORD104	21.000	41.752	1.988	2.477	Yes	0.663	1.008	0.553	1.000	0.993	0.500	0.980	1.009	0.500
SNORD6	2.000	4.175	2.088	2.245	Yes	0.039	1.056	0.742	0.689	1.029	0.574	0.643	0.977	0.567
SNORD1B	1.000	2.088	2.088	2.140	Yes	0.794	1.005	0.467	0.456	0.981	0.630	0.504	0.947	0.593
SNORD83A	4.000	9.394	2.349	2.199	Yes	0.648	1.048	0.556	0.776	1.021	0.444	0.448	0.919	0.607
SNORD43	6.000	15.657	2.609	2.183	Yes	0.219	1.008	0.646	0.388	1.005	0.648	0.760	1.022	0.540
SNORD20	10.000	41.752	4.175	3.860	Yes	0.593	1.055	0.566	0.864	1.063	0.537	0.760	1.044	0.540
SNORD38B	1.000	5.219	5.219	3.942	There is no this snoRNA in tissue									
SNORD57	4.000	41.752	10.438	6.000	Yes	0.094	1.050	0.697	0.689	1.029	0.574	0.865	0.999	0.527
SNORD25	2.000	22.963	11.482	4.502	Yes	0.781	1.010	0.535	0.955	1.007	0.481	0.714	0.944	0.553
SNORA64	1.000	15.657	15.657	4.663	No	0.188	0.762	0.657	0.272	0.723	0.685	0.608	0.922	0.573
SNORA71A	2.000	41.752	20.876	7.801	No	0.915	0.950	0.515	0.864	1.163	0.537	0.687	1.087	0.553
SNORD10	1.000	41.752	41.752	3.646	Yes	0.535	1.059	0.576	0.529	1.104	0.611	0.428	1.612	0.607
SNORD37	1.000	41.752	41.752	3.646	No	0.064	0.526	0.717	0.018	0.512	0.870	0.143	0.740	0.700

***Figure 5-6**, the snoRNAs more than 2 times change in S17/S15(the 'Yes' means the direction was same between data in tissue and Dseq2 data in serum, while 'No' means the direction was opposite between tissue and DESeq2, the dark pink means the small RNA was significant in tissue data while the light pink means with a trend).*

	RNAS15	RNAS17	RPKM-method DE	DESeq2 DE	direction in tissue	p value in tissue(AJCC0.V.123)	DE in tissue(AJCC0.V.123)	AUC in tissue(AJCC0.V.123)	p value in tissue(AJCC0.V.3)	DE in tissue(AJCC0.V.3)	AUC in tissue(AJCC0.V.3)	p value in tissue(AJCC012.V.3)	DE in tissue(AJCC012.V.3)	AUC in tissue(AJCC012.V.3)
RNU11	18.000	8.074	2.229	1.294	No	0.654	1.066	0.556	0.328	0.911	0.667	0.318	1.023	0.637
RNU2-50P	18.000	8.074	2.229	1.294	There is no this snRNA in tissue									

Figure 5-7*, the snRNAs more than 2 times change in S15/S17 (the 'Yes' means the direction was same between data in tissue and Dseq2 data in serum, while 'No' means the direction was opposite between tissue and DESeq2, the dark pink means the small RNA was significant in tissue data while the light pink means with a trend).*

	RNAS15	RNAS17	RPKM-method DE	DESeq2 DE	direction in tissue	p value in tissue(AJCC0.V.123)	DE in tissue(AJCC0.V.123)	AUC in tissue(AJCC0.V.123)	p value in tissue(AJCC0.V.3)	DE in tissue(AJCC0.V.3)	AUC in tissue(AJCC0.V.3)	p value in tissue(AJCC012.V.3)	DE in tissue(AJCC012.V.3)	AUC in tissue(AJCC012.V.3)
RNU12	6.000	16.148	2.691	1.486	No	0.593	0.964	0.566	1.000	0.984	0.500	0.743	1.016	0.547
RNU4-2	6.000	16.148	2.691	1.486	No	0.564	0.985	0.571	0.388	0.857	0.648	0.569	1.007	0.580
RNU6-254P	6.000	12.111	2.019	1.340	There is no this snRNA in tissue									

Figure 5-8*, the snRNAs more than 2 times change in S17/S15 (the 'Yes' means the direction was same between data in tissue and Dseq2 data in serum, while 'No' means the direction was opposite between tissue and DESeq2, the dark pink means the small RNA was significant in tissue data while the light pink means with a trend).*

5.2Comparison of the sequencing data with the matched OpenArray data

***Table 5-1**, The Taqman OpenArray data in S15/17*

Taqman	Fold change
hsa-miR-100-5p	23.587
hsa-miR-660-5p	16.221
hsa-miR-99a-5p	14.620
hsa-miR-192-5p	11.472
hsa-miR-130b-3p	10.238
hsa-miR-375	10.056
hsa-miR-152-3p	9.448
hsa-miR-92a-3p	6.498
hsa-miR-320a	6.190
hsa-miR-222-3p	5.502
hsa-miR-155-5p	4.758
hsa-miR-21-5p	4.084
hsa-miR-215-5p	3.945
hsa-miR-31-5p	3.670
hsa-miR-146a-5p	3.553
hsa-miR-148a-3p	3.531
hsa-miR-532-5p	3.411
hsa-miR-25-3p	3.294
hsa-miR-30a-5p	3.112
hsa-miR-130a-3p	3.053
hsa-miR-20a-5p	2.990
hsa-miR-636	2.990
hsa-miR-361-5p	2.884
hsa-miR-30d-5p	2.782
hsa-miR-345-5p	2.621
hsa-miR-27a-3p	2.585
hsa-miR-19a-3p	2.462
hsa-miR-328-3p	2.362
hsa-miR-410-3p	2.157
hsa-miR-335-5p	2.144
hsa-miR-340-5p	2.128
hsa-miR-324-3p	2.100
hsa-miR-339-3p	2.041
hsa-miR-148b-3p	2.002

***Table 5-2**, The sequencing data in S15/17*

Seqencing	Fold change
hsa-miR-4728-3p	244.277
hsa-miR-3605-3p	29.236
hsa-miR-615-3p	20.770
hsa-let-7b-3p	16.378
hsa-miR-141-3p	16.067
hsa-miR-3168	13.245
hsa-miR-32-5p	13.245
hsa-miR-660-5p	12.853
hsa-miR-10a-3p	7.224
hsa-miR-4732-5p	7.224
hsa-miR-31-5p	6.472
hsa-miR-200a-3p	5.719
hsa-miR-10a-5p	5.465
hsa-miR-130b-3p	5.399
hsa-miR-19a-3p	5.370
hsa-miR-29c-3p	5.370
hsa-miR-193b-5p	5.151
hsa-miR-7706	4.457
hsa-miR-204-5p	3.622
hsa-miR-375	3.546
hsa-miR-27a-3p	3.345
hsa-miR-181a-3p	3.236
hsa-miR-874-3p	3.215
hsa-miR-125b-2-3p	2.991
hsa-miR-21-3p	2.986
hsa-miR-320a	2.986
hsa-miR-148a-3p	2.861
hsa-miR-500a-3p	2.810
hsa-miR-100-5p	2.656
hsa-miR-130a-3p	2.546
hsa-miR-589-5p	2.529
hsa-miR-345-5p	2.246
hsa-miR-5189-5p	2.173
hsa-miR-148a-5p	2.107
hsa-miR-15b-3p	2.107
hsa-miR-15a-5p	2.072
hsa-miR-28-5p	2.026

***Table 5-3**, The Taqman OpenArray data in S17/15*

Taqman	Fold change
hsa-miR-142-3p	2.219
hsa-miR-15b-5p	2.549
hsa-miR-144-5p	2.639
hsa-miR-26a-5p	2.713
hsa-let-7d-5p	2.868
hsa-miR-30e-3p	10.196

***Table 5-4**, The sequencing data in S17/15*

Seqencing	Fold change
hsa-miR-186-5p	3.680
hsa-let-7d-5p	3.893
hsa-miR-26b-3p	4.299
hsa-miR-409-3p	4.337
hsa-miR-181a-2-3p	4.556
hsa-miR-143-3p	4.558
hsa-miR-23b-3p	4.561
hsa-let-7e-5p	5.220
hsa-miR-30b-3p	5.660
hsa-miR-374a-5p	5.695
hsa-miR-485-5p	5.695
hsa-miR-342-3p	5.847
hsa-miR-15b-5p	5.853
hsa-miR-424-3p	5.853
hsa-miR-30b-5p	5.992
hsa-miR-342-5p	6.249
hsa-miR-340-3p	6.644
hsa-miR-10b-5p	6.764
hsa-miR-223-3p	6.812
hsa-miR-335-3p	7.119
hsa-miR-132-3p	7.214
hsa-miR-6852-5p	7.669
hsa-miR-541-3p	7.804
hsa-miR-183-5p	7.831
hsa-miR-142-3p	8.332
hsa-miR-4446-3p	8.881
hsa-miR-139-5p	9.017
hsa-miR-671-3p	9.027
hsa-miR-654-3p	10.016
hsa-miR-483-3p	10.354
hsa-let-7f-5p	10.480
hsa-miR-301a-3p	11.997

hsa-miR-431-5p	11.997
hsa-miR-20a-5p	12.655
hsa-miR-148b-3p	13.060
hsa-miR-5010-5p	13.288
hsa-let-7a-5p	14.048
hsa-miR-769-5p	14.415
hsa-miR-98-5p	14.415
hsa-miR-323b-3p	14.928
hsa-miR-30a-3p	15.978
hsa-miR-326	18.180
hsa-miR-155-5p	20.968
hsa-miR-101-3p	22.780
hsa-miR-150-3p	31.607
hsa-miR-181c-5p	31.955
hsa-miR-3173-5p	35.119
hsa-miR-381-3p	35.119
hsa-miR-1301-3p	46.129
hsa-miR-30e-3p	53.722
hsa-miR-224-5p	56.950
hsa-miR-1237-3p	79.729
hsa-miR-3614-5p	140.950
hsa-miR-1226-3p	251.527

***Table 5-5**, The overlapped miRNA of S15/17 between Taqman OpenArray and sequencing data*

OVERLAP
hsa-miR-100-5p
hsa-miR-660-5p
hsa-miR-130b-3p
hsa-miR-375
hsa-miR-320a
hsa-miR-31-5p
hsa-miR-148a-3p
hsa-miR-130a-3p
hsa-miR-345-5p
hsa-miR-27a-3p
hsa-miR-19a-3p

***Table 5-6**, The overlapped miRNA of S17/15 between Taqman OpenArray and sequencing data*

OVERLAP
hsa-miR-142-3p
hsa-miR-15b-5p
hsa-let-7d-5p
hsa-miR-30e-3p

CHAPTER 6
INVESTIGATION OF THE ROLE OF BLOOD SMALL RNAS IN REGULATING CHEMORADIOTHERAPY RESPONSE IN EAC CELLS

6.1 Investigation of the baseline cellular levels of small RNAs between resistant and sensitive cells

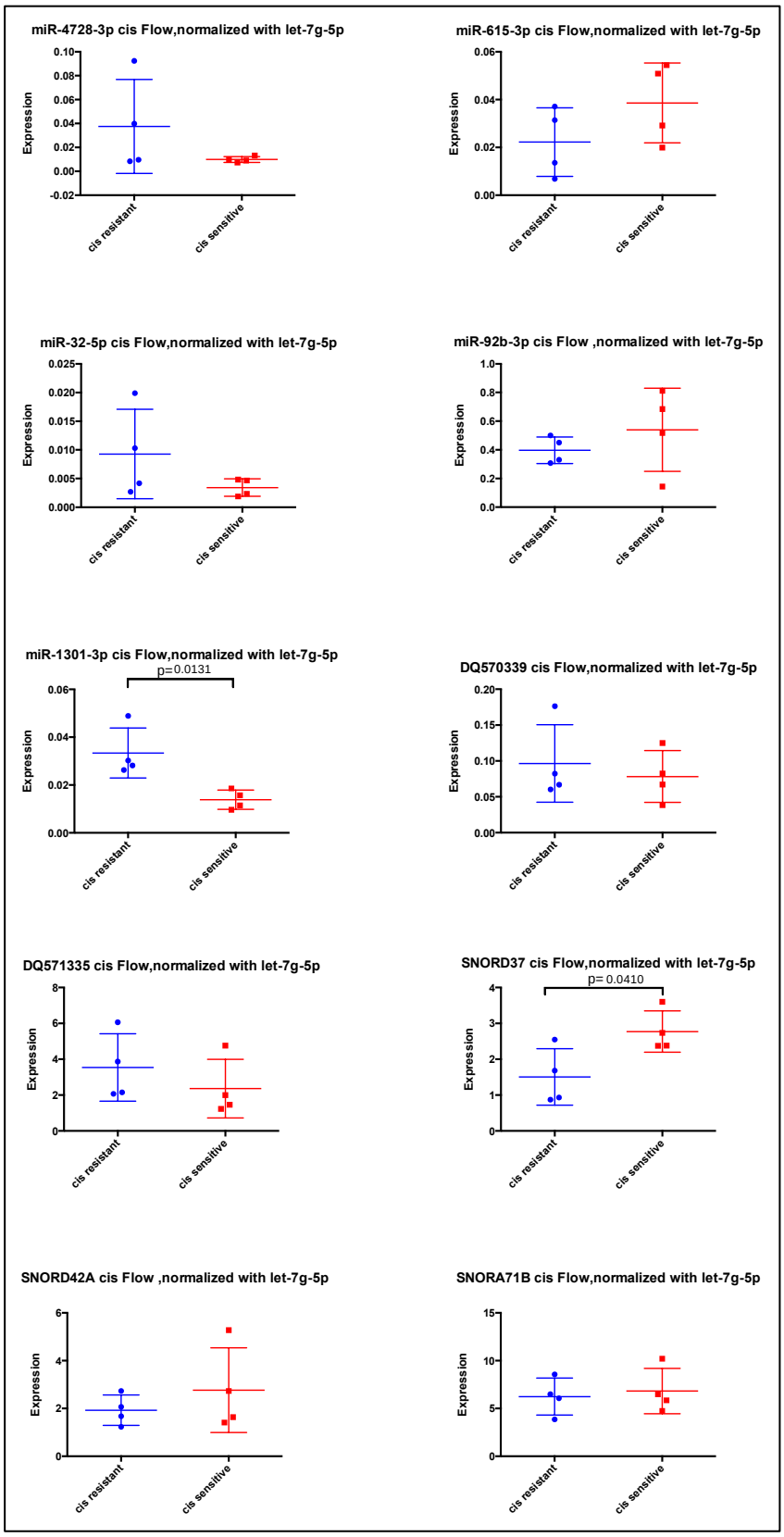

***Figure 6-1**, the small RNAs in Cisplatin resistant and sensitive groups by Flow Cytometry.*

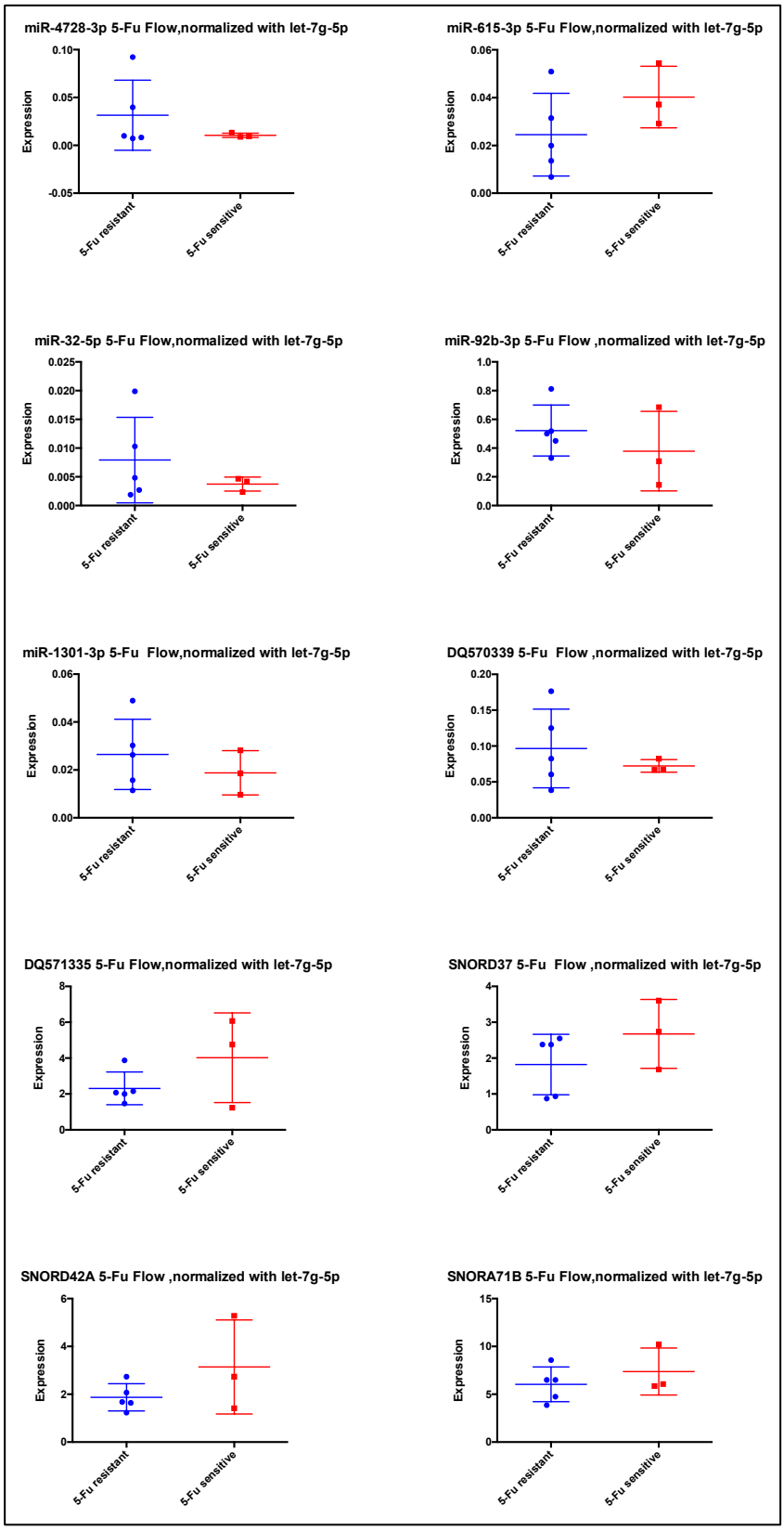
miR-4728-3p 5-Fu Flow,normalized with let-7g-5p
Expression
0.10
0.05
0.00
-0.05
5-Fu resistant
5-Fu sensitive
miR-615-3p 5-Fu Flow,normalized with let-7g-5p
Expression
0.06
0.04
0.02
0.00
5-Fu resistant
5-Fu sensitive
miR-32-5p 5-Fu Flow,normalized with let-7g-5p
Expression
0.025
0.020
0.015
0.010
0.005
0.000
5-Fu resistant
5-Fu sensitive
miR-92b-3p 5-Fu Flow ,normalized with let-7g-5p
Expression
1.0
0.8
0.6
0.4
0.2
0.0
5-Fu resistant
5-Fu sensitive
miR-1301-3p 5-Fu Flow,normalized with let-7g-5p
Expression
0.06
0.04
0.02
0.00
5-Fu resistant
5-Fu sensitive
DQ570339 5-Fu Flow ,normalized with let-7g-5p
Expression
0.20
0.15
0.10
0.05
0.00
5-Fu resistant
5-Fu sensitive
DQ571335 5-Fu Flow,normalized with let-7g-5p
Expression
8
6
4
2
0
5-Fu resistant
5-Fu sensitive
SNORD37 5-Fu Flow ,normalized with let-7g-5p
Expression
4
3
2
1
0
5-Fu resistant
5-Fu sensitive
SNORD42A 5-Fu Flow ,normalized with let-7g-5p
Expression
6
4
2
0
5-Fu resistant
5-Fu sensitive
SNORA71B 5-Fu Flow,normalized with let-7g-5p
Expression
15
10
5
0
5-Fu resistant
5-Fu sensitive

***Figure 6-2**, the small RNAs in 5-Fu resistant and sensitive groups by Flow Cytometry.*

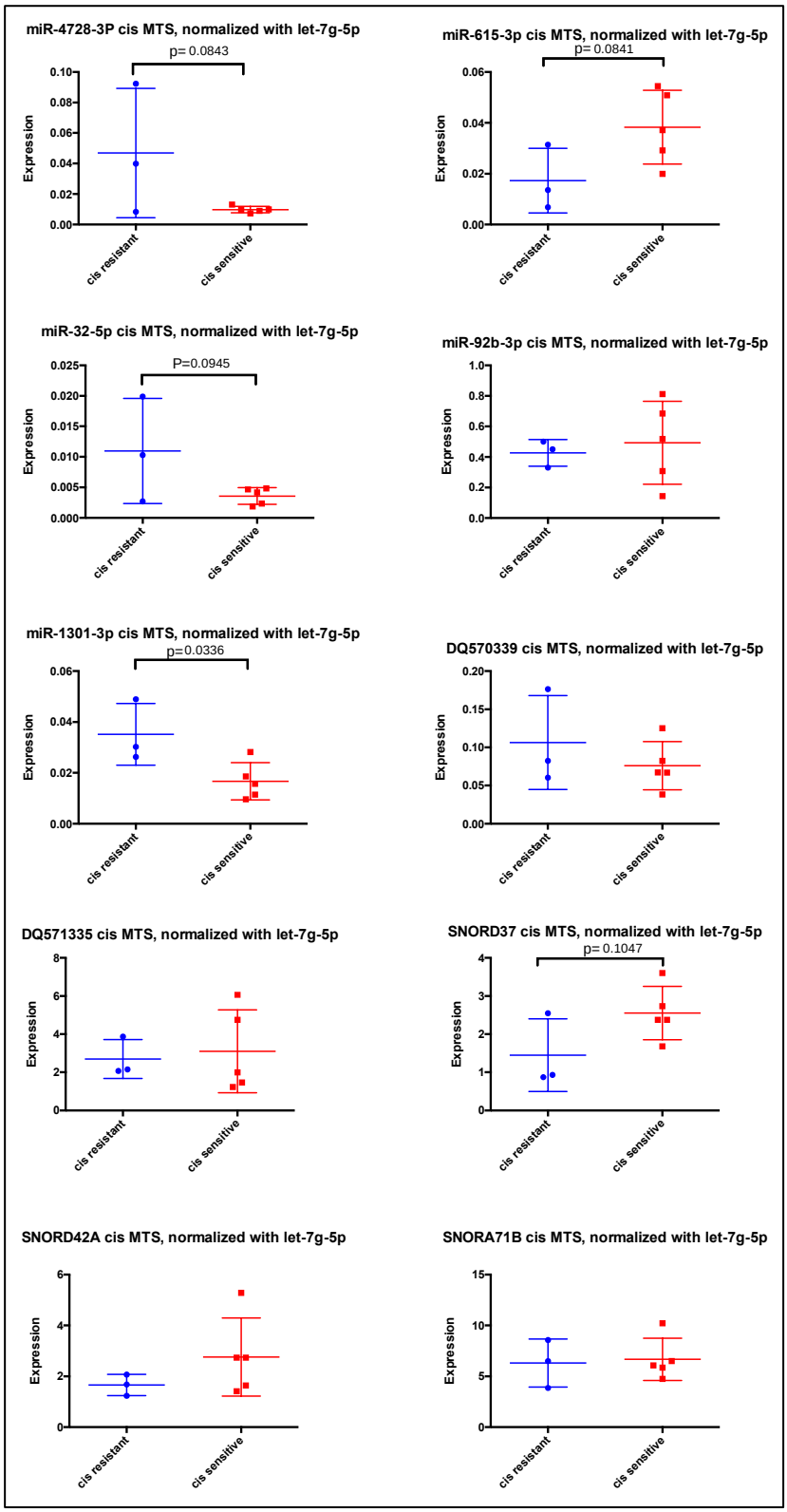

***Figure 6-3**, the small RNAs in Cisplatin resistant and sensitive groups by MTS.*

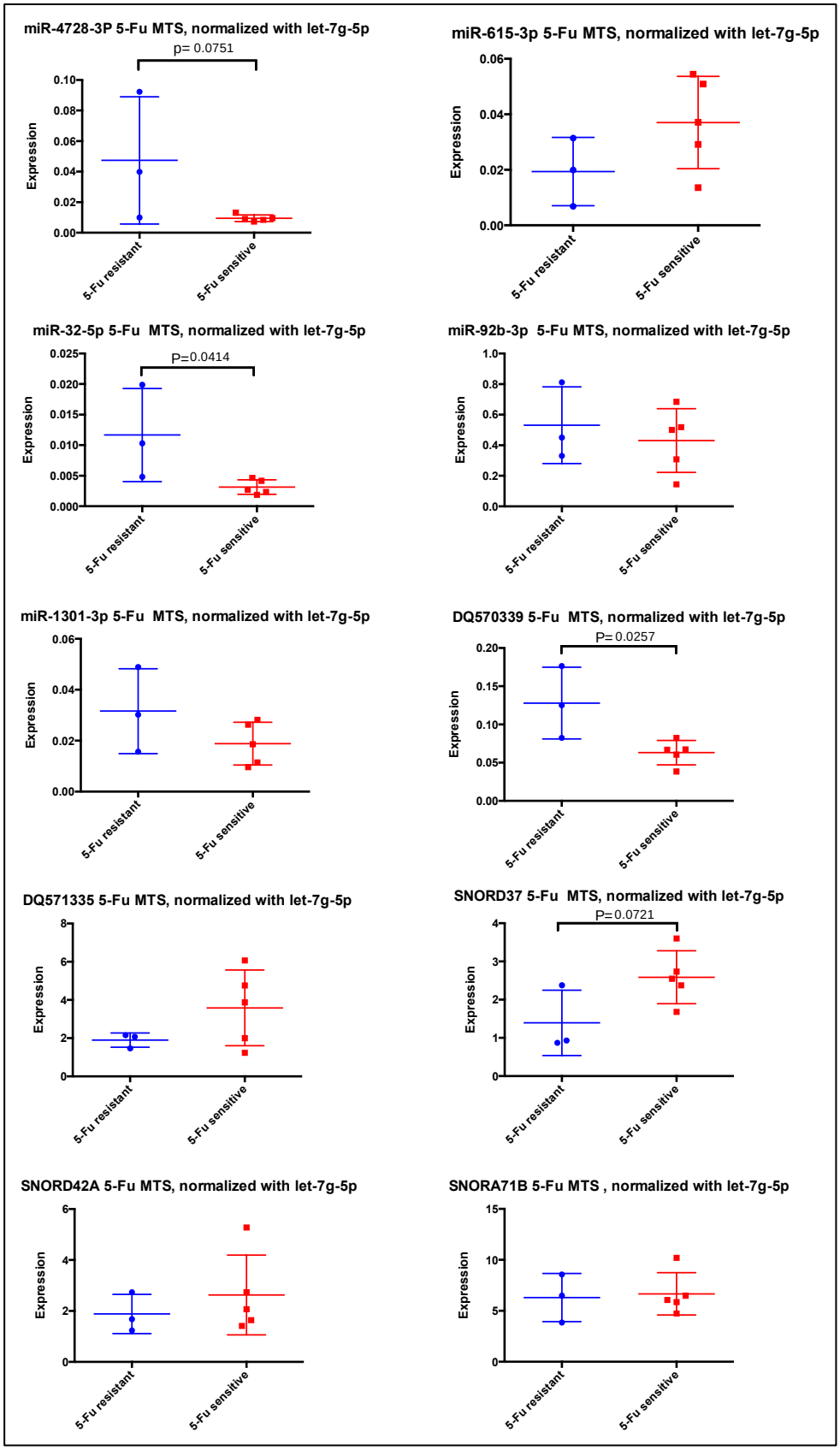

***Figure 6-4**, the small RNAs in 5-Fu resistant and sensitive groups by MTS.*

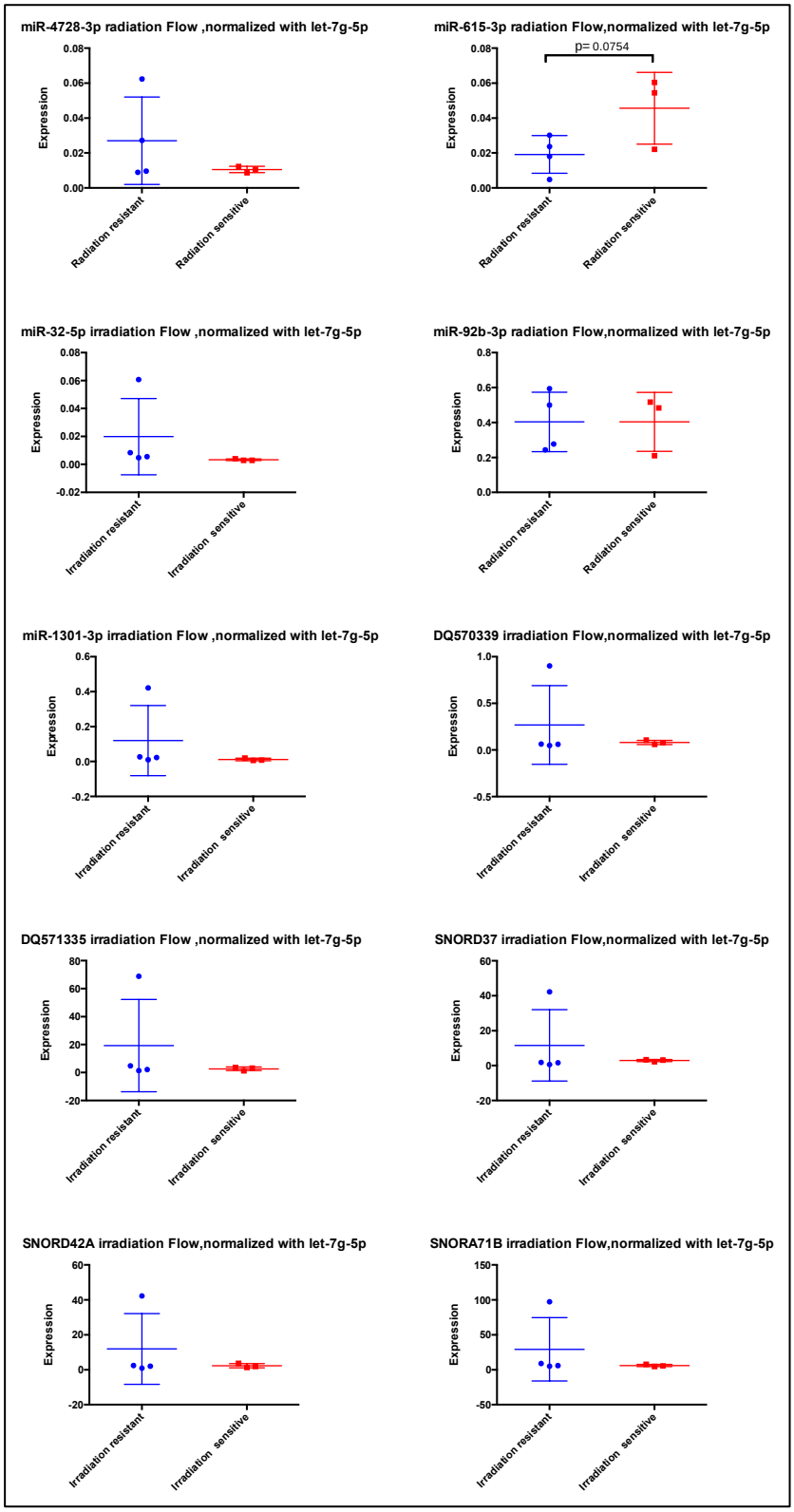

***Figure 6-5**, the small RNAs in radiation resistant and sensitive groups.*

6.2Investigation of the baseline cellular levels of small RNAs and their association with drug or radiation response by Spearman correlation

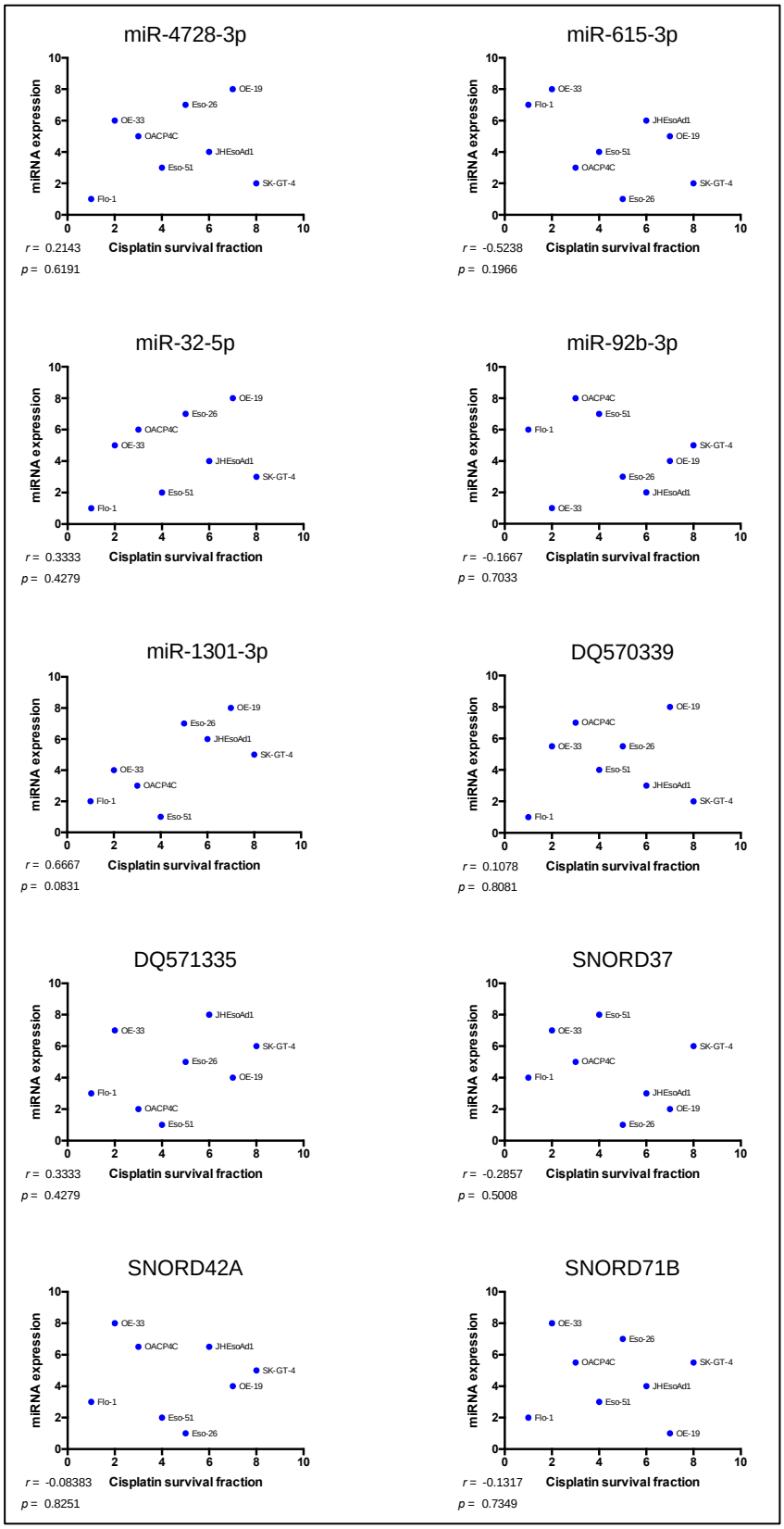
miR-4728-3p
miRNA expression
Cisplatin survival fraction
r = 0.2143
p = 0.6191
miR-615-3p
r = -0.5238
p = 0.1966
miR-32-5p
r = 0.3333
p = 0.4279
miR-92b-3p
r = -0.1667
p = 0.7033
miR-1301-3p
r = 0.6667
p = 0.0831
DQ570339
r = 0.1078
p = 0.8081
DQ571335
r = 0.3333
p = 0.4279
SNORD37
r = -0.2857
p = 0.5008
SNORD42A
r = -0.08383
p = 0.8251
SNORD71B
r = -0.1317
p = 0.7349

***Figure 6-6**, the relationship between small RNA and cisplation treatment response by Flow cytometry.*

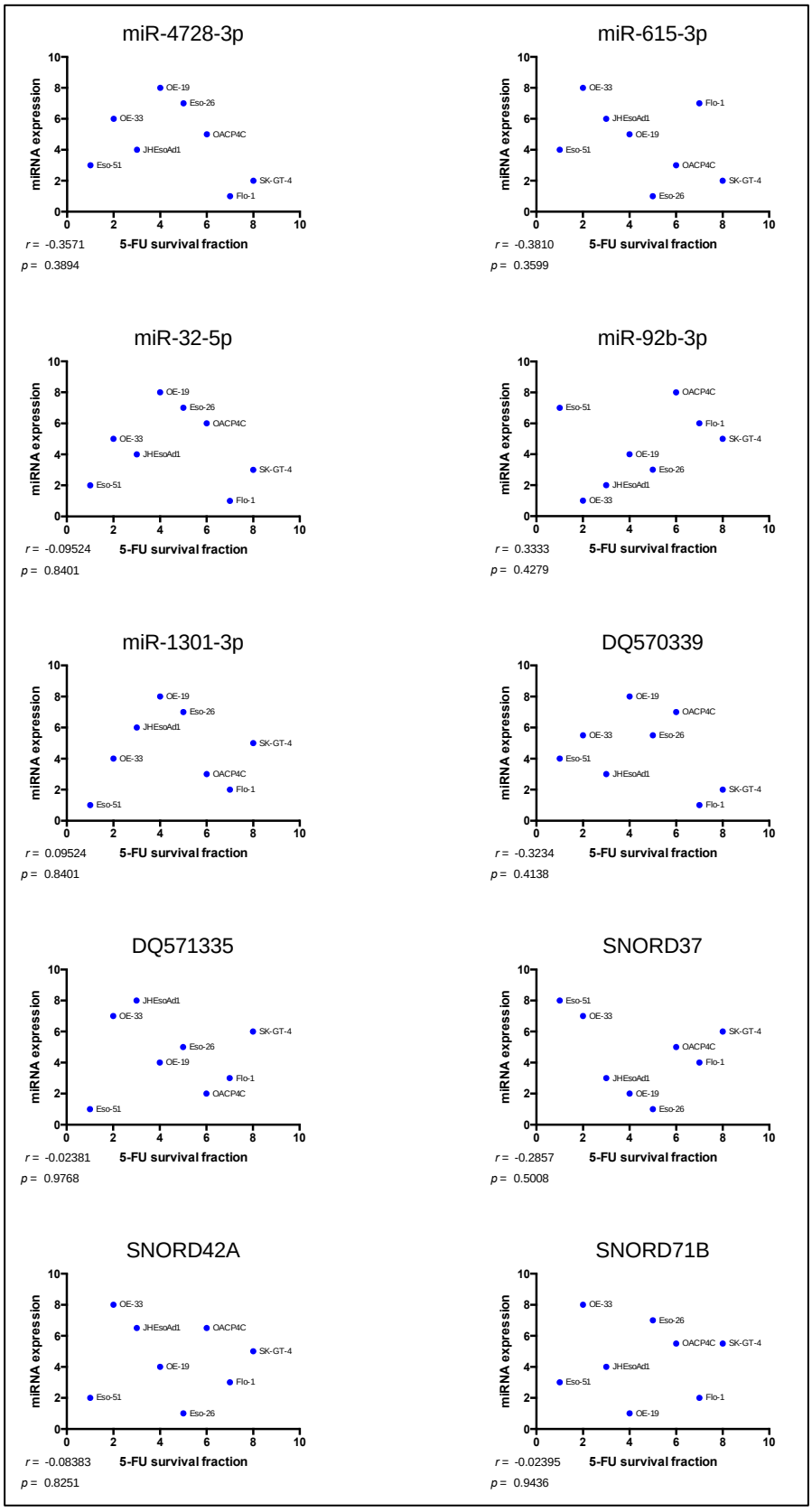
miR-4728-3p
miRNA expression
5-FU survival fraction
r = -0.3571
p = 0.3894
OE-19
Eso-26
OE-33
OACP4C
JHEsoAd1
Eso-51
SK-GT-4
Flo-1
miR-615-3p
r = -0.3810
p = 0.3599
miR-32-5p
r = -0.09524
p = 0.8401
miR-92b-3p
r = 0.3333
p = 0.4279
miR-1301-3p
r = 0.09524
p = 0.8401
DQ570339
r = -0.3234
p = 0.4138
DQ571335
r = -0.02381
p = 0.9768
SNORD37
r = -0.2857
p = 0.5008
SNORD42A
r = -0.08383
p = 0.8251
SNORD71B
r = -0.02395
p = 0.9436

Figure 6-7*, the relationship between small RNA and 5-Fu treatment response by Flow cytometry.*

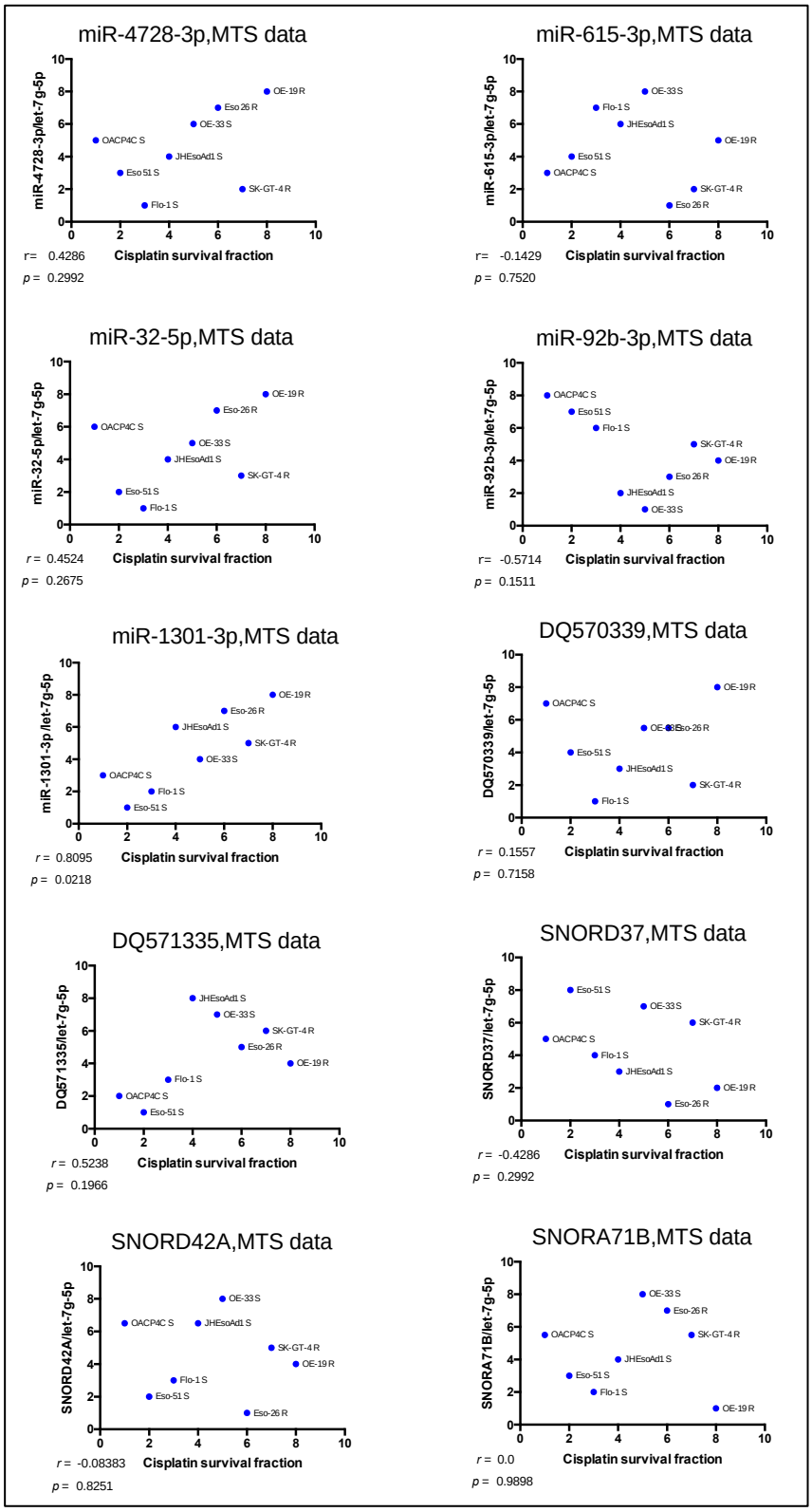

***Figure 6-8**, the relationship between small RNA and cisplation treatment response by MTS.*

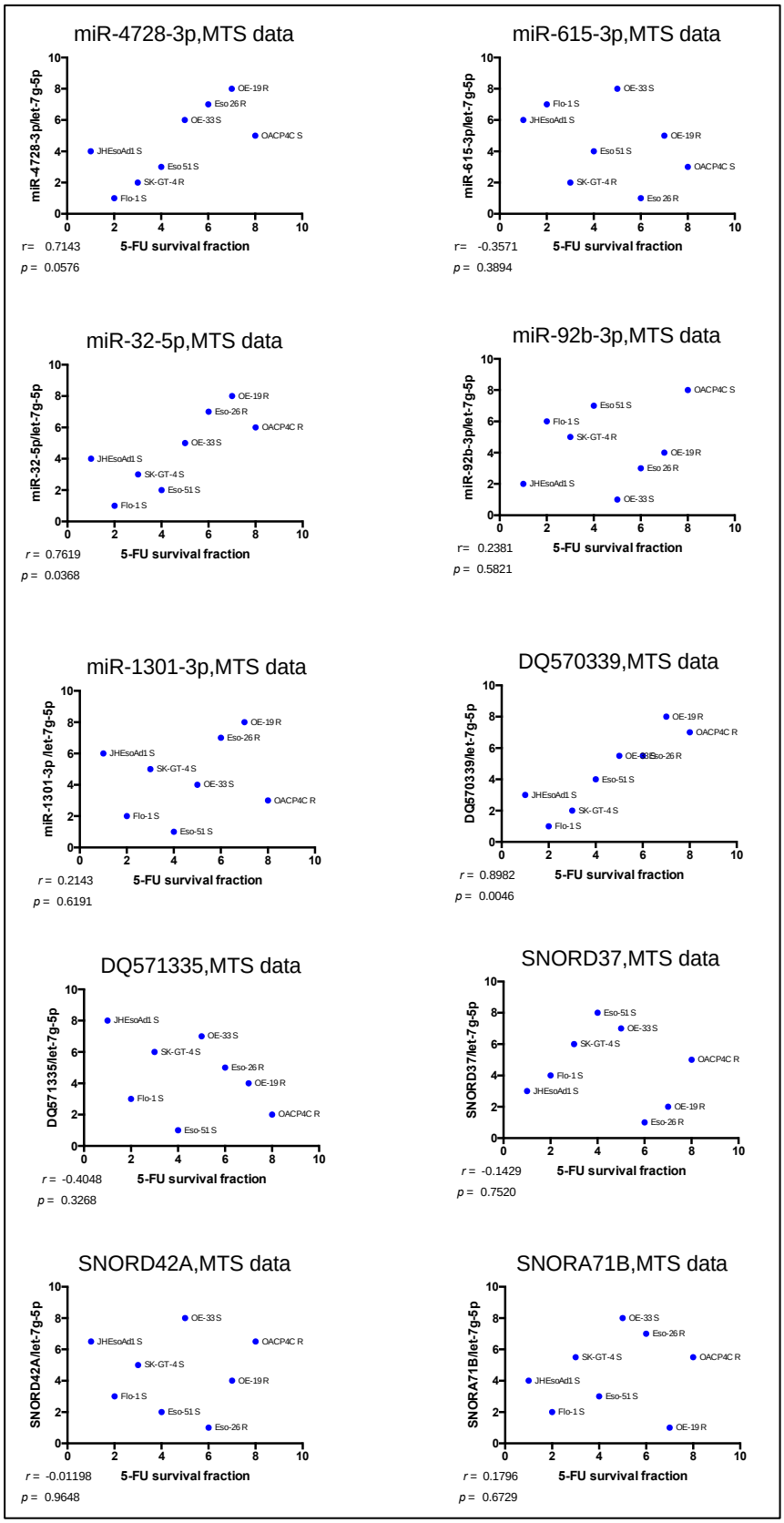
miR-4728-3p,MTS data
miR-4728-3p/let-7g-5p
OE-19 R
Eso 26 R
OE-33 S
OACP4C S
JHEsoAd1 S
Eso 51 S
SK-GT-4 R
Flo-1 S
r= 0.7143
p = 0.0576
5-FU survival fraction
miR-615-3p,MTS data
miR-615-3p/let-7g-5p
OE-33 S
Flo-1 S
JHEsoAd1 S
OE-19 R
Eso 51 S
OACP4C S
SK-GT-4 R
Eso 26 R
r= -0.3571
p = 0.3894
5-FU survival fraction
miR-32-5p,MTS data
miR-32-5p/let-7g-5p
OE-19 R
Eso-26 R
OACP4C R
OE-33 S
JHEsoAd1 S
SK-GT-4 S
Eso-51 S
Flo-1 S
r = 0.7619
p = 0.0368
5-FU survival fraction
miR-92b-3p,MTS data
miR-92b-3p/let-7g-5p
OACP4C S
Eso 51 S
Flo-1 S
SK-GT-4 R
OE-19 R
Eso 26 R
JHEsoAd1 S
OE-33 S
r= 0.2381
p = 0.5821
5-FU survival fraction
miR-1301-3p,MTS data
miR-1301-3p /let-7g-5p
OE-19 R
Eso-26 R
JHEsoAd1 S
SK-GT-4 S
OE-33 S
OACP4C R
Flo-1 S
Eso-51 S
r = 0.2143
p = 0.6191
5-FU survival fraction
DQ570339,MTS data
DQ570339/let-7g-5p
OE-19 R
OACP4C R
Eso-26 R
Eso-51 S
JHEsoAd1 S
SK-GT-4 S
Flo-1 S
r = 0.8982
p = 0.0046
5-FU survival fraction
DQ571335,MTS data
DQ571335/let-7g-5p
JHEsoAd1 S
OE-33 S
SK-GT-4 S
Eso-26 R
OE-19 R
Flo-1 S
OACP4C R
Eso-51 S
r = -0.4048
p = 0.3268
5-FU survival fraction
SNORD37,MTS data
SNORD37/let-7g-5p
Eso-51 S
OE-33 S
SK-GT-4 S
OACP4C R
Flo-1 S
JHEsoAd1 S
OE-19 R
Eso-26 R
r = -0.1429
p = 0.7520
5-FU survival fraction
SNORD42A,MTS data
SNORD42A/let-7g-5p
OE-33 S
JHEsoAd1 S
OACP4C R
SK-GT-4 S
OE-19 R
Flo-1 S
Eso-51 S
Eso-26 R
r = -0.01198
p = 0.9648
5-FU survival fraction
SNORA71B,MTS data
SNORA71B/let-7g-5p
OE-33 S
Eso-26 R
SK-GT-4 S
OACP4C R
JHEsoAd1 S
Eso-51 S
Flo-1 S
OE-19 R
r = 0.1796
p = 0.6729
5-FU survival fraction

***Figure 6-9**, the relationship between small RNA and 5-Fu treatment response by MTS.*

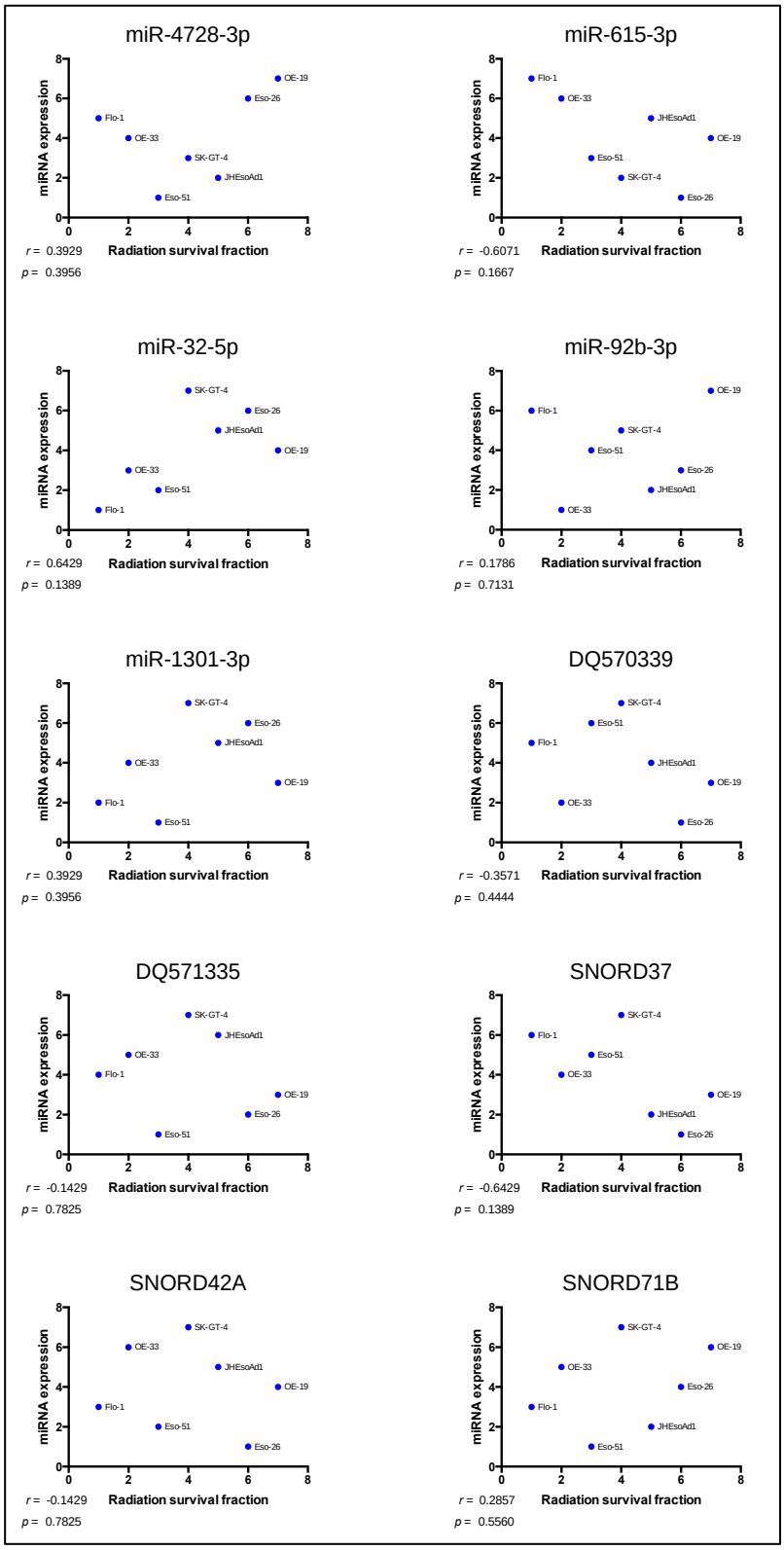

***Figure 6-10**, the relationship between small RNA and radiation treatment response by Clonogenic assay.*

6.3 The role of serum exosomes and their small RNAs in controlling cell growth in EAC cells

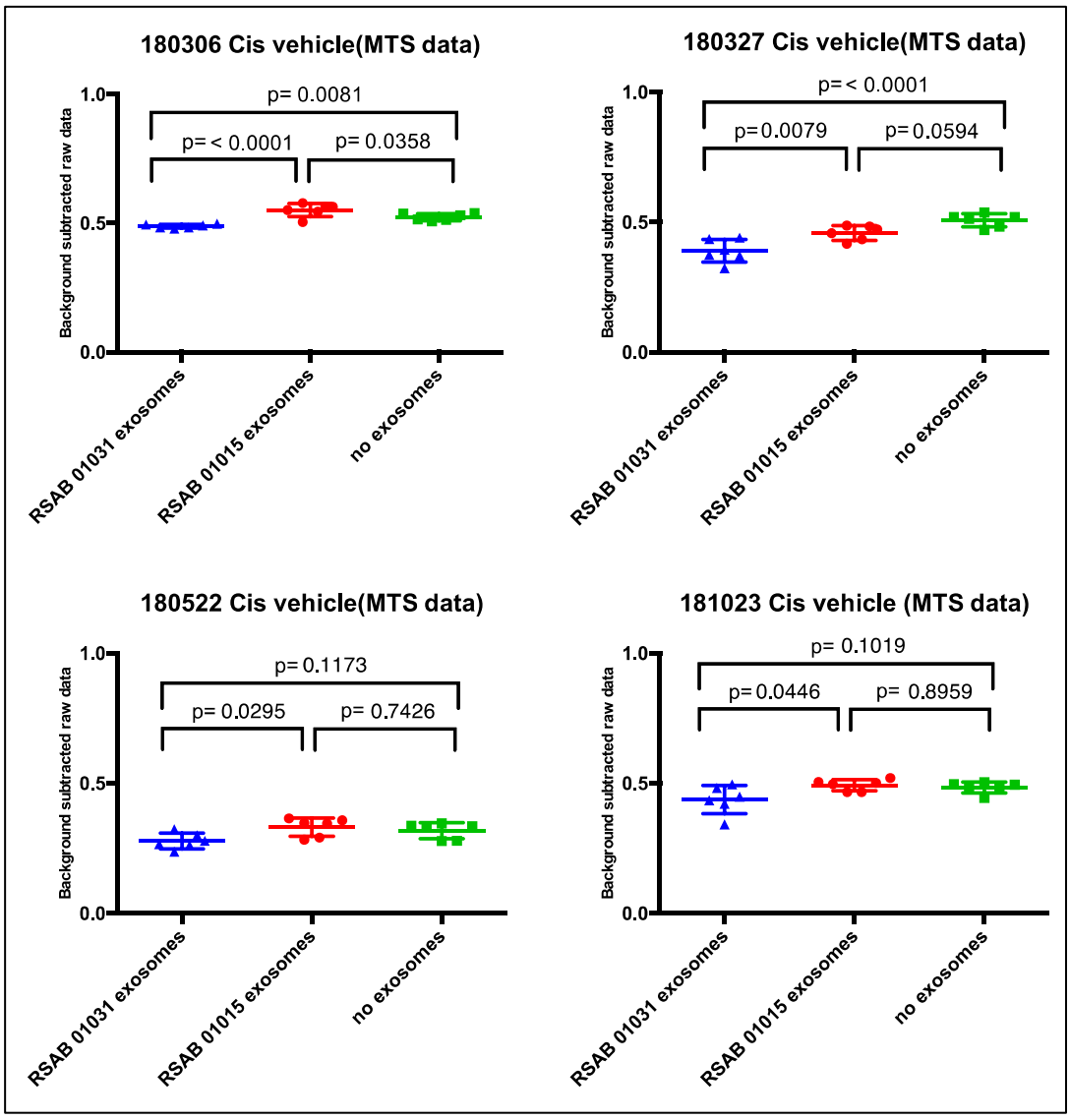

***Figure 6-11**, The MTS data showed exosomes from non-responder increased the cell viability.*

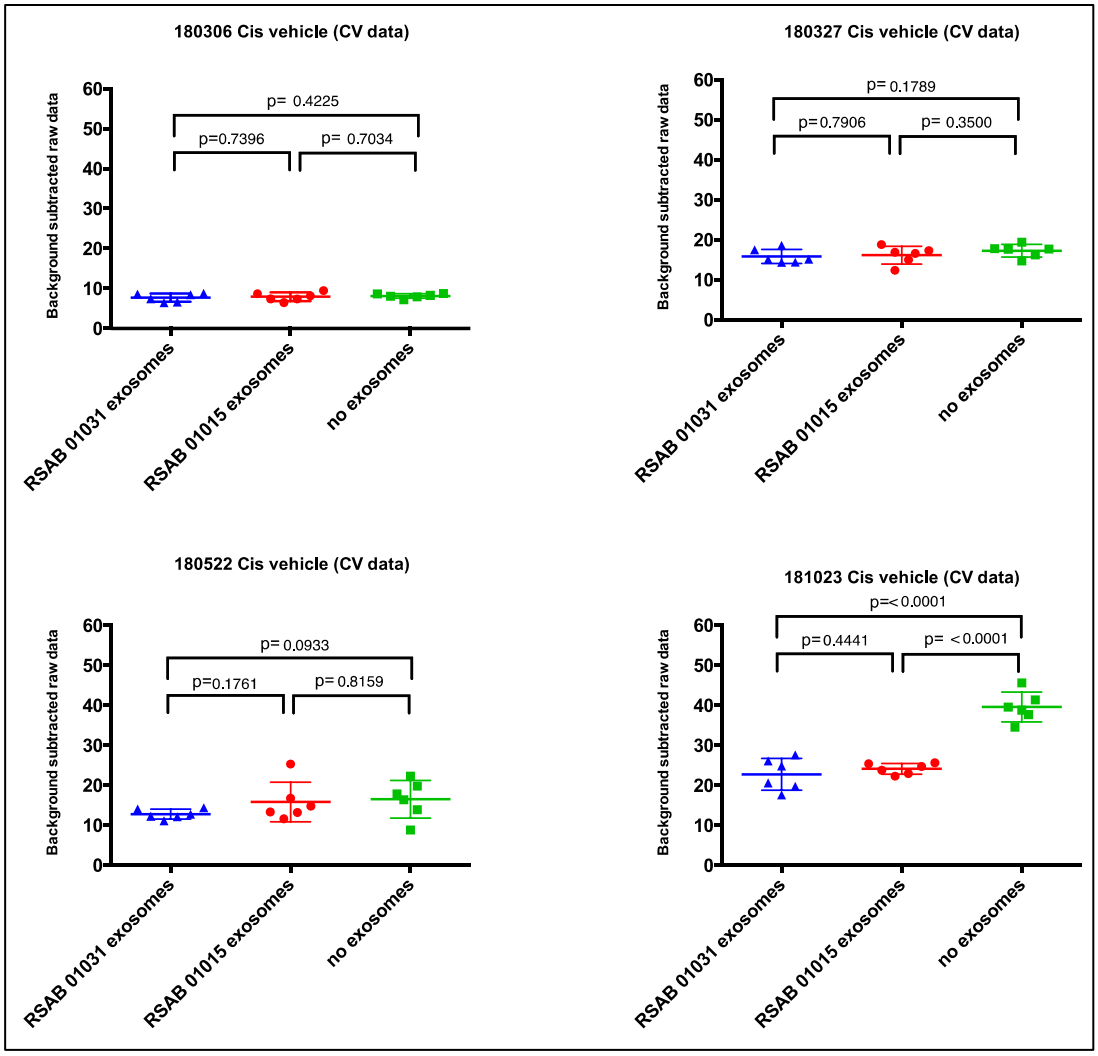

***Figure 6-12**, The effect of exosomes in affecting cell viability by CV data (large circle area analysis in 96 well plate)*

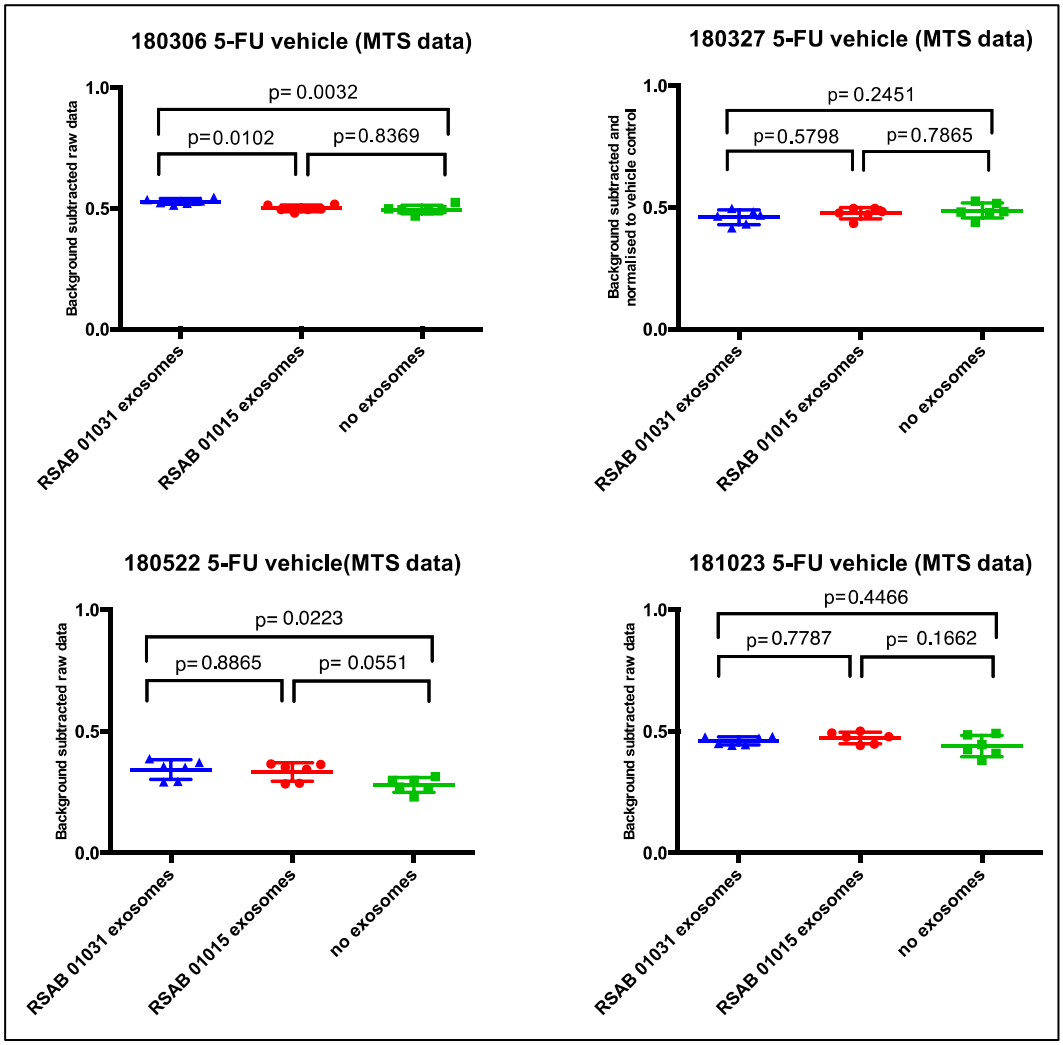

***Figure 6-13**, The exosomes showed no reproducible effects across the 4 independent 5-Fu vehicle control by MTS*

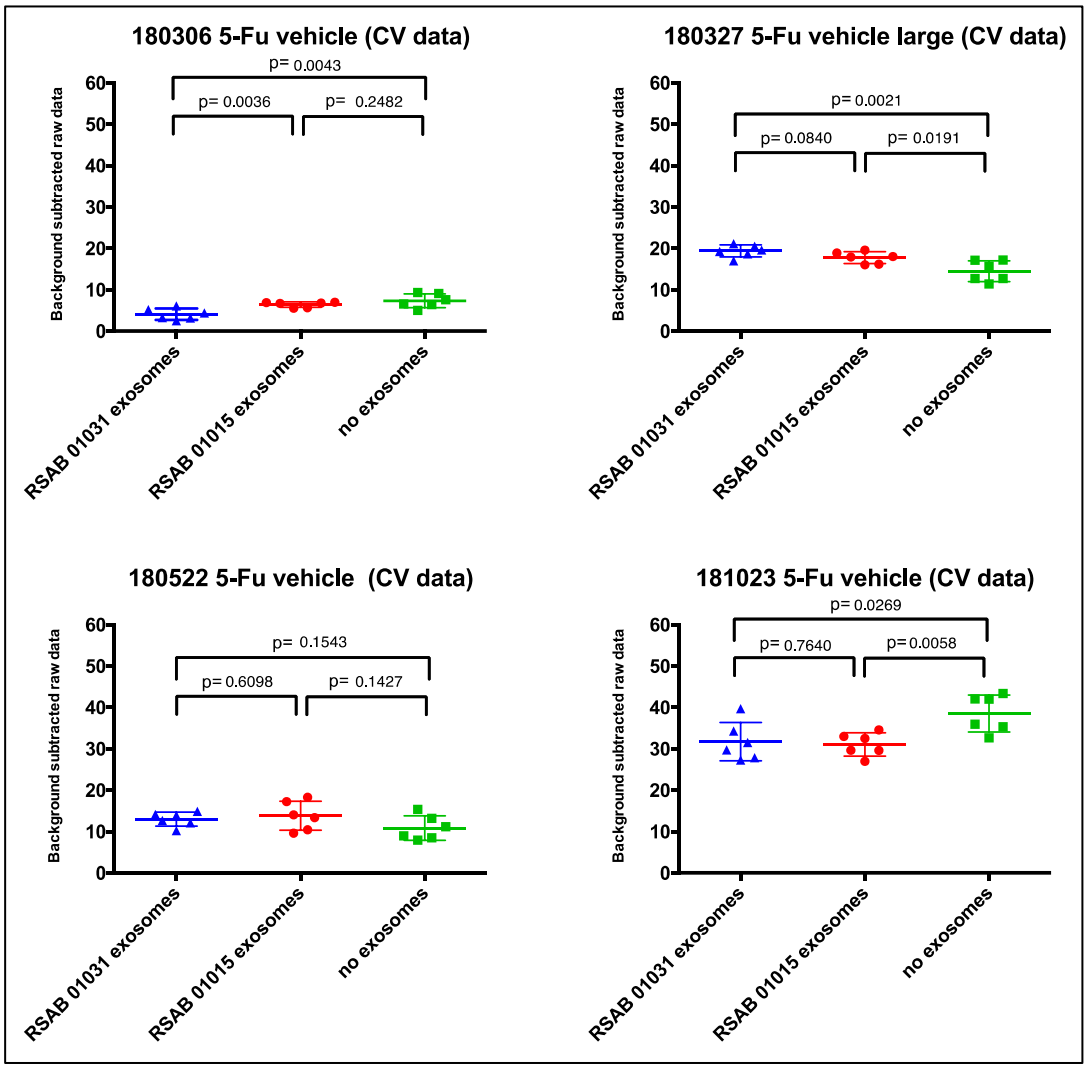

***Figure 6-14**, The exosomes showed no reproducible effects across the 4 independent 5-Fu vehicle control by CV data(large circle area analysis in 96 well plate)*

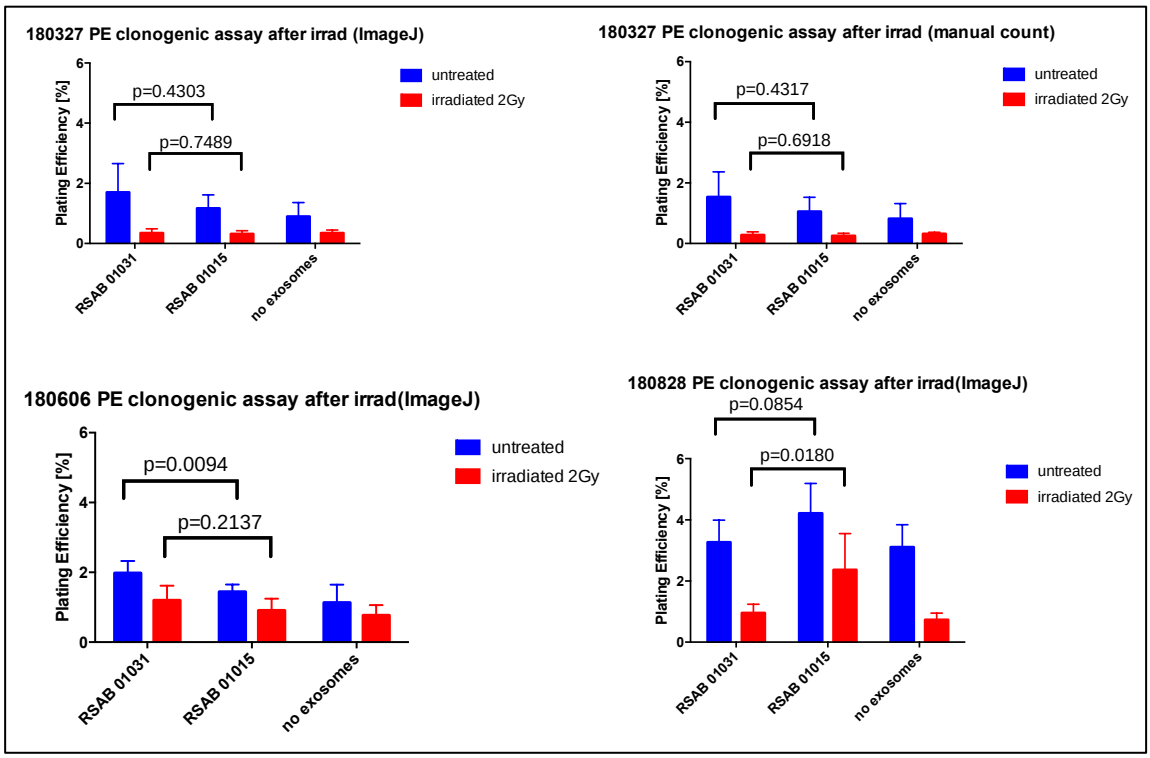

***Figure 6-15**, The exosomes showed no reproducible effects across the 3 independent irradiation experiments*

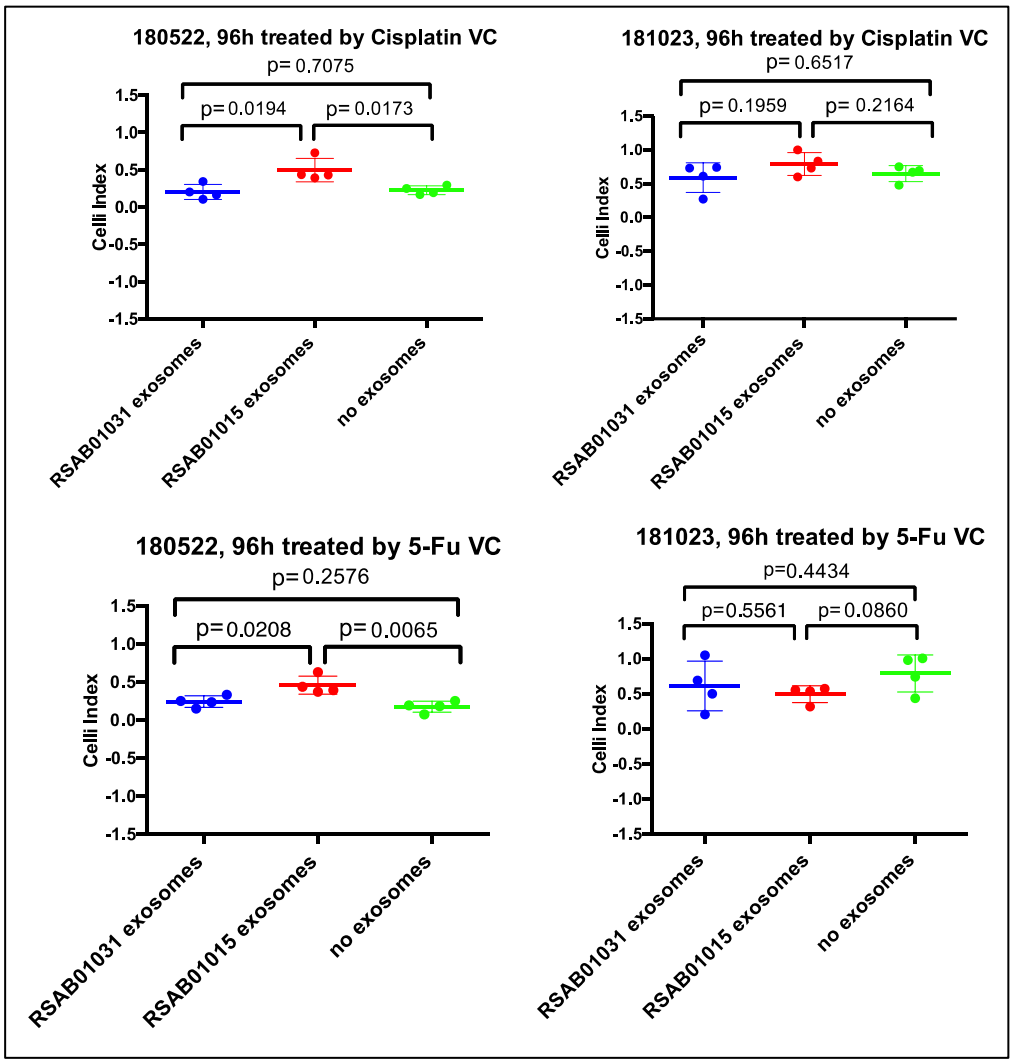

***Figure 6-16**, The effect of exosomes in affecting cell viability by xCelligence data (96h, Cell Index: the Xcelligence data normalized by subtract the data of VC)*

6.4 The role of serum exosomes and their small RNAs in controlling drug / radiation response in EAC cells

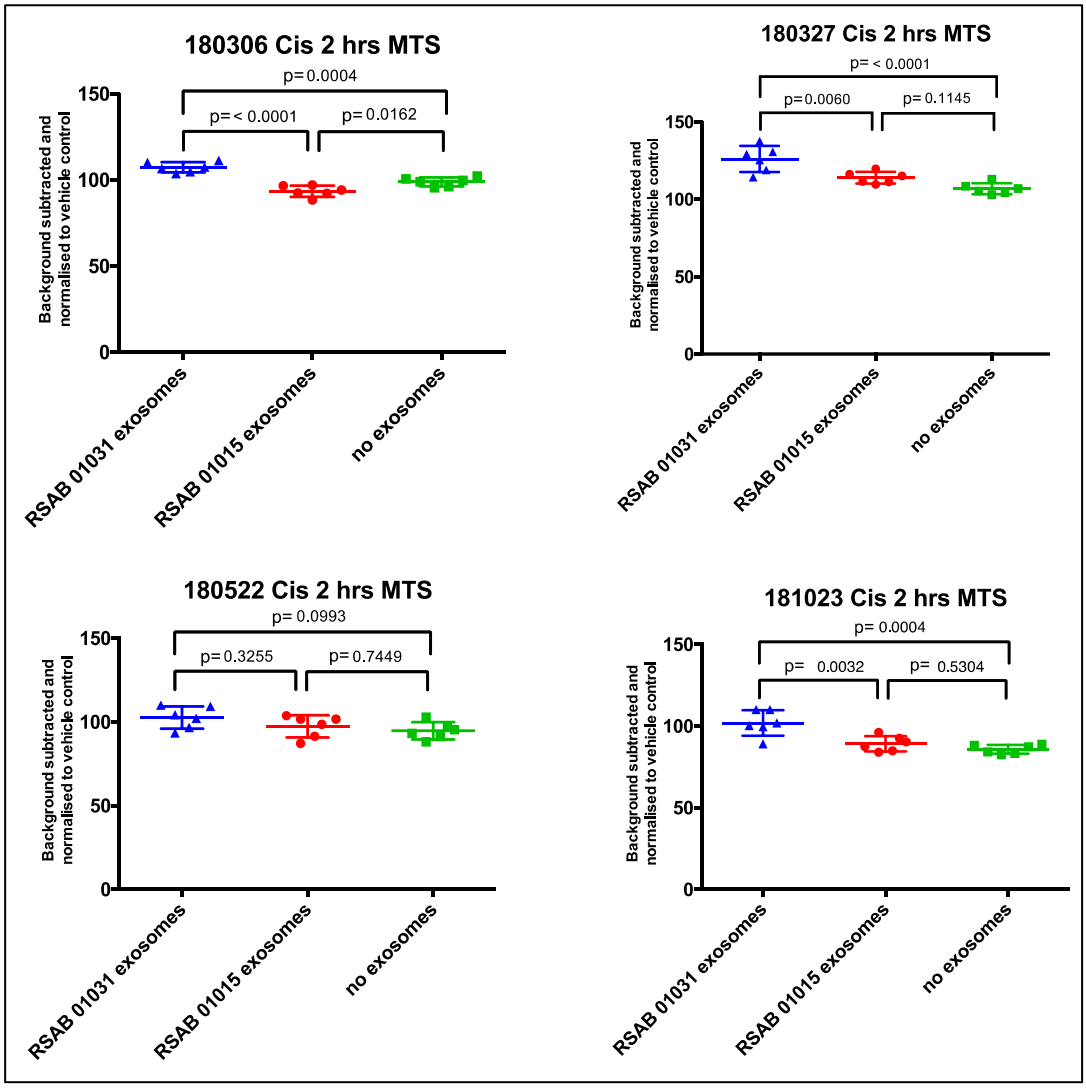

***Figure 6-17**, The effect of exosomes in affecting Cisplatin response by MTS data (the exosomes exposured cells treated by Cisplatin, and the MTS data was measured after 2h adding the MTS regents. All the data was normalized by vehicle control)*

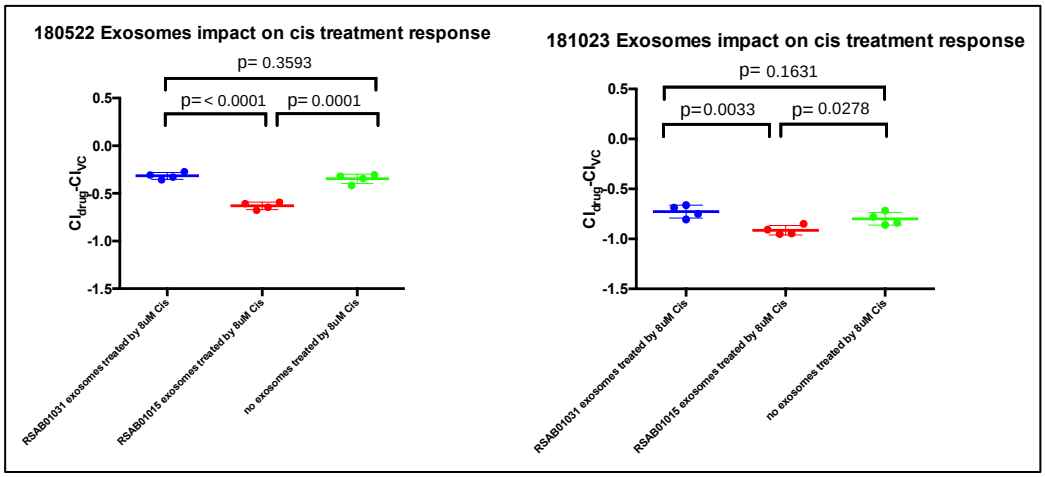

***Figure 6-18**, The effect of exosomes in affecting Cisplatin response by Xcelligence data (the exosomes exposured cells treated by Cisplatin, and the Xcelligence data was normalized by subtracting vehicle control).*

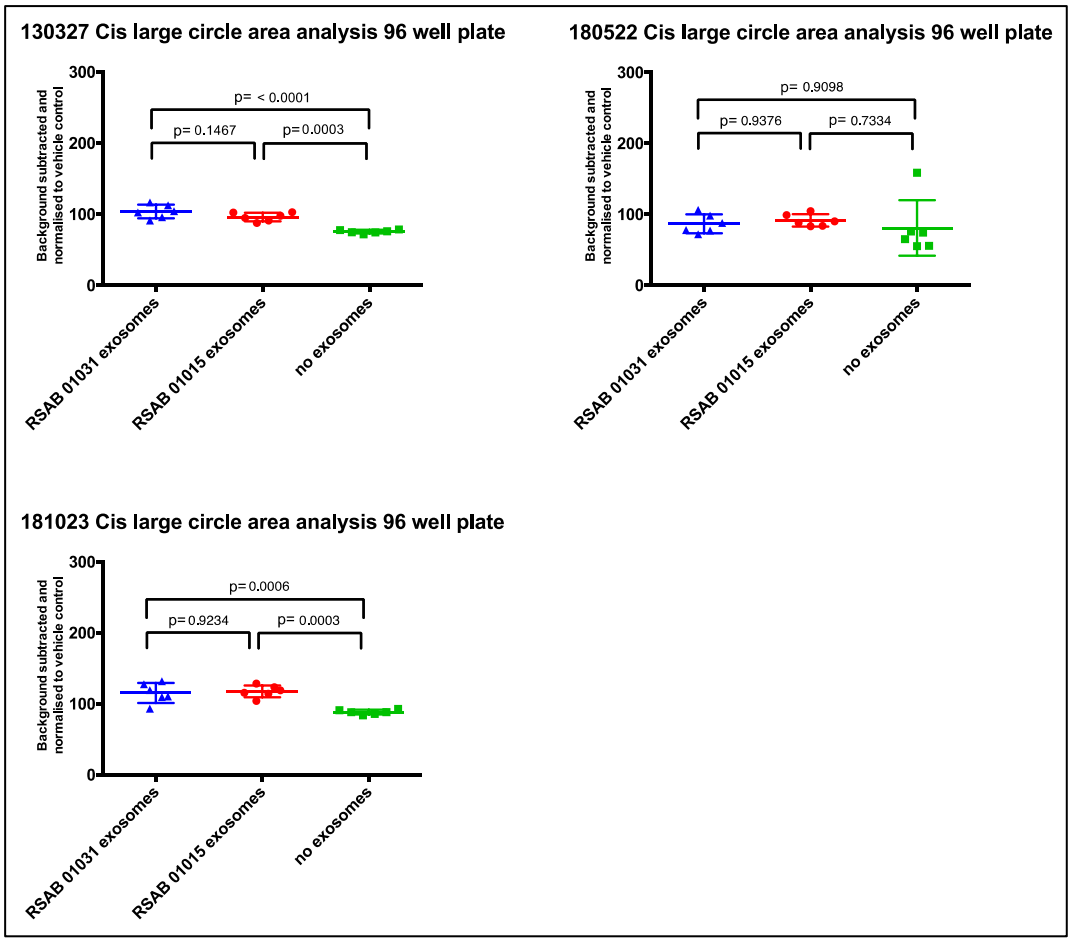

***Figure 6-19**, The effect of exosomes in affecting Cisplatin response by CV data (Background subtracted and normalized to vehicle control, large circle area analysis).*

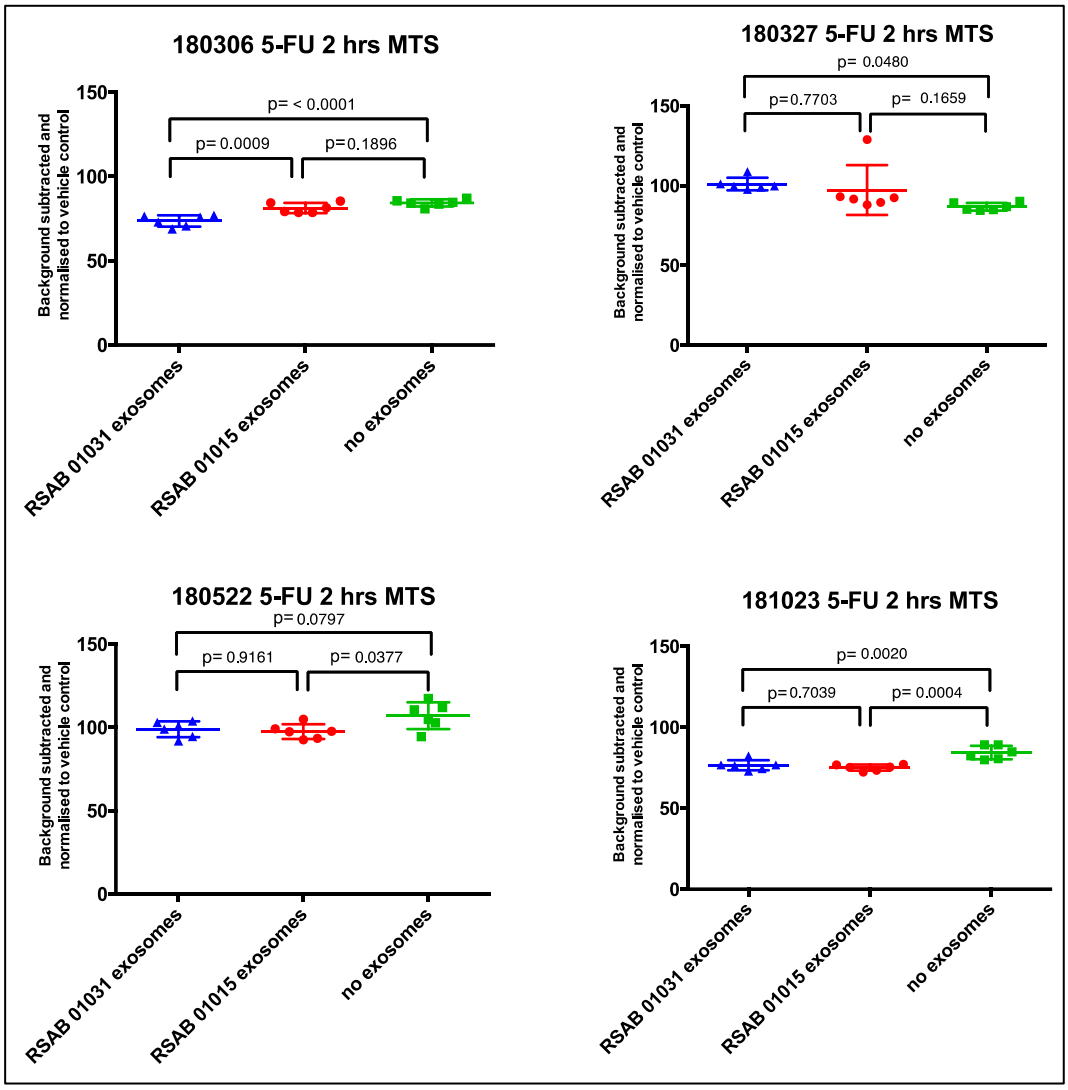

***Figure 6-20**, The effect of exosomes in affecting 5-Fu response by MTS data (the exosomes exposured cells treated by 5-Fu, and the MTS data was measured after 2h adding the MTS regents. All the data was normalized by vehicle control)*

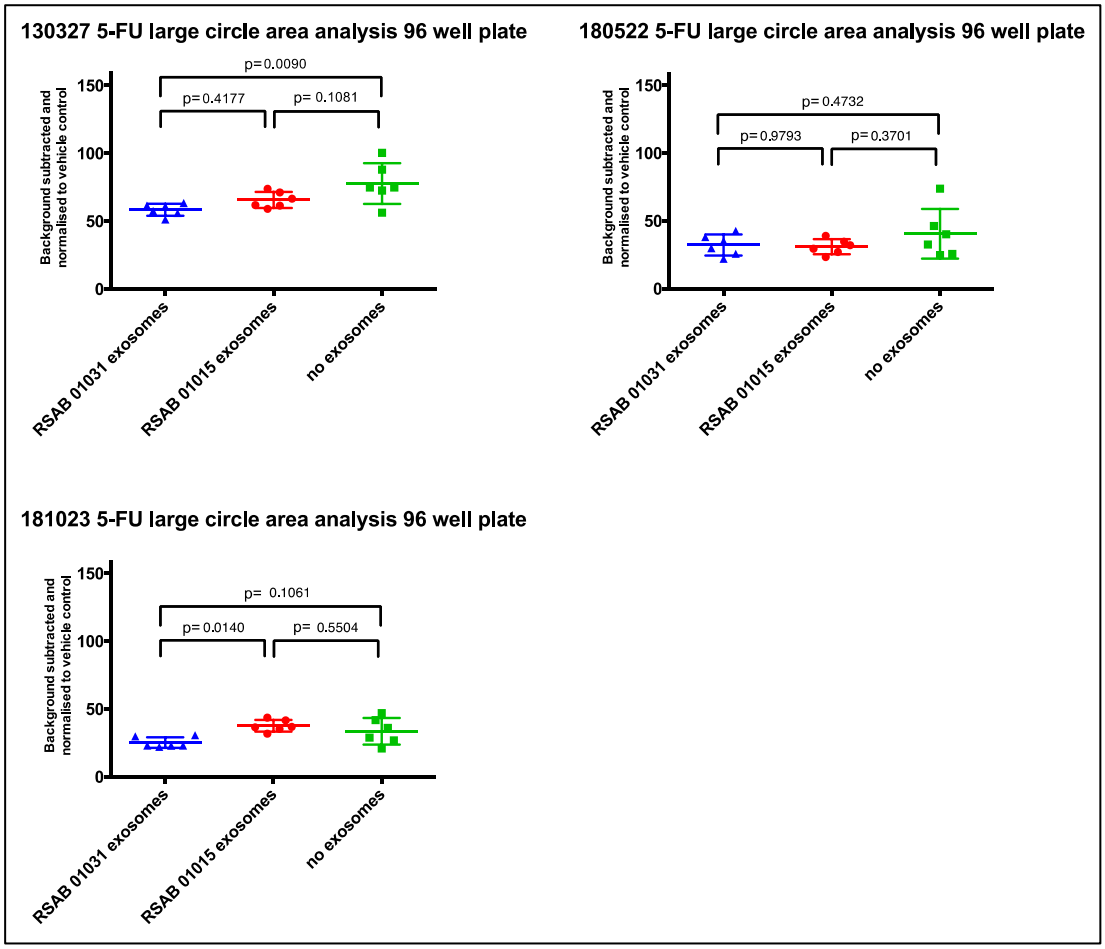

***Figure 6-21**, The effect of exosomes in affecting 5-Fu response by CV data (Background subtracted and normalized to vehicle control, large circle area analysis).*

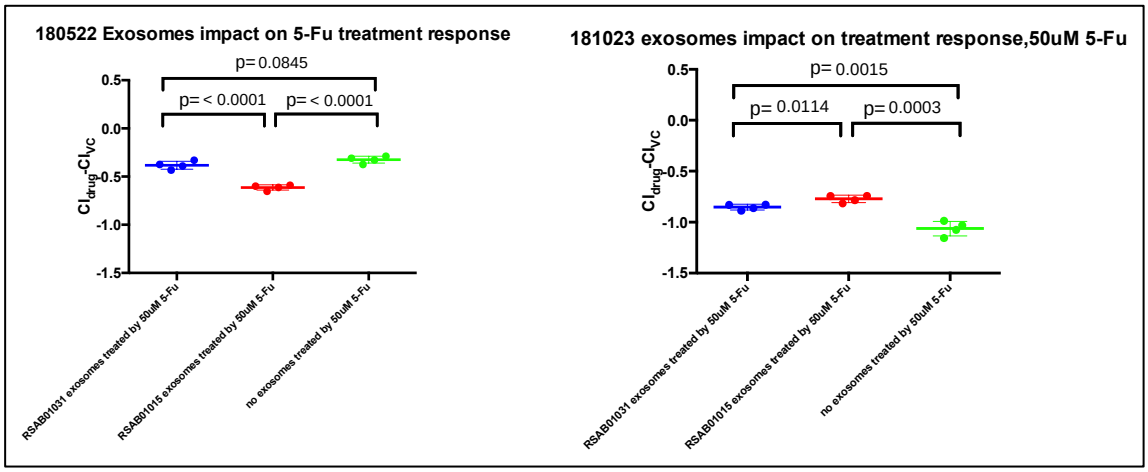

***Figure 6-22**, The effect of exosomes in affecting 5-Fu response by Xcelligence data (the exosomes exposured cells treated by 5-Fu, and the Xcelligence data was normalized by subtracting vehicle control).*

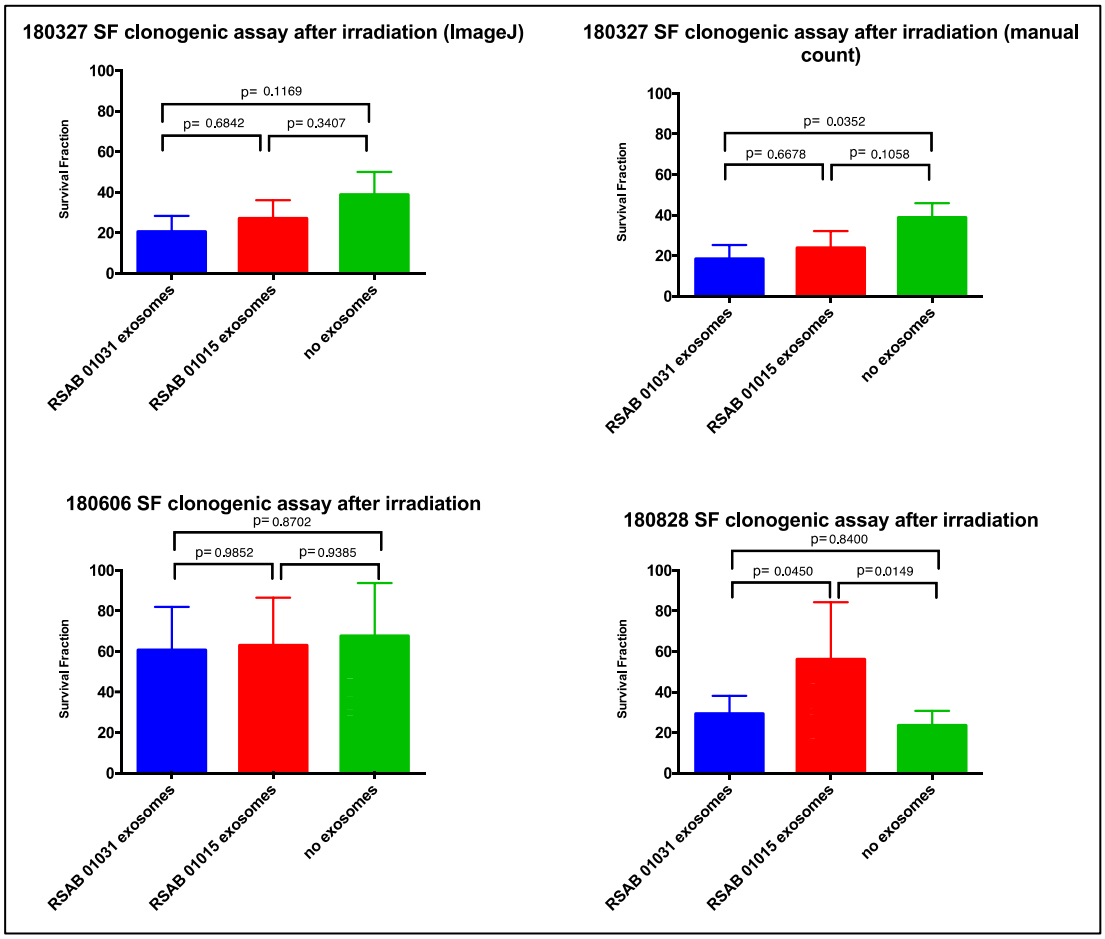

***Figure 6-23**, The effect of exosomes in affecting irradiation response by Clonogenic assay (the data was analysed by Image J software, the manual count was used as well as a compare and the results were similar between two methods).*